Hazard assessment of engineered nanomaterials – impacts on hepatic and renal models

Ali Kermanizadeh

Doctor of Philosophy

Heriot Watt University

January 2013

Abstract

This study was conducted as part of a large consortium (FP7 project – ENPRA) to investigate the potential hazard of a wide range of nanomaterials (one Ag, two ZnO, two MWCNTs and five TiO_2) on the liver and the kidneys for the purpose of risk assessment.

The *in vitro* C3A hepatocyte model demonstrated that Ag and ZnO NMs were consistently more potent with respect to cytotoxicity and cytokine production. In comparison the MWCNT and TiO_2 nanomaterials investigated revealed relatively lower toxicity. The cytotoxicity of ZnO may be related to its solubility, but this is less likely for the Ag NMs. Urea and albumin production were measured as indicators of hepatic function. These markers were only altered by the coated and uncoated ZnO, which significantly decreased albumin production. The C3A model also showed that the NM which induced a low cytotoxicity (TiO_2 and MWCNTs) generated intracellular ROS, induced oxidative stress (GSH depletion) and that an oxidative mechanism was involved in both the induction of IL8 protein production and genotoxicity.

The C3A cells were demonstrated to be a very good model to investigate nanomaterial induced effects on hepatocytes when compared to primary human hepatocytes. The results also suggested that biotransformation enzymes in hepatocytes are not important in terms of determining nanotoxicology.

In vivo mice models demonstrated that the instilled Ag, ZnO and positively charged TiO_2 result in distal effects on the liver in the form of oxidative stress. While all NMs with the exception of the two MWCNTs instilled via the lungs caused changes in gene expression in the liver in varying degrees.

The intravenous exposure of mice to the NMs resulted in a neutrophil influx into the liver. These leukocytes play an important in the initiation of the immune response to the NMs. However the NMs were not sufficient to cause any long term neutrophil mediated inflammation or damage to the liver tissue. Any changes that were observed after 24 hr post exposure in terms of leukocyte infiltration into the tissue, antioxidants status and changes in gene expression related to inflammation, oxidative stress and apoptosis had resolved 72 hr post exposure.

Next, we show that Kupffer cells are very important in the liver immune response to the NMs with a significant change in the cytokine profile following the enrichment of the macrophage population.

Finally, investigations using the HK-2 renal model demonstrated that ZnO and Ag NMs were consistently more potent with respect to cytotoxicity, cytokine production (IL6 and IL8) and intracellular reactive oxygen species production. These results were consistent with those observed in the hepatocyte models. We noted that short term sub-lethal exposure to the Ag and two of the TiO_2 NMs (positively charged and the 94 nm TiO_2) resulted in most evident DNA damage.

Acknowledgements

Firstly I would like to thank my brilliant supervisor Prof Vicki Stone for her continuous support and patience over the last three years. Her guidance has been invaluable in the completion of this PhD – without her input and knowledge achieving this task would have been extremely difficult.

I would also like to thank my colleagues and friends at Heriot Watt and Napier Universities for their all their help and making coming to work a total pleasure. In particular a massive thank you to Dr Celine Filippi, Dr David Brown, Dr Birgit Gaiser, Dr Helinor Johnston, Dr Gary Hutchison and Dr Lesley Young.

Next I would like to thank my mum and dad as well as my fantastic friends (a big mention to the beautiful Haley) for putting up with me and listening to all the Ali whinging and complaining.

Finally a special mention for all the partners and collaborators on the ENPRA project – Dr Ilse Gosens, Dr Mike Ward and Dr Sonja Boland have all been fantastic during this project.

ACADEMIC REGISTRY

Research Thesis Submission

Name*:*	Ali Kermanizadeh		
School/PGI:	School of Life Sciences		
Version: *(i.e. First, Resubmission, Final)*	Final	Degree Sought (Award and Subject area)	Doctor of Philosophy Nanotoxicology

Declaration

In accordance with the appropriate regulations I hereby submit my thesis and I declare that:

1) the thesis embodies the results of my own work and has been composed by myself
2) where appropriate, I have made acknowledgement of the work of others and have made reference to work carried out in collaboration with other persons
3) the thesis is the correct version of the thesis for submission and is the same version as any electronic versions submitted*.
4) my thesis for the award referred to, deposited in the Heriot-Watt University Library, should be made available for loan or photocopying and be available via the Institutional Repository, subject to such conditions as the Librarian may require
5) I understand that as a student of the University I am required to abide by the Regulations of the University and to conform to its discipline.

* *Please note that it is the responsibility of the candidate to ensure that the correct version of the thesis is submitted.*

Signature of Candidate*:*		Date:	

Submission

Submitted By *(name in capitals):*	Ali Kermanizadeh
Signature of Individual Submitting:	
Date Submitted:	

For Completion in the Student Service Centre (SSC)

Received in the SSC by *(name in capitals):*			
Method of Submission *(Handed in to SSC; posted through internal/external mail):*			
E-thesis Submitted (**mandatory for final theses**)			
Signature:		Date	

Contents

List of Figures

Chapter 6

List of Tables

Publications

Kermanizadeh A, Brown DM, Hutchison G, Stone V. (2013). Engineered nanomaterial impact in the liver following exposure via an intravenous route – the role of polymorphonuclear leukocytes and gene expression in the organ. Nanomedicine and Nanotechnology 4: 157. DOI:10.4172/2157-7439.1000157.

Kermanizadeh A, Gaiser BK, Hutchison GR, Stone V. (2012). An *in vitro* liver model – assessing oxidative stress and genotoxicity following exposure of hepatocytes to a panel of engineered nanoparticles. Particle and Fibre Toxicology 9:28 DOI: 10.1186/1743-8977-9-28.

Kermanizadeh A, Gaiser BK, Ward MB, Stone V. (2012). Primary human hepatocytes vs. hepatic cell line – assessing their suitability for *in vitro* nanotoxicology. Nanotoxicology DOI: 10.3109/17435390.2012.734341.

Kermanizadeh A, Pojana G, Gaiser BK, Birkedal R, Bilaničová D, Wallin H, Jensen KA, Sellergren B, Hutchison GR, Marcomini A, Stone V. (2012). *In vitro* assessment of engineered nanomaterials using a hepatocyte cell line: cytotoxicity, pro-inflammatory cytokines and functioal markers. Nanotoxicology DOI: 10.3109/17435390.2011.653416.

Johnston H, Brown D, Kermanizadeh A, Gubbins E, Stone V. (2012). Investigating the relationships between nanomaterial hazard and physicochemical properties: informing the exploitation of nanomaterials within therapeutic and diagnostic applications. Journal of Controlled Release 164: 307-313.

Gaiser BK, Hirn S, Kermanizadeh A, Kanase N, Fytianos K, Wenk A, Haberl N, Kreyling W, Stone V. (2012). Effects of silver nanoparticles on the liver and hepatocytes *in vitro*. Toxicological Sciences 131(2), 537–547.

Kermanizadeh A, Vranic S, Boland S, Moreau K, Squiban AB, Gaiser BK, Andrzejczuk LA, Stone V. (2013). An *in vitro* assessment of panel of engineered nanomaterials using a human renal cell line: Cytotoxicity, pro-inflammatory response, oxidative stress and genotoxicity. Submitted to BMC Nephrology.

Gaiser BK, Hirn S, Kermanizadeh A, Kanase N, Fytianos K, Wenk A, Haberl N, Kreyling W, Stone V. (2013). Effects of Titanium Dioxide Nanoparticles on the Liver and Hepatocytes *in vitro*. Submitted to Particle and Fibre Toxicology.

Chapter One

Nanomaterials, nanotoxicology and nanotechnology

1.1 Risk assessment of engineered nanoparticles (ENPRA) project

The aim of this study was to evaluate the toxicity of a panel of engineered nanomaterials (NMs) on the liver and the kidneys, conducted as part of the European Commission funded project ENPRA (Engineered Nanoparticle Risk Assessment). Overall, the project was concerned with revealing the risks associated with exposure to a panel of engineered NMs. Therefore a number of nano scale materials (EU commission recommendation) were utilised in this project including a variety of titanium oxide (TiO_2), zinc oxide (ZnO), silver (Ag) and multi-walled carbon nanotubes (MWCNT). These NMs were chosen as they are all mass produced and have applications in a diverse range of products and industries and might therefore possess a real risk to workers and the consumers.

The project co-ordination and management of all twenty one partners as well as all European and US collaborations was led by the Institute of Occupational Medicine (IOM). The extensive characterisation of the material panel was carried out principally by the OECD (Organisation for Economic Co-operation and Development) and the JRC (Joint Research Centre). The dose response toxicity of the different NMs (aiming to pin point the threshold dose) on areas of interest, in particular pulmonary (Edinburgh University, Universite Catholique de Louvain, Katholieke Universiteit Leuven and Helmholtz Zentrum Munchen – German centre for Environmental Health), cardiovascular (Katholieke Universiteit Leuven, University of Copenhagen), hepatic (Edinburgh Heriot Watt University, Institut fur umweltmedizinische Forschung), renal (Edinburgh Heriot Watt University, Universite Paris Diderot, Institut fur umweltmedizinische Forschung) and developmental (Vrije Universiteit Brussels, Rijksinstituut voor Volksgezondheid en Milieu) were investigated in detail *in vitro* and *in vivo* by the different partners. Furthermore, different end points such as oxidative stress, inflammation, genotoxicity and fibrogenicity were also examined at sub-lethal concentrations as a means of determining the mechanism of action of the toxicity of the NMs on the cells. From the gathered data the IOM will implement a risk assessment model for the investigated engineered NMs. This will be followed by the execution of a risk management strategy by the JRC – consumer product safety and quality unit.

1.2 Nanotechnology

The extremely rapid expansion of technological, scientific and commercial use of atomic or molecular scale materials, their assembly and their unique properties, has led to an escalating interest in the fields of nanoscience and nanotechnology (Maynard, 2007; Sandhiya, *et al*., 2009). Twenty years ago little was known about the technology outside a very small specialist circle. Fast forward to 2012 and over 1300 consumer products on the market claim to contain elements of nanotechnology with these numbers increasing on a daily basis (Woodrow Wilson, 2012). It is estimated that worldwide sales of nano-scale products will bypass 3 trillion US dollars by 2014 (Sandhiya, *et al*., 2009).

The prefix "nano" derived from the Greek nanos signifying dwarf - was specifically coined for particles containing tens or hundreds of atoms, with dimensions at the scale of less than 100 nm (Buzea, *et al*., 2007). It is this small size which is fundamental to the field of nanotechnology, although other particle parameters also determine their physical, biological and toxicological properties (Jones, *et al*., 2009). Nano has become a popular label for much of modern science. The nanometre is a metric unit of length, and denotes one billionth of a meter (10^{-9} m). To put the minuscule size of these materials into some perspective, a red blood cell is roughly 7,000 nm in diameter while a resting macrophage in tissue is 20,000 nm (Matsumoto, *et al*., 2010).

The foremost reason for producing and exploiting NMs is that they are fundamentally different from the bulk form of the same compound (Edwards-Jones, 2009). In theory this means that previously unexploited beneficial properties of a given material can be explored in its nano size range (Edwards-Jones, 2009). As a result the amount of interest in nanotechnology has risen exponentially across many fields aiming to exploit a wealth of opportunities. These applications include medicine, cosmetics, textiles, electronics and engineering (Tetley, 2007). Paradoxically, however, there is concern that the increased release of engineered NMs could be potentially hazardous for people living and working with these materials due to the radical alterations in their chemical and physical properties (Hoet, *et al*., 2004).

1.3 Sources of NMs

Nanostructured materials did not come into existence with the recent emergence of the field of nanotechnology. Nanominerals are widely distributed throughout the atmosphere, oceans, surface and underground waters, soils and in most living organisms - even within proteins and viruses (Yang, *et al*., 2012). Nanoparticles play an important role in the lives of ocean-dwelling phytoplankton which remove carbon dioxide from the atmosphere. Phytoplankton growth is limited by iron availability. In the ocean the iron source is composed of nanocolloids and mineral nanoparticles supplied by rivers, glaciers and deposition from the atmosphere (Riech, *et al*., 2006). On land, nm-scale hematite (iron oxide) catalyzes the oxidation of manganese, resulting in the rapid formation of minerals that absorb heavy metals in water and soils. The rate of this oxidative reaction is increased when NMs are present (Riech, *et al*., 2006). Furthermore, NMs such as fullerenes occur naturally from combustion processes such as forest fires and volcanoes (Oberdorster, *et al*., 2005). Naturally occurring processes generating nano-sized structures in liquid phase include erosion and chemical disintegration of organic (plant or microorganism debris) or geological (e.g. clays) parent materials (Boyle, *et al*., 2005). Thus nanomaterials are not new. Yet it is only with the recent advances in the manufacture of sophisticated synthesis and characterisation tools that the manipulation of matter near atomic scale has become possible and the study and industrial use of nano-sized materials has become a reality.

Humans have been exposed to airborne NMs throughout their evolution. However this exposure has increased dramatically in the last century due to the introduction of anthropogenic materials (derived from human activity) due to the industrial revolution (Oberdorster, *et al*., 2005). The principal source of these unintentional anthropogenic NMs are internal combustion engines, power plants, jet engines, metal and polymer fumes, heating, cooking (frying, grilling) and electric motors (Nel, *et al*., 2006). The most widely debated and studied source of unintentional NMs are the ultrafine air pollution particulates mainly focused in urban surroundings and generally produced from combustion processes and as industrial by-products such as carbon black (Donaldson, *et al*., 2002). There have been numerous studies on the adverse health effects in susceptible groups associated with exposure to these environmental NMs (Donaldson, *et al*, 2002; Gilmour, *et al*., 2004). These individuals have suffered from complications such as chronic obstructive pulmonary disease (COPD), asthma and cardiovascular problems in part at least due to exposure to these air particulates.

In addition to direct release into the atmosphere, engineered NMs enter the environment by three main sources. Firstly, some nanomaterials are produced in mass quantities and undoubtedly released into the atmosphere at some point during the manufacturing process (Oberdorster, *et al*., 2005). Secondly, NMs in personal products such as cosmetics are continually washed off (Nel, *et al*., 2006). Finally, the use of NMs in products such as fuel cells and aerosols may leak into the atmosphere (Oberdorster, *et al*., 2005).

Engineered NMs are deliberately and specifically produced and labelled according to their shape (e.g. nanotubes or nanowires). Currently there are two widely used methods of generating nanomaterials. The top-down method is the refinement of a starting bulk material into nano-scale dimensions using mechanical or chemical energy. An opposite approach, termed bottom-up, is to synthesise the NM from atomic or molecular species via chemical reactions (e.g. sol-gel processing, chemical vapour deposition (CVD), plasma or flame spraying synthesis, laser pyrolysis, atomic or molecular condensation) allowing for the precursor particles to grow in size. The formation and growth of the NMs is controlled either by exhaustion of one of the reactants or on the introduction of the chemical that would block the reaction, or physical restriction of the volume available for the growth of the individual nanoparticles by using templates (Gutsch, *et al.*, 2005). Both approaches can incorporate the use of gas, liquid, supercritical fluids, solid states or in vacuum (Gutsch, *et al*., 2005).

Metal NMs are principally produced by gas-phase condensation using a vacuum chamber that consists of a heating element. The process utilises a gas, which is typically inert, at pressures high enough to promote particle formation but low enough to allow the production of spherical materials. The metal is then taken to temperatures far above the melting point, but less than the boiling point, so that an adequate vapour pressure is achieved. Gas is continuously introduced into the chamber and removed by pumps. This gas flow removes the evaporated metal away from the hot element. As the gas cools metal vapour, nano-sized particles form. These particles are liquid since they are still too hot to be solid. The liquid particles collide in a controlled environment so that they grow to specification. As the liquid particles are further cooled under control, they become solid and no longer grow (Gutsch, *et al*., 2005). Generally human exposure to these NMs can be described as intentional as they are deliberately produced for a specific purpose so it is crucial to establish any potential hazardous side effects these particulates may possess.

1.4 Everyday exploitation of NMs

Currently, there is intensive developmental work across many industries that utilise nanoscale materials and their assembly. The levels of interest in nanotechnology has risen to such an extent that commercialisation of NMs are often government supported in a large number of countries including the USA, UK, Japan, Korea, Taiwan, Singapore, Australia, China and Malaysia (Lines, 2008).

One of the most prominent areas of research and interest in NM exploitation is the field of nanomedicine as a means of accurate, early diagnosis and effective treatment of disease with fewer side effects. The use of nanomaterials has been extremely successful as a means of non invasive early diagnostic imaging. Nanotechnology enabled molecular imaging techniques including optical, nuclear, ultrasound, computed tomography (CT) and magnetic resonance imaging (MRI) have become extremely successful (Caruthers, *et al*., 2007).

Early diagnosis is ineffectual without effective therapy; therefore large investments have been made to apply nanotechnology to the treatment of disease. One example of current NM use is the dermatological application of liposomal drugs (i.e. hydrocortisone) (Banerjee, 2001). Advances in the field of nanomedicine have allowed for the packaging of liposomal chemotherapeutic agents. The surface attachment of polyethylene glycol is used to increase the circulating half life of the liposome. The technique is widely employed against leukaemia and neutropenia (i.e. Abraxane a nano-sized version of Paclitaxel is more effective than the previously administered formulation) (Wagner, *et al*., 2006).

One of the most important up-to-date manipulations of nanotherapeutics is the development of particles that can deliver specific therapy (chemical, genetic or radioactive) while remaining undetected by the immune system as well as having negligible side effects on healthy tissue (Caruthers, *et al*., 2007). In addition, these strategies allow materials to be tracked non-invasively to provide predicted efficacy and greatly improve the outcome of the treatment. One idea that has much popularity is the use of light absorbing nanomaterials (i.e. non toxic gold) for cancer treatment. The concept is based on the exposure of a region of tissue to a pulse laser with a wavelength for which the diseased cells have a greater absorption rate than the healthy tissue. At the appropriate wavelength, exposure of the NMs to the laser can trigger a photothermal effect in the particle whereby electronic oscillations at

the surface are converted to heat, which raises the particulate temperature killing the cancer cells (Avedisian, *et al*., 2009).

Nanomaterials - such as carbon nanotubes (CNTs) - are widely used in the shielding and absorbance of electromagnetic radiation, thermal conductivity and hydrogen storage. Furthermore, CNTs have excellent thermal, electrical and mechanical properties so they are often found as semiconductor tags for numerous bio-assays (Lines, 2008). NMs are also incorporated in the textile industry. For years nylon and polypropylene products have been integrated within nanomaterials due to their long term anti-microbial characteristics - even after extensive thermal cycling (Benn, *et al*., 2008). Nano-scale zinc and copper oxide can be readily incorporated into the synthetic fibres prior to the spinning process with virtually no effect on the colour, clarity, gloss or the physical properties of the material (Lines, 2008). Applications include clothing, healthcare facilities and institutions, water filters and home furnishings. This anti-microbial activity can also be imparted to food processing and food services as well as general paints and coatings. Other NMs are used in a wide range of electronics such as storage media, flat panel displays, vacuum microelectronics, field emission cathodes and photonic band gap materials and devices (Mazzola, 2003). The use of nano-sized materials as a source of fuel has gathered in popularity and importance especially with the continuous escalation in prices of traditional fuels. There has been much interest in the use of metal oxide NMs as low temperature electrolytes in solid oxide fuel cells (Wildgoose, *et al*., 2005).

Modern cosmetics often contain nano-sized components, such as nano emulsions, nanosomes, nanocapsules, niosomes or liposomes which are microscopic vesicles consisting of traditional cosmetic materials (Nohynek, *et al*., 2008). One of the largest applications of insoluble NM is their use in sunscreen products. The global production of nanomaterials for sunscreen products was estimated to be over 1,000 tonnes during 2003/2004 and is on a yearly increase (Nohynek, *et al*., 2008; Teow, *et al*., 2011). Titanium dioxide (TiO_2) and zinc oxide (ZnO) are principally utilised in these products (Nohynek, *et al*., 2008).

As demonstrated, NMs are increasingly used in a wide variety of industries, with this trend set to further increase in the next few decades (Mamalis, 2007). However, successful exploitation of nanomaterials will require risk evaluation which would allow an improved

understanding of the implication of exposure to NMs because any human or environmental hazard would severely slow down this rapidly expanding field (Maynard, 2007).

1.5 Risk assessment of NM exposure to human health

NMs can be produced from most chemicals, however many of the materials currently in industrial use are manufactured transition metals, carbon, silicon and metal oxides (Dreher, *et al*., 2004). As the field of nanotechnology develops, the potential for public and occupational exposure will also increase. Therefore, there is an urgent necessity to consider the possibility of any detrimental health corollaries with this sudden increase and exposure to nanomaterials. This is achieved in the form of a critical risk assessment (Papp, *et al*., 2008). Simply put, the risk is assessed based upon the level of exposure to the manufactured NM, toxicology of the material in question, route of exposure and its bio-persistence. Hence, it is necessary to identify the hazards associated with NM exposure both *in vitro* and *in vivo*, consequently assembling a knowledge base on the perils associated with NM exploitation on human health (Hoet, *et al*., 2004).

In order for any nanomaterial to be considered a potential hazard to human health it must first be biologically available. In other words exposure must occur and the NM must be available in sufficient quantities to exert toxic effects on the host. Consequently, the extent of exposure and the potential hazard will vary within different occupational groups (healthy vs. immune compromised or genetic disorder), surroundings (good ventilation, filtration, respirators and appropriate protection masks and gloves vs. poor ventilation and working conditions) and consumers (amount of day to day NM exposure) (Maynard, *et al*., 2007). Secondly, the material in question whether in powder, aerosol, liquid or aggregate form should have the potential to initiate a response not associated with the same chemical in bulk form (Maynard, *et al*., 2007). At this point it is important to note that NMs are often bound within materials or coated with various proteins and are rarely available in a ‘free form’. However as part of a risk assessment it is important to strategise for NM release into the atmosphere and the environment (Papp, *et al*., 2008). Release of silver NMs from anti-microbial socks into the environment following consequential washes is an example of this (Benn, *et al*., 2008).

With conventional risk assessment paradigms the potential hazard can be evaluated via toxicity and health outcomes (dose and route). However with engineered NMs a third

component needs to be considered - namely the characterisation of the material (Hoet, *et al*., 2004; Maynard, 2007). It has been suggested that for any comprehensive toxicity testing of a given NM, physiochemical parameters such as surface area, surface chemistry, size distribution and material charge have to be thoroughly characterised (Oberdorster, *et al*., 2005). It is important to note that understanding the hazard and establishing the dose and route of exposure will only allow for quantification of engineered NM risk. Controlling exposure and reducing the potential risk is fully dependent on safe workplaces and products.

1.6 Physicochemical characteristics of NMs

All NMs have the commonality of their very small size, however there are numbers of physicochemical variables that have a significant influence on the nanomaterial properties and toxicity. These include variations in their dimensionality, morphology, chemical composition, surface structure, charge, surface coating, solubility and agglomeration (Nel, *et al*., 2006; Tsuji, *et al*., 2006). For any toxicity study it is essential to try to understand the impact of these characteristics.

1.6.1 Importance of NM size

Nanomaterials have a very large surface area and high particle number per unit mass compared to the bulk form of the same compound. For example, one carbon particle with a diameter of 60 µm has a mass of 0.3 µg and a surface area of 0.01 mm^2. The same mass of carbon in nanoparticulate form, where each particle has a diameter of 60 nm, has a surface area of 11.3 mm^2 and consists of 1×10^9 nanoparticles. The ratio of surface area to volume or mass for a particle with a diameter of 60 nm is 1000 times greater than a particle with a diameter of 60 µm (Buzea, *et al*., 2007). As the material in the nano-scale form presents a much larger surface area for chemical reactions, reactivity is enhanced roughly 1000 fold (Roduner, 2006). As chemical reactivity generally increases with decreasing material size, surface coatings and other modifications can have complicating effects, even reducing reactivity with decreasing size in some instances (Roduner, 2006). The atoms situated on the surface of a NM have less neighbours than bulk atoms, resulting in lower binding energy per atom with decreasing size (Roduner, 2006). A consequence of reduced binding energy per atom is a melting point reduction with particle radius (Roduner, 2006). One such example is the melting temperature of 3 nm gold NMs, which is more than 300 degrees lower than the

melting temperature of bulk gold (Roduner, 2006). This size related unique physicochemical characteristic might be extremely beneficial as a source of new applications and products, however it has been shown that this property also accounts for size dependent toxicity i.e. as size decreases toxicity increases (Johnston, *et al*., 2010). In other words engineered NMs may partly behave like new chemical substances.

1.6.2 Importance of NM shape and structure

The first important distinction of NMs is that they are either in the form of thin films or fixed nano-scale objects or unconstrained particles (Jones, *et al*., 2009). The morphology of a nanoparticle plays a crucial role in their classification, property and toxicity. In general NMs can be classified based on their number of dimensions. Nanoparticles with one dimension are typically engineered as a monolayer in the form of thin films or surface coatings (computer chips or hard coatings on eye wear) (Huang, *et al*., 2009). Two dimensional NMs include nano-scale structures which are mostly films with nanostructures firmly attached to a substrate or nano filters used for particle separation and filtration. Carbon nanotubes are an example of a material which can be nano-scale in two dimensions (Buzea, *et al*., 2007). 3D materials are nano-scaled in all three dimensions and include colloids and free nanoparticles with various morphologies.

High aspect ratio nanomaterials (HARN – any nanomaterial that has one dimension out with the nano scale) include: nanowires, nanohelices, nanopillars, nanotubes and nanobelts. Low aspect ratio NMs include spherical, helical, oval, cubic, pillar and prism shaped particles (Aitkin, *et al*., 2006; Buzea, *et al*., 2007) (Figure 1.1). The effects of the shape of NMs with regards to their toxicity is not fully understood, however the shape might affect the deposition and absorption in the body (Oberdorster, *et al*., 2005).

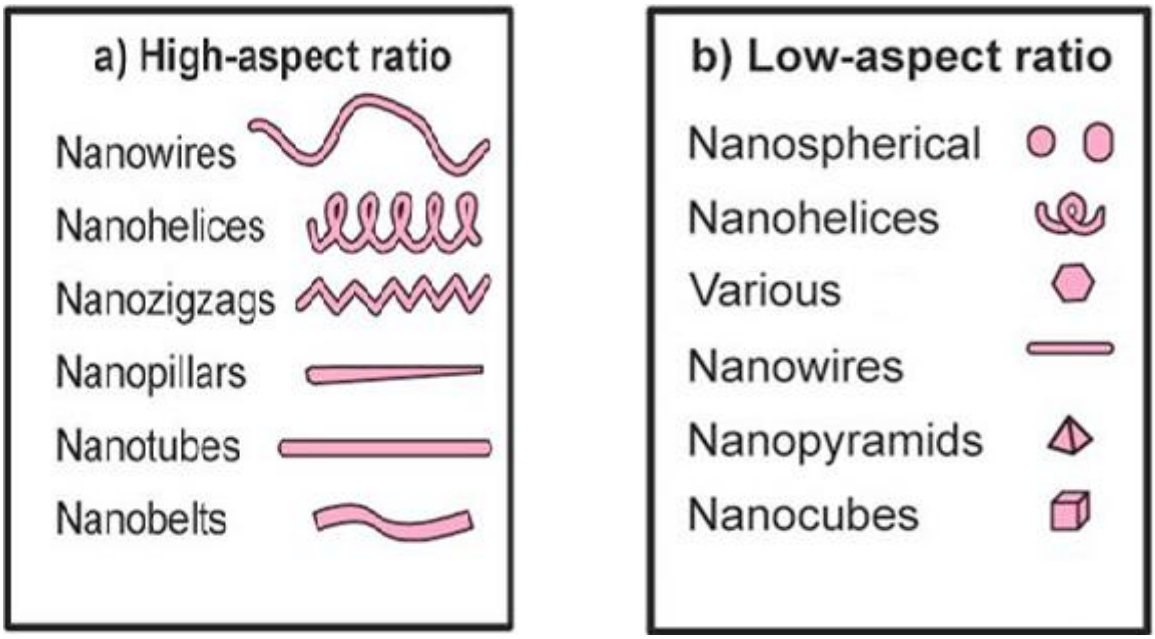

Figure 1.1. Different forms of some **a)** high and **b)** low-aspect ratio NMs. (Image adapted from Buzea, *et al*., 2007).

1.6.3 Importance of nanomaterial composition

Any NM can be composed of a single constituent material or be a composite of two or more materials. For the purposes of characterisation, nanomaterials are often categorised as carbon based, organic and inorganic polymers as well as metal and metal oxide compounds or composites (Grill, *et al*., 2009). The engineered NM composites currently include coated, encapsulated and mixed structures (Grill, *et al*., 2009). The biological effects and toxicity of these materials will vary drastically depending on the surface chemistry, impurities and the particular reactive groups on the surface of the NM (Oberdorster, *et al*., 2005).

1.6.4 Importance of NM uniformity and agglomeration

NMs can exist as dispersed aerosols, suspensions/colloids or in an agglomerate state based on their chemistry and electromagnetic properties (Handy, *et al*., 2008). In colloid chemistry, particles may remain dispersed or alternatively aggregate which may remove the material from the liquid phase. In practise, even apparently stable dispersions will gradually agglomerate out of the aqueous phase over time (Buzea, *et al*., 2007). The rate of agglomeration of NMs in an aqueous medium will partly depend on particle – particle collision frequency and the attractive - repulsive properties of the materials involved (i.e. surface charges on two positively charged materials) (Handy, *et al*., 2008). After the initial

collision, particles may remain as single particles, or form particle – particle, particle – cluster or cluster – cluster agglomerates. The agglomeration phenomena, has many implications, such as the attachment of materials to the walls of experimental equipment (glassware, scientific instruments) (Handy, *et al*., 2008). There are also toxicological implications regarding the fate and behaviour of the materials, and the types of ecosystems and organisms exposed. In an agglomerated state, NMs may behave as one larger particle, hence losing the chemical and toxicological characteristics associated with nanomaterials. Any attempt to prevent aggregation or agglomeration of NMs will alter body distribution and drastically affect the toxicity in the examined biological systems (Oberdorster, *et al*., 2005). Therefore the existence of free mono-dispersed NMs is extremely important for any *in vitro* toxicity test. This being said, it is important to consider the tendency of nanomaterials to agglomerate, as any natural human exposure may and in probability does not involve individual particulates but instead much larger agglomerates would be incorporated (Hirano, 2009). To this end, any prior knowledge into the physiological properties of the material and mechanism of human encounter will be extremely advantageous for the inauguration of all experiments and analysis of the results (Hirano, 2009; Jones, *et al*., 2009).

1.6.5 Importance of NM charge on behaviour and toxicity

The surface charge of a nanomaterial is principally imposed by its composition and surface attachments. This charge can be positive, negative or neutral. The charge of the NM plays a crucial role in its agglomeration state (Handy, *et al*., 2008; Nafee, *et al*., 2009). The weakening of the electrostatic repulsive forces (zeta potential falling below 30 mV) is usually associated with originally well dispersed particles coming together (Lakshminarasimhan, *et al*., 2008). However it is now understood that the charge also influences the toxicity of the NM. Recent studies have demonstrated that cationic nanomaterials induce certain cell damage through their interaction with anionic components of the glycoproteins on the surface of epithelial cells (Fischer, *et al*., 2003). Furthermore surface charge of a nanomaterial may influence its uptake and its eventual location within a cell (Yue, *et al*., 2011).

1.7 Nanotoxicology – a brief historical review

The rapid expansion of nanotechnology is a very profitable industry and promises to have great benefits for mankind. However there is growing concern about the effects of engineered

NMs on the environment and potential toxicity to workers and consumers of these nano products. To ease these concerns and fears, regulatory, industrial and funding agencies have been financing projects to evaluate the toxicological profiles of mass produced engineered NMs (Oberdorster, *et al*., 2007).

The roots of nanomaterial toxicity can be traced back to the early 1990s where the current paradigm of nanotoxicology was being formed with greater understanding of the toxicity of metal fumes, dust, silica, asbestos and other synthetic fibres and more recently air pollution particles such as PM_{10} (extremely small sub-divisions of solid or liquid matter suspended in a gas or liquid smaller than 2.5 μm) (Oberdorster, *et al*., 2007). The understanding that materials in the nano-scale have their unique biological properties was the turning point in the field of nanotoxicology. In the early 20^{th} century numerous studies investigated the exposure to NMs without the realisation of the importance of ultrafine particles (Oberdorster, *et al*., 2007). The first study to bring into focus the importance of anthropogenic NMs was in the 1970s where combustion engine emissions were characterised (Whitby, *et al*., 1975). An important milestone in the history of nanotoxicology was the discovery that NMs are taken up by cells and are capable of translocation to other tissues and organs from the sites of exposure (Oberdorster, *et al*., 2007). This was significant as this ability is unique to ultrafine particles; (30 nm intratracheally instilled gold particles were observed to cross the alveolar-capillary barrier and accumulated in platelets (Berry, *et al*., 1977)). This was followed by revolutionary experiments by a German group demonstrating the deposition of inhaled particles in the lower respiratory tracts in humans (Heyder, *et al*., 1986). This and subsequent deposition studies confirmed the realization that NMs have unique toxicological properties (Oberdorster, *et al*., 2007).

The first direct *in vivo* comparison of nano and micro particles was carried out in 1990 with TiO_2 (Ferrin, *et al*., 1990) and Al_2O_3 particles (Oberdorster, *et al*., 1990). These studies showed significantly higher levels of pulmonary inflammation and interstitial translocation associated with nano sized materials. In 1992 an important paper was published concluding the increased toxicity associated with NMs is due to their large surface area and their ability to translocate. In other words, same mass dose exposure of these compounds might not exhibit any toxicity in micro or bulk form (Ferrin, *et al*., 1992). In 1998, a pulmonary toxicity study of fine and ultrafine nanoparticles demonstrated that in addition to size other characteristics such as surface area and chemistry are also extremely important in particle

toxicology (Donaldson, *et al*., 1998). It is now widely accepted that for any comprehensive toxicological study all aspects of NM physicochemical properties must be investigated (Oberdorster, *et al*., 2007).

The first comprehensive step in establishing oxidative stress as a possible mechanism for small material pathogenesis was a 1980s asbestos study (asbestos has size and shape similarities to carbon nanotubes). The team demonstrated that asbestos was responsible for cell damage and subsequent pathogenesis. The same group later showed that antioxidants such as glutathione reduce asbestos pathogenicity (Mossman, *et al*., 1983; 1986). Other mainstream studies at this time were linking particle induced oxidative stress and inflammation (Janssen, *et al*., 1993). Furthermore, trials into the adverse effects of harmful particulates, in particular PM_{10} and better understanding of stress responsive pro-inflammatory transcription factors resulted in the generalisation of the oxidative stress hypothesis to nanomaterials (Oberdorster, *et al*., 2007). The next important milestone in the history of nanotoxicology was the realisation that some NMs are capable of acting as haptens and induce an antibody mediated immune response (e.g. recognised and processed fullerenes as protein conjugates) (Chen, *et al*., 1998).

One of the important concepts of nanotoxicology in the early 21st century was the idea that the physicochemical properties of different NMs influence the adsorption of certain proteins or lipids from different body compartments, hence governing the subsequent destination of the particle in the body (Muller, *et al*., 2004).

Although there have been huge leaps forward in terms of the current understanding into the toxicity of NMs, there are major knowledge gaps yet to be filled. One important factor that has to be considered for any future experimentation is that any toxicological information on nanomaterials must be considered at relevant human exposure levels. Any material irrespective of size would have detrimental effects at high enough doses (Oberdorster, *et al*., 2007). For any *in vivo* or *in vitro* toxicity study to have any real relevance, doses must be low enough to anticipate for possible human exposure.

1.8 Routes of NM exposure

Biological systems usually integrate multiple pathways of toxicity into a limited number of pathological outcomes including: inflammation, apoptosis, necrosis, fibrosis, metaplasia and carcinogenesis (Nel, *et al*., 2006). With the ever increasing sources of NMs, we are constantly bombarded with materials of all shapes and sizes. It is widely accepted that the skin, lungs and the gastrointestinal tract (GT) are in constant contact with the external environment, so it is not surprising to find all three systems being primary exposure sites for NMs (Yokel, *et al*., 2011) (Figure 1.2). However, as has been previously discussed, most materials are able to translocate to secondary target organs located at a distance from the original point of entry (Figure 1.2).

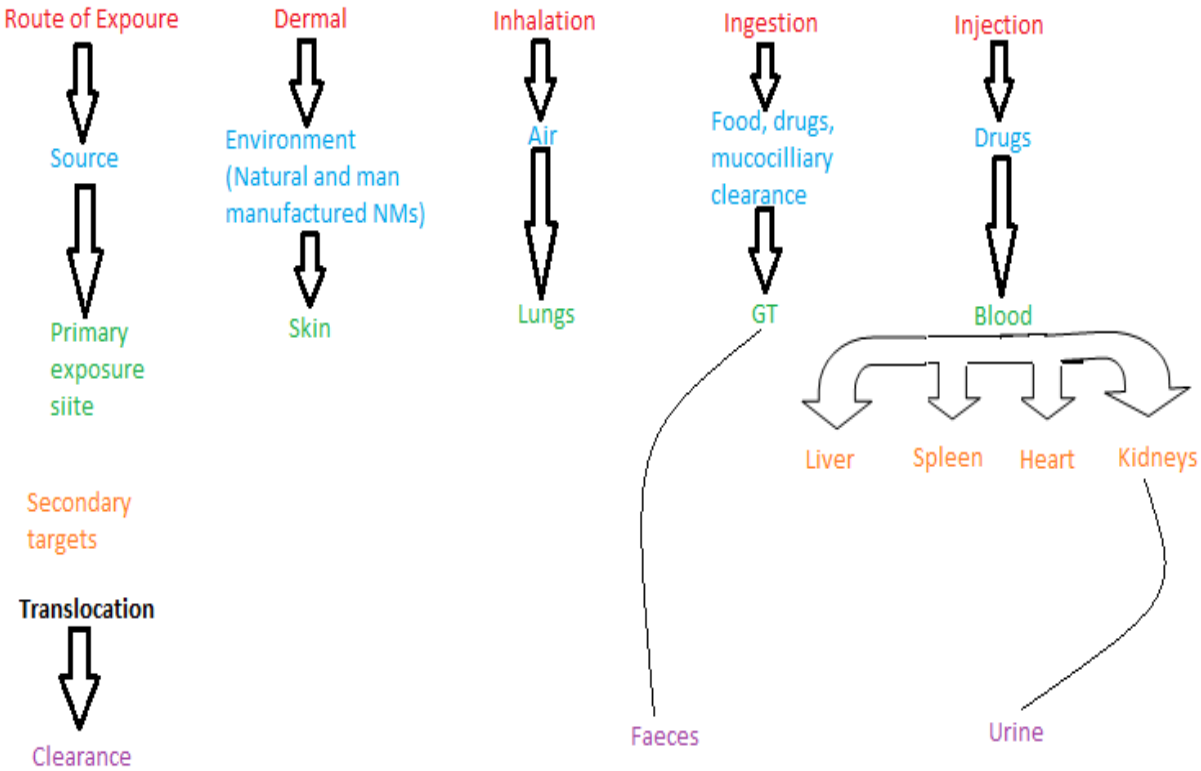

Figure 1.2. Routes of exposure and potential destiny of the NM dependant on its physicochemical properties and protein exposure. (Adapted from Yokel, *et al*., 2011).

1.8.1 NMs and the skin

Although in general nanomaterial toxicity is associated with inhalation, there is an ever increasing concern of subsequent translocation to secondary target organs following dermal exposure (Hoet, *et al*., 2004). It has been suggested that certain NMs are able to penetrate the skin and are distributed throughout the body via the circulatory system (Oberdorster, *et al*., 2005). Nanomaterial based products are commonly used in a wide range of cosmetic products including conditioners, sunscreens and lotions. These emulsions combine traditionally utilised materials emulsified in water and oils in the nano-scale. This alteration in size renders the products transparent and much more pleasant to the touch (Nohynek, *et al*., 2008). The use of titanium dioxide and zinc oxide NMs has drastically improved the transparency of sunscreen products, hence there has been a noticeable improvement in the protection of skin against UV damage (WHO – accessed July 2012). Furthermore the development of liposome vesicles has been extremely beneficial to the cosmetic industry as they have been proven to improve skin stability and tolerance to ingredients such as vitamins and antioxidants (Nohynek, *et al*., 2008). In addition to cosmetic products, airborne NMs are also capable of coming in contact with the skin.

The first point to be addressed regarding NM toxicity and the skin, is the organs structural integrity. The skin is composed of several layers including the stratum corneum, stratum spinosum and stratum basale which form a tight protective layer for the underlying dermis and the subcutaneous layer making the organ fairly impermeable. A study using a series of substances has demonstrated that human skin is relatively impermeable compared to the skin of the rat (magnitude of 11 fold) (Ravenzwaay, *et al*., 2004). Subsequent studies utilising TiO_2 have shown that both micro and nano-scale materials remain on the skin surface and do not penetrate through the layers (Crosera, *et al*., 2009).

It is important to state that compromised skin (dermal abrasion, cuts, eczema or severe sunburn) may have a greater susceptibility to penetration of NMs, as illustrated by an American group showing deeper penetration of quantum dots in damaged skin (Zhang, *et al*, 2008). However, it has been argued that skin inflammation produces a significant thickening of the epidermis layer hence enhancing the barrier properties of the skin (Nohynek, *et al*., 2008). Overall, the current weight of evidence suggest that nanomaterials are unable to penetrate the human skin, hence there is little chance of toxicity from exposure to cosmetic

products and very little chance of translocation of these NMs to secondary organs (Crosera, *et al*., 2009).

1.8.2 Inhalation of nanomaterials

Inhaled NMs deposit in different sites of the respiratory tract by diffusion. The method by which they are transported through the lung is predominately influenced by endocytosis, phagocytosis or transcytosis across epithelial and endothelial cells (Papp, *et al*., 2008). This in turn might result in the NMs being released into the blood and being transported to a varied range of secondary target organs including the liver, kidneys, lymph nodes, spleen, heart, and even the brain (most likely via the olfactory nervous system) (Mailander, *et al*., 2009; Sadauskas, *et al*., 2009b). As previously mentioned the surface properties of each individual nanomaterial are extremely important in their interaction with the pulmonary and immune cells and possibly their final destination (Mailander, *et al*., 2009).

Any pathogenic effects of inhaled NMs are dependent on a substantial lung burden which is determined by rates of deposition and clearance (clearance in turn is influenced by material size and surface properties) (Muhlfeld, *et al*., 2008). It is understood that nanomaterials deposit throughout the lung, penetrating as deep as the alveolar regions (Hoet, *et al*., 2004). The upper pathways of the lung are predominately cleared by mucociliary transport, while alveolar clearance is mediated by pulmonary macrophages (Muhlfeld, *et al*., 2008). The phagocyte influenced clearance of NMs is associated with release of pro-inflammatory cytokines, reactive oxygen species and a host of other mediators and chemokines. This mode of toxic impact or pathogenicity is usually associated with cases in which the deposition rate of NMs exceeds the clearance rate (Hoet, *et al*., 2004). Furthermore numerous studies have demonstrated that the deposition of solid NMs - such as single walled carbon nanotubes in experimentally large doses - resulted in granuloma formation in the lung (Lam, *et al*., 2003; Poland, *et al*., 2008). Currently, it is assumed that in the majority of instances, inhaled NMs are cleared from the lung and do not cause toxic effects on the organ, as long as the clearance mechanism is unaffected by the nanomaterial characteristics or the exposure is not in large enough doses to hamper the clearance mechanism (this is associated with toxicity and pathogenesis) (Hoet, *et al*., 2004).

1.8.3 Nanomaterials and the intestinal tract

Ingestion of NMs can occur directly from food, water or orally administered medicines. It is believed that the vast majority of ingested nanomaterials are rapidly passed through the gastrointestinal tract and lost via the faeces (Papp, *et al*., 2008). However, a minor fraction of NMs are translocated from the lumen of the intestinal tract, perhaps via Peyer's patches containing M cells and normal intestinal enterocytes (Yamanaka, *et al*., 2008). Once again surface properties of nanomaterials play an important role in their translocation from the intestinal tract. It has been suggested that charged materials exhibit poor bio-availability due to electrostatic repulsion and mucus entrapment (Hoet, *et al*., 2004). Once in sub-mucosal tissue, NMs are capable of entering both the lymphatics and the blood capillaries. In a 1990 study mice were fed polystyrene spheres ranging from 50 nm to 3 microns for a period of ten days. It was found that as much as 26% of the 100 nm materials were detectable in the blood (Jani, *et al*., 1990).

There is conflicting data on the mechanisms of the toxicity of NMs in the gastrointestinal tract. However, it has been suggested that the disruption of the epithelial barrier function by apoptosis of the enterocytes is a possible mechanism for mucosal inflammation (Hoet, *et al*., 2004).

1.8.4 NMs in the blood

In addition to the translocated NMs from pulmonary and gastrointestinal exposure (Sections 1.8.2 and 1.8.3), direct injection of materials loaded with drugs and diagnostics are the principle routes of NM entry in the circulatory system. The presence of nanomaterials in the blood allows distribution to a wide range of target organs including the liver, kidneys, heart and spleen. When NMs reach systemic circulation they can interact with plasma proteins, platelets, coagulation factors, erythrocytes and white blood cells. The binding to plasma proteins in particular is thought to be extremely important in the distribution and excretion of NMs (Hagens, *et al*., 2007). It seems that the addition of serum might result in reduced cytotoxicity *in vitro* in some instances as demonstrated by Lovric and colleagues. They showed quantum dots pre-treated with bovine serum albumin result in a smaller number of cell dying compared with cells treated with unmodified materials (Lovric, *et al*., 2005).

Furthermore, it seems sensible to incorporate serum into *in vitro* experiments in order to extrapolate results to *in vivo* situations (Hagens, *et al*., 2007).

It has been shown that certain materials (i.e. titanium dioxide) can be found inside human red blood cells (Rothen-Rutishauser, *et al*., 2006). This is a very interesting finding as erythrocytes do not have phagocytic receptors. This seems to suggest that in this case cellular uptake does not involve phagocytosis or endocytosis (Rothen-Rutishauser, *et al*., 2006). Red blood cells must incorporate a non specific mechanism for NM uptake which might be diffusion or the utilisation of trans-membrane channels. It is understood that intracellular TiO_2 NMs are not membrane bound and have direct access to cellular DNA and organelles which undoubtedly increases their toxic potential (Rothen-Rutishauser, *et al*., 2006). Finally, it might be possible that some materials can cross the trans-placental barrier. Although there is very limited information in this area, data exists from a very interesting study in which pregnant mice were intraperitoneally injected with soluble fullerenes (C_{60}). At high concentrations all embryos died, while at lower concentrations abnormalities were observed around the head region of the embryos (Tsuchiya, *et al*., 1996). This study indicates that the NMs were transferred to the embryo via the trans-placental passage or directly from the peritoneal cavity into the uterus (Tsuchiya, *et al*., 1996).

1.8.5 Eventual fate of the nanomaterials

Under normal circumstances materials absorbed by the gastrointestinal tract will be directly transported to the liver via the portal vein. The liver is fully capable of active removal of hazardous substances from the blood. However there is contradictory evidence about the percentage and the properties of overall number of NMs that are cleared from the blood in this manner.

It seems unlikely that inert NMs - such as fullerenes and carbon nanotubes can be metabolized by enzymes within the body (Hagens, *et al*., 2007). Therefore, it seems sensible to hypothesise that NMs with functionalised groups are more susceptible to enzyme activity. There are numerous routes in which an absorbed NM can be excreted. The first of these elimination pathways is renal clearance. A recent study showed that intact fullerene and single walled carbon nanotubes were detectable in the urine from rats three and half hours following intravenous injection of the materials (Singh, *et al*., 2006). However this is not

always the case as NM size as well as its chemical properties all influence clearance. This is demonstrated in a study in which quantum dots were still present in the lymph nodes and bone marrow of mice 133 days after the initial injection (Hardman, 2006).

Bile is another excretion route suggested by some as the clearance mechanism of certain NMs. In a 2001 study polystyrene NMs (50 and 500 nm) were intravenously injected into rats. It was discovered that a fraction of 50 nm materials were internalised by the hepatocytes. After a 24 hour period 5% of the total dose was excreted in the bile (Nagayama, *et al*., 2001). The larger NMs however were predominately phagocytosed by the Kupffer and endothelial cells (Nagayama, *et al*., 2001). This seems to suggest that bile secretion of nano particulates is size dependent. Another potential excretion routes for NMs could be breast milk. However corroborating data is currently unavailable to confirm these routes (Hagens, *et al*., 2007). It is also believed certain nanomaterials are degraded in the lysosomes of certain immune cells (Stern, *et al*., 2012).

1.9 Engineered NMs used to investigate toxicity to the liver and the kidneys

Many engineered NMs are manufactured from a diverse group of substances, hence for a risk assessment study a varied range needs to be evaluated for a comprehensive toxicity profile. It is very possible that each nanomaterial will differ in the levels of toxicity and the mechanism by which they exert these adverse effects. The ENPRA particle panel was appraised fully in order to establish the toxicity of each material on liver and kidneys.

1.9.1 Silver

Nanosilver particles generally contain 20-15000 silver atoms. At the nano-scale, silver exhibits remarkably unusual physical, chemical and biological properties. Due to its strong antibacterial activity, silver coatings are used on various textiles as well as coatings on certain medical implants. Furthermore, the NM is used for treatment of wounds and burns or as a contraceptive as well as being marketed as a water disinfectant and room spray (Chen, *et al*., 2008b). With ever increasing intimate exposure to silver NMs it is very important to establish the concentration in which the material becomes toxic to human cells. From a historical point of view it is assumed that apart from some mild cases of argyria, silver is relatively non toxic to mammalian cells (Drake, *et al*., 2005). However as discussed previously, once a substance

reaches the nano-scale it can have completely different properties. It is known that materials smaller than an aerodynamic diameter of 2.5 µm can penetrate down to the alveoli of the lungs. Most commercialised silver nanomaterials are smaller than 100 nm, therefore exposure of NMs in the lung could induce impacts such as oxidative stress in lung epithelial cells. With a highly pro-oxidative environment such as the intra-alveolar spaces of the lung and their extremely large surface area, it might be sensible to assume that silver NMs could be sufficient facilitators of free radical generation (Chen, *et al*., 2008). In addition silver NMs can easily be translocated to secondary organs via endocytosis and transcytosis. A 2001 study shows that silver particles of 15 nm rapidly decrease in numbers in the lung following inhalation and intratracheal instillation. These particulates were later located in the blood and other organs including the liver and the kidneys (Takenaka, *et al*., 2001). The authors note that up to 20% of the silver was observed in the liver (Takenaka, *et al*., 2001).

Silver NMs are regularly utilised in water disinfection and food preservation, so there is a very real possibility for the materials reaching the gastrointestinal tract. Intestinal particles are readily taken up by Peyer's patches or the enterocytes. Once in sub-mucosal tissue, silver NMs are able to enter the lymphatics and capillaries. It seems that despite this, any toxicity associated with ingestion of silver NMs seems to be localised to the liver and is not observed systemically (Carlson, *et al*., 2008; Hussain, *et al*., 2005; Takenaka, *et al*., 2001).

As for the mechanism of toxicity of silver NMs, it has been suggested that exposure significantly decreases cellular mitochondrial function, followed by apoptosis like morphological changes in exposed BRL 3A cells (Hussain, *et al*., 2005). The same team have indicated that depletion of GSH levels and increased oxidative stress was associated with the mitochondrial perturbation (Hussain, *et al*., 2005).

In this study one silver NM (<20 nm, NM 300) was investigated. The materials were capped with PVP (polyvinylpyrolidone) to improve dispersion in aqueous media (Table 3.1).

1.9.2 Multi walled carbon nanotubes

Carbon nanotubes (CNTs) consist of a network of carbon atoms arrayed in graphene sheets, rolled up into tubes with a diameter in the nano-scale. There are two classes of CNTs: single

walled (SWCNT) – composed from only one CNT layer and the multi walled (MWCNT) variety generated from two or more layers of rolled-up graphene sheets. These NMs have unique physical and chemical properties making them an ideal candidate in a multitude of industrial applications including high resistance composites and electronic devices (De Nicola, *et al*., 2009). CNTs are also widely used in diagnostic and therapeutic tools for the detection and treatment of diseases including certain cancers (Ferrari, 2005). In addition, burning of natural gases, such as propane and methane is a source of CNT release into the atmosphere (Murr, *et al*., 2004). CNTs have the tendency to aggregate and form rope - like structures which has to be considered in any toxicological study (Donaldson, *et al*., 2006; Poland, *et al*., 2008).

The toxicity of CNTs is widely documented. Adverse effects observed include pulmonary inflammogenicity (Ellinger-Ziegelbaur, *et al*., 2009), with the effects of SWCNTs being higher than that of MWCNTs. In contrast *in vitro* exposure of RAW264.7 macrophage cell line to SWCNTs was associated with the active production of transforming growth factor β and reduced levels of the pro-inflammatory cytokines TNF-α and IL1-β (Shvedova, *et al*., 2005). In the same study no ROS activity was identified. In a contrasting study however it was shown that SWCNTs enriched with iron generated considerable amounts of hydroxyl radicals (Kegan, *et al*., 2006). Therefore it seems that iron contamination of CNTs might influence the toxicity of the materials.

The toxicity of asbestos to mesothelial cells is well recognized. This has led many to draw comparisons between asbestos and the fibrous, rigidly shaped and non-soluble CNTs (Donaldson, *et al*., 2011; Murphy, *et al*., 2012). To this end many studies have been carried out and it has been shown that well dispersed CNTs are less toxic than agglomerated CNTs, at least in mesothelioma cells (Wick, *et al*., 2007). Thus the degree of agglomeration seems paramount in evaluating the toxicity of any CNT (Wick, *et al*., 2007). This being said it is important to note that due to the nature of the materials and van der Waals forces there will always be some degree of agglomeration despite the concentration and type of dispersant utilised (Mitchell, *et al*., 2007).

In this study two entangled MWCNTs of different length (NM 400 - D: 5-35 L: 700-3000; NM 402 - D: 6-20 L: 700-4000) was investigated as representatives of engineered CNTs in industry (Table 3.1).

1.9.3 Zinc oxide

Zinc oxide (ZnO) NMs have been shown to have great benefits in society and are currently being applied in a broad range of industries including cosmetics (sunscreens), biosensors and numerous electronic goods as well as being a constituent of metal fumes in welding (Deng, *et al*., 2009). Furthermore, due to their antibacterial properties these materials have huge potential in the development of prophylactic drugs. Many studies have focused on the influence of ZnO NMs on bacterial growth. An example of one such study demonstrates that ZnO severely inhibits the growth of *E.coli* and protects intestinal cells from an enterotoxigenic form of the bacteria (Roselli, *et al*., 2003), while another group have publicized that the particulate has bacteriostatic effects against *Staphylococcus aureus* and *Streptococcus agalactiae* (Huang, *et al*., 2008).

A recent *in vivo* study in which mice were exposed to ZnO NMs (272 nm) via an oral route resulted in significant accumulation of materials within the liver as well as cellular injury. The authors also noted elevated levels of alanine aminotransferase and alkaline phosphates in serum as well as pathological lesions in the liver (Sharma, *et al*., 2012b). In the same study ZnO exposure was associated with induction of oxidative stress and DNA damage within the liver (Sharma, *et al*., 2012b). The same team have also shown *in vitro* oxidative stress and genotoxicity in HepG2 (liver cell line) following exposure to the ZnO NMs (Sharma, *et al*., 2012a). In another set of trials it was shown that ZnO NMs have significant toxic effects on aortic endothelial cells, with 50% of cells dying after a 4 hr incubation period with the 50 nm materials (Gojova, *et al*., 2007). Furthermore, another study on mouse neural stem cells revealed that a 24 hr incubation with 30, 60 and 200 nm ZnO materials results in manifestation of a clear dose dependant toxicity on the cells. The team propose that the ZnO NMs induces apoptosis of the treated cells (Deng, *et al*., 2009).

In this study two different engineered ZnO NMs were utilised. Firstly, NM 110 which is an uncoated 100 nm material. The second ZnO NM (NM 111) (130 nm) was coated with Triethoxycaprylylsilane - a silicone based surfactant and functions as a binding agent and emulsifier (to allow better dispersion) (Table 3.1).

1.9.4 Titanium dioxide

Titanium dioxide (TiO_2) NMs have a wide range of uses including the production of paints, paper, plastics, food additives and colorants, as well as in pharmaceutical and cosmetic industries (Jin, *et al*., 2008). In addition, due to the unique ability of anatase TiO_2 NMs to strongly absorb UV light with very low scattering, it is widely utilised in sunscreen products and self cleaning windows (Jin, *et al*., 2008). There are three natural forms of TiO_2 – with rutile being its most common form. Rutile is the preferred polymorph of TiO_2 because it has the lowest molecular volume of three forms. Anatase, the second mineral form of TiO_2, is most commonly found in nature as small isolated and sharply developed crystals in a tetragonal system. Brookite, the least common naturally occurring form of TiO_2 crystallises in an orthorhombic system (Dubrovinsky, *et al*., 2001).

Currently there are conflicting views on the adverse effects of the TiO_2 nanomaterials. On one side of the argument it is suggested that in sufficient doses TiO_2 can cause inflammation, fibrosis, and pulmonary damage. It has also been shown that after translocation from the primary site of exposure the NM can induce oxidative stress - mediated toxicity in many cell types by producing large amounts of free radicals (Jin, *et al*., 2008; Kang, *et al*., 2008; Wang, *et al*., 2007b). Oxidative stress can damage proteins, lipids and nucleic acids, leading to interference in cell signalling and modulation of transcription factors (i.e. NFκ-B). This in turn can result in cell death due to oxidative DNA damage and increased cellular nitric oxide (Jin, *et al*., 2008).

It has been shown that exposure of rats via an IV route to 50 mg/kg of 100 nm TiO_2 nanomaterials resulted in pathological lesions within the liver. Furthermore there was an increase in reactive oxygen species and a down regulation of intracellular antioxidants within liver cells (Meena, *et al*., 2012). In a similar study injection of 5 nm TiO_2 NM resulted in liver DNA damage, histopathological changes and hepatocyte apoptosis. This was associated with increases in mRNA expressions of TNF-α, IL6, IL4 and IL1-β (Ma, *et al*., 2009). In another study 25 nm TiO_2 NMs resulted in increased DNA strand breaks in HepG2 cells (Petkovic, *et al*., 2011).

However, in a contrasting study there was no cytotoxicity to human derived Caco-2 cells following 24 hr exposure to TiO_2 NMs. The team did discover however that the NMs were

able to cross the epithelial lining of the intestinal model by transcytosis and penetrate into the cells (Koeneman, *et al*., 2009)

TiO_2 nanomaterials in general have very low solubility, hence once in solution there is a tendency for the particulates to agglomerate which has to be considered in cytotoxicity and molecular pathogenesis studies (Kang, *et al*., 2008). It is also interesting to note that in a related study TiO_2 NMs did not cause toxicological injury to mammalian cells under dark conditions (Xia, *et al*. 2006).

In this study five different TiO_2 materials were investigated. First of these NMs was photocat 7 (NM 101) (7 nm anatase). There were also three 10 nm anatase TiO_2 NMs (one neutrally charged, one positively and one negatively charged NM – termed NRCWE 001, NRCWE 002 and NRCWE 003 respectively). The final TiO_2 was NRCWE 004 (anatase 94 nm) (Table 3.1).

Chapter Two

Liver and the kidneys - the nanotoxicological concerns with these organs

2.1 The Liver

The liver is considered by many as the metabolic centre of the body. The organ has a crucial role in metabolic homeostasis, as it is responsible for the storage, synthesis, metabolism and redistribution of carbohydrates, fats and vitamins (Kmiec, 2001). The liver produces large numbers of serum proteins, mainly albumin, an array of enzymes and acute phase proteins. The organ is also the principal detoxification centre of the body, removing xenobiotics and waste products by metabolism or biliary excretion (Kmiec, 2001). As previously mentioned, some NMs are capable of distributing from the site of exposure to a number of secondary organs, one of which is the liver.

2.2 The blood supply to the liver

The two main vessels supplying the liver with blood are the hepatic artery, which delivers oxygenated blood from the heart (constituting around 35% of overall blood supply) and the hepatic portal vein which delivers blood rich in nutrients, vitamins and xenobiotics from the small intestine (65% of the total blood supply) (Figure 2.1). The hepatic vein returns de-oxygenated blood to the heart via the vena cava, while other incoming and outgoing blood vessels are connected by sinusoid vessels (Kmiec, 2001). It is important to understand the blood supply as this is the main route of the NM translocation from the primary exposure site to this organ. This being said the liver sinusoid which is a fenestrated blood vessel (associated with supply of oxygen rich blood from the hepatic artery and nutrient rich blood from the portal vein) has also been implicated as a potential route for nanomaterial access to the liver (Shi, *et al*., 2010a)

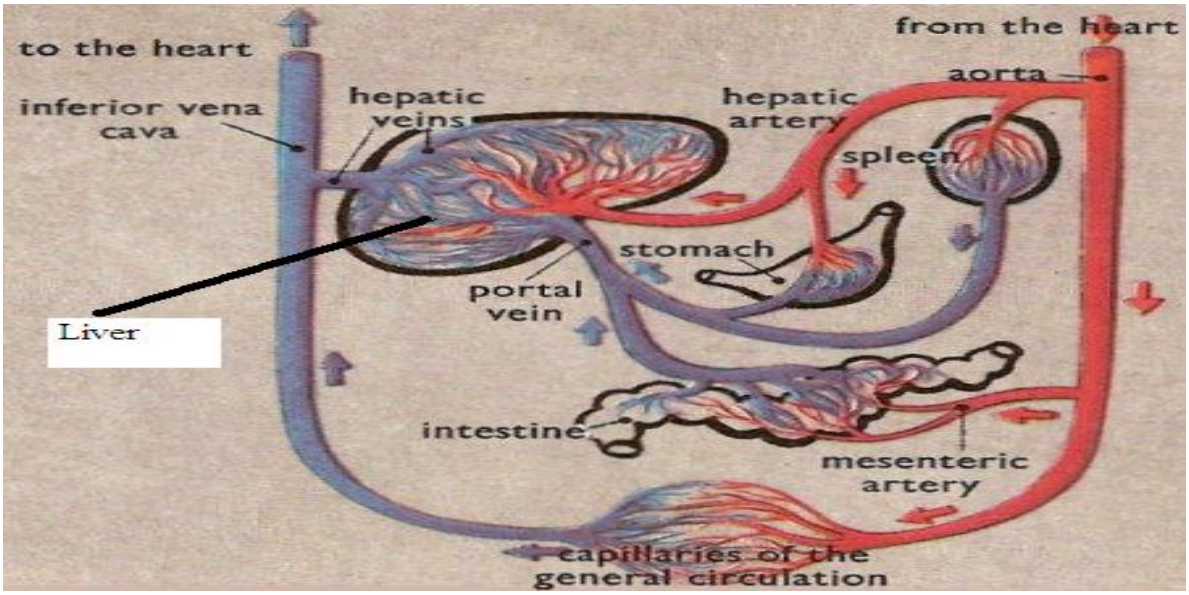

Figure 2.1. Blood supply to the liver**.** (Adapted from Kanel, *et al*., 2005)

2.3 Cells important in normal liver function

The liver is a dark red/brown coloured organ divided into four lobes which can be further organised into smaller structural hexagonal units known as liver lobules composed of parenchymal and nonparenchymal cells (Kmiec, 2001).

2.3.1 Hepatocytes

Parenchymal cells which are principally the hepatocytes constitute the major cellular compartment of the liver (approximately 65% of total liver volume). Hepatocytes are polyhedral multifaceted cells with eight or more faces, and range between 25-30 μm in length (Kmiec, 2001). In addition, many mammalian hepatocytes are bi-nucleated or polyploid (Kmiec, 2001). These cells participate in almost all functions that are attributed to the liver. One of the most important of these roles is the release of glucose in the process of glycogenolysis and producing glucose from non carbohydrate substrates via gluconeogenesis (Kmiec, 2001). Hepatocytes are the only known cells that inactivate ammonia in the urea cycle. These cells are responsible for the manufacture of important serum proteins such as acute phase proteins (i.e. complement components) crucial in mammalian innate immune system (Kmiec, 2001). They also play a substantial role in the metabolism of exogenous and endogenous lipids and catabolism of blood - derived cholesterol enriched protein (Kmiec, 2001). Hepatocytes also produce bile components such as bile acids, cholesterol,

phospholipids and conjugated bilirubin (breakdown product of normal heme catabolism) (Kmiec, 2001). Moreover, hepatocytes synthesize a wide array of hormones and cytokines including IL8 (Dong, *et al*., 1998), IL6 (Saad, *et al*., 1995), TNF-α (Saad, *et al.*, 1995) and MCP-1 (Dong, *et al*., 1998). In a healthy liver parenchymal cells very rarely divide, however, upon severe injury hepatocytes proliferate at extremely rapid rates to restore the organ mass (Kmiec, 2001). It is understood that the metabolic heterogeneity of the hepatocytes is at least partially determined by their location inside the lobule. Periportal hepatocytes localized at the periphery of the lobule are in a micro-environment rich in oxygen, substrates and hormones in the blood from the terminal afferent vessels. In contrast, perivenous hepatocytes (located around the central vein) function with blood partially depleted of oxygen and nutrients but rich in carbon dioxide and other metabolism products (Kmiec, 2001).

The cytochrome P450 (CYP450) superfamily are a number of heme containing enzymes that are involved in a diverse array of substrate specific and catalytic activities (Guengerich, 2001). The CYP450 enzymes and their co-factors are embedded in the membrane of the endoplasmic reticulum and play a crucial role in the metabolism of drugs, chemicals and endogenous substrates in the liver (Westerink, *et al*., 2007). Due to their importance in healthy functioning hepatocytes this superfamily is usually investigated as markers for normal cells *in vitro* (Villeneuve, *et al*., 2004).

It is widely argued that *in vitro* hepatocyte systems (including cell lines and systems without optimal artificial extracellular matrices) might not be ideal for functional and metabolic studies as the cells lose key liver specific functions especially their cytochrome P450 activity (Kim, *et al*., 2011a; Mingoia, *et al*., 2007). Hence the cells used in such experiments are not fully representative of primary hepatocytes *in vivo*. The use of cell lines in an *in vitro* scenario however does have its advantages as the cells are cheaper and easier to maintain and much more suitable candidates for high throughput toxicology screening compared to primary cells.

2.3.2 Sinusoidal endothelial cells

Sinusoidal endothelial cells of the liver (SEC) (3% of total liver volume) differ in many structural and functional aspects from other endothelial cells of the body (Fainboim, *et al*.,

2007). Firstly, they do not have a basement membrane and are often embraced by the cytoplasmic processes of underlying hepatic stellate cells (Fainboim, *et al*., 2007). SECs form an important filtration barrier between macromolecules (might also include NMs) and blood cells and hepatocytes – preventing direct contact and influencing the extent of exchange of various substances. SECs form a continuous lining of the liver sinusoids separating parenchymal cells (hepatocytes) and hepatic stellate cells from direct contact with the blood (Kmiec, 2001). They are flat elongated cells with numerous thin cytoplasmic processes. These cells are separated by sieve plates (fenestrations of 100-200 nm in clusters of 10-50 pores representing 6% of the endothelial surface) (Kmiec, 2001). SECs contain a large number of lysosomes, phagosomes and micro and macro-pinocytotic vesicles (Fainboim, *et al*., 2007). The main functions of the SECs are assumed to be the formation of a general barrier against pathogenic agents, as well as serving as a selective sieve for certain substances from the blood to the stellate cells and hepatocytes (main mechanism for this is understood to be receptor mediated endocytosis) (Kmiec, 2001). The receptor mediated endocytosis of substances such as collagen, hyaluronic acid, fibronectin, entacin and chondroitin sulphate proteoglycan is a major physiological role for SECs (Kmiec, 2001). In addition, SECs exhibit a number of other receptors including specific receptors for fibronectin, LPS (TLR4), scavenger receptors (i.e. for mannose), CD14 (LPS binding protein receptor), IL1, IL6, TNF-α, TGF-β, PGE_2, PGD_2, oestrogen, glucagon, and C5a (Kmiec, 2001).

The liver is continuously exposed to food and microbial antigens from the intestine. In addition, the liver as the primary metabolic organ produces a multitude of new antigens. Therefore the risk of self-immunity seems extremely high in the liver. However, the liver has acquired specialized mechanisms of immune tolerance in order to avoid over-activation of the immune system. SECs are not only involved in the clearance of particulate and soluble antigens, but are also extremely important in the process of the development of specific tolerance to non-pathogenic antigens (Tiegs, *et al*., 2009). SECs have the capacity to function as non-professional antigen presenting cells (APCs), as they constitutively express both MHC class I and II, co-stimulatory molecules including CD80, CD86, CD40 as well as CD4, CD11, CD54 and VCAM-1 - all necessary or at least beneficial for recognition, processing and presentation of antigens to T lymphocytes (Tiegs, *et al*., 2009). Although SECs stimulate the proliferation of naive CD4 cells, these lymphocytes do not proliferate towards a Th1 phenotype - instead they demonstrate characteristics most associated with Th2 cells (cytokine profile IL10, TGF-β) (Tiegs, *et al*., 2009) (Figure 2.2). The IL10 produced by the SECs and

Kupffer cells (which will be discussed in detail in section 2.3.3) decreases the constitutive expression of MHC class II as well as CD80 and CD86 and completely diminishes the activity of mannose receptor responsible for antigen uptake, resulting in specific T cell anergy (Tiegs, *et al*., 2009). In addition, SECs produce the negative co-stimulatory molecule PD-L1, inducing CD8 cell tolerance (Tiegs, *et al*., 2009). It is important to note that although in normal healthy conditions in the liver, tolerance is favoured over immunity; the immune system of the organ is more than capable of clearing pathogenic antigens. It has been shown that activation of TLR3 (polyl:C binding) or TLR4 (LPS binding) induces CD8 mediated hepatitis. In addition as SECs constitutively express MHC class I, they are able to cross present antigens to CD8 cells (Kmiec, 2001).

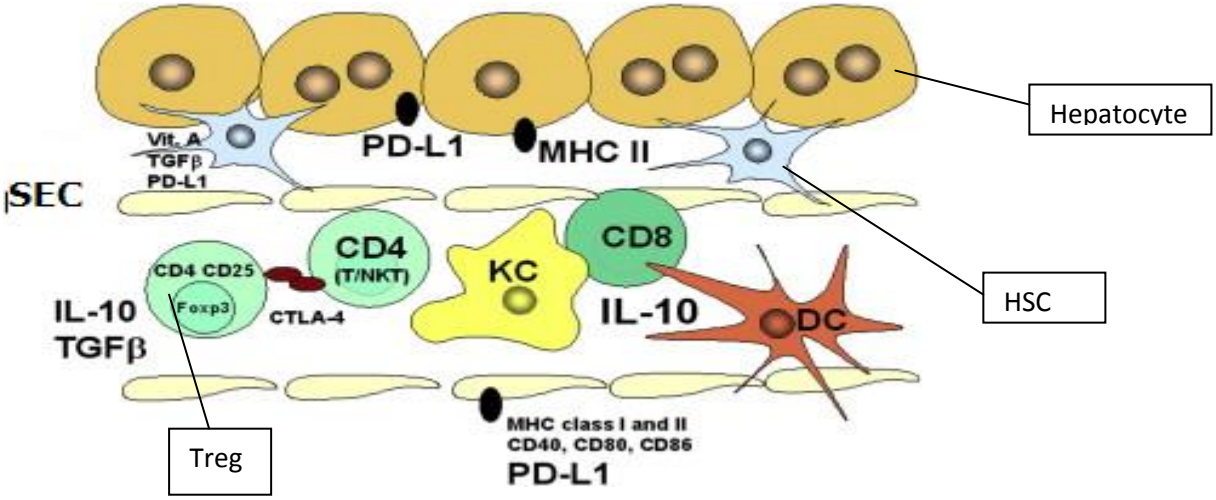

Figure 2.2. Cell types and their interaction with in the liver**.** (Adapted from Tiegs, *et al*., 2009)

2.3.3 Kupffer cells

Kupffer cells (KC) (20% of total cell numbers in a healthy liver) are the resident macrophages of the liver. These cells represent the largest number of macrophages in the mammalian body. KCs are responsible for the clearance of gut-derived bacteria and potential bacterial toxins such as endotoxins and peptidoglycans (Kmiec, 2001). These cells very much resemble other macrophages in the body – characterised by numerous microvillious projections, blebs and lamellipodia (Tiegs, *et al*., 2009). KCs are generally concentrated in the periportal region of the liver which allows monitoring of the blood entering the organ (Kmiec, 2001). These macrophages are positioned to have constant contact with gut-derived antigens. It is hypothesized that due to the constant exposure to low levels of gut bacterial products, KCs are in a permanent semi-activated state (Tiegs, *et al*., 2009). Under

pathological conditions, bacteria that bypass the intestinal barrier are the most important activators of KCs. These macrophages have the largest array of surface receptors designed for identification of most gut-derived antigens. Some of these receptors include mannose receptors, IgG receptors (FcγRII and III), scavenger receptors type I and II, FcαRI, Complement receptors, C5a receptor, a wide range of TLRs including TLR4, cytokine receptors (IL1, IL2-β, IL6, TGF-β, TNF-α), platelet activating factor receptors, glucagon receptors and Fas (CD95) (Kmiec, 2001). In addition, similar to other macrophages, once KCs are activated they are capable of producing an array of mediators involved in wide range of functions including: protein degradation, modulation of cell function and defence mechanisms and cytotoxicity. Some of the most crucial of these secretory products include MMP-13, proteoglycans, NO, PAF, IL1-α, IL1-β, IL6, IL8, IL12, IL18, IL21, IL23, TNF-α, TGF-β, reactive oxygen species, lysozyme and osteopontin (Baffy, 2009). In contrast to SECs which only remove soluble molecules from circulation, KCs can accumulate process and present both soluble and particulate antigens from the portal circulation (Kmiec, 2001). Beside these typical macrophage duties, the KCs have the essential role of removing damaged erythrocytes from the blood, and subsequently degrading haemoglobin and re-circulating iron (Kmiec, 2001).

Although KCs have the capacity for initiating and sustaining an immune response to eliminate pathogenic antigens, under normal circumstances they are extremely important in the maintenance of liver tolerance (Tiegs, *et al*., 2009). It is understood that following the initial activation and production of a pro-inflammatory response, KCs release IL10 which down-regulates the production of TNF-α and IL6 and other potentially damaging pro-inflammatory cytokines (Tiegs, *et al*., 2009).

2.3.4 Hepatic stellate cells

Hepatic stellate cells (HSC) (6% of the total number of liver cells) are located in the perisinusoidal spaces in direct locality to the endothelial cell layer with their cell bodies often compressed between the hepatocytes (Kmiec, 2001). HSCs exhibit two phenotypes: a quiescent one in a normal liver and an activated form in a diseased liver. The inactive HSC are characterised by abundant lipid droplets and a low proliferative rate. The activated cells however lose their lipid vacuoles, while demonstrating increased proliferation and enhanced production/secretion of extracellular matrix components (Kmiec, 2001). The non-activated

HSCs have a number of functions in a healthy liver. One of the most important of these functions is the metabolism of retinoid. More than 85% of vitamin A in the body is stored in the liver and about 90% of all the retinoid in the liver is in the lipid droplets of the HSCs (Kmiec, 2001). HSCs are also one of the major producers of extracellular matrix components and ECM-degrading enzymes. In a healthy liver, HSCs express all the major isoforms of hepatocyte growth factor, transforming growth factor β and insulin-like growth factors (Kmiec, 2001). These cells are also involved in the synthesis of erythropoietin and plasminogen activation system (Kmiec, 2001). Once activated, HSCs play a pivotal role in the initiation and progression of liver fibrosis. The secretion of leptin (hormone that plays a key role in regulating energy intake and energy expenditure i.e. in metabolism) by activated HSCs seems to be very important in modulation and activity of many pro-inflammatory cytokines (Tiegs, *et al*., 2009). In addition it is now believed that HSCs can function as antigen presenting cells (APCs) and present protein or lipid antigens to conventional T cells as well as CD1d - restricted T cells and Natural killer T (NKT) cells (Tiegs, *et al*., 2009).

Like other cells in the liver, HSCs are involved in maintenance of tolerance in the liver. As already mentioned HSCs store vitamin A and many believe that CD4 cells coming in contact with such cells can be converted to induced regulatory T cells via vitamin A - derived retinoic acid (Tiegs, *et al*., 2009). Moreover, activated HSCs express the negative co-stimulator PD-L1 (Programmed Death Ligand-1 or CD274 binds PD-1 on activated T cells and induces apoptosis in target cells) as well as being major sources of TGF-β (Tiegs, *et al*., 2009).

2.3.5 Other cells in the liver

Morphological data has indicated that the liver sinusoids contain a large and heterogeneous population of resident lymphocytes, which compromises the conventional αβ T cells, pit cells (natural killer cells – $CD3^{-}CD56^{+}$), γδ T cells, NKT cells and small numbers of B lymphocytes (Tiegs, *et al*., 2009). In addition, there is a subset of professional antigen presenting cells resident in the liver which are the dendritic cells (DC). These cells comprise of both myeloid and plasmacytoid DCs (Baffy, 2009). These liver DCs express very low levels of MHC class II and co-stimulatory molecules (CD80, CD86, CD40) – hence exhibiting an immature phenotype (Tiegs, *et al*., 2009). These cells produce large levels of IL10, stimulating a Th2 cytokine response. In addition IL10 enhances the expression of CCR5 (chemokine receptor) while down-regulating CCR7 expression by the DCs thus

preventing homing to secondary lymphoid tissue (Tiegs, *et al*., 2009). Finally it is important to mention a specialized group of regulatory T cells ($CD4^+CD25^+Foxp3^+$), which are extremely important in maintaining liver tolerance by producing substantial amounts of IL10 (Tiegs, *et al*., 2009).

2.4 Albumin

Albumin is the most abundant protein in serum, containing 585 amino acids and a molecular weight of 66 kDa. This highly soluble globular protein is present in human plasma at normal concentrations between 35 and 50 gram/litre (Roche, *et al*., 2008). Albumin is synthesized in the liver and catabolised by all metabolically active tissues. Albumin makes a large contribution to plasma colloid osmotic pressure due to its small size and abundance (35-50% of total plasma proteins by weight). It has many important physiological and pharmacological functions. Albumin is responsible for the transportation of metals, fatty acids, cholesterol, bile pigments, insoluble organic substances (e.g. unconjugated bilirubin), drugs as well as being a key element in the regulation of osmotic pressure and distribution of fluid between different compartments (Roche, *et al*., 2008). In normal conditions albumin has a half life of about 20 days and its plasma concentration represents equilibrium not only between its synthesis in the liver and its catabolism (Peters, 1996).

2.5 Urea

Ammonia plays a central role in nitrogen metabolism. It is a major by-product of protein and nucleic acid catabolism. The nitrogen from ammonia can incorporate into urea, amino acids, nucleic acids and many other nitrogenous compounds (Sands, 2003). Ammonia is present in body fluids as both NH_3 and NH_4^+ - these are constantly in equilibrium. NH_3 can diffuse freely across membranes via aquaporins (Sands, 2003), while NH_4^+ is carried in the liver by an active transport system – termed the RhB glycoprotein system (Sands, 2003). In a healthy human the blood ammonia concentrations are normally below 35 µmol/L. This is important as ammonia is neurotoxic at higher concentrations. Excessive cerebral ammonia uptake in hyperammonaemic states leads to astrocytic glutamine accumulation and cerebral oedema, a major factor in hepatic encephalopathy (Häussinger, *et al*., 2008).

The liver is the most important site of ammonia metabolism. The organ is responsible for removal of most of the toxic ammonia. By doing so, the liver also plays a major role in the metabolic regulation of systemic pH, due to the fact that hydrogen ions released from NH_4^+ during the synthesis of urea neutralize the excess bicarbonate produced by the breakdown of amino acids (Häussinger, *et al*., 1990). Urea is electrically neutral and is transported across biological membranes by facilitated diffusion. Urea transporters in the liver include aquaglyceroporin - AQP9, and urea transporter UT-B1 (Sands, 2003). Urea is excreted by the kidney, and is normally present in plasma and body fluids at a concentration of 3.0–6.5 mmol/l (Häussinger, *et al*., 2008).

2.5.1 Sources of ammonia

Whereas urea production takes place largely within the liver, much of the ammonia used in urea synthesis is derived, directly or indirectly, from extra-hepatic tissues. Ammonia is largely released from the intestine and the kidneys, with the liver, resting muscle, and brain acting to remove ammonia from the blood (Olde Damink, *et al*., 2002). A large proportion (25%) of all the nitrogen utilized in urea synthesis reaches the liver via the portal vein, from ammonia formed in the small intestine and colon. Furthermore, most of the nitrogen transported to the liver for incorporation into urea is carried not as ammonia but as amino acids, such as alanine or glutamine (Olde Damink, *et al*., 2002).

Once in the liver, glutamate and glutamine are major sources of ammonia. Glutamate is released directly from proteins, but more importantly it is formed from other amino acids (with the exception of lysine and threonine) released from protein breakdown in aminotransferase reactions. Glutamate is directly formed by deamidation of glutamine, and from proline and histidine (Olde Damink, *et al*., 2002). Ammonia is released from glutamate by its oxidative deamination by glutamate dehydrogenase, a mitochondrial enzyme. This enzyme is present in most tissues, but it has utmost activity in the liver (Olde Damink, *et al*., 2002). Amino acids can also be transaminated with glyoxalate to form glycine, which is deaminated by glycine oxidase to yield ammonia.

Ammonia can also be generated by the deamidation of glutamine and asparagine and in the histidine lyase reaction, as well as serine, threonine, cysteine, cystathione and homoserine, in pyridoxal phosphate-dependent deamination reactions, which occur mainly in the liver. Most

of the ammonia produced from purine nucleotides is derived from adenosine monophosphate (AMP), in a reaction catalysed by adenylate deaminase. This pathway becomes particularly important during exercise when ammonia formation and release from muscle is increased (Olde Damink, *et al*., 2002).

The intestine is also a major site of ammonia production. Some 15–30% of the urea synthesized by the liver is degraded by bacterial ureases in the gut, with the liberation of ammonia and carbon dioxide. A second source of ammonia from the gut, quantitatively of equal importance, is the intestinal mucosa itself. The small intestine produces a significant quantity of ammonia, which comes primarily from the metabolism of glutamine removed from arterial blood (Morris, 2002).

2.5.2 Urea production

Approximately 90% of surplus nitrogen in humans enters the urea cycle for irreversible conversion to urea, which is excreted by the kidneys, with approximately 30 grams of urea being excreted daily in healthy adults. Using tracer techniques, it has been observed that calculated urea production exceeds urinary urea excretion by about 20–30%. This difference is attributed to extra-renal losses, largely accounted for by the intestinal hydrolysis of urea (Beliveau-Carey, *et al*., 2003). Short term regulation of urea synthesis occurs at the levels of substrate provision and enzyme activities, whereas long term control is transcriptionally affected by changes in enzyme concentrations. Substrate provision for the urea cycle depends on amino acid delivery, the activity of amino acid transport systems and amino acid metabolizing enzymes (Beliveau-Carey, *et al*., 2003).

It is important to note that changes in urea-cycle enzyme expression can occur following alterations in dietary protein. In such time glucagon, insulin and glucocorticoids are extremely important mediators (Morris., 2002). When protein intake is increased, there is a proportional increase in the total hepatic content of all urea cycle enzymes resulting in increased urea production. Long term regulation of urea cycle enzymes occurs primarily at the level of transcription (Morris., 2002). Glucagon, which increases during starvation and glucocorticoids predominately associated with protein breakdown are both involved with increased enzyme levels and urea production (vom Dahl, *et al*., 1991). Glucagon also

regulates urea synthesis by activation of mitochondrial glutaminase, amino acid transport, *N*-acetylglutamate synthesis, and stimulation of hepatic proteolysis (vom Dahl, *et al*., 1991).

2.5.3 Urea and ammonia metabolism in liver disease

Urea synthesis is greatly reduced in severe liver disease, in parallel with glutamine synthesis. This tends to be correlated with deterioration in other markers of hepatocellular function (Racine-Samson, *et al*., 1996). In patients with liver disease, there is a tendency for blood ammonia levels to rise. The main reason for this is presumably the failure of the liver, because of hepatocellular dysfunction, to remove ammonia from the portal venous blood (Racine-Samson, *et al*., 1996). One hypothesis in this study was that NM exposure could interfere with urea synthesis by hepatocytes hence it seems an important endpoint to study in order to gain a better understanding of how these particular ENPRA NMs are affecting liver function.

2.6 C reactive protein

C reactive protein (CRP) is a protein synthesised and secreted by the hepatocytes of the liver in response to inflammatory cytokines, in particular IL6. It is a member of the pentraxin family of proteins - composed of five identical subunits arranged in a cyclic pentameter shape. These subunits are non-covalently bonded and have a total molecular weight of 118,000 daltons (McWilliam, *et al*., 2010). Although CRP is often used clinically as a marker for inflammation, it also functions as a key component of the innate immune response to inflammation and infection. It plays this role by mediating phagocytosis, activating the complement cascade and by producing further inflammatory cytokines (Gabay, *et al*., 1999). CRP forms complexes by binding to a range of molecules, such as polysaccharides and peptopolysaccharides present on bacteria, parasites and fungi (Gabay, *et al*., 1999). CRP also plays a role in clearance of cellular debris by binding components of damaged host cells (both membrane and intracellular components) (McWilliam, *et al*., 2010). These CRP–ligand complexes bind to Fc receptors on phagocytic cells (neutrophils, macrophages, etc.) mediating phagocytosis of pathogens opsonised by CRP and stimulating a pro-inflammatory response via the production of further cytokines (IL1, TNF-α). CRP–ligand complexes are also able to bind to C1q, the first component of the classical complement cascade, which again triggers phagocytic activity (Du Clos, *et al*., 2004).

CRP (the prototypical acute phase protein in humans) was discovered in 1930 by Tillett and Francis (McWilliam, *et al*., 2010). They studied the sera of patients with acute pneumococcal pneumonia and identified a substance in the sera that formed a precipitate when combined with the C polysaccharide of the pneumococcal cell wall. As patients recovered, the ability of their sera to form this precipitate disappeared. Likewise, sera from healthy individuals did not form this precipitate. Ultimately, this "C reactive" component was found to be a protein and was given the name "CRP" (McWilliam, *et al*., 2010).

In humans, plasma levels of CRP can increase markedly as much as 1000 fold or more, after an acute inflammatory stimulus, largely reflecting increased synthesis by hepatocytes. It is important to note however that CRP induction is part of a larger picture of re-orchestration of liver gene expression during inflammatory states, the acute phase response, in which synthesis of many plasma proteins are increased (Du Clos, *et al*., 2004). At least 40 plasma proteins are defined as acute phase proteins, based on changes in circulating concentration after an inflammatory stimulus. This group includes clotting proteins, complement factors, anti-proteases, and transport proteins. These changes presumably contribute to defensive or adaptive capabilities of the host immune response (Du Clos, *et al*., 2004).

2.6.1 Experimental evidence of CRP in action

CRP has been shown to play a protective role in a variety of inflammatory conditions, including protecting mice from lethal challenge with bacterial LPS and various mediators of inflammation (Black, *et al*., 2004). In addition, CRP has been found to delay the onset and development of experimental allergic encephalomyelitis, an aseptic animal model of multiple sclerosis (Szalai, *et al*., 2002). In a murine model of chemotactic factor-induced alveolitis, CRP has also been shown to inhibit the influx of neutrophils and protein into the lungs (Black, *et al*., 2004).

In addition to these mouse models, a polymorphism in the human CRP gene resulting in a lower basal level of CRP has been associated with an increased risk of developing systemic lupus erythematosus (Black, *et al*., 2004).

CRP is an ancient protein whose initial role as a pattern recognition molecule may have been to defend against bacterial infections, but whose present biological role appears quite

complex. It is likely that the activity of CRP in humans, either pro- or anti-inflammatory is dependent on the context in which it is acting. Therefore it seems important that CRP is studied in order to gain a better understanding of the effects of engineered nanomaterials on the human liver and the eventual clearance of these materials from the organ.

2.7 Inflammation

The term inflammation is derived from the Latin "inflamatio" meaning to set on fire (Scott, *et al*., 2004). It is an extremely complicated process involving the innate and adaptive immune systems with many cells and molecules contributing to the generation of different physiological and pathological outcomes; such as wound healing and infection (Coussens, 2002). An inflammatory response can be initiated by both antigen dependent or independent stimulation (Baniyash, 2006). The former is initiated by pathogen associated membrane proteins (PAMPs) - mainly nucleotide-binding oligomerization domain (NOD) proteins and Toll like receptors (TLRs) inducing the production of lipid mediators, cytokines and chemokines from neutrophils, macrophages, and mast cells. These events lead to a co-ordinated increase in vascular permeability, up regulation of adhesion molecules (L-, P-, and E-selectins in early stages and $\alpha 4\beta 1$, $\alpha 1\beta 4$ integrins binding vascular cell adhesion molecule -1 (VCAM-1) and mucosal vascular addressin cell adhesion molecule 1 (MadCAM-1) at later junctures on the blood vessels, important for direction and migration of leukocytes to site of injury (Carneiro, *et al*., 2008).

This is subsequently followed by activation of phagocytes and promotion of their microbicidal action, pursued shortly by activation of natural killer cells and the release of cytokines (IFN-γ) essential for enhancing cytotoxicity and further activation of macrophages which are the most important cells as a source of growth factors, cytokines and modulating tissue repair (Beutler, 2004; Hamerman, *et al*., 2005).

The main mediators of inflammation are TNF-α, I-1, IL6, prostaglandins (PGE_2 believed by many to be the most potent mediator of them all), leukotrienes, histamine, bradykinan and PAF (Coussens, 2002). Collectively they control inflammatory cell populations, up-regulate vascular permeability and adhesion, increase cytotoxicity of natural killer cells, pain as well

promoting production of phagocytes and acute phase proteins from the liver (Coussens, 2002).

Chemokines are crucial for directing cells to the targeted areas of inflammation. Some of these important soluble proteins include neutrophil attracting factors like IL8, C5a, Kalikerin and monocyte guiding proteins such as monocyte chemo-attractant proteins 1, 2 and 3, Tumour growth factor β (TGF-β) and macrophage inflammatory proteins 1α and 1β (Carneiro, *et al*., 2008).

2.8 Oxidative stress

The recent abundant evidence suggesting the involvement of oxidative stress in the pathogenesis of various disorders and diseases has attracted much attention both in the scientific community and general public.

Reactive oxygen species (ROS) and other free radicals are critical intermediates in the normal physiology and pathophysiology of the liver in particular with regards to the hepatocytes (Diesen, *et al*., 2009). ROS are important in the creation of oxidative stimuli required for normal physiologic homeostasis of hepatocytes. However, the equilibrium between ROS generation and the antioxidant defence within a cell can be disrupted resulting in an overall net oxidative stress (Kang, 2002). In the liver, free radicals triggered by ROS are created by the neutrophils, Kupffer cells, mitochondria, and cytochrome P450 (Kang, 2002). The damage created by oxidative stress affects all cells within the liver by inducing inflammation, ischemia, apoptosis and necrosis. ROS affect the pathophysiology of many diseases such as atherosclerosis, adult respiratory distress syndrome, cystic fibrosis, cataracts, cancer, liver disease, diabetes, neurological conditions and ischemia/reperfusion injuries (Lieber, 1997). Currently, it is believed that ROS also affects signal transduction pathways that when unbalanced may lead to hepatic inflammation, necrosis, fibrosis, and/or apoptosis (Diesen, *et al*., 2009) as has been shown in the lung and other cell types (Clift, *et al*., 2010). ROS include superoxide (O_2^-), hydrogen peroxide (H_2O_2) and hydroxyl radical (OH^-). Of these, those with an unpaired electron are known as ‘‘radicals’’ (Diesen, *et al*., 2009). Superoxide (O_2^-) is the most common radical that can serve as a precursor for several other ROS species. It is important to note however, that O_2^- by itself is also a potent oxidant. Superoxides are

constitutively produced by mitochondria as a by product of oxidative phosphorylation, as the mitochondria reduce approximately 1 – 3% of respiratory oxygen molecules to superoxide anions (Nohl, *et al*., 2003). Mitochondria contain enzymes and compounds that consume ROS, including superoxide dismutase that converts superoxide anion (O_2^-) to hydrogen peroxide (H_2O_2), catalases (H_2O_2 dismutases) and peroxidases that reduce H_2O_2 to water, frequently by employing the reducing power of NAD(P)H. Metals including iron and copper can further react with hydrogen peroxide to produce hydroxyl radicals via the Fenton reaction (Nohl, *et al*., 2003). The Fenton reaction recycles iron from Fe (II) to Fe (III) by oxidizing superoxide anion to oxygen. Hydroxyl radicals are then created resulting in an increase in the levels of bioactive iron. This process can occur in Kupffer cells in pathologic conditions such as cirrhosis (Nohl, *et al*., 2003). The ability of superoxide to activate this reaction makes it an important factor in oxidative stress.

Reactive oxygen species are necessary for many normal physiological functions. Reactive oxygen species are implicated in cell signalling and are considered by some to be the second messengers that can trigger cytokine, hormone, and growth factor release from certain cells (Diesen, *et al*., 2009). ROS can also affect gene expression, as well as playing a role in the normal induction of apoptosis though the exact mechanisms are currently unclear (Diesen, *et al*., 2009). Since ROS are ubiquitous in the normal physiology of so many processes, it is not surprising that when excess ROS are produced they subsequently affect many normal functions of a healthy cell.

2.9 Antioxidants

To combat excess ROS, the body utilizes antioxidants. Endogenous antioxidants are usually small molecules that are able to prevent or limit oxidative damage by detoxifying ROS (Glantzounis, *et al*., 2005). Common antioxidants in hepatocytes include glutathione (GSH), glutathione peroxidase, and reductase enzymes superoxide dismutase (SOD), hemeoxygenase (HO), peroxidases and metal binding proteins (Glantzounis, *et al*., 2005). Low molecular weight compounds, such as bilirubin, melatonin, lipoicacid, coenzyme Q and uric acid also have antioxidant properties (Glantzounis, *et al*., 2005). Antioxidants can be classified into hydrophilic (e.g. GSH) and hydrophobic (e.g. α-tocopherol) categories allowing protection for all components within the cell (Teixeira, *et al*., 2012).

Glutathione is a ubiquitous tri-peptide which primarily functions to react with hydrogen peroxide utilising glutathione peroxidase to create glutathione disulfide (GSSG). GSH also scavenges other ROS molecules and prevents oxidation of protein sulfhydryl groups (Diesen, *et al*., 2009). In addition to glutathione, catalase and peroxidases are able to break down hydrogen peroxide to less reactive metabolites. Catalase converts hydrogen peroxide to water and oxygen, while peroxidase is also able to reduce it to water with reducing equivalents, usually thiol-containing molecules such as thioredoxin. Thioredoxin contains two sulfhydryl groups, which are oxidized to a disulfide. Another antioxidant enzyme - superoxide dismutase (SOD), catalyzes the reaction of two superoxide radical anions with each other, leading to the formation of one molecule of molecular oxygen and one molecule of hydrogen peroxide (Glantzounis, *et al*., 2005). Peroxide is relatively stable but in the presence of a transit ion metal may form hydroxyl radicals. It is well known that transition metals may create reactive oxygen species (e.g. via Fenton reaction), therefore it is a very real possibility that metal binding proteins may also have antioxidant properties (Diesen, *et al*., 2009). Iron may be bound by transferrin and lactoferrin, while ceruloplasmin and albumin bind copper. Haemoglobin and myoglobin both contain iron and heme. When exposed to excessive oxidative stress, the heme group and the iron may disassociate, thus promoting lipid peroxidation. When this occurs, haemoglobin binding proteins such as haptoglobin and heme binding proteins like hemopexin, bind these proteins to decrease the level of lipid peroxidation (Diesen, *et al*., 2009).

Exogenous antioxidants may also be consumed through the diet: common dietary forms include vitamin C (ascorbate), vitamin E, carotenoids, and plant phenols. Lipophilic α-tocopherol, the active form of vitamin E, scavenges peroxyl radicals and prevents lipid peroxidation (Birlouez-Aragon, *et al*., 2003). Carotenoids are a source of vitamin A and also scavenge free radicals, while plant phenols are able to scavenge ROS and to chelate metals (Diesen, *et al*., 2009).

2.10 Distribution and deposition of the NMs in the liver (current understanding)

There is some evidence that nanomaterials administered via intravenous (IV), intraperitoneal (IP) and inhalation routes will eventually reach the liver (Chen, *et al*., 1999; Semmler-Behnke, *et al*., 2008). The organ has prominent importance as it receives NMs at extremely high volumes compared to other organs and alongside the kidneys might be responsible for

the clearance of these materials from the blood (Chen, *et al*., 1999). In a recent study, mice were injected with gold NMs sized 2 and 40 nm. It was observed that the 40 nm materials administered via the IV route were only located within the mice Kupffer cells of the liver (Sadauskas, *et al*., 2007). The uptake of 2 nm NMs was slower and only some of the Kupffer cells internalising the materials with the rest being traced to some of the macrophages in the spleen (Sadauskas, *et al*., 2007). Intraperitoneal administration of the NMs resulted in less intense staining of the Kupffer cells (still markedly higher than other organs). Instead the particulates were located within the macrophages of the mesenterial lymph nodes and lymphatic tissues of the spleen and the small intestine (Sadauskas, *et al*., 2007). These findings are extremely interesting as after IP injection the NMs pass numerous lymph nodes packed with macrophages and other immune system cells, yet the majority travel to the liver and are taken up by the Kupffer cells. These and other findings indicate that Kupffer cells could well be central to the elimination of NMs that reach the liver (Sadauskas, *et al*., 2007; 2009a; Xiong, *et al*., 2008). It is believed that NMs are potentially taken up by the Kupffer cells via trancytosis (Sadauskas, *et al*., 2009a).

2.11 Neutrophils and the liver

Neutrophils also referred to as polymorphonuclear leukocytes (PMNs) are the most abundant of all white blood cells comprising of up to 70% of all leukocytes (Freitas, *et al*., 2009). Neutrophils are the front line effectors of the innate immune system: after differentiation these short lived cells circulate in the bloodstream for up to 7 hr before migrating into tissues (Quinn, *et al*., 2004). These cells are solely responsible for surveillance and constituting the first line of defence against foreign antigens (Nauseef, 2007). Hence it is not surprising that in the event of an inflammatory response there is usually an increase in PMN numbers, mobility, tissue influx and phagocytic ability (Freitas, *et al*., 2009). Neutrophils are the most active phagocytic cells in the hosts immune system arsenal. They are capable of ingestion of antigens into specialised phagosomes and producing a wide array of cytotoxic agents to eliminate the foreign particle (Nauseef, 2007). The role of PMNs in disposal of NMs is not yet fully understood, however it has been shown that nanomaterial exposure in the lungs results in a large increase in PMN numbers in the tissue (Donaldson, *et al*., 2003).

In order to gain entry into the liver neutrophil rolling and adhesion requires up-regulation of β integrins, selectins and endothelial receptors (Jaeschke, *et al*., 2006). It has been shown that

the most common neutrophil mediated response in the liver is governed by the adhesion of the cells to hepatocytes (via ICAM-1 binding Mac-1) (Bautista, 2002; Ramaiah, *et al*., 2007). This adhesion triggers the formation of reactive oxygen species (ROS) by NADPH oxidase and release of proteases through the degranulation of the PMNs. This process could lead to neutrophilic hepatitis characterised by self aggravating mechanisms resulting in chronic disease (Bautista, 2002).

2.12 The kidneys

Human kidneys are fist sized organs located at either side in the lower abdomen. The kidneys are principally responsible for the removal of metabolic waste. This term is generally taken as nitrogenous waste; namely urea and ammonia, however it is widely accepted that other waste products and toxic substances such as carbon dioxide, bile and possibly nanomaterials are excreted through urine (Wang, *et al*., 2009). The blood and all tissue fluids contain a variety of solutes including glucose and salts dissolved in water. The concentrations (relative and absolute) of these solutes have to be tightly regulated as does their total concentration relative to water (Raven, *et al*., 2008). This solute concentration must be kept constant in both the blood and tissue fluids (osmoregulation) (Raven, *et al*., 2008). The two processes of excretion and osmoregulation are governed by the urinary system and the kidneys.

2.13 Blood supply to the kidneys

The kidneys receive blood from the renal arteries, left and right, which branch directly from the dorsal aorta. Despite their relatively small size, the kidneys receive approximately 20% of the entire cardiac output (Roberts, *et al*., 2000). Each renal artery branches into segmental arteries, dividing further into interlobar arteries which penetrate the renal capsule and extend through the renal columns between the renal pyramids. The interlobar arteries then supply blood to the arcuate arteries that run through the boundary of the cortex and the medulla. Each arcuate artery supplies several interlobular arteries that feed into the afferent arterioles that supply the glomeruli (Figure 2.3) (Raven, *et al*., 2008). After filtration in the glomeri occurs, the blood moves through a small network of venules that surround the kidney tubule structures before they converge into interlobular veins. As with the arteriole distribution, the veins follow in the same pattern, the interlobular veins provide blood to the arcuate veins

flowing back to the interlobar veins, which form the renal vein exiting the kidney for transfusion of blood (Raven, *et al*., 2008).

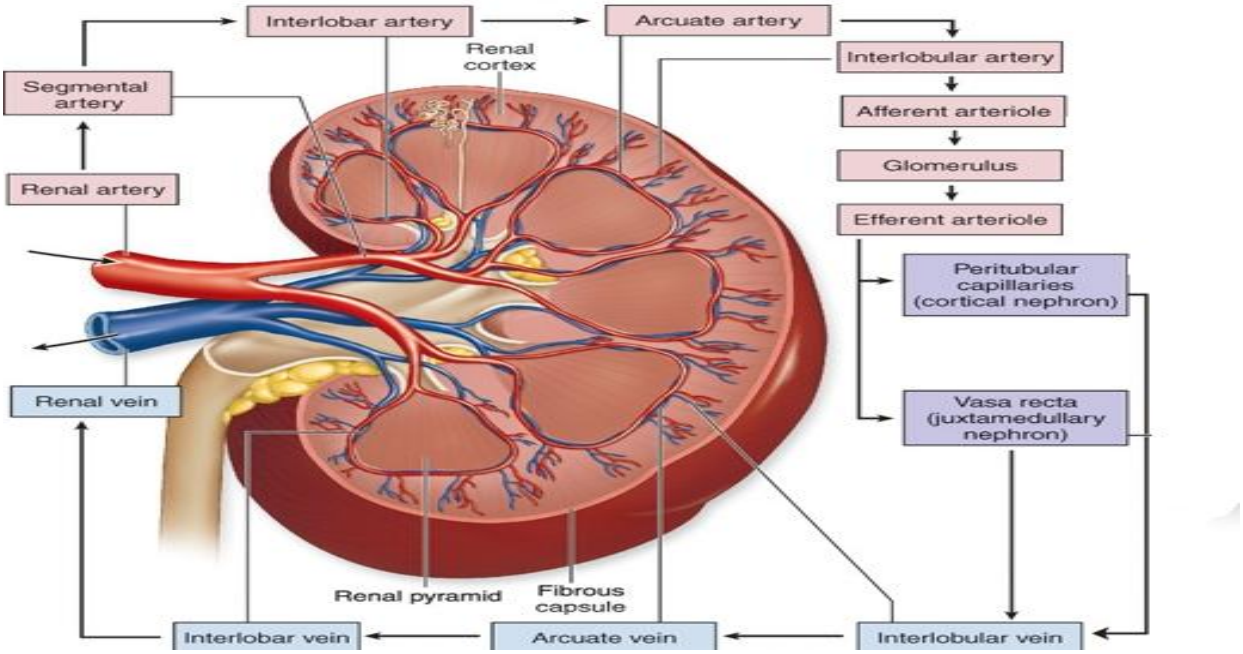

Figure 2.3. The blood supply to the kidney (Adapted from Raven, *et al*., 2008).

2.14 A healthy functioning kidney

Each kidney contains about one million functioning filtering units (nephrons). Mammalian kidneys contain a mixture of juxtamedullary nephrons which are characterised by long loops (loop of Henle) dipping into the medulla and cortical nephrons with shorter loops (Raven, *et al*., 2008).

Each nephron consists of a long tubule and associated small blood vessels. The blood enters the nephrons via afferent arterioles. Here the blood is filtered by the glomerulus - the blood pressure forces through the porous capillary walls (Wang, *et al*., 2009). Erythrocytes and plasma proteins are too large to enter the glomerular filtrate but large quantities of plasma, containing water and dissolved molecules and potentially NMs, leave the vascular system at this step. The filtrate immediately enters the Bowman's capsule and is in turn released into the proximal convoluted tubule located in the cortex (Raven, *et al*., 2008). Water is re-absorbed as it passes through the loop of Henle. After leaving the loop the fluid is delivered to distal convoluted tubules in the cortex that drains into a collecting duct (Roberts, *et al*.,

2000). The collecting ducts from the millions of different nephrons empty into one of the two ureters. Most of the water and dissolved solutes are re-absorbed during the passage through this tubule system. This selective re-absorption in the collecting duct is driven by an osmotic gradient produced by the loop of Henle (Raven, *et al*., 2008). The re-absorption of glucose, amino acids and other essential molecules needed in the body is driven by active transport and other co-transport carriers, with the maximum rate of transport achieved when the carriers are saturated (Jaitovich, *et al*., 2009). If a person has a higher than normal blood glucose level (above 180 mg/ml; individuals suffering from diabetes mellitus) the glucose in the filtrate is expelled in the urine (Villar, *et al*., 2009). The secretion of foreign molecules and waste products involves the transport of these entities across the membranes of the blood capillaries and kidney tubules into the filtrate. This process is similar to re-absorption but proceeds in the opposite direction (Raven, *et al*., 2008).

Urine with high H^+ concentration helps maintain the acid-base balance of the blood within a narrow range (pH 7.35 - 7.45). Moreover, the excretion of water in urine contributes to the maintenance of blood volume and pressure (i.e. large volumes of urine excreted reduce blood volume) (Roberts, *et al*., 2000). The purpose of kidney function is therefore homeostasis – maintaining the constancy of the internal environment (Villar, *et al*., 2009).

2.15 Proximal convoluted tubules

Water is only able to pass through a cell through osmosis; however this process is not possible between two isotonic solutions. Therefore some mechanism is needed to create an osmotic gradient between glomerular filtrate and the blood to allow re-absorption of water (Raven, *et al*., 2008). Virtually all the nutrient molecules in the filtrate are re-absorbed back into the systemic blood by the proximal convoluted tubules. In addition, two-thirds of the sodium chloride and water filtered into the Bowman's capsule is immediately re-absorbed across the walls of the proximal convoluted tubules (Raven, *et al*., 2008). The re-absorption is driven by the active transport of Na^+ out of the filtrate and into the surrounding peritubular capillaries. Cl^- follows Na^+ passively because of electrical attraction and water follows because of osmosis (Jaitovich, *et al*., 2009). As NaCl and water are removed from the filtrate in proportionate amounts, the filtrate remaining in the tubule is still isotonic to the blood plasma (Jaitovich, *et al*., 2009). The luminal surface of the epithelial cells of this segment of the nephron is covered with densely packed microvilli named the brush border cells. The

microvilli greatly increase the luminal surface area of the cells. The cytoplasm of these cells are densely packed with mitochondria - largely found in the basal region within the foldings of the basal plasma membrane. The mitochondria are needed in order to supply the energy for the active transport of sodium ions out of the proximal tubule. Cuboidal epithelial cells lining the proximal tubule have extensive lateral inter-digitations between neighbouring cells (Roberts, *et al*., 2000). The agonist re-absorption of the proximal tubular contents after interruption of circulation in the capillaries surrounding the tubule often leads to disturbance of the cellular morphology of the proximal tubule cells, including the ejection of cell nuclei into the tubule lumen (Roberts, *et al*., 2000).

2.16 Loop of Henle

As previously stated, the function of the loop of Henle is to create a gradient of increasing osmolarity from the cortex to the medulla (Figure 2.4). This allows water to be re-absorbed by osmosis in the collecting duct as it runs down the medulla past the loop of Henle (Roberts, *et al*., 2000).

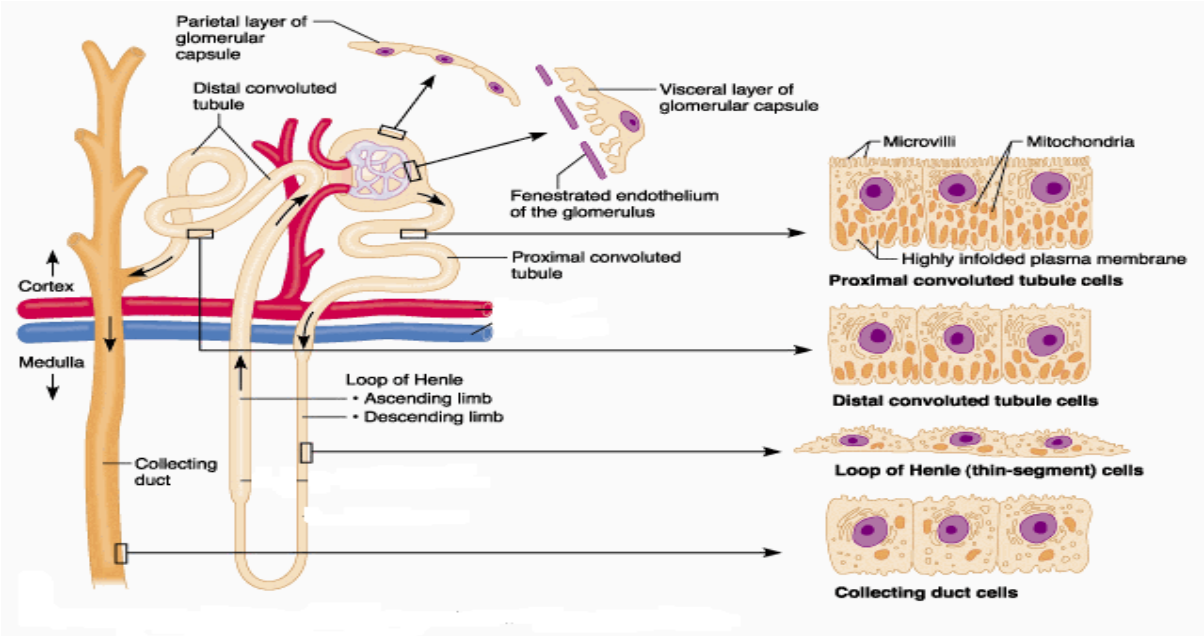

Figure 2.4. Mammalian nephron (Adapted from Roberts, *et al*., 2000).

The descending and ascending limbs of the loop of Henle differ structurally and in their permeability. This produces a gradient of increasing osmolarity from the cortex to the medulla (Figure 2.4) (Raven, *et al*., 2008). The ascending limb of the loop of Henle is

composed of a thick layer of low simple cuboidal epithelium cells, while the descending limb is compiled of relatively thin layers of simple squamous epithelial cells (Raven, *et al*., 2008). The entire ascending limb is impermeable to water. This thick portion allows active transportation of Na^+ out of the tubule with Cl^- following passively. The descending limb is thin and permeable to water but not to NaCl. The Na^+ and Cl^- are lost by the ascending limb, therefore the osmalarity of the interstitial fluid is higher than the descending limb, hence water moves out of the limb by osmosis (Roberts, *et al*., 2000). The sodium chloride pumped out of the ascending limb of the loop is re-absorbed from the surrounding interstitial fluid into the vasa recta renis (capillaries in the medulla) (Raven, *et al*., 2008).

2.17 Distal convoluted tubules and the collecting duct

The filtrate reaching the distal convoluted tubules is hypotonic and by the time it reaches the collecting duct it is removed by a strong osmotic gradient into the surrounding blood vessels (Raven, *et al*., 2008). The osmotic gradient normally remains constant but the permeability of the distal convoluted tubule and the collecting duct is adjusted by anti-diuretic hormone (ADH) (Raven, *et al*., 2008). When the animal needs to conserve water the posterior pituitary gland secretes more ADH. The increase in the hormones correlates with a rise in the number of water channels in the plasma membrane of the collecting duct cells resulting in the release of hypertonic urine (Roberts, *et al*., 2000). In addition the re-absorption of NaCl in the distal convoluted tubules and the collecting duct is under the control of the hormone aldostrone (Raven, *et al*., 2008).

2.18 Immunology of the kidneys

In the immune system, a complex orchestration of cytokines and other molecules act in a paracrine, autocrine or endocrine fashion to control the differentiation, proliferation and activity of immune cells. The kidneys maintain a delicate equilibrium between pro-inflammatory cytokines and their inhibitors. Therefore, any cytokine response to infection or injury is a well-coordinated and precisely controlled process aimed at maintaining the body homeostasis (Carrero, *et al*., 2008).

It is important to distinguish between local and systemic inflammation. Locally produced pro-inflammatory mediators include IL8, IL12, IL18, TNF-α and IFN-γ and IL6. In the

kidney these cytokines are produced predominately by T helper lymphocytes and macrophages. Th1 cytokines stimulate the synthesis of nitric oxide and other inflammatory mediators, the functional activity of cytotoxic T cells, natural killer cells and activated macrophages, altogether exerting a pro-inflammatory action. On the other hand, Th2 cytokines inhibit macrophage activation, T cell proliferation and the production of pro-inflammatory cytokines, therefore are involved in anti-inflammatory processes. Th1 and Th2 responses are mutually inhibitory (Carrero, *et al*., 2008). Many believe that day to day immunity of the kidneys is predominately controlled by the macrophages. Studies in which urine samples were collected from patients with acute rejection episodes following kidney transplantation demonstrated significantly higher levels of IFN-γ and TNF-α. Elevated concentrations of these pro-inflammatory cytokines in urine unaccompanied by high concentrations of IL2, seems to suggest an ongoing undetected nonspecific macrophage-mediated Th1 immune response, capable of amplifying the allo-immune response in the early phases of post surgery, leading to immunity (Karczewski, *et al*., 2009).

This being said it is important to mention that the renal epithelial cells are also able to contribute to the immune response in the organs by producing a wide array of cytokines and chemokines under certain conditions including IL10 (Liu, *et al*., 2012), MCP-1 (Liu, *et al*., 2012), vascular endothelial growth factor a (VEGF-a) (Fernandez-Martinez, *et al*., 2012), IL6 (Fitzgerald, *et al*., 2012) and IL8 (Fitzgerald, *et al*., 2012).

Over all it seems that unlike the liver, in the kidneys immunity is favoured over tolerance. Hence all lymphoid and myeloid cells such as dendritic cells, natural killer cells, neutrophils and the lymphocytes contribute to the immunity of the kidneys (Carrero, *et al*., 2008).

2.19 Distribution and deposition of the NMs in the kidney (current understanding)

The kidneys are particularly susceptible to xenobiotics due to their high blood supply and their ability to concentrate toxins (L'azou, *et al*., 2008). In theory both the glomerular structures (during plasma filtration) and tubular epithelial cells may be potentially exposed to nanomaterials. Previous experiments have demonstrated that mice exposed to copper NMs had severe damage to the proximal tubular cells (Chen, *et al*., 2006), while Wang and colleagues observed glomerulonephritis and pathological degeneration of the renal proximal convoluted tubules following oral TiO_2 administration (Wang, *et al*., 2007a). The kidney is

composed of different cell types with varying levels of sensitivity to toxic substances. Mesenglial cells for example are perivascular pericytes located within the central portion of glomeular tuft between the capillary loops and are involved in the control of glomeular hemodynamics. They encounter blood filtrate in large volumes and are very possibly one of the cell types most likely to encounter NMs *in vivo* (L'azou, *et al*., 2008). Proximal tubule cells are characterised by well-developed basal infolding and an apical brush border and characterised by their ability for intense pinocytic activity. Furthermore they are capable of variable transport and co-transport of various materials (Cartiera, *et al*., 2009). Hence these cells were an ideal candidate for an *in vitro* nanotoxicological investigation.

2.20 Aims

To evaluate adverse effects of a range of manufactured nanomaterials on the liver and kidneys (due to their potential for NM accumulation, both organs have an essential role in maintaining health and their contrasting immunological profiles) as part of the Seventh Framework programme (FP7) project ENPRA. A number of endpoints were thoroughly investigated. These included cytotoxicity, oxidative stress, inflammation and genotoxicity. In addition we utilised a full dose reposnse which will provide information for the development of structure activity relationships and risk assessment model to be implemented by the JRC.

Chapter Three

Materials and methods

This work was conducted as part of a large collaborative project. All of the methods described below were conducted by Ali Kermanizadeh. Methods conducted by collaborators are provided in the appendices and are indicated below as appropriate.

3.1 Equipment

Throughout all experiments the following equipment were utilised: Sartorius ME36S balance, Ultrawave Q series ultrasonic sonicator, ESCO class II BSC Airstream biohazard safety cabinet, New Brunswick Galaxy 170S incubator, Grant OLS 200 water bath, Dynex Magellen Biosciences MRX Revelation plate reader, FLUOstar Optima Microplate reader, Grabt-Bio PMS-1000 Orbital Microplate shaker, Hitachi S-4800 Type II Field Emission Gun-Scanning Electron Microscope and Tecnai 12 and Joel 2010 Transmission Electron Microscopes.

3.2 Nanomaterials

Nanomaterials were purchased as stated: NM 101 (Hombikat UV100; rutile with minor anatase; 7 nm), NM 110 (BASF Z-Cote; zinkite, uncoated, 100 nm), NM 111 (BASF Z-Cote; zinkite coated with triethoxycaprylylsilane, 130 nm), NM 300 (RAS GmbH; Ag capped with polyoxylaurat Tween 20 - < 20 nm), NM 400 (Nanocyl; entangled MWCNT, diameter 30 nm), NM 402 (Arkema Graphistrength C100; entangled MWCNT, diameter 30 nm). These NMs were originated from the European Commission Joint Research Centre (JRC, Ispra, Italy). The above mentioned nanomaterials were sub-sampled by the JRC under Good Laboratory Practice conditions and preserved under argon in the dark until use. The NRCWE samples were procured by the National Research Centre for the Working Environment (NRCWE). Sub-sampling was completed by NRCWE into 20 ml Scint-Burk glass pp-lock with Alu-Foil (WHEA986581; Wheaton Industries Inc.) after pooling and mixing 0.1 to 1 kg of the material to cover the need of the ENPRA project. NRCWE 001, TiO_2 rutile 10 nm was purchased from NanoAmor (Houston, USA) and was also used for production of NRCWE 002 (TiO_2 rutile 10 nm with positive charge) and NRCWE 003 (TiO_2 rutile 10 nm with negative charge) using the procedures described below (Section 3.3). NRCWE 004 (TiO_2 rutile 94 nm) was purchased from NaBond. The Ag was supplied in de-ionised water (85%) with 7% stabilizing agent (ammonium nitrate) and 8% emulsifiers (4% each of Polyoxyethylene Glycerol Trioleate and Tween 20). All other materials were supplied as dry

powders. The complete list of investigated nanomaterials including information provided by the suppliers is reported in Table 3.1.

NM	NM Code	Average Size (nm) (Supplier information)	Additional information	CAS - number
TiO_2	NM 101	7 nm	anatase, thermal	13463-67-7
ZnO	NM 110	100 nm	uncoated	1314-13-2, *EINECS* 215-222-5
ZnO	NM 111	130 nm	triethoxycaprylylsilane coated	1314-13-2, 2943-75-1 *EINECS* 215-222-5, 220-941-2
Ag	NM 300	< 20 nm	Polyoxylaurat Tween 20 capped	7440-22-4
MWCNT	NM 400	30 nm 5 µm long	short entangled	7782-42-5, *EINECS* 231-955-3
MWCNT	NM 402	30 nm 5 µm long	long entangled	7782-42-5, *EINECS* 231-955-3
TiO_2	NRCWE 001	10 nm (XRD)	rutile	13463-67-7
TiO_2	NRCWE 002	10 nm (XRD)	rutile	-
TiO_2	NRCWE 003	10 nm (XRD)	rutile	-
TiO_2	NRCWE 004	94 nm (XRD)	rutile	13463-67-7

Table 3.1. List of engineered nanomaterials investigated, with the original source codes, the nominal sizes and properties as provided by the supplier.

3.3 Surface functionalisation of titanium dioxide (conducted by the NRCWE)

The surface functionalistion of NRCWE 002 and NRCWE 003 was carried in the National Research Centre for the Working Environment in Copanhagen. Details are provided in appendix 1.

3.4 Nanomaterial characterisation (conducted by University Ca' foscari Venice)

The majority of the work in characterising the panel of ENPRA nanomaterials was taken place at the Department of Environmental Sciences, Informatics and Statistics, University Ca' Foscari Venice. Details are provided in appendix 2.

Primary and aggregate size range, shape and crystal structure of the test materials were determined by Transmission Electron Microscopy (TEM) on a Jeol (Tokyo, Japan) 3010 transmission electron microscope operating at 300 kV. Surface areas and pore volumes were obtained by nitrogen adsorption on a Micrometritics ASAP2000 Accelerated Surface Area and Porosimetry System at an adsorption temperature of -196°C, after pre-treating the sample under high vacuum at 300°C for 2 hr (Brunauer, *et al.*, 1938). The selected degassing conditions may affect the coating on some of the powder nanomaterials.

3.5 Dynamic light scattering

The hydrodynamic size distributions of the NMs dispersed in William's E medium (Life Technologies, UK), Keratinocyte serum free media (K-SFM) (Life Technologies, UK), RPMI with 10% fetal calf serum (FCS) (Sigma, UK) and HepatoZyme (Life Technologies, UK) were determined in the 1 - 128 µg/ml concentration range (equivalent to the cell exposure concentration range utilised in this study) by dynamic light scattering (DLS) using a Malvern Metasizer nano series – Nano ZS (USA).

3.6 Atomic absorption spectroscopy (AAS)

Stock solution of standards was prepared for both Ag and Zn in water ranging from 4 down to 0.1 ppm. The Ag and ZnO NMs (NM 300, NM 110 and NM 111) were dispersed in the ENPRA dispersant and sonicated (section 3.8). To ascertain the dissolution of ZnO and Ag,

the materials were diluted in both ultrapure and filtered water and Minimum Essential Medium Eagle (MEM) (Invitrogen, UK) with 10% FCS, 2 mM L-glutamine, 100 U/ml Penicillin/Streptomycin, 1 mM sodium pyruvate, and 1% non essential amino acids (termed complete medium). The nanoparticle dispersions and blank samples were incubated in triplicate for 24 hr at 37°C, 5% CO_2 (identical exposure conditions as used for the treatment of cells). The NMs were centrifuged at 13000 g for 1 hr before the supernatant was passed through a 5000 KDa (25 nanometers) ultrafilteration column (Sartorius, USA). Supernatants were stored at 4°C until accessed by AAS. The analysis was carried out using a Perkin Elmer AAnalyst 200 Atomic Absorption Spectrometer (Ag and Zn Hollow Cathode Lamp).

3.7 Cell culture

The human hepatoblastoma C3A cell line was obtained from the American Type Culture Collection (ATCC) (USA). The cells were maintained in complete C3A medium (Section 3.5), at 37ºC and 5% CO_2.

The primary human hepatocytes were purchased from Life Technologies, UK. The cells were maintained in Williams E medium (Life Technologies, UK) with 5% FCS, 10 µM dexamethasone in DMSO, 100 U/ml Penicillin/Streptomycin, 4 µg/ml bovine insulin, 2 nM Glutamax and 15 mM of HEPES, at 37ºC and 5% CO_2.

The immortalized adult human renal proximal tubule epithelial cells (HK-2) were obtained from the ATCC (USA). The cells were maintained in Keratinocyte Serum Free Medium (Life Technologies, UK) containing 25 µl of bovine (pituitary) extract, 0.2 ng/ml human recombinant epidermal growth factor and 100 U/ml penicillin/streptomycin (termed K-SFM) or RPMI (Sigma, France) with 10% FCS and 100 U/ml penicillin/streptomycin (termed complete RPMI), at 37ºC and 5% CO_2. Two different media were utilised to allow comparisons of cytotoxicity and a better understanding of how the nanomaterials behave in different media with varying amounts of protein.

3.8 Nanomaterial treatment

NMs were dispersed in MilliQ de-ionised water with 2% FCS. For coated ZnO (NM 111), the particles were wetted with 0.5 % vol ethanol before the addition of the dispersion media. The

nanomaterials were sonicated for 16 mins without pause following the protocol developed for ENPRA (Jacobsen, *et al*., 2010). Following the sonication step, all samples were immediately transferred to ice (all NMs were used within 15 mins of being sonicated).

To ascertain the toxicity of nanomaterials to the cells ten concentrations between 0.16 μg/cm^2 and 80 μg/cm^2 were utilised (corresponding to 0.5 μg/ml to 256 μg/ml) by diluting in complete medium for each cell type (at room temperature). All NM treatments were carried out in the dark.

3.9 WST-1 cell viability assay

The WST-1 assay is based on the enzymatic cleavage of tetrazolium salt to a water soluble formazan dye by the mitochondria (tetrazolium reductase) in viable cells. An expansion in the number of viable cells results in an increase of overall activity of mitochondrial dehydrogenases, hence more WST-1 is converted to the formazan which can be detected and quantified. This absorbance value is representative of cell viability (Al-Nasiry, *et al*., 2007).

All cells were seeded in 96 well plates (10^4 cells per well in 100 μl of the cell culture medium) and incubated for 24 hr at 37ºC and 5% CO_2. The following day the cells were exposed to the materials or controls for 24 hr at 37ºC, 5% CO_2. Subsequent to NM treatment, cell supernatants were collected and frozen at -80ºC and later used for enzyme linked immunosorbent assays (ELISA), FACSArray, urea analysis and CYP450 activity measurement where appropriate. The cells were washed twice with phosphate buffered saline (PBS), followed by the addition of 10 μl of the WST-1 cell proliferation reagent (Roche, USA) and 90 μl of fresh medium. Cells were then incubated for 1 hr at 37ºC, 5% CO_2. The plates were spun for 2 mins at 1000 g. The supernatant was transferred to a fresh plate and the absorbance measured by dual wavelength spectrophotometry at 450 nm and 630 nm using a micro-plate reader (supernatants were transferred into fresh plates in order to decrease the potential interference of the NMs during the measurement of the absorbance).

3.10 Alamarblue cell viability assay

Alamarblue is a non-toxic, cell-permeating compound that is blue in colour and virtually non-fluorescent. Upon entering cells, resazurin is reduced to resorufin, which produces very

bright red fluorescence. Viable cells continuously convert resazurin to resorufin, thereby generating a quantitative measure of viability and cytotoxicity (Al-Nasiry, *et al*., 2007).

The cells were plated and exposed to the selected NMs as previously described (Section 3.7 and 3.8). The supernatants were removed and the plates washed twice with PBS. Alamarblue cell proliferation reagent (Invitrogen, UK) (10 µl) and 90 µl of fresh medium was added to each well. The plates were incubated for 2 hr at 37ºC, 5% CO_2. The supernatant from each well was then transferred to a fresh plate and the absorbance measured using a spectrophotometer at a wavelength of 570 nm.

3.11 Enzyme-linked Immunosorbent assay (ELISA)

After exposure, the cell supernatants were collected and stored at -80ºC. The supernatants were centrifuged at 1000 g and cytokine and albumin levels determined by ELISA according to the manufacturer's instructions. Human IL8, TNF-α and IL6 ELISA kits were purchased from Invitrogen (UK), human CRP ELISA from Immune systems (Paignton, UK), human albumin ELISA from Bethyl laboratories (USA), rat cytokine-induced neutrophil chemoattractant-1 (CINC-3) from R and D Systems (USA) and rat IL10 from Abcam (USA).

As a positive control the hepatocytes were treated with 10 µg/ml of LPS for 24 hr (Sigma, UK).

3.12 Cytometric Bead Array cytokine and chemokine analysis

The levels of human IL6, IL8, TNF-α and monocyte chemo-attractant protein 1 (MCP-1) produced by the HK-2 cells and IL6, TNF-α, and IFN-γ produced by a co-culture of primary rat hepatocyte and Kupffer cells was measured using the BD™ Cytometric Bead Array cytokine flex sets (bead based immunoassay) according to the manufacturer's instructions.

In this assay flow cytometry is used to discriminiate between different bead population based on size and fluorescence. The flex sets employ micro particles with discrete fluorescence intensities to detect soluble anylates (in this case different cytokines or chemokines). Each bead provides a capture surface for a specific protein and is analogous to an individually coated well of an ELISA plate.

3.13 Urea assay

In order to investigate the effects of NM exposure on urea production, a QuantiChrom Urea assay kit (BioAssay Systems, USA) was utilised. After exposure to the materials, the C3A cell supernatants were collected (Section 3.6). All samples were diluted (1:50) in distilled water and 50 µl of each sample was added to appropriate wells. Working reagent (200 µl) made from two components (reagent A: – *o*-phthalaldehyde <0.40%, Brij 35 <0.04%, sulphuric acid 10% and reagent B: – Primaquine diphosphate <0.08%, boric acid <0.8%, sulphuric acid 22% and Brij 35 <0.04%) was also added to all wells (1:1). The plates were incubated for 30 mins at room temperature and the absorbance read at a wavelength of 430 nm on a plate reader.

3.14 Antioxidant pre-treatment of hepatocytes

The C3A cells were seeded in 96 well plates at 10^4 cells per well in 100 µl of the complete cell culture medium and incubated for 24 hr at 37ºC and 5% CO_2. In order to investigate the possible intervention of antioxidants on cytotoxicity, ROS or cytokine production from the hepatocytes, they were pre-treated with 100 µM of Trolox (6-hydroxy-2,5,6,7,8-tetramethylchroman-2-carboxylic acid) in complete medium for 1 hr. The medium containing the antioxidant was removed before the addition of the nanomaterials as described above (Section 3.7).

3.15 2',7'-dichlorfluorescein-diacetate (DCFH-DA) assay

C3A cells were seeded on a 96 well plate in complete phenol red free (reduce interference) C3A medium ($1x10^4$ cells per well) and incubated at 37°C, 5% CO_2 for 24 hr. The cells were exposed to the NMs or equivalent control (hydrogen peroxide 100 µM – positive control) in complete medium for up to 24 hr.

DCFH-DA is air, light and temperature sensitive so great care was taken when preparing the final working concentration. Following incubation, cells were rinsed and 100 µl of 2 mM DCFH-DA was added before the plates were incubated in the dark at room temperature for 1 hr. Cells were rinsed again and 200 µl of 90% DMSO in PBS was added and incubated on a shaker for 5 mins at room temperature. The plates were wrapped in foil to protect from light

before being centrifuged for 2 mins at 250 g. This was followed by the measurement of 150 µl of supernatant in black 96 well plates at an excitation wavelength of 485 nm and emission wavelength of 520 nm.

3.16 HE Oxidation (conducted by Université Paris Diderot-Paris 7)

The dihydroethidium (HE) oxidation experiment was carried by partners at the Université Paris Diderot-Paris 7, with the details provided in appendix 3.

3.17 Measurement of total glutathione

The protocol is adapted from Senft, *et al*., 2000. A 3 ml cell suspension of cultured cells ($1x10^6$ cells per ml) was added to 6 well plates and incubated overnight at 37°C and 5% CO_2. The cells were exposed to the NMs or equivalent control dispersant in complete medium for 24 hr before being scraped into ice cold phosphate buffered saline and centrifuged (700 g for 2 mins). The cell pellet was re-suspended in ice-cold lysis buffer, mixed and incubated on ice for 10 mins before being centrifuged at 15000 g for 5 mins to generate lysates and protein pellets. Glutathione was quantified in the lysate by reaction of sulfhydryl groups with the fluorescent substrate *o*-phthaladehyde (OPT) (OPT reacts with intracellular GSH to generate fluorescence) using a fluorimeter with an excitation wavelength of 350 nm and emission wavelength of 420 nm.

The protocol was slightly modified to include measurements of total glutathione by reducing oxidase glutathione dimers (GSSG) by addition of 7 µl of 10 mM sodium dithionite to all samples and incubating at room temperature for 1 hr.

The rat and mice liver tissues were thawed on ice and homogenised in 2 ml of lysis buffer on ice and centrifuged (700 g for 5 mins). The pellet was re-suspended in ice-cold lysis buffer (Senft, *et al*., 2000), mixed and incubated on ice for 10 mins before being centrifuged at 15000 g for 5 mins. Glutathione was quantified in the lysate by reaction of sulfhydryl groups with the fluorescent substrate OPT using a fluorimeter with an excitation wavelength of 350 nm and emission wavelength of 420 nm.

3.18 FPG modified Comet assay

The FPG (formamidopyrimidine [fapy] – DNA glycosylase) modified Comet assay was used to measure DNA strand breaks and specific oxidative DNA damage such as 7, 8-dihydro-8-oxoguanine, 8-oxoadenine, fapy-guanine etc., based on the method described by Speit, *et al*., 2004. In this study the tail moment (Wilkland, *et al*., 2003) was measured using an automatic image analyser (Comet Assay IV; Perceptive Instruments, UK) connected to a fluorescence microscope. Images were captured using a stingray (F-033B/C) black and white video camera.

After a 4 hr NM treatment (or positive control - 60 µM of H_2O_2), the cells were rinsed twice with PBS and detached using trypsin before being suspended in 5 ml of culture medium. Cells were centrifuged for 10 mins at 250 g, 4ºC and re-suspended at a concentration of 1.5 x 10^6 cells/ml in complete medium. A 20 µl volume of calculated cell suspension was added to 240 µl of 0.5% low melting point agarose. Next, 125 µl of the mixture was added to pre-coated slides (1.5% agarose) in triplicate. Following 10 mins of solidification on ice, slides were lysed overnight at 4ºC in lysis buffer (2.5 M NaCl, 100 mM EDTA, 10 mM Tris-base, pH 10, containing 10% DMSO and 1% TritonX-100). The slides were washed three times for 5 mins with FPG-enzyme buffer (40 mM HEPES, 100 mM KCl, 0.5 mM EDTA, 0.2 mg/ml BSA - pH 8), covered with 100 µl of either buffer or FPG in buffer (1:30), sealed with a cover slip and incubated for 30 mins at 37ºC. FPG cleaves DNA at locations of oxidation leading to a greater tail for cells exhibiting oxidative DNA damage (Wilkland, *et al*., 2003). All slides were then transferred into a black chilled electrophoresis tank. After alkaline unwinding (pH 13) for 20 mins, electrophoresis was performed for 15 mins at 270 mA, 24 V. Slides were neutralized three times for 5 mins using a neutralization buffer (0.4 M TrisBase, pH 7.5). Before analysis, slides were dried in air for 10 mins and stained with GelRed (2 in 10000, 40 µl per slide). A total of 50 cells were analyzed per slide per experiment.

The longer term genotoxic ability of Ag NM (NM 300) was also investigated. The C3A cells were exposed to the NMs for 24 hr before being allowed to recover for 72 hr. The cells were then detached by treating with trypsin before being transferred to a new flask. After 48 hr the cells were treated with the Ag NMs for 24 hr, with the whole process being repeated for a period of 8 weeks.

3.19 Cytochrome P450 assay

After exposure, the hepatocyte supernatants (from both the control and treated cells as described in Section 3.7) were collected and stored at -80ºC. The supernatants were centrifuged at 1000 g and a DetectX® P450 activity kit (ArborAssays, USA) was utilised to quantitatively measure the enzymatic activity of CP450s from the C3A and primary hepatocytes according to the manufacturer's instructions.

3.20 Transmission Electron Microscopy (TEM)

The hepatocytes were seeded in 6 well plates in cell culture medium (minimum of 1 x 10^6 cells per well) and incubated at 37°C, 5% CO_2 for 24 hr. Cells were exposed to 5 µg/cm^2 of the chosen NMs for 4 hr (control cells were treated with fresh medium). The samples were thoroughly washed with fresh medium (x2) before being removed from the plastic and transferred to BEEM capsules. The tubes were spun for 5 mins at 1000 g, before the addition of 1 ml of 2.5% gluteraldehyde in PBS for 2 hr. The cells were then washed (x3) with PBS followed by the addition of 1 ml of 1% osmium tetroxide in PBS to the pellet for 10 mins before being rinsed five times with PBS and two times with distilled water. The samples were dehydrated in 50%, 70%, 90% and 100% ethanol for 10 mins each. After the removal of the ethanol a 50:50 mixture of resin and ethanol was added for 45 mins before being replaced with 100% resin and incubated for 24 hr. The samples were embedded and cured before being fastened to a trimming block. An ultramicrotome was used to produce a final trapezoid shape of around 1 mm or less. The samples were cut into 50-100 nm sections and transferred onto TEM grids. The grids were coated with 5 nm of evaporated carbon prior to imaging to minimise charging. A FEI Tecnai TF20 FEGTEM microscope fitted with a Gatan Orius SC600 CCD camera and an Oxford Instruments 80 mm^2 X-Max EDX detector was utilised to image the cells and perform chemical analysis via energy dispersive X ray (EDX) analysis. The TEM analysis was carried out at the Leeds Nanoscience and Nanotechnology Research Equipment Facility.

3.21 Scanning Electron Microscopy (SEM)

C3A and the primary hepatocytes were seeded on 10 mm sterile cover-slips in 24 well plates ($2x10^5$ cells per well in 500 µl of the cell culture medium) and incubated for 24 hr at 37ºC

and 5% CO_2. Cells were exposed to 5 μg/cm^2 of the chosen NMs for 4 hr. The cells were washed with 0.1 M sodium cacodylate buffer (pH 7.3) before being fixed with 2% gluteraldehyde for 2 hr at 4°C. The cells were washed (x3) with 0.1 M sodium cacodylate buffer before being dehydrated in 50%, 70%, 90% and 100% acetone for 10 mins each. The samples were then critical point dried and mounted on aluminium stubs and sputter coated with gold for 45 sec. A FEI Quanta 3D SEM was utilised to image the cell and NMs surface interaction. A special mention to Mrs Marian Millar for her invaluable help with the SEM analysis.

3.22 Statement of Animal Welfare

The animal studies related to this project were either conducted by Dr Ilse Gosens (RIVM, The Netherlands) or myself in Edinburgh. All work conducted by the RIVM is described in appendix 4.

All UK experiments involving animal cells described were performed under a Project License and Personal License issued by the United Kingdom Home Office. Sprague Dawley rats (male, 3 months old) and C57BL/6 mice (female, 10 weeks old) were obtained from Biomedical Research Resources, Royal Infirmary Edinburgh (Edinburgh, UK) and housed in conditions approved by the UK Home Office. The animals were caged in pairs with free access to food and water and at a temperature of 23 ± 1°C. The animals were kept under specific pathogen free conditions.

3.23 Rat liver cells isolation and culture

Liver cells were isolated using a classical two-step collagenase perfusion method, modified to obtain higher yields of cells. Briefly, after a first anterograde perfusion through the hepatic portal vein, the liver was perfused in a retrograde fashion through the inferior vena cava with a Hank's buffered salt solution devoid of calcium (HBSS) (Sigma, UK) before being perfused with L15 medium (Life Technologies, UK) supplemented with HEPES (10 mM), glutamine (2 mM), Gentamycin (50 μg/ml) and 40 U/ml of collagenase (Roche) for 25 min. The liver was then cut down to small pieces, rinsed with ice-cold cell culture medium before being incubated again in the collagenase solution for 10 min. The resulting cell suspension was then filtered with a nylon gauze and then left to sediment for 15 min at 4°C. The cell pellet and the

unsettled cells in the supernatant were collected for further processing and Kupffer cell isolation (termed second pass cells). The settled cell suspension was spun down at 300 g and the supernatant discarded. A typical isolation resulted in a suspension of $70x10^6$ single cells and duplet/triplet with over 90% viability, as assessed by trypan blue exclusion.

The freshly isolated cells were seeded on rat tail collagen (Serve, Germany) or matrigel (BD, UK) coated 96 well plates in HepatoZyme medium at 37ºC and 5% CO_2 for a minimum of 4 hr before NM treatment (10^4 cells per well).

3.24 Rat liver cell characterisation

This work was carried out principally by my colleague Dr Celine Filippi at Heriot Watt University and is described in appendix 5 and 6.

3.25 Kupffer cell isolation and enrichment

For the isolation of Kupffer cells, the fraction of cells mentioned above (Section 3.23) was centrifuged at 800 g and the supernatant discarded. The pellet was used to positively select Kupffer cells using a magnetic-bead based cell purification system (MACS) (Miltenyi Biotech, Germany) with an anti CD163-PE coupled antibody (MCA342PE) (AbD Serotec, UK) and Anti PE microbeads (Miltenyi Biotech, Germany). Briefly following the addition of the primary PE conjugated antibody the cells were incubated in the dark for 10 mins at 4°C. The cells were washed with autoMACS Rinsing solution (Miltenyi Biotech, Germany) to remove unbound primary antibody. The Anti PE microbeads were added (20 µl per 10^7 cells). The cells were mixed well and incubated for 15 mins at 4°C in the dark. The cells were once again washed and added to the column. The Kupffer cells magnetically attached to the column while the other cell types were eluted. This typically increased the Kupffer cell content from 4% to 30% of the cell suspension.

3.26 Intravenous injections

Prior to injections the NMs were dispersed in sterile water with 2% mouse serum according to the ENPRA protocol (Jacobsen, *et al*., 2010). C57/BL6 mice were randomly assigned into cages in groups of two before being injected via the lateral tail vein using a 27 gauge needle.

All animals were kept under isoflurane anaesthesia during the injection process (placed on a thermostat controlled heating device at 37°C). Animals were exposed to either a single dose of the different nanomaterials (128 µg/ml – 100 µl) or three doses of 100 µl of 64 µg/ml every 24 hr. A positive control of LPS (50 µl - 100 µg/ml) was also employed. The mice were dissected 6, 24, 48 and 72 hr after the single IV injection, or 72 hr after the triple injection regime (anaesthetised before being killed by cervical dislocation). The liver was then divided into four pieces. The middle lobe was divided into two – one section was frozen in liquid nitrogen for GSH measurements (about 0.2 g of tissue), while the other half was stored in RNAlater® (Life Technologies, UK). The left lobe was removed for myeloperoxidase (MPO) analysis (about 0.3g of tissue). The Right lobe was preserved in 10% formaldehyde for immunohistochemistry (about 0.3g of tissue).

3.27 Myeloperoxidase assay

A mouse MPO ELISA kit (Hycult Biotech, USA) was utilised to quantify neutrophil influx into the liver tissue. Briefly, the tissue was lysed in a lysis buffer consisting of 5 mM EDTA, 10 mM Tris, 10% glycerine, 1 mM phenylmethylsulfonyl fluoride, 1 µg/ml leupeptin and 28 µg/ml aprotinin (pH 7.4). The samples were centrifuged twice at 1500 g for 15 mins at 4°C and the supernatant removed to reduce contamination with cell debris. All samples were diluted 4 fold before being used in the ELISA kit according to the manufacturer's instructions.

3.28 Immunohistochemistry

The fixed tissue sections (section 3.26) were transferred to embedding cassettes before being dehydrated in 70% ethanol (2 changes, 1 hr each), 80% ethanol (2 changes, 1 hr each), 95% ethanol (2 changes, 1 hr each), 100% ethanol (3 changes, 1 hr each) and Histoclear II **(**3 changes, 1 hr each). The tissues were then embedded in paraffin wax (56-58ºC - 2 changes, 1.5 hr each). The blocks were cut into thin slices (4 µm) before being transferred to a 45ºC water bath. The paraffin sections were moved onto polysine glass slides, brushed into position before being dried overnight at 37ºC. The slides were rehydrated in Histoclear II (2 changes, 3 mins), Histoclear II 1:1 with 100% ethanol (3 mins), 100% ethanol (2 changes, 3 mins), 95% ethanol (3 mins), 70% ethanol (3 mins), and 50% ethanol (3 mins). The sections were then washed in tris buffered saline (TBS) plus 0.025% triton (2 x 5 mins) and blocked

with 10% FCS in TBS for 2 hr at room temperature. The primary antibody diluted in TBS with 1% BSA (rat anti-mouse Ly-6B.2 alloantigen – AbD Serotec, UK) was applied (100 µl per slide). The slides were incubated overnight at 4°C.

The slides were rinsed 2 x 5 mins in TBS plus 0.025% triton and incubated in 0.3% H_2O_2 in TBS for 15 mins. The horse radish peroxidise (HRP) conjugated secondary antibody was applied (human anti rat IgG2b: HRP – AbD Serotec, UK) before incubation at room temperature for 1 hr. The slides were rinsed 3 x 5 in TBS and developed with 100 µl of DAB substrate kit (Abcam, USA). The slides were washed and mounted with Mowiol 4-88 (Polysciences Inc., UK).

3.29 Intratracheal instillation

The installation procedures were carried out at Centre for Environmental Health Research, National Institute for Public Health and the Environment (Netherlands). Deatils are provided in Apppendix 4.

3.30 RNA isolation, RT reaction and Real time PCR

Liver samples were homogenised in liquid nitrogen using a mortar and pestle. Homogenised tissues were stored at -80°C before RNA was extracted and isolated using the MagMAX™ -96 Total RNA Isolation Kit (Ambion, USA). RNA concentration and purity were measured on a Nanodrop 2000c system (Thermo Scientific, UK). The High Capacity cDNA RT kit (Applied Biosystems, UK) was used according to the protocol to transcribe RNA into cDNA. Equal quantities of RNA from 3 animals in the same treatment group were pooled and 300 ng of RNA were used in RT reactions.

PCRs were conducted in triplicate on a 7900 RT fast PCR system and SDS 2.3 software in 384 well plates (Applied Biosystems, USA), using TaqMan kits with FAM dye under standard TaqMan conditions for 50 cycles. The following Applied Biosystems kits were used: Mouse kits Mm00437762-m1 – B2m (housekeeping gene); Mm00436450-m1 – CXCL2; Mm00439614-m1 – IL10; Mm00443258-31 – TNF-α; Mm00437858-m1 – C3; Mm00438864-m1 – Fas ligand; Mm00516023-m1 – ICAM-1; Mm00802090-m1 – albumin and Mm00446190-m1 – IL6.

3.31 Statistical analysis

The statistical significance of the results was assessed using ANOVA (analysis of variance test), with a Tukey multiple comparison, using the Minitab 15 programme. ANOVA analysis was specifically selected as it allows for comparisons to be made between the means of several treatment groups. All findings were considered significant if the p value was below 0.05. The null hypothesis for ANOVA analysis is that the means from different treatment groups are the same. Therefore, if the null hypothesis is rejected (i.e. if $p<0.05$), it can be concluded that at least one group differs from the rest. To reveal which groups were different from one another a Tukey comparison was incorporated within the test. This test determines if there are any significant differences between the different groups. If these differences are evident it establishes what groups are significantly different from each other. Accordingly within this study it is absolutely critical to consider if the different particle treatments differ to the control groups. All experiments were repeated a minimum of three times.

Chapter Four

In vitro assessment of engineered nanomaterials using C3A hepatocytes: Cytotoxicity, pro-inflammatory cytokines and function markers

Based on publication: Kermanizadeh A, Pojana G, Gaiser BK, Birkedal R, Bilaničová D, Wallin H, Jensen KA, Sellergren B, Hutchison GR, Marcomini A, Stone V. (2012c). *In vitro* assessment of engineered nanomaterials using a hepatocyte cell line: cytotoxicity, pro-inflammatory cytokines and functioal markers. Nanotoxicology DOI: 10.3109/17435390.2011.653416.

4.1 Aims and chapter outline

To investigate the potential of the panel of engineered NMs to induce an inflammatory response in the hepatoblastoma cell line (C3A), measured by the release of pro-inflammatory cytokines (IL6, IL8 and TNF-α), C reactive protein (CRP) and the functional markers albumin and urea.

4.2 Characteristics of nanomaterials and exposure media

Investigated NMs were characterised by a combination of analytical techniques in order to infer primary physical and chemical properties useful to understand their toxicological behaviour. A list of the measured physical and chemical properties of selected NMs is presented in Table 4.1. All of this data was generated by University Ca' foscari Venice, but it is included here as characterisation of NM is fundamental to understanding their toxicity.

ENM code	ENM type	Phase	XRD Size [nm]	TEM Size	Primary characteristics by TEM analysis	Surface area (BET) [m^2/g]	Known coating	Size in MEM (DLS) Ψ
NM101	TiO_2	Anatase €	9	4-8 /50-100	Two structures found; type 1 show agglomerates in the 50 - 1500 nm range	322	none	185, 742
NM110	ZnO	Zincite	70 to > 100	20-250 / 50-350	Mainly 2 euhedral morphologies: 1) aspect ratio close to 1 (20 - 250 nm range and few particles of approx. 400 nm) 2) Ratio 2 to 7.5 (50-350 nm). Minor amounts of particles with irregular morphologies observed.	14	none	306
NM111	ZnO	Zincite	58-93	20-200 / 10-450	As NM110, but with different size distributions. 1) Particles with aspect ratio close to 1 (~90% in the 20-200 nm range); 2) particles with aspect ratio 2 to 8.5 (~90% in the 10-450 nm ratio).	18	Trie-othoxy-capry-lsilane 130	313
NM300	Ag	Ag	7[$] 14[£] <18 / 15 / > 100[#]	8-47 (av.: 17.5)	Mainly euhedral NM; minor fractions have either elongated (aspect ratio up to ~ 5) or sub-spherical morphology	NA	none	12, 28, 114
NM400	MWCNT	-	-	D: 5-35 L: 700-3000	Irregular entangled kinked and mostly bent MWCNT (10-20 walls). Some CNTs were capped and some cases multiple caps were found due to overgrowth. Fe/Co	298	none	*

					catalysts (6-9 nm, average 7.5 nm) were found inside the tubes.			
NM402	MWCNT	-	-	D: 6-20 L: 700-4000	Entangled irregular, mostly bent MWCNT (6-14 walls). Some tubes were capped by unknown material. Some nano-onions (5-10 nm) and amorphous carbon structures mixed with Fe (5-20 nm). Residual catalyst was observed. Individual catalyst particles up to 150 nm were also detected.	225	none	*
NRCWE 001	TiO_2	Rutile[§]	10	80-400	Irregular euhedral particles detected by TEM	99	none	203
NRCWE 002	TiO_2	Rutile	10	80-400	Irregular euhedral particles detected by TEM	84	Positive charged	287
NRCWE 003	TiO_2	Rutile	10	80-400	Irregular euhedral particles detected by TEM	84	Negative charged	240, 1487
NRCWE 004	TiO_2	Rutile	App. 100	1-4/ 10-100/ 100-200/ 1000-2000	Five different particle types were identified: 1) irregular spheres, 1-4 nm (av. Diameter); 2) irregular euhedral particles, 10-100 nm (longest dimension); 3) fractal-like structures in long chains, 100-200 nm (longest dimension); 4) big irregular polyhedral particles, 1-2µm (longest dimension); 5) large irregular particles with jagged boundaries, 1-2 µm (longest dimension).			339

[€] 1 percent rutile found in one of two samples analyzed
[$] wet XRD in capillary tube
[£] dried samples
[#] sample with deposits
[§] ca. 6% anatase was observed in one of two samples analyzed
* Not detectable by DLS due to the very large aspect ratio
Ψ Intensity based size average in biological media after 15 mins.

Table 4.1. Main physical and chemical properties of tested ENMs (Reproduced from Kermanizadeh, *et al*., 2012c).

4.3 Impact of the selected panel of NMs on C3A cell viability

From the WST-1 data it was evident that there was a dose dependent decrease in cell viability at 24 hr across the entire nanomaterial panel (Figure 4.1). However, an LC_{50} could only be determined for exposures to Ag (NM 300) 2 μg/cm^2, uncoated ZnO (NM 110) 7.5 μg/cm^2 and coated ZnO (NM 111) 15 μg/cm^2 after a 24 hr exposure (Figure 4.1b, c and d). The Alamarblue data obtained also showed similar results across the ten NMs. However, this assay gave a slightly higher LC_{50} value (Table 4.2). The WST-1 assay was relatively more sensitive over the steepest part of the curve when compared to the Alamarblue. Silver materials (NM 300) induced the greatest level of toxicity within the C3A cells, followed by the uncoated ZnO (NM 110) and coated ZnO (NM 111) NMs. All of the TiO_2 and MWCNT NMs were considered to be low toxicity materials as the LC_{50} was not reached after a 24 hr exposure to the C3A cells at the range investigated.

We also investigated the toxicity of the ENPRA dispersants namely NM 300 dispersant termed (NM 300 DIS) and 0.5% ethanol in complete C3A medium. We found no toxicity of either dispersant to the C3A cells (data not shown) so we conclude that all observed toxicity is due to exposure to the NMs investigated.

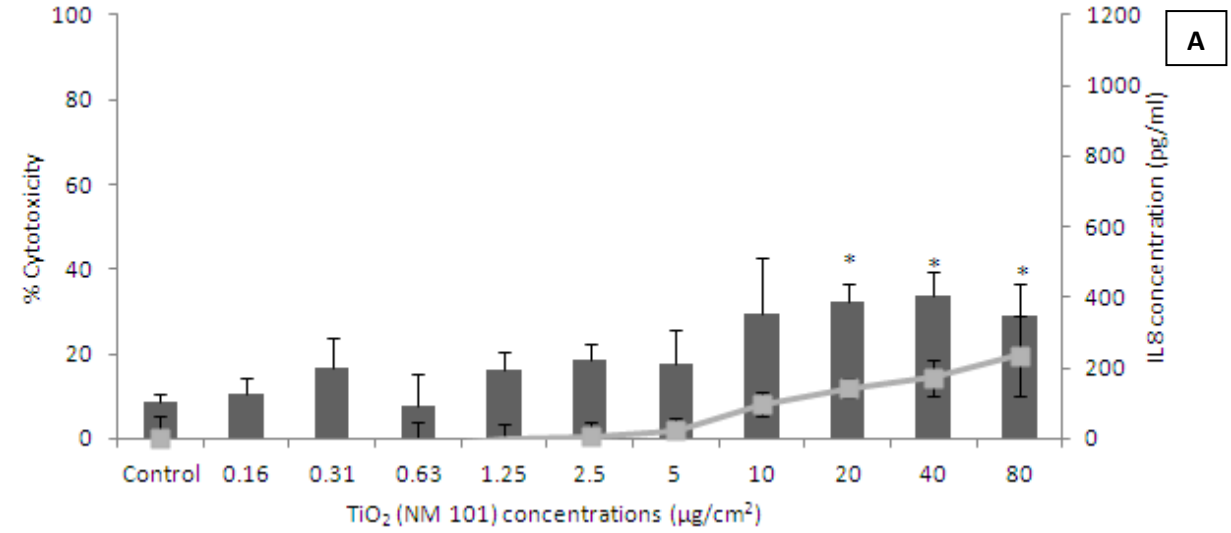
A
% Cytotoxicity
IL8 concentration (pg/ml)
Control
0.16
0.31
0.63
1.25
2.5
5
10
20
40
80
TiO2 (NM 101) concentrations (µg/cm2)

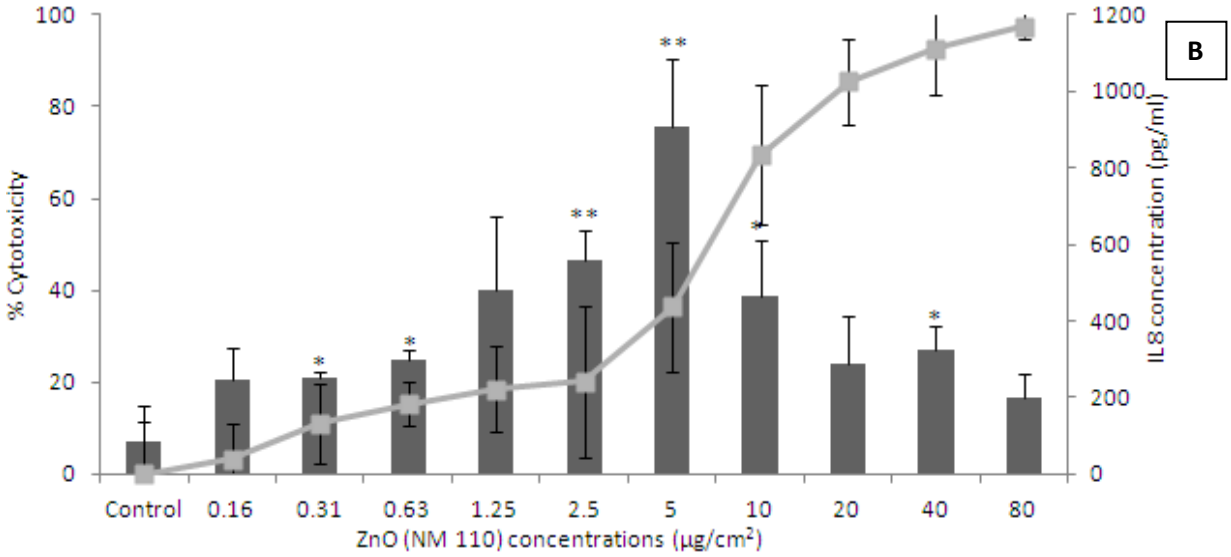
B
% Cytotoxicity
IL8 concentration (pg/ml)
Control
0.16
0.31
0.63
1.25
2.5
5
10
20
40
80
ZnO (NM 110) concentrations (µg/cm2)

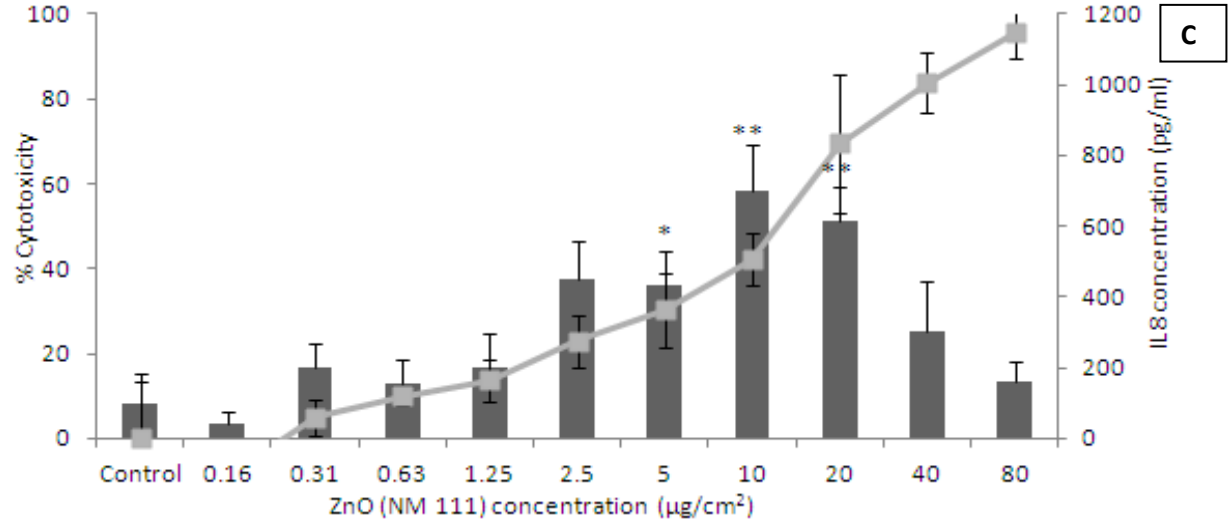
C
% Cytotoxicity
IL8 concentration (pg/ml)
Control
0.16
0.31
0.63
1.25
2.5
5
10
20
40
80
ZnO (NM 111) concentration (µg/cm2)

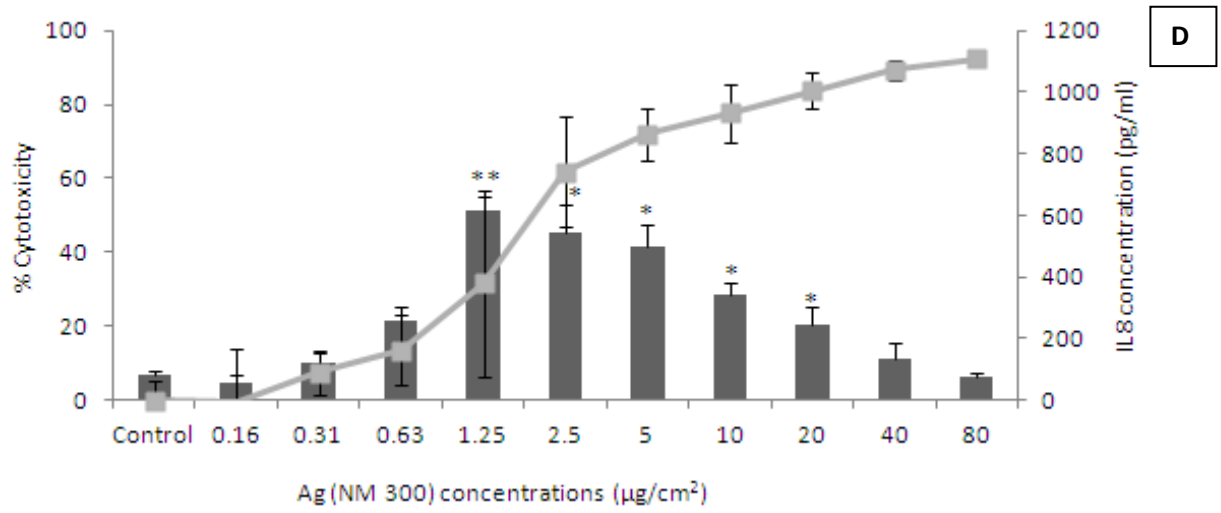
D
% Cytotoxicity
IL8 concentration (pg/ml)
Control
0.16
0.31
0.63
1.25
2.5
5
10
20
40
80
Ag (NM 300) concentrations (µg/cm²)

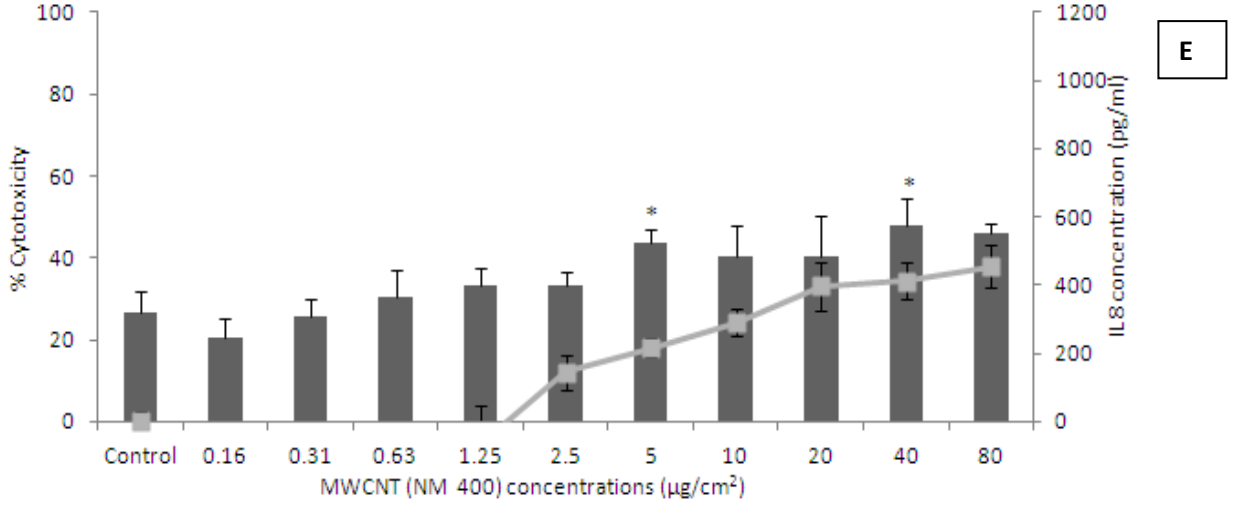
E
% Cytotoxicity
IL8 concentration (pg/ml)
Control
0.16
0.31
0.63
1.25
2.5
5
10
20
40
80
MWCNT (NM 400) concentrations (µg/cm²)

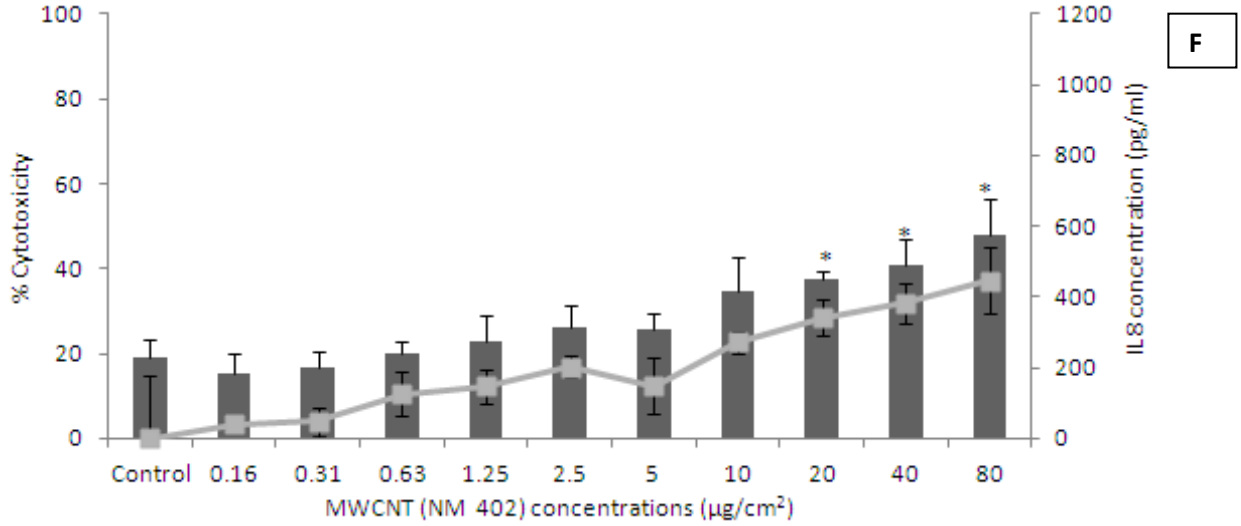
F
% Cytotoxicity
IL8 concentration (pg/ml)
Control
0.16
0.31
0.63
1.25
2.5
5
10
20
40
80
MWCNT (NM 402) concentrations (µg/cm²)

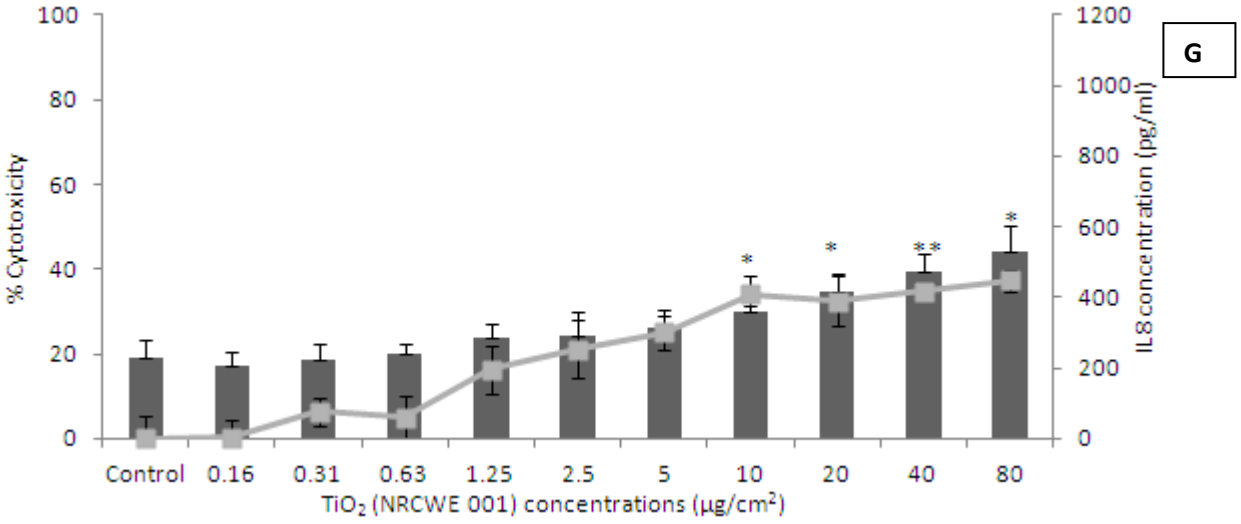
G
% Cytotoxicity
IL8 concentration (pg/ml)
Control
0.16
0.31
0.63
1.25
2.5
5
10
20
40
80
TiO2 (NRCWE 001) concentrations (µg/cm2)

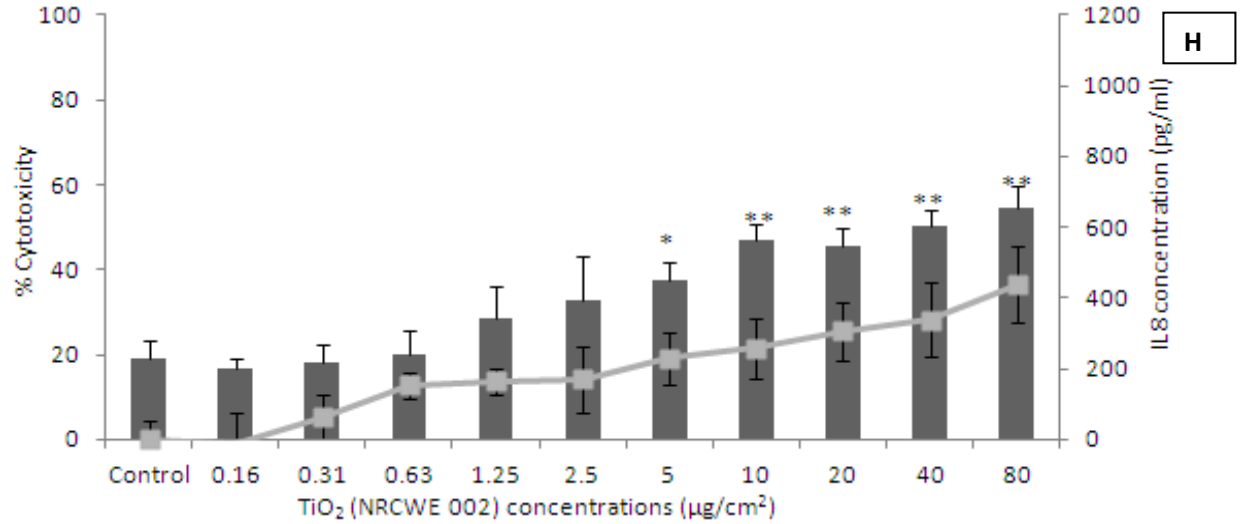
H
% Cytotoxicity
IL8 concentration (pg/ml)
Control
0.16
0.31
0.63
1.25
2.5
5
10
20
40
80
TiO2 (NRCWE 002) concentrations (µg/cm2)

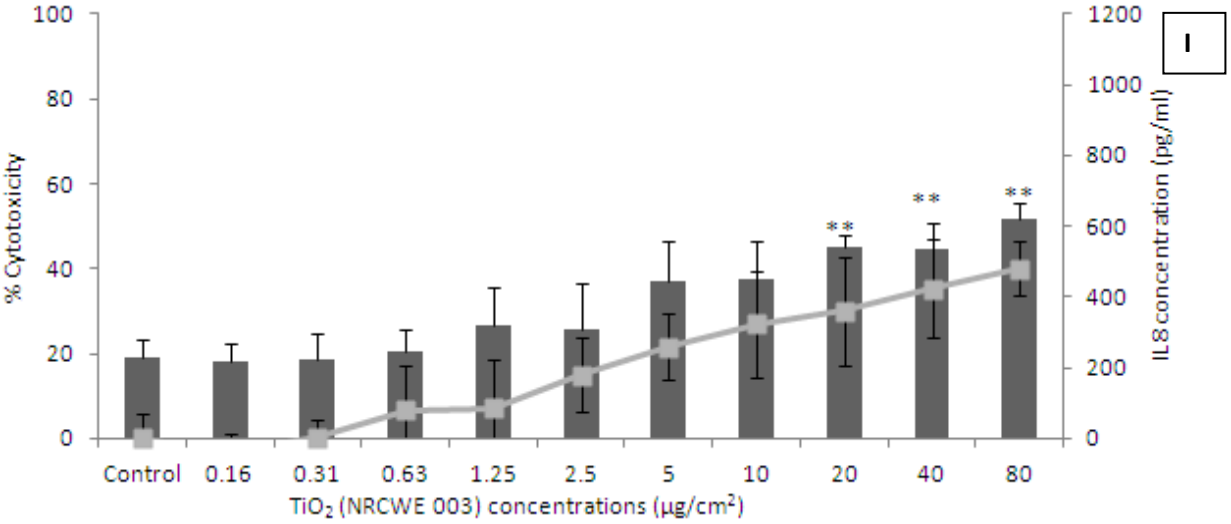
I
% Cytotoxicity
IL8 concentration (pg/ml)
Control
0.16
0.31
0.63
1.25
2.5
5
10
20
40
80
TiO2 (NRCWE 003) concentrations (µg/cm2)

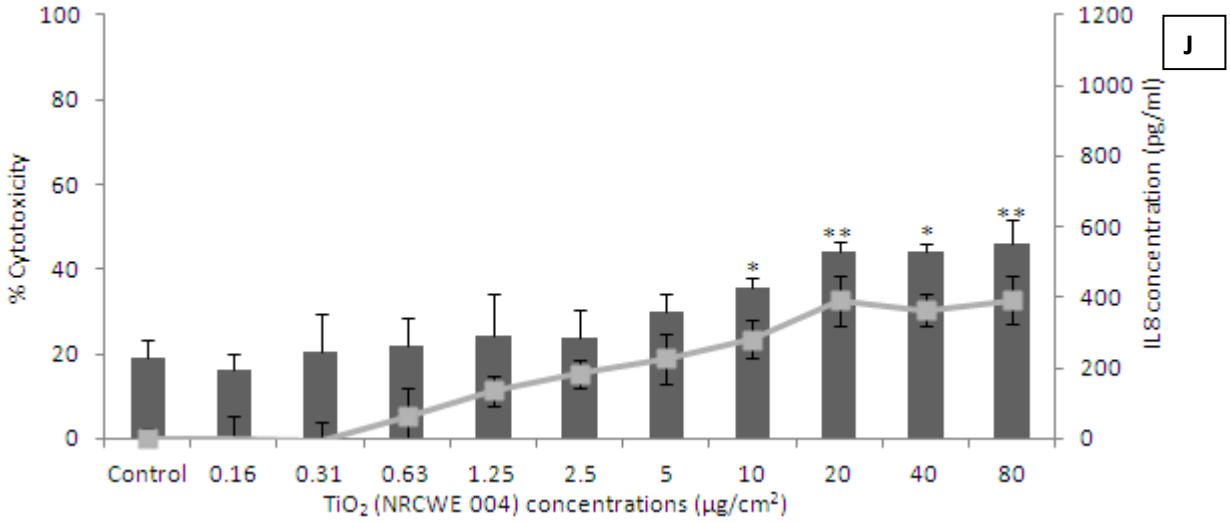

Figure 4.1. Cytotoxicity (grey line) and IL8 production (black bars) by C3A cells following exposure to a panel of engineered nanomaterials. The cells were exposed to cell medium (control)/medium and dispersant for NM 300 and NMs for 24 hr with cytotoxicity measured via WST-1 assay. IL8 production within cell supernatants was measured by ELISA. Values represent mean ± SEM (n=3), significance indicated by * = $p<0.05$ and **= $p<0.005$, when material treatments are compared to the control. **A)** NM 101 **B)** NM 110 **C)** NM 111 **D)** NM 300 **E)** NM 400 **F)** NM 402 **G)** NRCWE 001 **H)** NRCWE 002 **I)** NRCWE 003 **J)** NRCWE 004.

	LC_{50} (WST-1) - µg/cm^2	**LC_{50} (Alamarblue) - µg/cm^2**
NM 101	LC_{50} not reached up to 80 µg/cm^2	LC_{50} not reached up to 80 µg/cm^2
NM 110	LC_{50} between 5 and 10 µg/cm^2	LC_{50} around 10 µg/cm^2
NM 111	LC_{50} is between 10 and 20 µg/cm^2	LC_{50} around 20 µg/cm^2
NM 300	LC_{50} is between 1.25 and 2.5 µg/cm^2	LC_{50} is between 2.5 and 5 µg/cm^2
NM 400	LC_{50} not reached up to 80 µg/cm^2	LC_{50} not reached up to 80 µg/cm^2
NM 402	LC_{50} not reached up to 80 µg/cm^2	LC_{50} not reached up to 80 µg/cm^2
NRCWE 001	LC_{50} not reached up to 80 µg/cm^2	LC_{50} not reached up to 80 µg/cm^2
NRCWE 002	LC_{50} not reached up to 80 µg/cm^2	LC_{50} not reached up to 80 µg/cm^2
NRCWE 003	LC_{50} not reached up to 80 µg/cm^2	LC_{50} not reached up to 80 µg/cm^2
NRCWE 004	LC_{50} not reached up to 80 µg/cm^2	LC_{50} not reached up to 80 µg/cm^2

Table 4.2. WST-1 and Alamarblue cytotoxicity following 24 hr exposure of C3A hepatocytes to NM 101 (TiO_2 - 7 nm), NM 110 (ZnO - uncoated 100 nm), NM 111 (ZnO - coated 130 nm), NM 300 (Ag - <20 nm) and NM 400 (MWCNT), NM 402 (MWCNT), NRCWE 001 (TiO_2 - rutile 10nm), NRCWE 002 (TiO_2 - rutile 10 nm with positive charge), NRCWE 003 (TiO_2 - rutile 10 nm with negative charge) and NRCWE 004 (TiO_2 - rutile 94 nm) NMs.

Identifying the soluble fraction of Ag and ZnO NMs added to the cells is extremely important for the discrimination between effects induced by the NMs and dissolved elements therein. Therefore, 24 hr dissolution of NM 110, NM 111 and NM 300 was investigated in pure water and the C3A complete medium at 1, 16 and 128 µg/ml (Table 4.3). It was observed that silver (NM 300) had very low, but dose-dependent solubility in water (<0.01%). This solubility was slightly lower in the C3A medium. It is important to note that the C3A medium contained 3 x 10^{-4} mg of water soluble Zn/ml. The solubility of the NM 110 samples was between 6 x 10^{-4} and 3.73 x 10^{-4} mg/ml in water (1 and 128 µg/ml). In C3A medium, this concentration varied from 7 x 10^{-4} to 5.92 x 10^{-4} mg/ml in from the lowest to the highest concentration. The solubility of NM 111 in water was lower than NM 110 (2 x 10^{-4} to 1. 72 x 10^{-4} mg Zn/ml from the lowest to highest concentration). These results suggest that about 40 to 50% of the added ZnO NMs were dissolved in the cell-medium after 24 hr. The amount of dissolved Ag was low and less than 1 % by weight.

Treatment (µg/ml)	**NM 110**		**NM 111**		**NM 300**	
	H_2O	Medium	H_2O	Medium	H_2O	Medium
1	59.90%	46.70%	17.60%	38.90%	< 0.01%	< 0.01%
16	31.68%	33.12%	10.06%	25.13%	0.78%	0.19%
128	29.14%	23.36%	13.43%	26.48%	0.59%	0.47%

Table 4.3. Percentage values of the Ag (NM 300) and the ZnO nanomaterials (NM 110, NM 111) dissolved in Water and C3A complete medium following 24 hr of incubation at 37°C, 5% CO_2.

4.4 Impact of the engineered NMs on C3A hepatocyte IL8 production

Changes in cytokine production as a consequence of NM exposure were assessed within the supernatant of exposed hepatocytes and quantified via ELISA. For the low toxicity TiO_2 and MWCNT samples (NM 101, NM 400, NM 402, NRCWE 001, NRCWE 002, NRCWE 003 and NRCWE 004) the IL8 production increased in a dose dependent manner, reaching statistical significance compared to the control at high exposure concentrations (Figure 4.1a, e, f, g, h, i and j). However, in the presence of the highly toxic particles Ag and ZnO (NM 110, NM 111 and NM 300) there was a significant increase in the level of IL8 protein production that peaking around the LC_{50} values, followed by a decrease in the amounts of the cytokine produced as the toxicity increased (Figure 4.1b, c and d).

4.5 Impact of the NMs on C3A hepatocyte IL6, TNF-α and CRP production

Secretion of IL6, TNF-α and CRP into the supernatant of exposed C3A hepatocytes was quantified using ELISA analysis. There was no significant increase or decrease in the production of IL6, TNF-α or CRP after the exposure of the C3A cells to any of the selected nanomaterials (data not shown).

4.6 Impact of engineered NMs on urea and albumin production by C3A hepatocytes

In order to establish whether any of the NMs affected urea and albumin production, four exposure concentrations were chosen for each material. These concentrations included the LC_{50} and three subsequently lower concentrations for the highly toxic materials (NM 110, NM 111 and NM 300) and two high and two low concentrations for the low toxicity nanomaterials (80, 20, 2.5 and 0.31 $\mu g/cm^2$). It was observed that none of the investigated NMs were able to modify urea production following a 24 hr exposure period (Figure 4.2). There was a significant decrease in levels of albumin secreted at LC_{50} concentrations for both ZnO NMs – NM 110 and NM 111 (compared to the control) (Figure 4.2b and c). However, none of the other eight NMs were capable of affecting albumin production by hepatocytes.

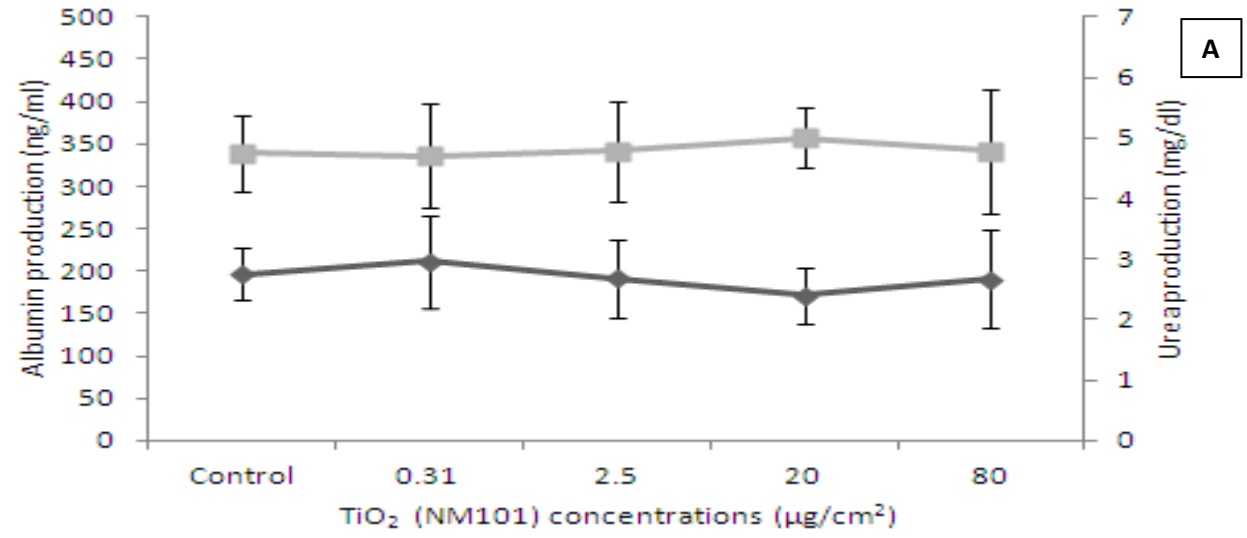
A
Albumin production (ng/ml)
Ureaproduction (mg/dl)
500
450
400
350
300
250
200
150
100
50
0
7
6
5
4
3
2
1
0
Control
0.31
2.5
20
80
TiO2 (NM101) concentrations (µg/cm2)

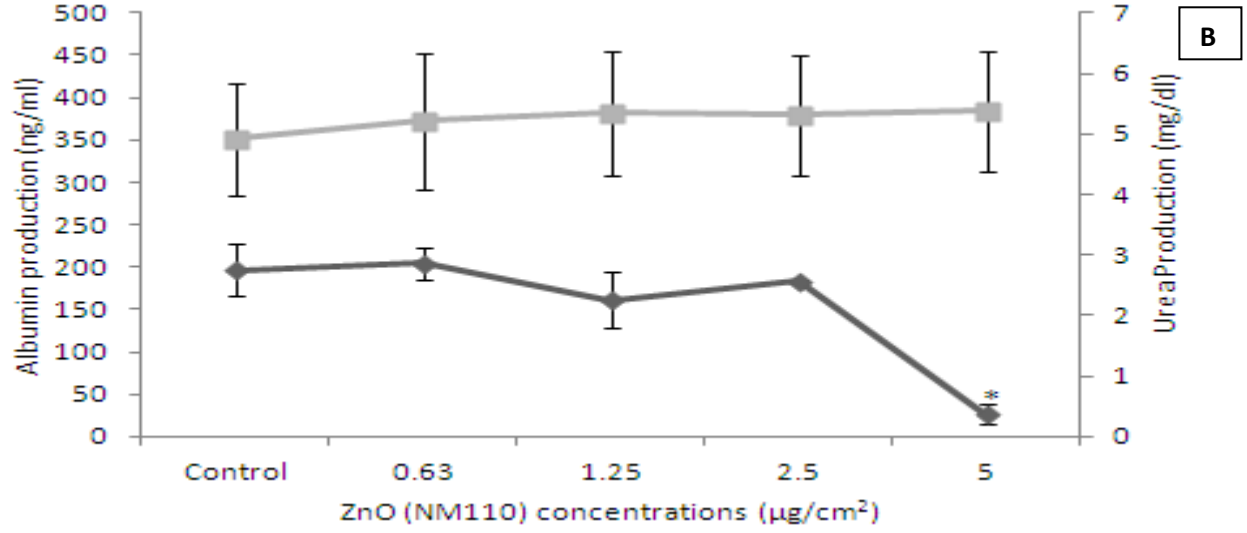
B
Albumin production (ng/ml)
UreaProduction (mg/dl)
500
450
400
350
300
250
200
150
100
50
0
7
6
5
4
3
2
1
0
*
Control
0.63
1.25
2.5
5
ZnO (NM110) concentrations (µg/cm2)

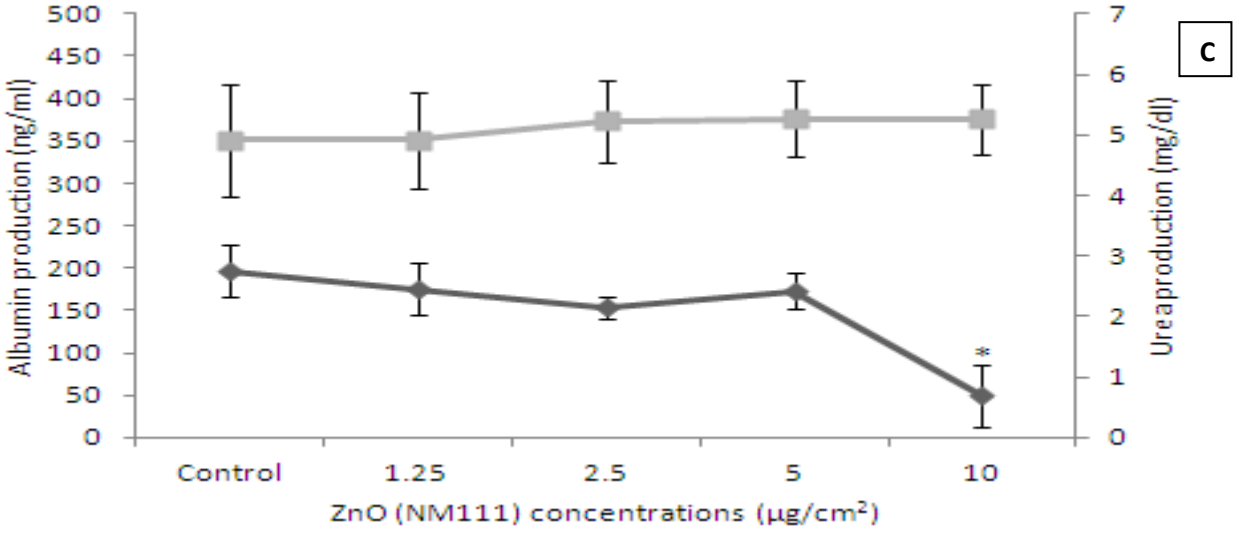
C
Albumin production (ng/ml)
Ureaproduction (mg/dl)
500
450
400
350
300
250
200
150
100
50
0
7
6
5
4
3
2
1
0
*
Control
1.25
2.5
5
10
ZnO (NM111) concentrations (µg/cm2)

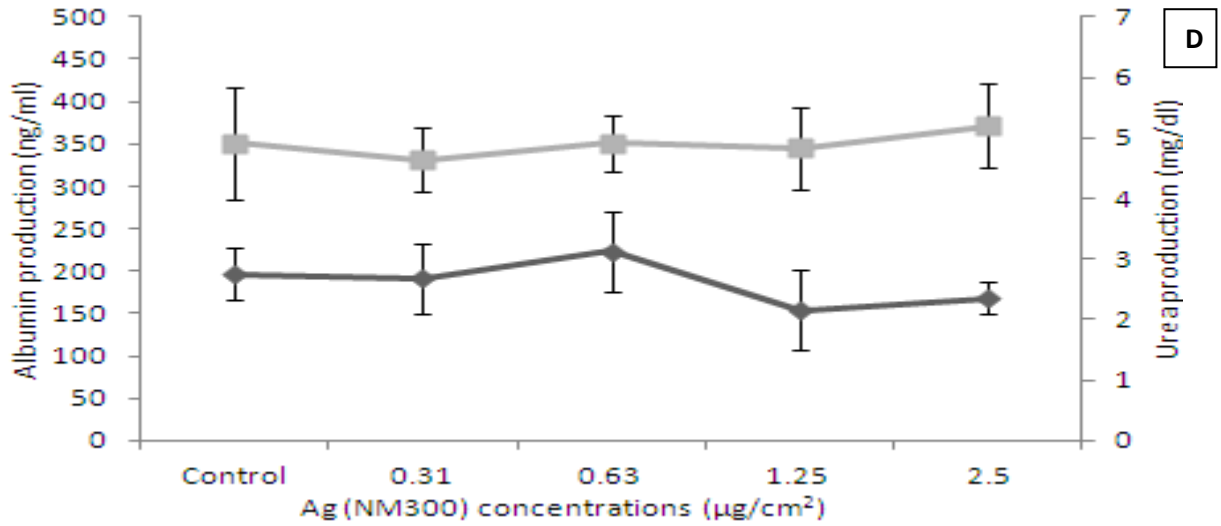
D
Albumin production (ng/ml)
Urea production (mg/dl)
Control
0.31
0.63
1.25
2.5
Ag (NM300) concentrations (µg/cm²)

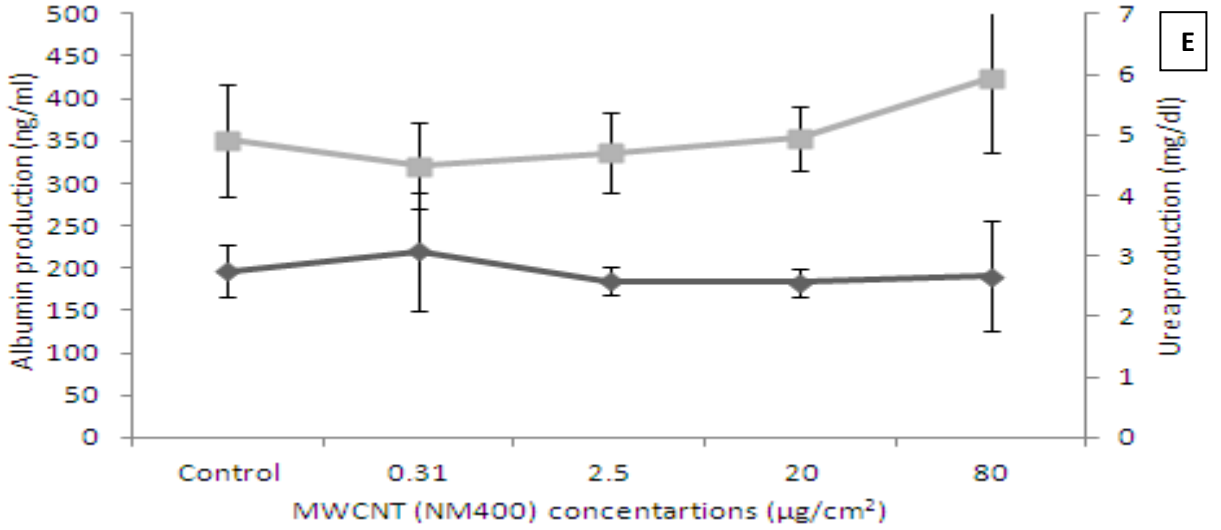
E
Albumin production (ng/ml)
Urea production (mg/dl)
Control
0.31
2.5
20
80
MWCNT (NM400) concentartions (µg/cm²)

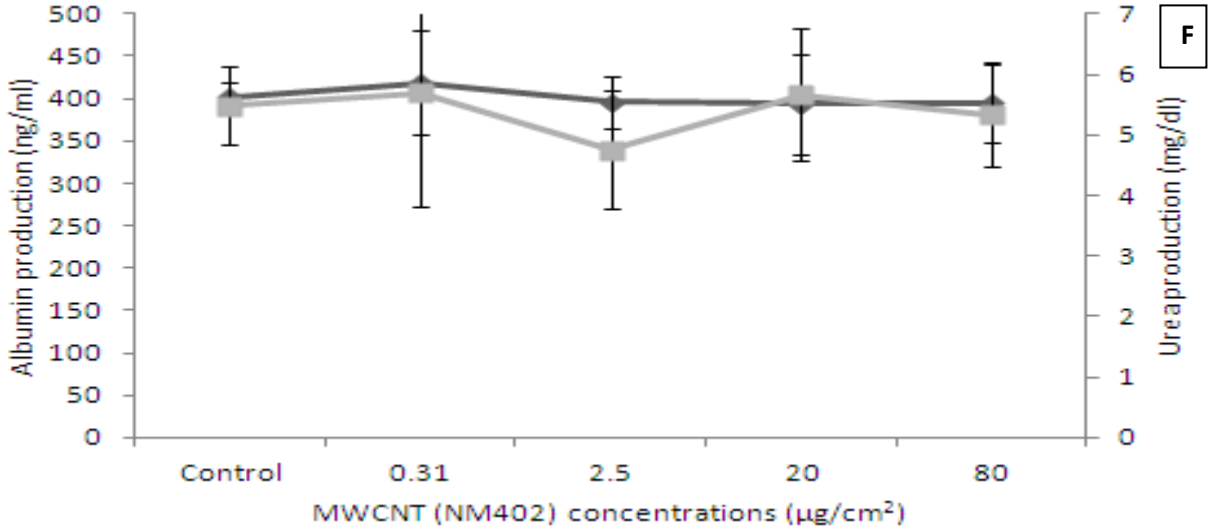
F
Albumin production (ng/ml)
Urea production (mg/dl)
Control
0.31
2.5
20
80
MWCNT (NM402) concentrations (µg/cm²)

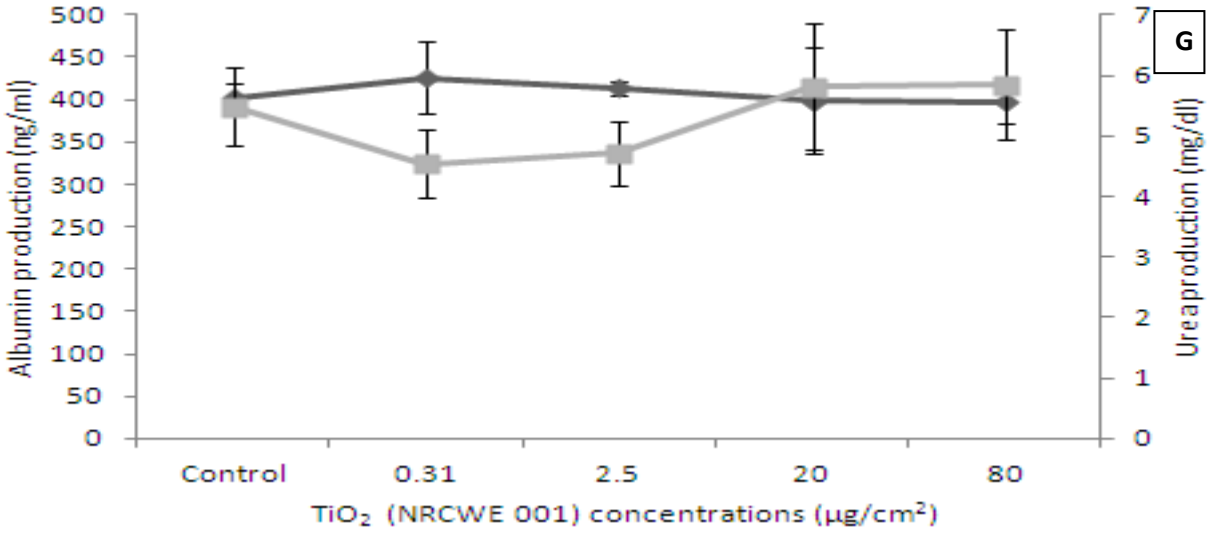
G
Albumin production (ng/ml)
Ureaproduction (mg/dl)
500
450
400
350
300
250
200
150
100
50
0
7
6
5
4
3
2
1
0
Control
0.31
2.5
20
80
TiO2 (NRCWE 001) concentrations (µg/cm2)

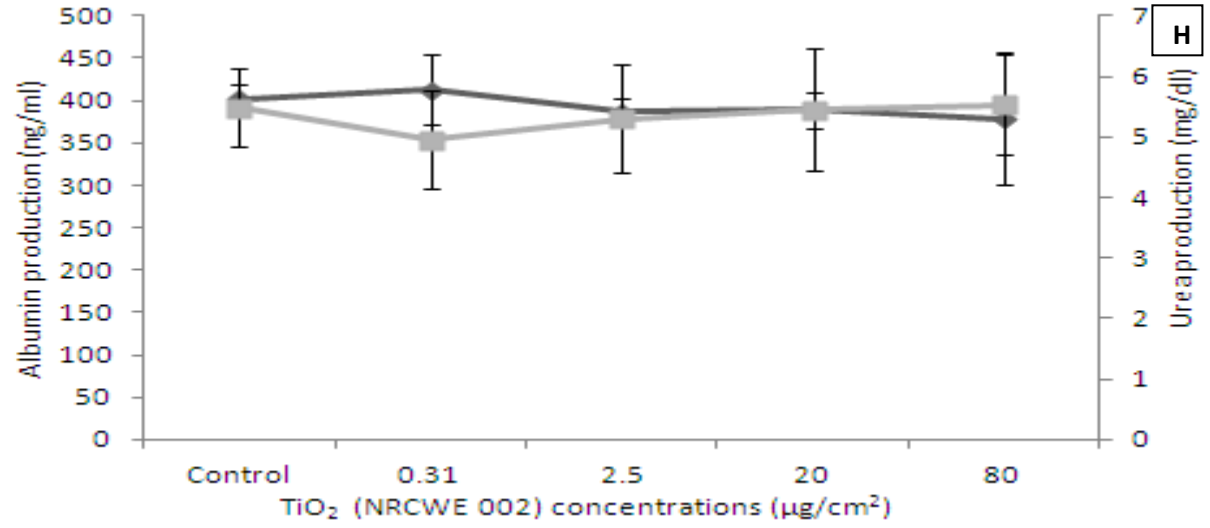
H
Albumin production (ng/ml)
Ureaproduction (mg/dl)
500
450
400
350
300
250
200
150
100
50
0
7
6
5
4
3
2
1
0
Control
0.31
2.5
20
80
TiO2 (NRCWE 002) concentrations (µg/cm2)

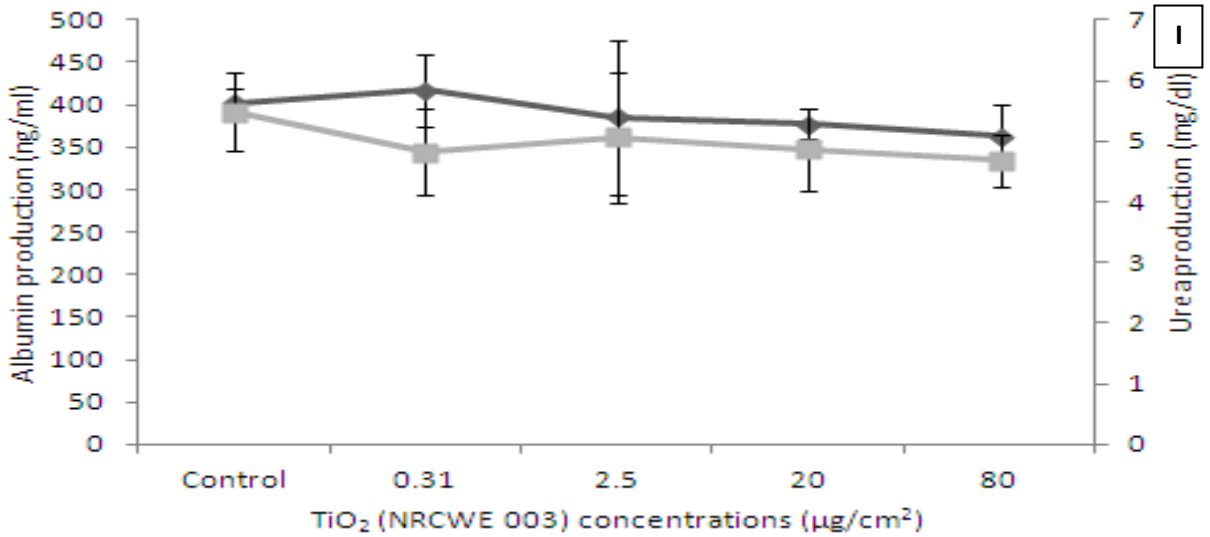
I
Albumin production (ng/ml)
Ureaproduction (mg/dl)
500
450
400
350
300
250
200
150
100
50
0
7
6
5
4
3
2
1
0
Control
0.31
2.5
20
80
TiO2 (NRCWE 003) concentrations (µg/cm2)

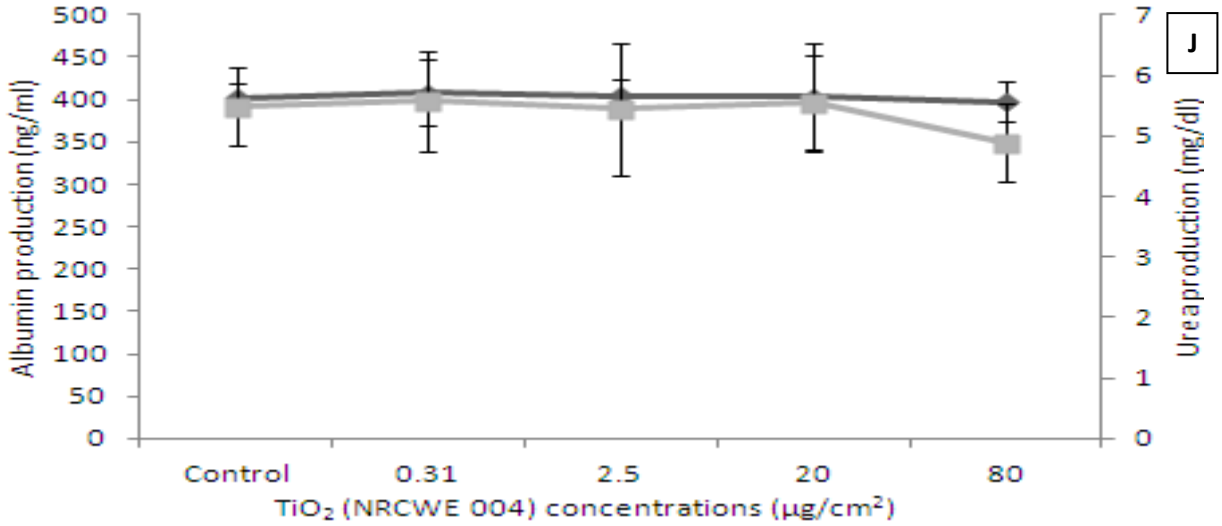

Figure 4.2. Albumin production (black line) and urea secretion (grey line) from C3A cells in the presence of a panel of engineered nanomaterials. Cells were exposed to medium (control) or NMs for 24 hr. Values represent mean ± SEM (n=3), significance indicated by * = $p<0.05$, compared to the control. **A)** NM 101 **B)** NM 110 **C)** NM 111 **D)** NM 300 **E)** NM 400 **F)** NM 402 **G)** NRCWE 001 **H)** NRCWE 002 **I)** NRCWE 003 **J)** NRCWE 004.

4.7 Discussion

As part of the FP7 project – ENPRA we investigated the potential hazard of a wide range of nanomaterials on a variety of targets for risk assessment. For this reason, the wide dose response ranges were used in order to allow calculation of values such as LC_{50} for comparisons between different materials and cell target types both *in vitro* and *in vivo*.

In this chapter the focus was on the impact of the investigated nanomaterials on C3A cells with respect to cytotoxicity, pro-inflammatory cytokine production and markers of function. The data shows that the nanomaterials vary in terms of their toxicity and impact on cell function after acute (24 hr) exposure *in vitro*.

This acute *in vitro* cytotoxicity study indicates that the NM panel can be segregated into a low (TiO_2 and MWCNT) and a high toxicity group (Ag and coated and uncoated ZnO) (Table 4.2). The silver NMs were the most toxic with an LC_{50} as low as 2 $\mu g/cm^2$. Our results are similar to previous studies in which hepatocytes exposed to uncoated 5–10 nm Ag particles for a period of 24 hr were toxic at concentrations as low as 0.5 µg/ml (Kawata, *et al*., 2009; Park, *et al*., 2010). It has been shown that at nano-scale, silver exhibits remarkably unusual physical, chemical and biological properties (Chen, *et al*., 2008).

The coated and uncoated ZnO NMs also exhibited significant toxicity to C3A cells (NM 110 – LC_{50} 7.5 $\mu g/cm^2$ and NM 111 - LC_{50} 15 $\mu g/cm^2$). In a recent set of trials, it was shown that ZnO NMs have significant toxic effects on aortic endothelial cells, with 50% of cells dying after a 4 hr incubation period with 50 nm particles (Gojovo, *et al*., 2007). In another study on mouse neural stem cells, a 24 hr incubation with 30, 60 and 200 nm ZnO particles resulted in manifestation of a clear dose dependant toxicity to the cells (LC_{50} 8-20 $\mu g/cm^2$). The authors proposed that the ZnO induced apoptosis of the treated cells (Deng, *et al*., 2009).

Both Ag and ZnO have been reported elsewhere to exhibit solubility resulting in the release of ions that contribute to the toxicity of these NMs (Fabrega, *et al*., 2011; Kim, *et al*., 2011b; Park, *et al*., 2011; Song, *et al*., 2010; Wong, *et al*., 2010; Zheng, *et al*., 2011). Our assessment of dissolution in complete C3A medium showed that less than 1% of Ag (NM 300) dissolves in this medium after 24 hr of incubation so it is very unlikely that the toxicity witnessed is due to the release of ions. Similarly in a recent study A549 cells (alveolar cell line) were

exposed to both Ag NMs and ions in a dose dependant manner. The authors noted very low toxicity following exposure to the Ag^+ at the lower concentrations (Foldbjerg, *et al*., 2011). Furthermore our Ag solubility findings are similar to studies in which it was noted that very little silver is dissolved in the tested media (Chappell, *et al*., 2011; Gaiser, *et al*., 2011). However it seems that the two ZnO NMs (NM 110 and NM 111) were partially soluble in the medium utilised, so there is a real possibility that the high toxicity of these materials is in part due to the release of ions. Around 40 to 50% of the added ZnO NMs were found as soluble Zn in the cell medium utilised. Some soluble Zn (2.9 µg/ml) was already present in the original cell medium, but addition of the NM 110 and NM 111 increased the concentrations in a dose-dependent manner up to 128 µg/ml in the cell medium. Further understanding of the dissolution kinetics of these partially soluble compounds in both the test item preparation step and in the cell media are crucial for further understanding of the toxicology of these nanomaterials.

It has been suggested that in sufficient doses TiO_2 can cause pulmonary inflammation, fibrosis and damage (Jin, *et al*., 2008). Based on recent *in vivo* studies, inflammation may persist for several months, but does not reach the level of inflammation induced by quartz (Roursgaard, *et al*., 2011). It has also been shown that after translocation from the primary site of exposure, the NMs can induce oxidative stress - mediated toxicity in many cell types by producing large amounts of free radicals (Jin, *et al*., 2008; Kang, *et al*., 2008; Wang, *et al*., 2007b). All five TiO_2 were of relatively low toxicity to the C3A cells (LC_{50} at 24 hr was not reached in the presence of any of the NMs up to 80 µg/cm^2). Similarly, in a study using Caco2 cells it was found that there was no cytotoxicity following a 24 hr exposure to TiO_2 NMs (Jin, *et al*., 2008). Xia, *et al*., discovered however, that TiO_2 nanomaterials did cross the epithelial lining of the intestinal model by transcytosis, albeit at low levels. TiO_2 was able to penetrate into and through the cells without disrupting junctional complexes (Xia, *et al*., 2006). It is also interesting to note that a recent study suggests that TiO_2 NM exposure did not result in any toxicological effects to intestinal cells under dark conditions (Koeneman, *et al*., 2010). Our exposures here were also conducted in the dark. In addition the data presented here indicates that relatively high TiO_2 exposure concentrations can induce production of the pro-inflammatory cytokine IL8, which agrees with other *in vitro* studies (Monteiller, *et al*., 2007).

Finally, the data showed the MWCNTs tested were relatively non-toxic to the C3A cells at the times and concentrations tested. The toxicity of MWCNTs is widely documented, with adverse effects observed as pulmonary inflammogenicity (Ellinger-Ziegelbauer, *et al*., 2009), hepatotoxicity (Ji, *et al*., 2009), dermal and ocular irritation (Kishore, *et al*., 2009) as well as monocyte (De Nicola, *et al*., 2009) and macrophage (Hirano, *et al*., 2008) mediated pathogenesis to name but a few. Like other nanomaterials, CNTs may be capable of entering the bloodstream and can be translocated to secondary organs. Most of the manufactured MWCNTs are of an inhalable size and although most dust by mechanical agitation is coarse they could be potentially dangerous to anyone exposed (Hoet, *et al*., 2004). It has been shown that the cytotoxicity of SWCNTs is higher than that of MWCNTs (Shvedova, *et al*. 2005). *In vitro* exposure of RAW264.7 macrophage cell line to SWCNTs was associated with the active production of TGF-β and reduced levels of the TNF-α and IL1-β (Shvedova, *et al*. 2005), with no increase in intracellular ROS production (Shvedova, *et al*. 2005). The data presented here also supports the activity of MWCNT to induce the production of the pro-inflammatory cytokine IL8, but only at relatively high exposure concentrations.

Although some NMs adsorb proteins and form a protein corona (Montes-Burgos, *et al*., 2010) which could influence uptake and fate of the particle, we believe it is physiologically more relevant for the hepatocytes to be exposed to the NMs in a medium containing serum as for any nanomaterial to reach the liver, it will be exposed to numerous proteins along the way. In addition, the C3A cells require 10% serum to survive *in vitro*.

The ability of NMs to compromise the viability of the C3A was investigated using both the WST-1 and Alamarblue assays. Although data gathered revealed both assays were very similar across the ten nanomaterials, WST-1 was more sensitive over the steepest part of the curve when compared to the Alamarblue assay.

Hepatocytes are responsible for the manufacture of important serum proteins. They play a substantial role in the metabolism of lipids (Kmiec, *et al*., 2001) and synthesize many hormones and cytokines including IL8 (Dong, *et al*., 1998), IL6 (Saad, *et al*., 1995) TNF-α (Saad, *et al*., 1995) and CRP (Vermeire, *et al*., 2005). IL8 is a chemokine mediating the activation and migration of a wide variety of inflammatory cells including macrophages and mast cells into tissue, hence playing a pivotal role in initiation of an inflammatory response (Puthothu, *et al*., 2006). As described above there was a significant increase in the levels of

IL8 produced by the C3A cells in the presence of nanomaterials, with these levels peaking around the LC_{50} mark for the highly toxicity materials (Ag and the two ZnO NMs). The decrease in cytokine production at concentrations above the LC_{50} in the presence of the toxic concentrations of NMs is likely due to the fact the cells were dying preventing cytokine production. In the presence of low toxicity NMs (TiO_2 and MWCNT), C3A cells produced increased levels of IL8 peaking only at the highest concentrations suggesting that they cause a lower pro-inflammatory response than Ag and ZnO. These experiments seem to suggest that the *in vitro* hepatocyte nanomaterial-induced inflammation seems to include IL8 production from the cells. It is interesting to note that exposure of the liver cell line HepG2 to microorganisms (*Brucella*) *in vitro* also results in an increase of IL8 secretion from the cells (Delpino, *et al*., 2010). These findings suggest that IL8 seems to mediate hepatocyte inflammation in response to a number of stress factors, including NMs.

There was no change in the levels of IL6, TNF-α or CRP following exposure of the C3A cells to any of the investigated nanomaterials suggesting that the inflammatory response is limited. There is a real possibility that for a more realistic representation of cytokine secretion in the liver incorporation of other cells (i.e. Kupffer cells) into the *in vitro* system might be essential (Sadauskas, *et al*., 2007) (Chapter 9).

Both urea and albumin were quantified as measures of liver function. Following exposure of C3A cells to the panel of nanomaterials. It was discovered that there was no significant decrease or increase in the levels of urea production. There was no change in the levels of albumin following nanomaterial exposure, with the exception of both ZnO NMs. These results suggest that with the exception of ZnO, despite varying degrees of cell death, none of the nanomaterials investigated affected hepatocyte function *in vitro* in terms of albumin and urea production. It is interesting that although silver was the most toxic nanomaterial investigated in terms of viability, this did not translate into the effect on cell function at sub lethal concentrations.

4.8 Conclusions

In conclusion, the *in vitro* hepatocyte model demonstrated that Ag and ZnO NMs were consistently more potent with respect to cytotoxicity and cytokine production. In comparison the MWCNT and TiO_2 nanomaterials investigated revealed relatively lower toxicity. The

cytotoxicity of ZnO may be related to its solubility, but this is less likely for the Ag NMs. Urea and albumin production were measured as indicators of hepatic function. These markers were only altered by the coated and uncoated ZnO, which significantly decreased albumin production.

Chapter Five

Assessing oxidative stress and genotoxicity following exposure of C3A cells to the ENPRA panel of engineered nanomaterials

Based on publication: Kermanizadeh A, Gaiser BK, Hutchison GR, Stone V. (2012). An *in vitro* liver model – assessing oxidative stress and genotoxicity following exposure of hepatocytes to a panel of engineered nanoparticles. Particle and Fibre Toxicology 9:28 DOI: 10.1186/1743-8977-9-28.

5.1 Aims and chapter outline

To investigate the ability of NMs with diffrent physicochemical characteristics to induce ROS production and oxidative stress in hepatocytes *in vitro*, in order to relate this oxidative stress to pro-inflammatory protein production and genotoxicity.

In order to determine whether oxidative stress is induced by the different nanomaterials in the C3A cell line, the levels of cellular antioxidant glutathione (GSH) was measured. The effects of the overall oxidative stress depends upon the size of these changes, with a cell being able to overcome small perturbations (small to medium changes can induce cell signalling leading to activation of genes e.g. via NFkB signalling - control inflammation) and regain its original state. However, more severe oxidative stress can cause cell death. Even moderate oxidation can trigger apoptosis, while more intense stress may cause necrosis.

Furthermore, the levels of intracellular hydrogen peroxide (H_2O_2) was measured using the DCFH-DA assay - fluorogenic probes convenient and sensitive to monitor oxidative activity.

Finally, the short term genotoxic properties of the panel of materials was investigated using the widely utilised FPG modified comet assay.

5.2 Impact of the nanomaterials on depletion of GSH in C3A hepatocytes

Analysis of the total glutathione contents of C3A cells revealed a dose dependant decrease compared to the control cells at 24 hr following exposure to five of the ten nanomaterials investigated. These NMs were NM 110 (ZnO uncoated), NM 111 (ZnO coated), NM 300 (Ag), NM 400 and NM 402 (MWCNTs) (Figure 5.1b, c, d, e and f). The three NMs previously shown to be the most cytotoxic to C3A cells as measured by the WST-1 assay (Ag NM 300, ZnO NM 110 and 111) (Chapter 4) (Kermanizadeh, *et al*., 2012c) also proved to induce relatively greater glutathione depletion than the other investigated NMs (Figure 5.1b, c and d - the LC_{50} is indicated).

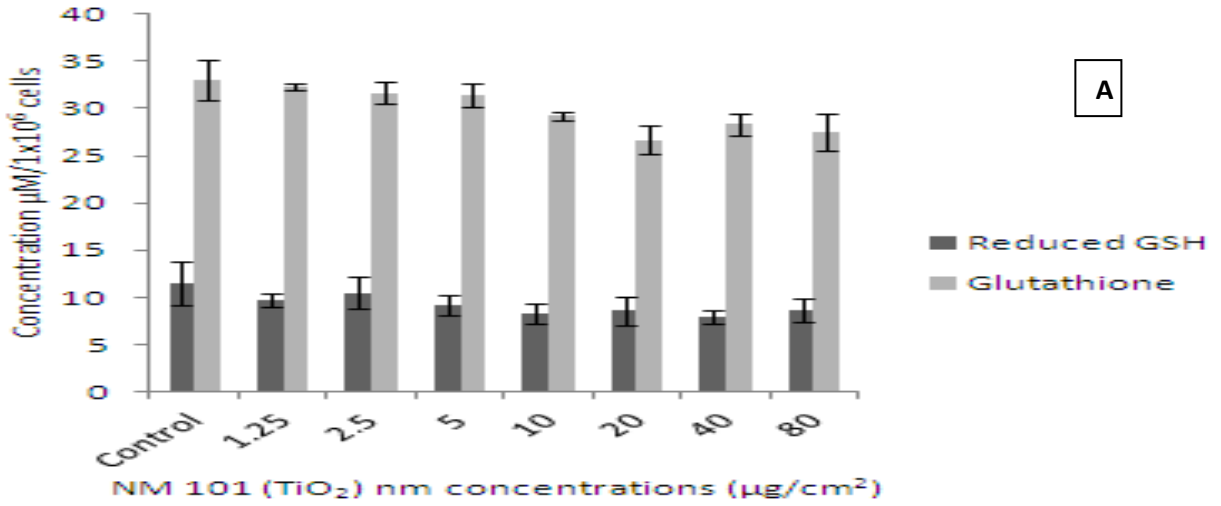
A
Concentration µM/1x10⁶ cells
0
5
10
15
20
25
30
35
40
Control
1.25
2.5
5
10
20
40
80
NM 101 (TiO₂) nm concentrations (µg/cm²)
Reduced GSH
Glutathione

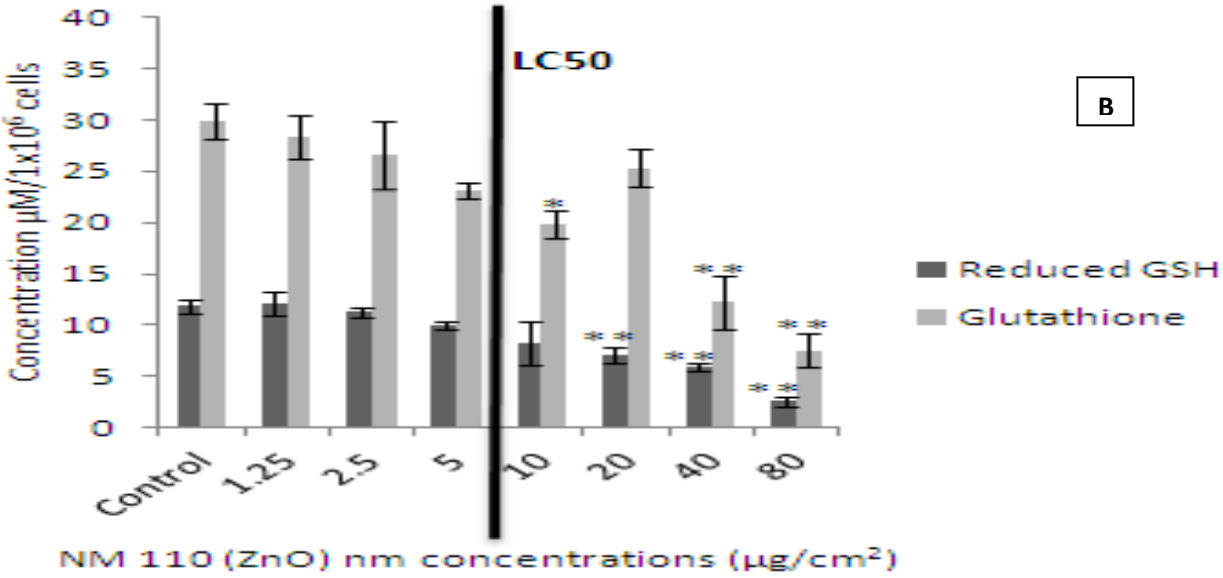
B
LC50
Concentration µM/1x10⁶ cells
0
5
10
15
20
25
30
35
40
Control
1.25
2.5
5
10
20
40
80
NM 110 (ZnO) nm concentrations (µg/cm²)
Reduced GSH
Glutathione

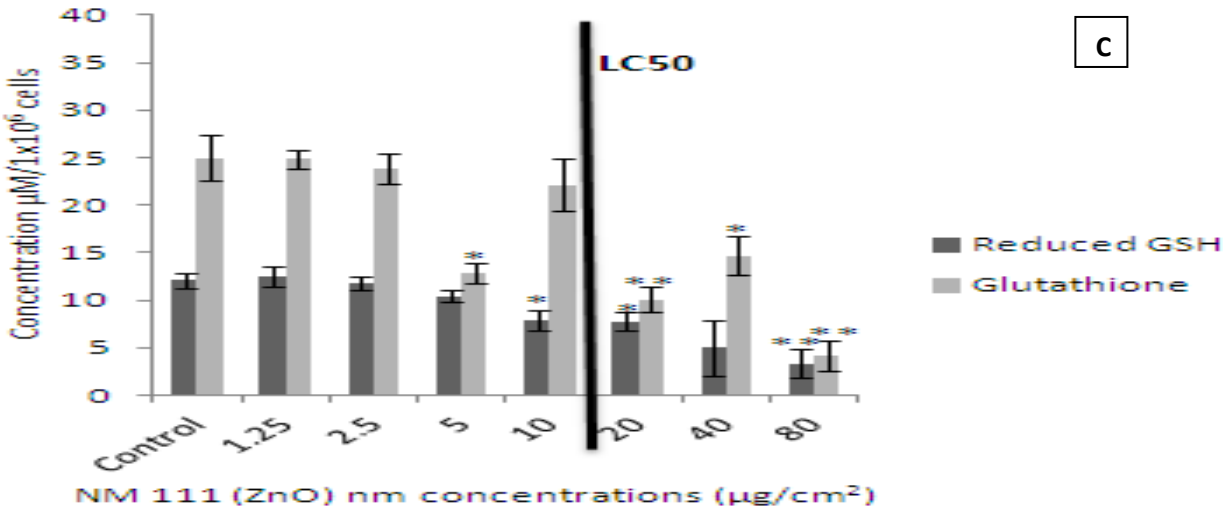
C
LC50
Concentration µM/1x10⁶ cells
0
5
10
15
20
25
30
35
40
Control
1.25
2.5
5
10
20
40
80
NM 111 (ZnO) nm concentrations (µg/cm²)
Reduced GSH
Glutathione

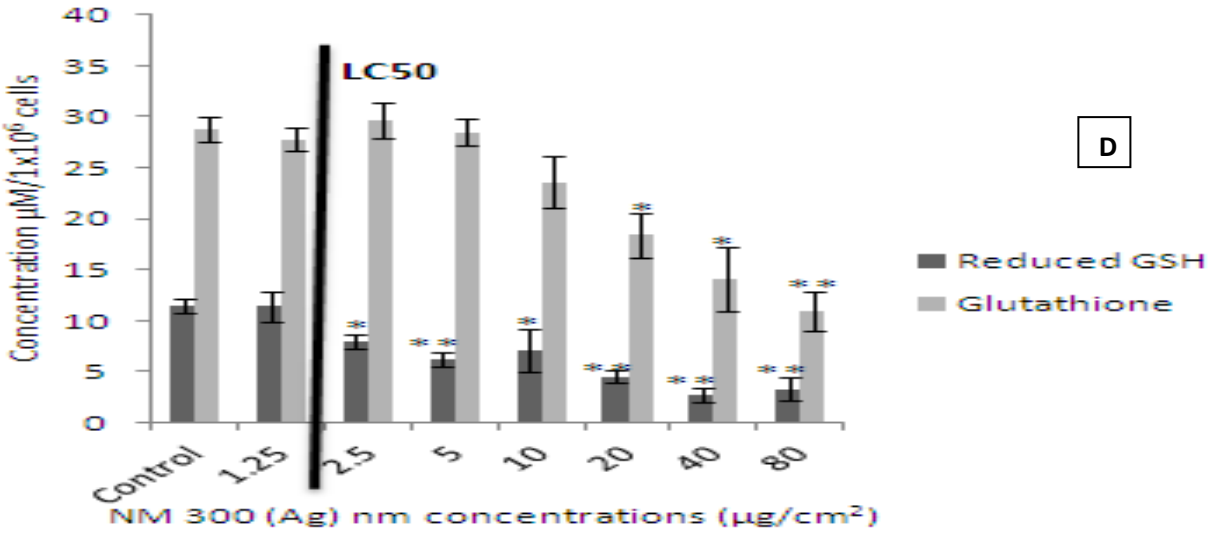
D
LC50
Concentration µM/1x10^6 cells
Reduced GSH
Glutathione
Control
1.25
2.5
5
10
20
40
80
NM 300 (Ag) nm concentrations (µg/cm²)

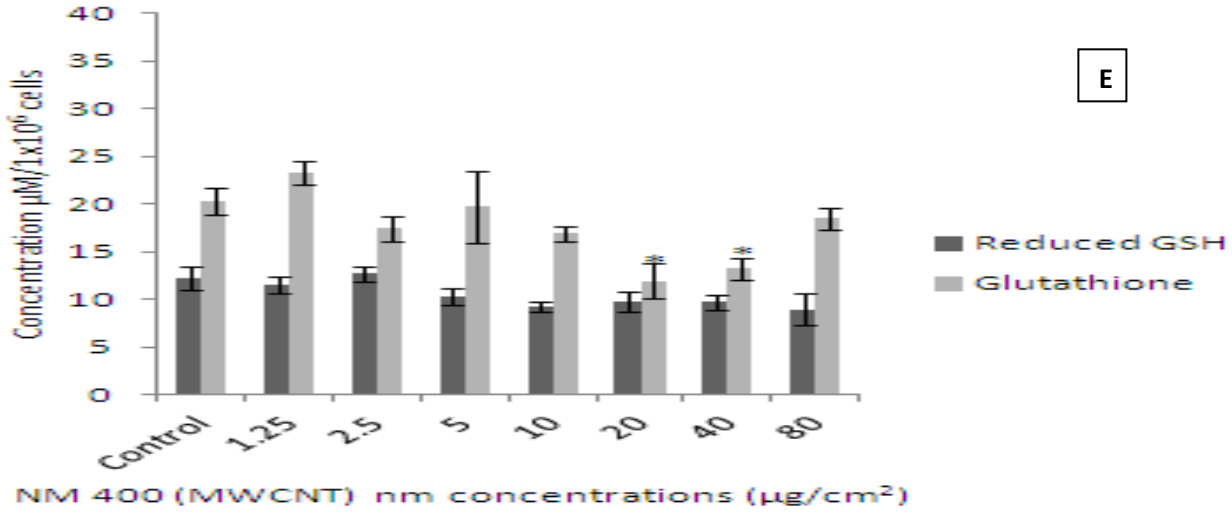
E
Concentration µM/1x10^6 cells
Reduced GSH
Glutathione
Control
1.25
2.5
5
10
20
40
80
NM 400 (MWCNT) nm concentrations (µg/cm²)

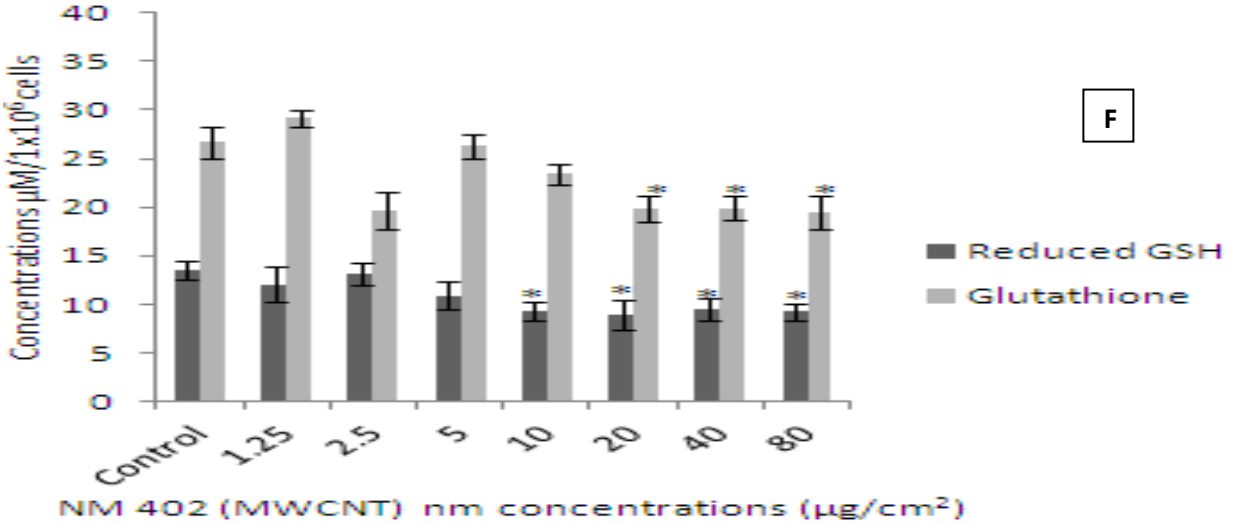
F
Concentrations µM/1x10^6cells
Reduced GSH
Glutathione
Control
1.25
2.5
5
10
20
40
80
NM 402 (MWCNT) nm concentrations (µg/cm²)

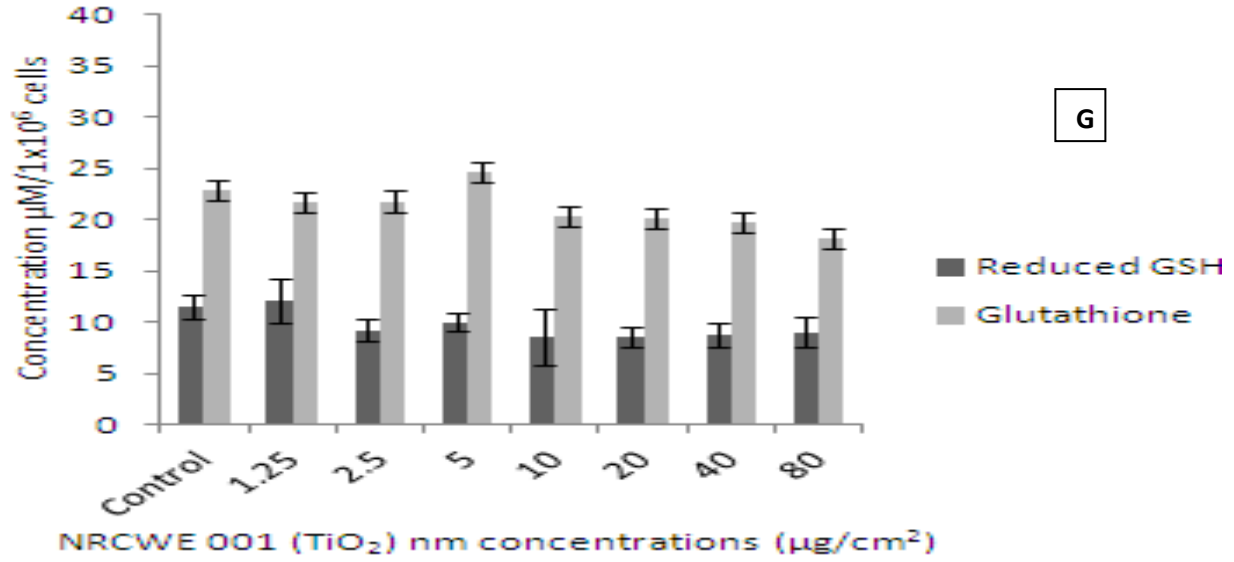
G
Concentration µM/1x10⁶ cells
40
35
30
25
20
15
10
5
0
Control
1.25
2.5
5
10
20
40
80
Reduced GSH
Glutathione
NRCWE 001 (TiO₂) nm concentrations (µg/cm²)

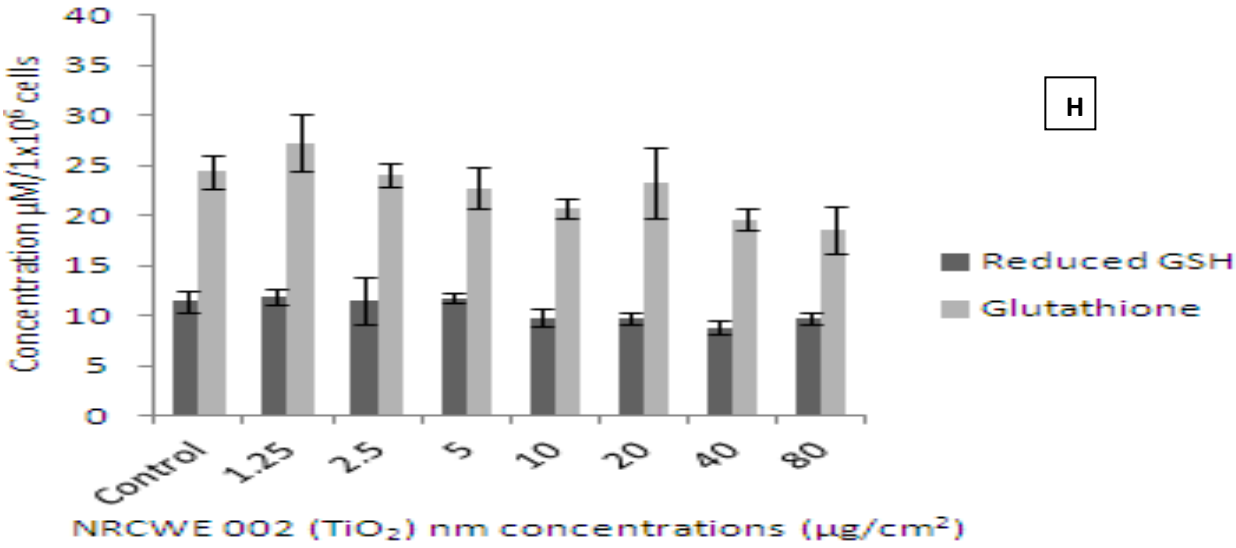
H
Concentration µM/1x10⁶ cells
40
35
30
25
20
15
10
5
0
Control
1.25
2.5
5
10
20
40
80
Reduced GSH
Glutathione
NRCWE 002 (TiO₂) nm concentrations (µg/cm²)

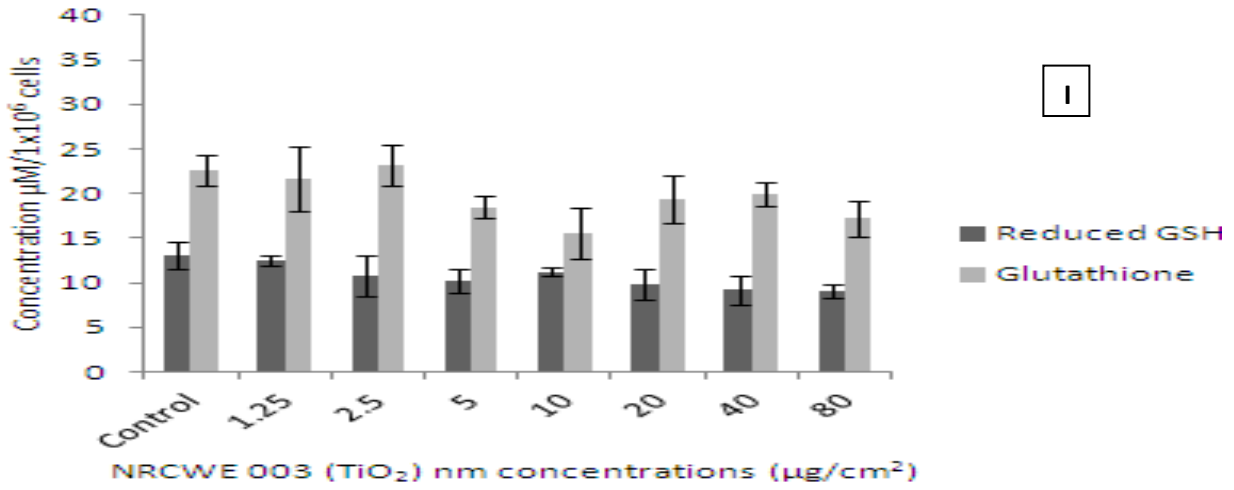
I
Concentration µM/1x10⁶ cells
40
35
30
25
20
15
10
5
0
Control
1.25
2.5
5
10
20
40
80
Reduced GSH
Glutathione
NRCWE 003 (TiO₂) nm concentrations (µg/cm²)

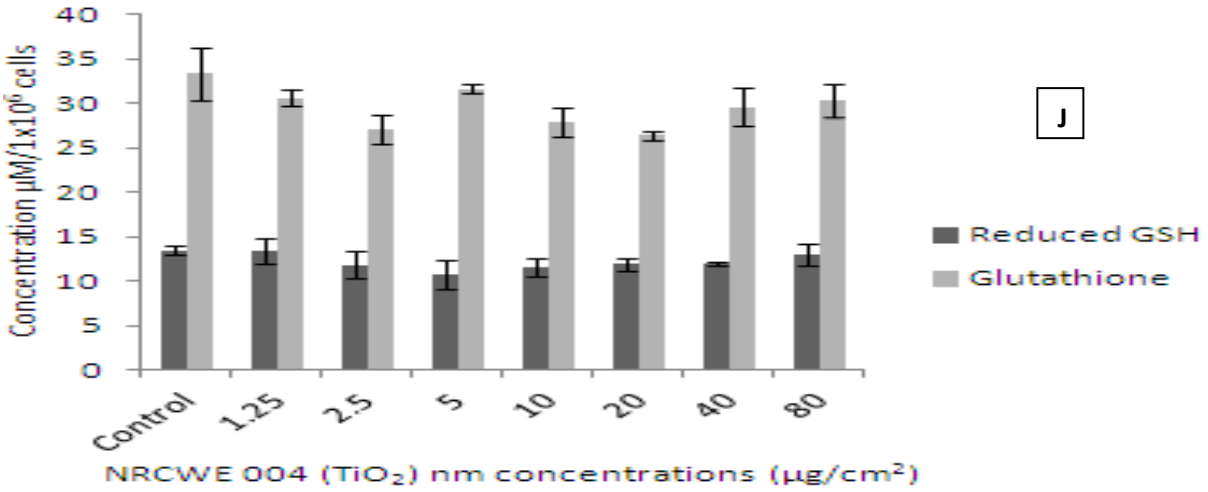

Figure 5.1. Effects of NM exposure on reduced GSH and total glutathione levels in C3A cells. The cells were exposed to cell medium (control) and increasing concentrations of selected NMs for 24 hr. Values represent mean ± SEM (n=3), significance indicated by *= $p<0.05$ and **= $p<0.005$ compared to the control. **A)** NM 101 **B)** NM 110 **C)** NM 111 **D)** NM 300 **E)** NM 400 **F)** NM 402 **G)** NRCWE 001 **H)** NRCWE 002 **I)** NRCWE 003 **J)** NRCWE 004. LC_{50} values are indicated for NMs where this value was measurable. For all other NMs the LC_{50} was not reached following exposure up to 80 µg/cm^2 after a 24 hr incubation.

5.3 Measurement of intracellular ROS

The 2',7'-dichlorfluorescein-diacetate assay is based on the principle of DCFH being oxidized to fluorescent dichlorofluorescein (DCF) in the presence of intracellular ROS. Six different exposure time points were chosen (2, 4, 6, 8, 12 and 24 hr). It was noted that the 6 hr exposure was optimal for the highest levels of intracellular ROS production (data not shown). We noted a dose dependent increase in the levels of DCF fluorescence after exposure to the low toxicity nanomaterials (TiO_2 and MWCNT NMs - Figure 5.2a, e, f, g, h and j). Following exposure to the highly toxic ZnO (NM 110) and Ag (NM 300) NMs, there was no significant increase in intracellular ROS levels. After exposure of the cells to coated ZnO (NM 111) there was a small but significant increase of fluorescence up to the LC_{50} value before a sharp drop at the higher concentrations. The levels of DCF fluorescence after the exposure to the highly toxic NMs were markedly lower than those witnessed after exposure to the low toxicity nanomaterials (Figure 5.2b, c and d).

In order to investigate whether an antioxidant could prevent the NM-induced ROS production within the hepatocytes – the cells were pre-treated with the vitamin E derivative – Trolox for 1 hr before the addition of the nanomaterials. Trolox prevented the NM induced DCF fluorescence with the inhibition most evident for the two MWCNTs (Figure 5.3).

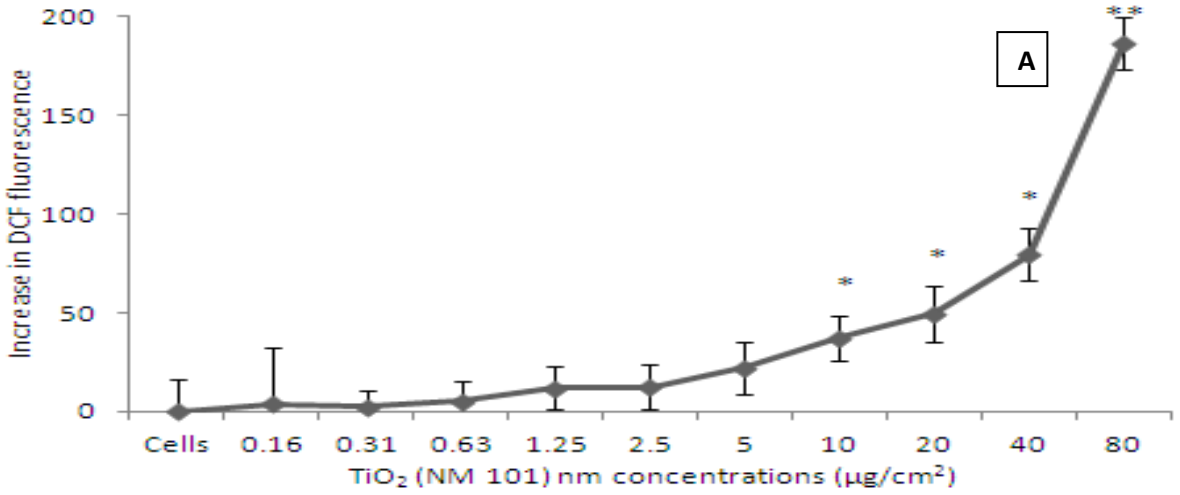
A
Increase in DCF fluorescence
200
150
100
50
0
Cells
0.16
0.31
0.63
1.25
2.5
5
10
20
40
80
TiO2 (NM 101) nm concentrations (µg/cm2)
*
*
*
**

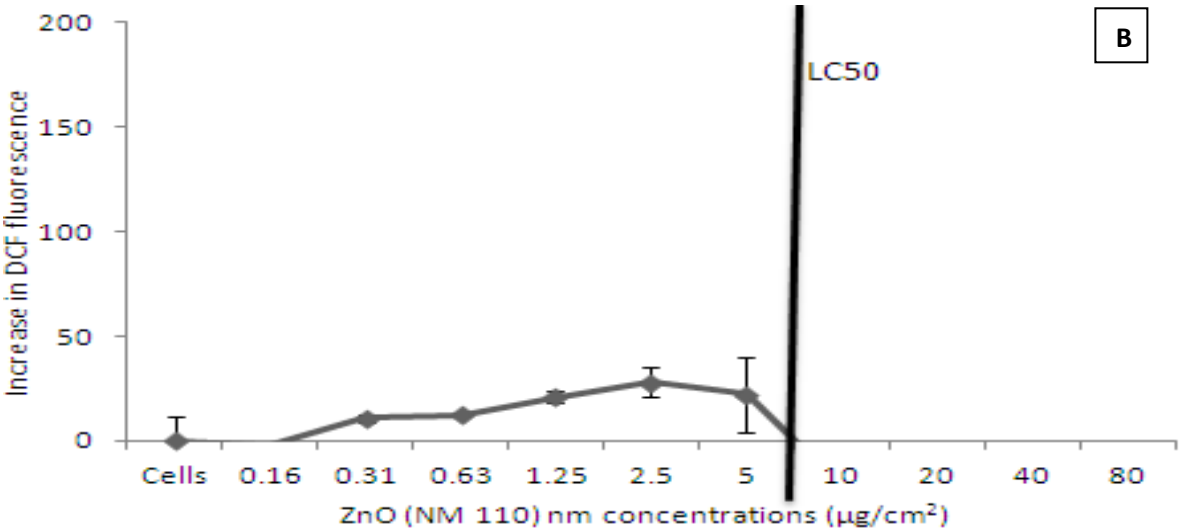
B
LC50
Increase in DCF fluorescence
200
150
100
50
0
Cells
0.16
0.31
0.63
1.25
2.5
5
10
20
40
80
ZnO (NM 110) nm concentrations (µg/cm2)

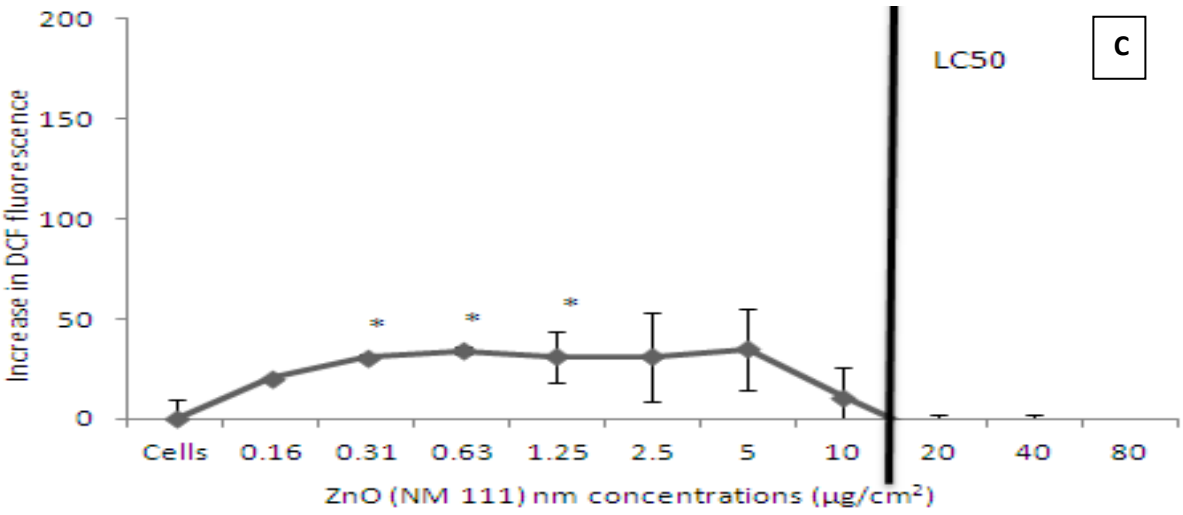
C
LC50
Increase in DCF fluorescence
200
150
100
50
0
Cells
0.16
0.31
0.63
1.25
2.5
5
10
20
40
80
ZnO (NM 111) nm concentrations (µg/cm2)
*
*
*

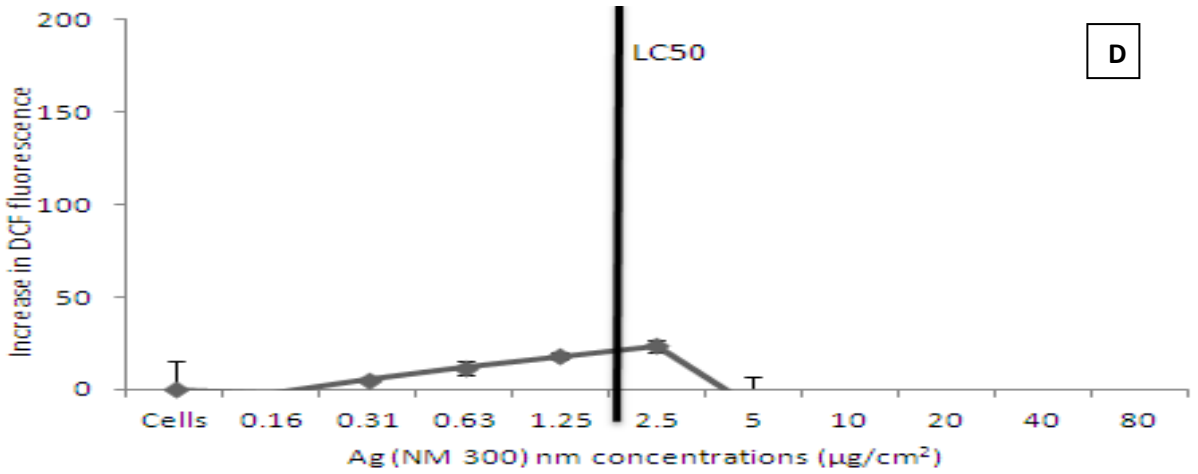
200
150
100
50
0
Increase in DCF fluorescence
LC50
D
Cells
0.16
0.31
0.63
1.25
2.5
5
10
20
40
80
Ag (NM 300) nm concentrations (µg/cm²)

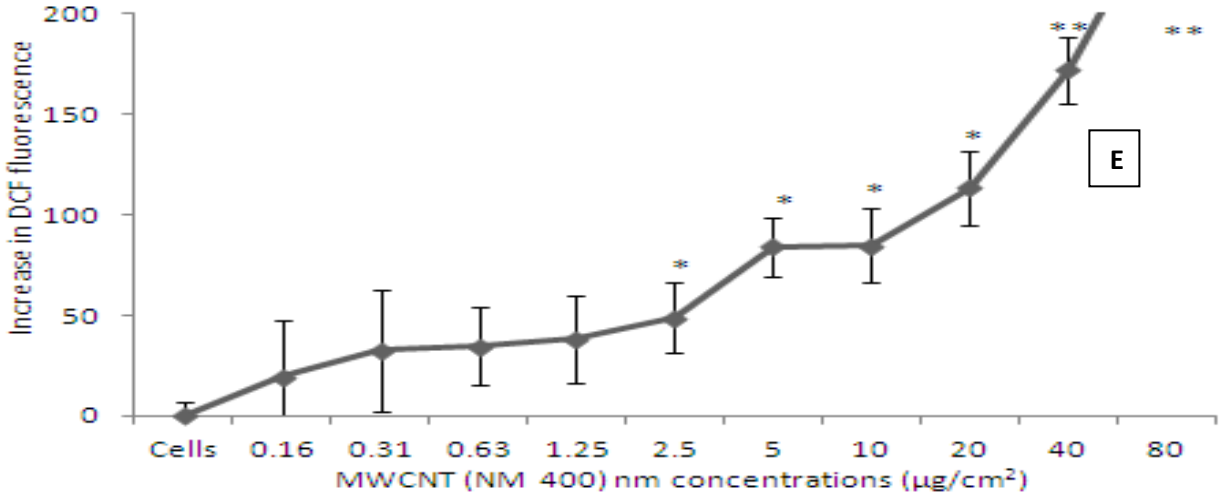
200
150
100
50
0
Increase in DCF fluorescence
E
* *
*
*
*
*
* *
Cells
0.16
0.31
0.63
1.25
2.5
5
10
20
40
80
MWCNT (NM 400) nm concentrations (µg/cm²)

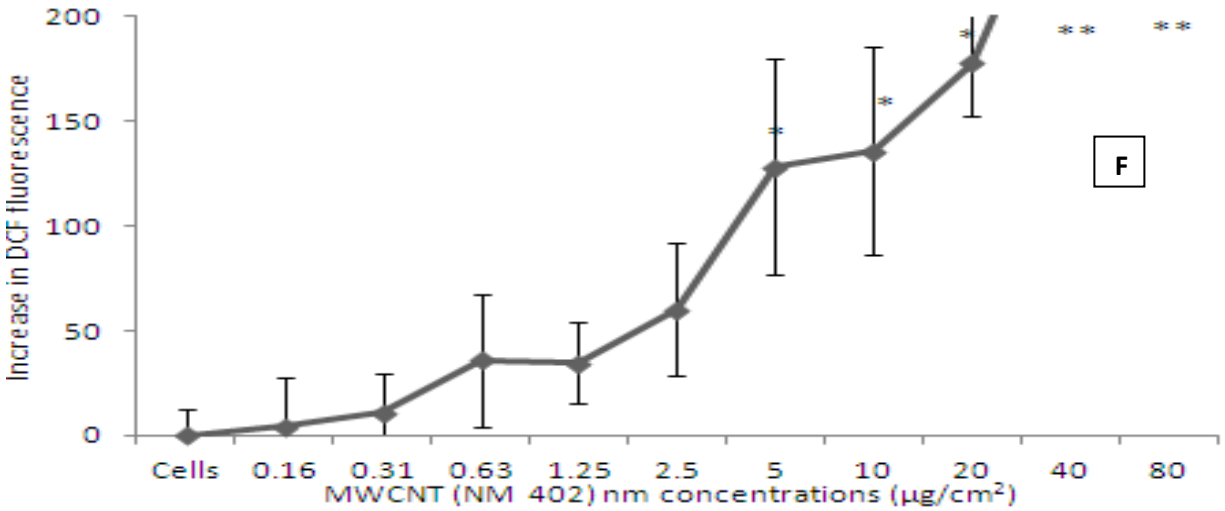
200
150
100
50
0
Increase in DCF fluorescence
F
* *
* *
*
*
*
Cells
0.16
0.31
0.63
1.25
2.5
5
10
20
40
80
MWCNT (NM 402) nm concentrations (µg/cm²)

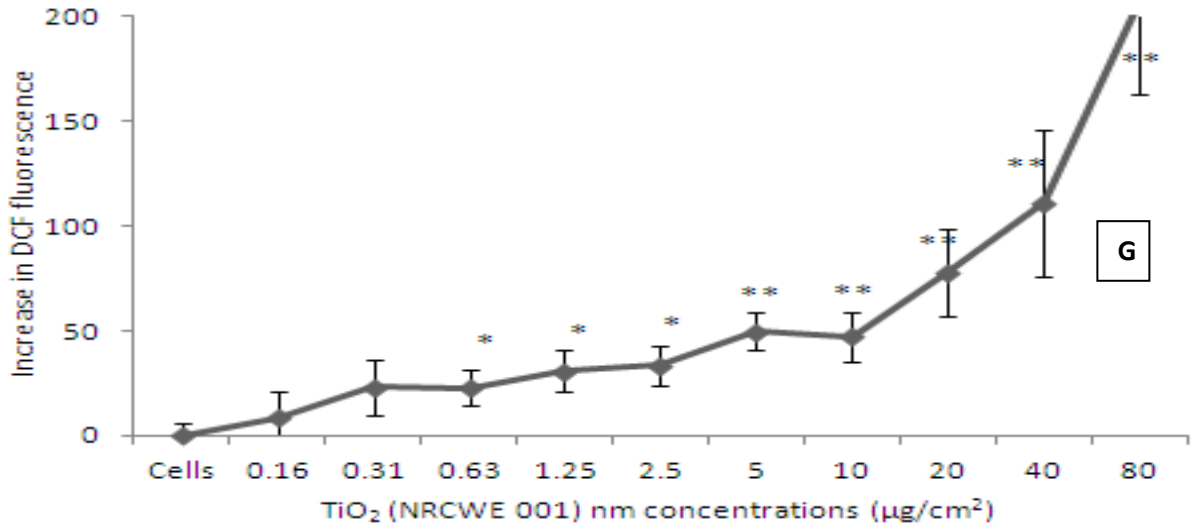
Increase in DCF fluorescence
200
150
100
50
0
Cells
0.16
0.31
0.63
1.25
2.5
5
10
20
40
80
TiO2 (NRCWE 001) nm concentrations (µg/cm2)
G

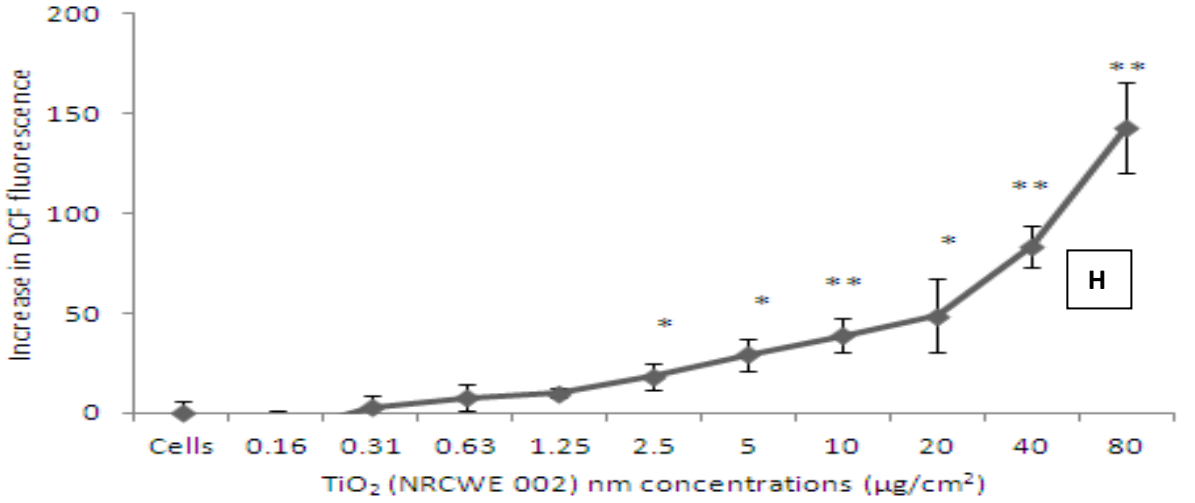
Increase in DCF fluorescence
200
150
100
50
0
Cells
0.16
0.31
0.63
1.25
2.5
5
10
20
40
80
TiO2 (NRCWE 002) nm concentrations (µg/cm2)
H

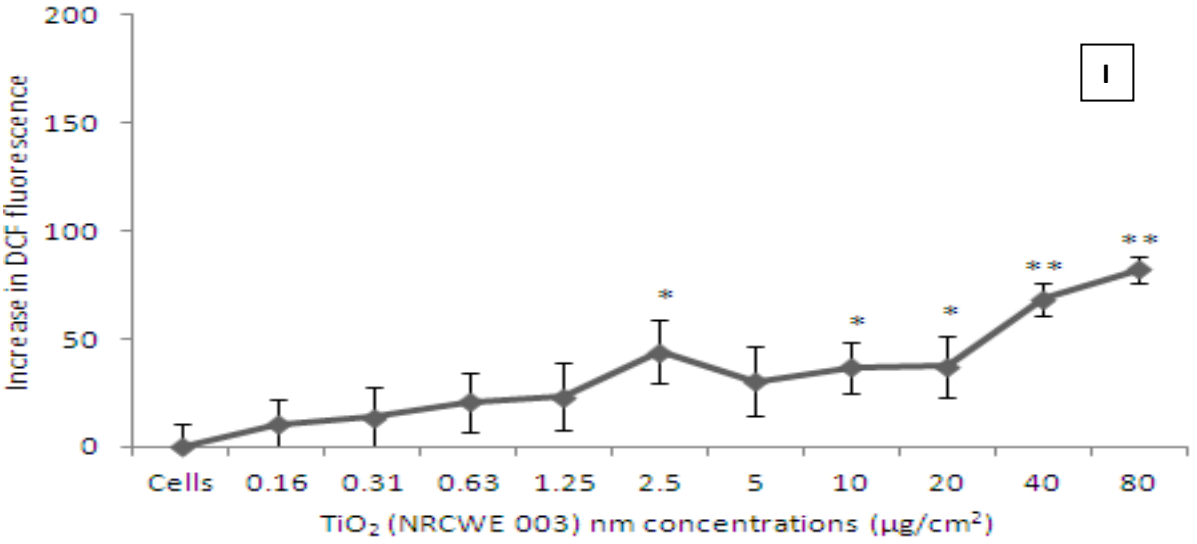
Increase in DCF fluorescence
200
150
100
50
0
Cells
0.16
0.31
0.63
1.25
2.5
5
10
20
40
80
TiO2 (NRCWE 003) nm concentrations (µg/cm2)
I

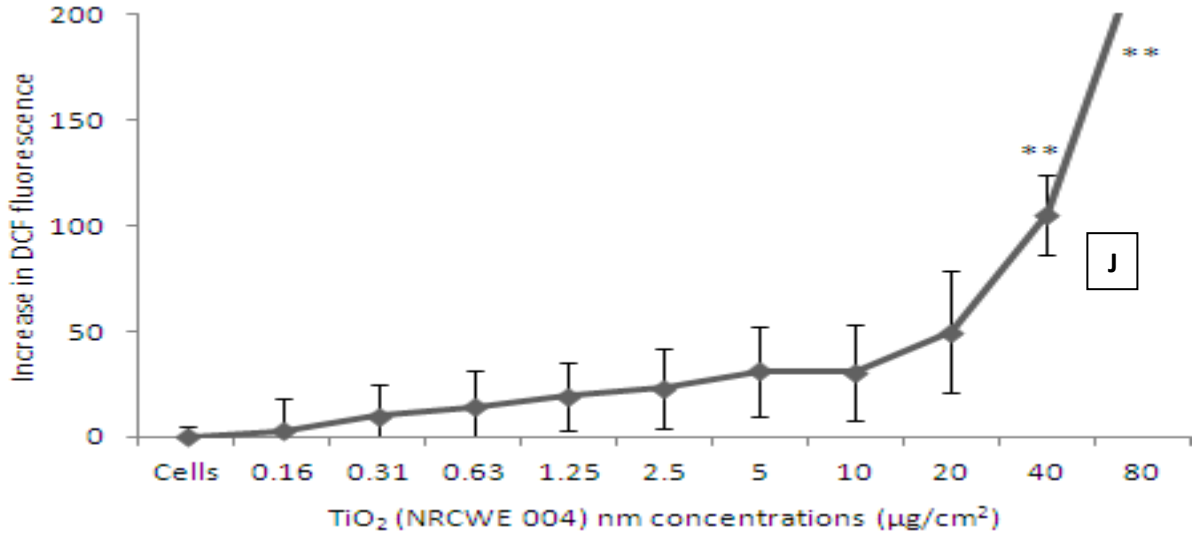

Figure 5.2. Effects of increasing concentration of NMs on the oxidation of DCFH to DCF in the C3A cells. The cells were exposed to cell medium (control) or NMs for 24 hr. Results are shown as mean fluorescence intensity minus corresponding control traces (± SEM) from three experiments (n=3), significance indicated by * = $p<0.05$ and ** = $p<0.005$, when NM treatments are compared to the control. **A)** NM 101 **B)** NM 110 **C)** NM 111 **D)** NM 300 **E)** NM 400 **F)** NM 402 **G)** NRCWE 001 **H)** NRCWE 002 **I)** NRCWE 003 **J)** NRCWE 004. LC_{50} values are indicated for NMs where this value was measurable. For all other NMs the LC_{50} was not reached following exposure up to 80 µg/cm^2 after a 24 hr incubation.

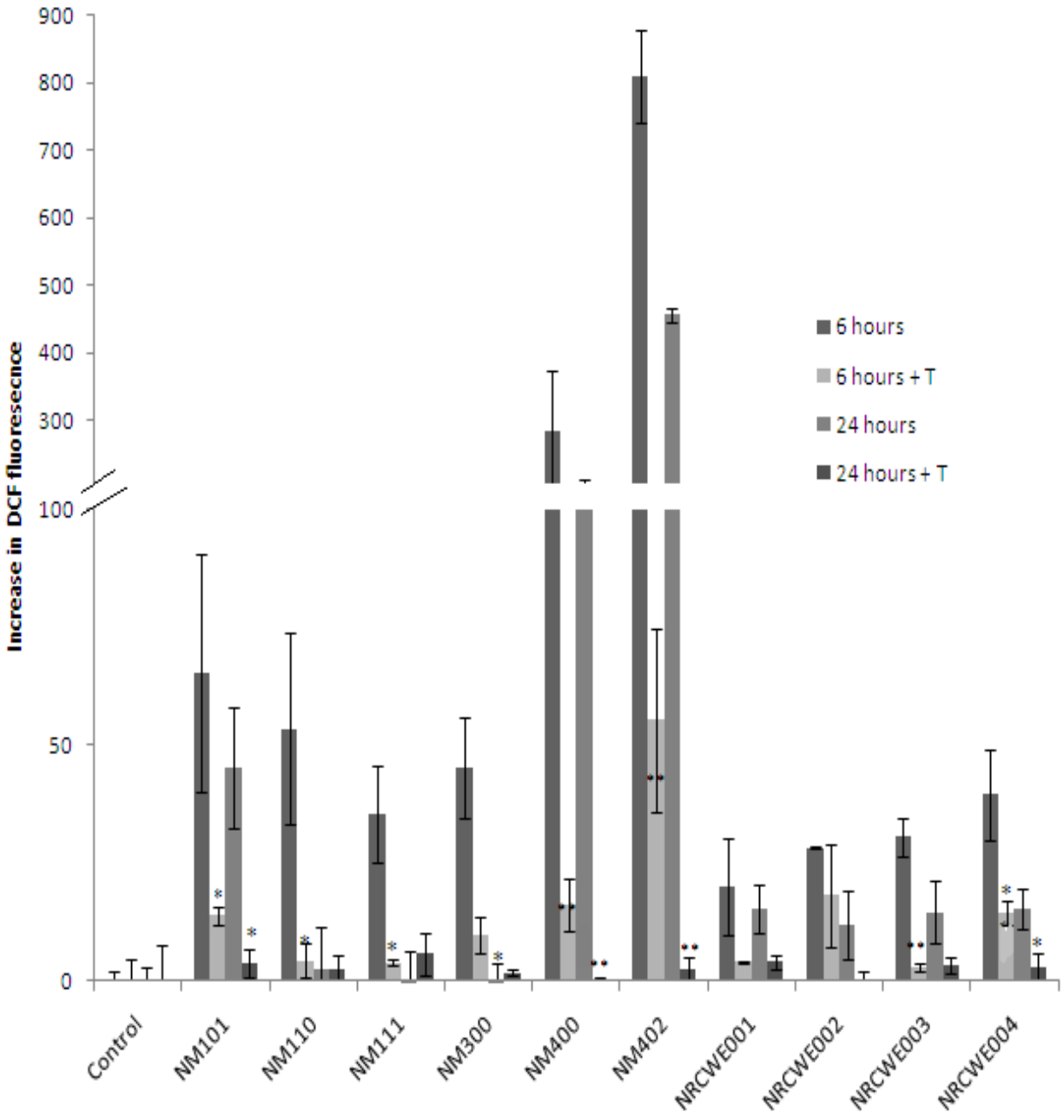

Figure 5.3. Effect of 20 µg/cm^2 of ENPRA nanomaterials on the oxidation of DCFH to DCF in C3A cells with and without Trolox pre-treatment. The cells were exposed to cell medium (control) or NMs for 6 or 24 hr. Results are exposed as mean fluorescence intensity minus corresponding control traces (±SEM) from three experiments (n=3), significance indicated by * = $p<0.05$ and ** = $p<0.005$, when decrease in fluorescence is compared to cells not treated with Trolox (T) before exposure to the NMs.

5.4 The effect of Trolox pre-treatment on cytotoxicity and IL8 production from C3A cells

As shown in chapter 4, three of the ENPRA panel of nanomaterials were highly cytotoxic (Ag, coated and uncoated ZnO). As shown there was also an increase in levels of IL8 production following exposure to the NMs investigated while no change in the levels of IL6, TNF-α or C reactive protein were observed. Therefore the aim was to investigate the effects of the pre-treatment with an external antioxidant on cytotoxicity and IL8 production from the C3A cells. The hepatocytes were pre-treated with Trolox for 1 hr before being exposed to four of the highest concentrations of the nanomaterials used previously (5 $\mu g/cm^2$ to 80 $\mu g/cm^2$).

The pre-treatment with Trolox prevented the cytotoxicity induced by five of the ten nanomaterials investigated (NM 110 (ZnO uncoated), NM 111 (ZnO coated), NM 300 (Ag), NRCWE 001 (TiO_2 rutile 10 nm) and NRCWE 004 (TiO_2 rutile 94 nm)) (Figure 5.4c, e, g, m and s). We also observed that Trolox reduced IL8 secretion for all NMs with the exception of Ag, whereas IL8 secretion appeared increased, however these changes were not significant (Figure 5.4h).

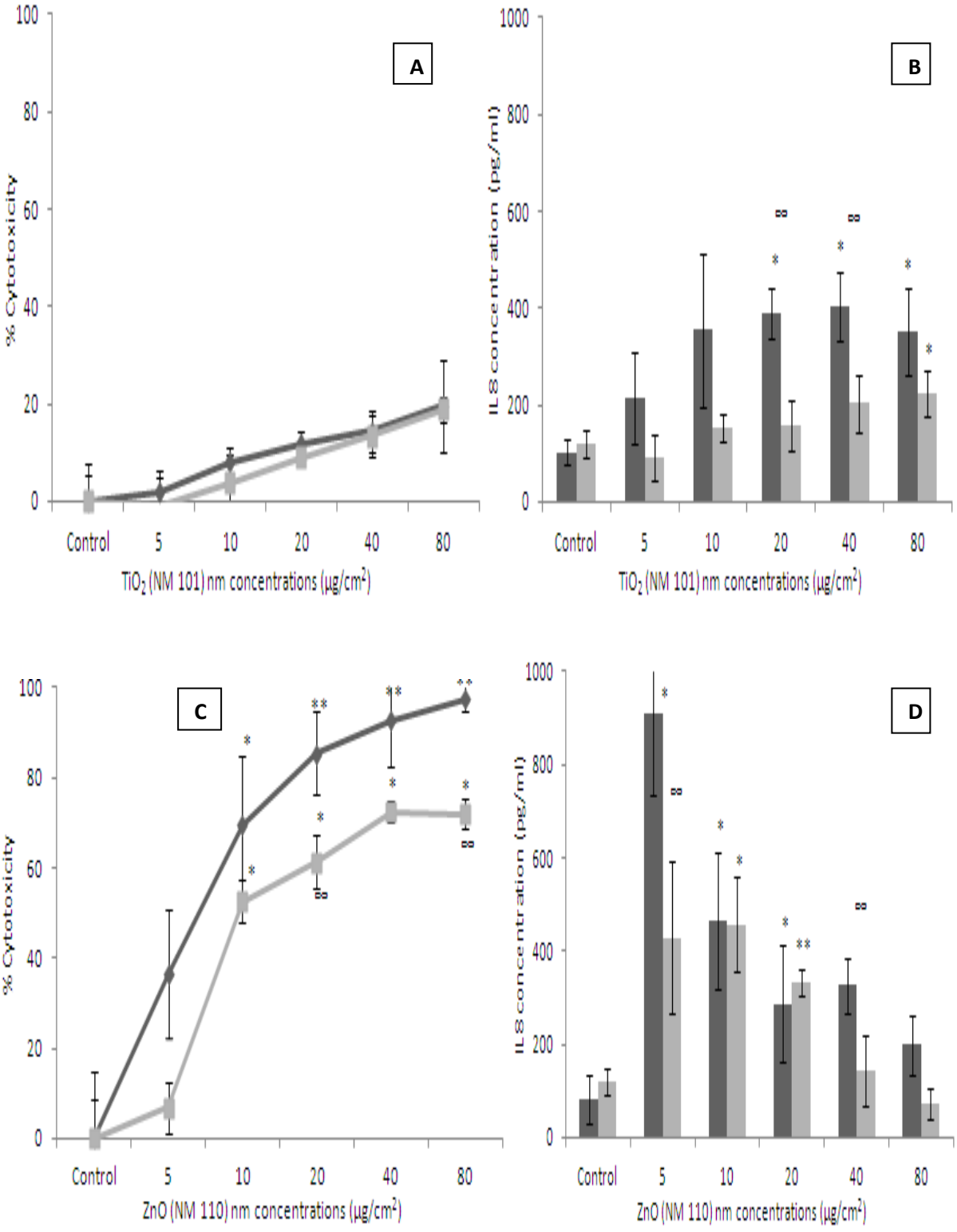
A
B
C
D
% Cytotoxicity
IL8 concentration (pg/ml)
Control
5
10
20
40
80
TiO2 (NM 101) nm concentrations (µg/cm2)
ZnO (NM 110) nm concentrations (µg/cm2)

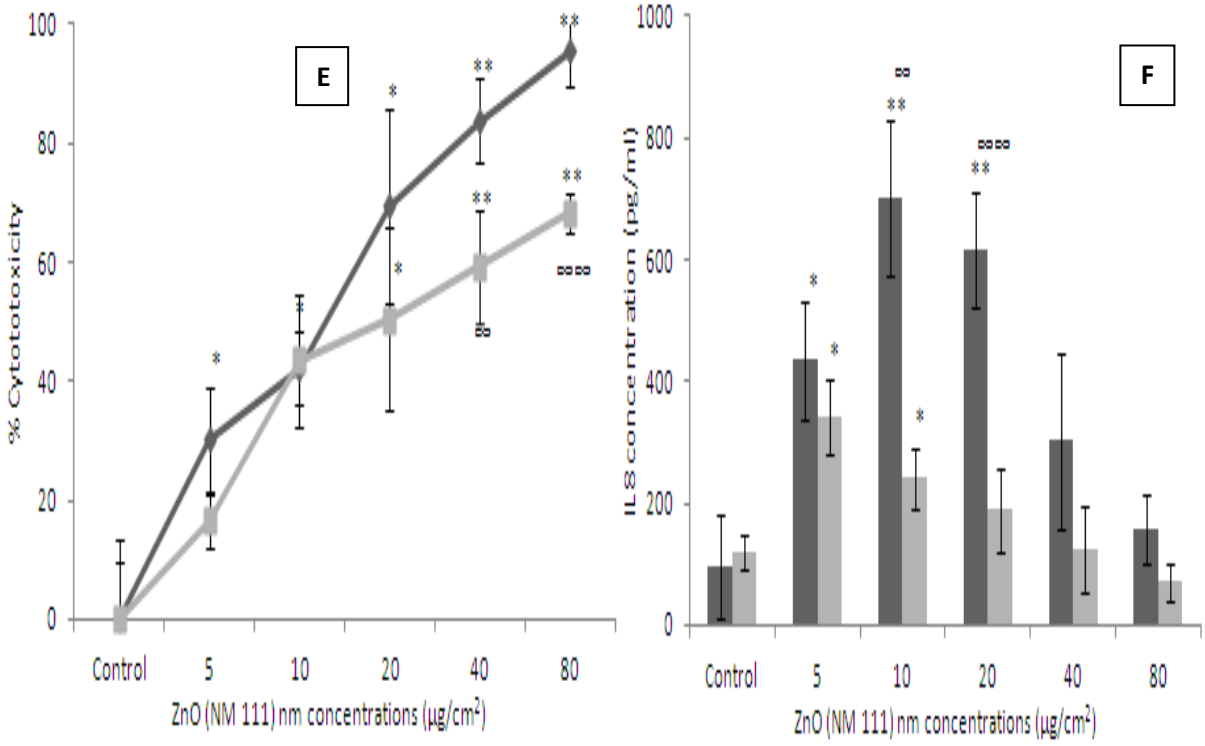
E
% Cytotoxicity
100
80
60
40
20
0
Control
5
10
20
40
80
ZnO (NM 111) nm concentrations (µg/cm²)
F
IL8 concentration (pg/ml)
1000
800
600
400
200
0
Control
5
10
20
40
80
ZnO (NM 111) nm concentrations (µg/cm²)

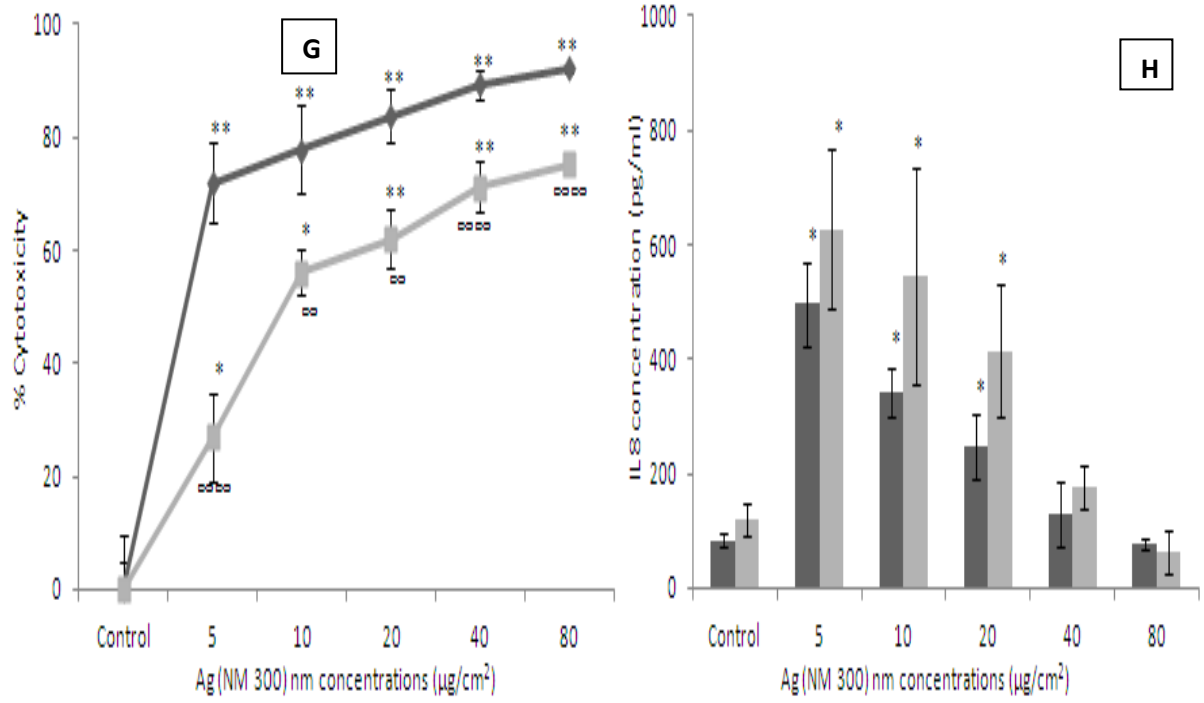
G
% Cytotoxicity
100
80
60
40
20
0
Control
5
10
20
40
80
Ag (NM 300) nm concentrations (µg/cm²)
H
IL8 concentration (pg/ml)
1000
800
600
400
200
0
Control
5
10
20
40
80
Ag (NM 300) nm concentrations (µg/cm²)

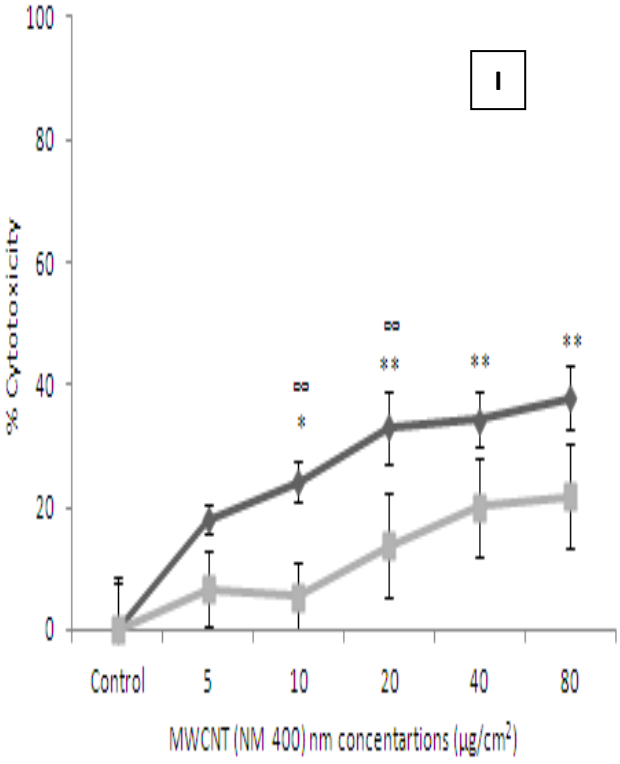
I
% Cytotoxicity
100
80
60
40
20
0
Control
5
10
20
40
80
MWCNT (NM 400) nm concentartions (µg/cm²)

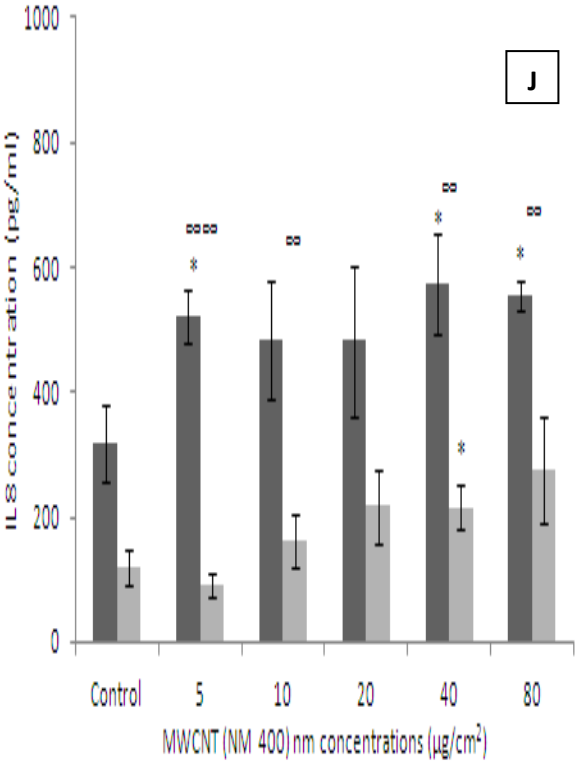
J
IL8 concentration (pg/ml)
1000
800
600
400
200
0
Control
5
10
20
40
80
MWCNT (NM 400) nm concentrations (µg/cm²)

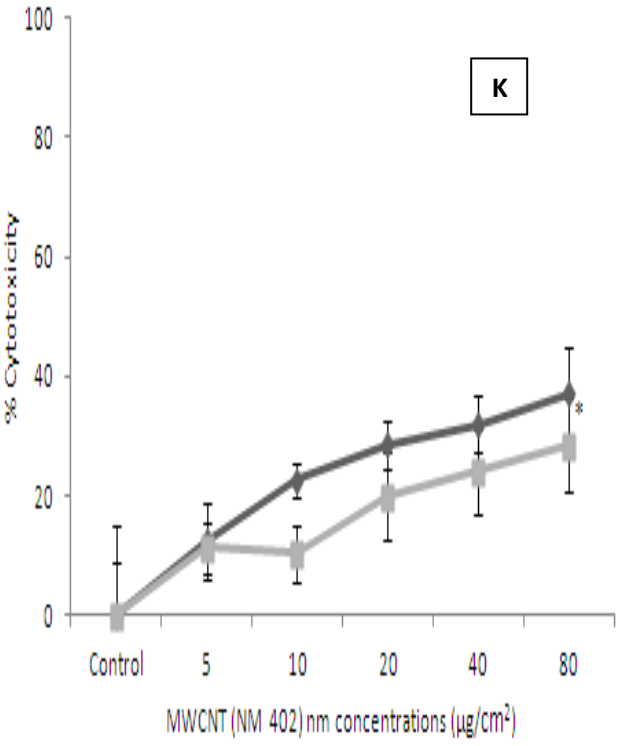
K
% Cytotoxicity
100
80
60
40
20
0
Control
5
10
20
40
80
MWCNT (NM 402) nm concentrations (µg/cm²)

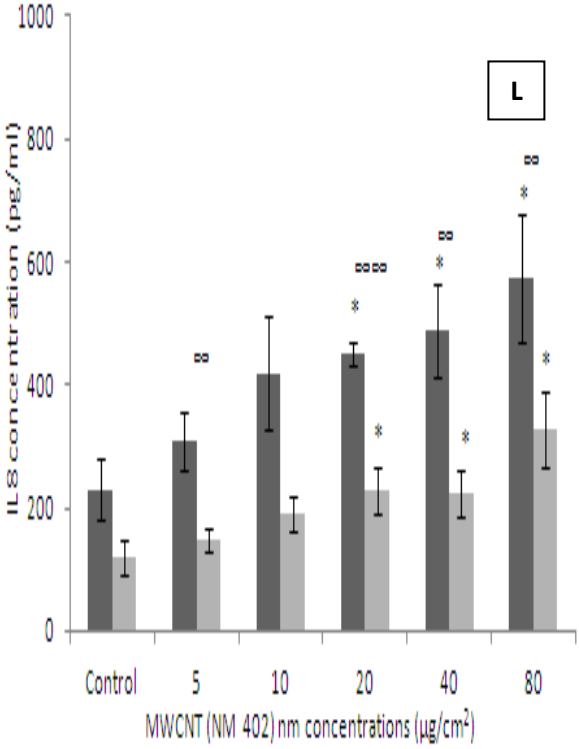
L
IL8 concentration (pg/ml)
1000
800
600
400
200
0
Control
5
10
20
40
80
MWCNT (NM 402) nm concentrations (µg/cm²)

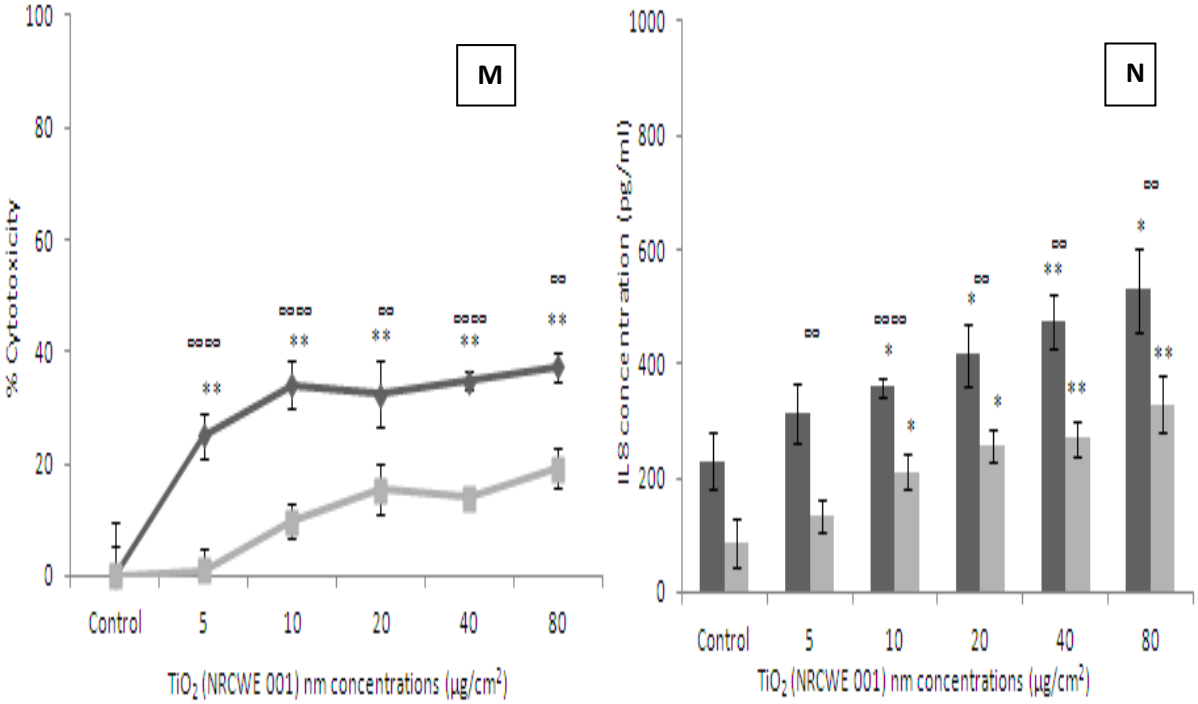
M
% Cytotoxicity
100
80
60
40
20
0
Control
5
10
20
40
80
TiO2 (NRCWE 001) nm concentrations (µg/cm2)

N
IL8 concentration (pg/ml)
1000
800
600
400
200
0
Control
5
10
20
40
80
TiO2 (NRCWE 001) nm concentrations (µg/cm2)

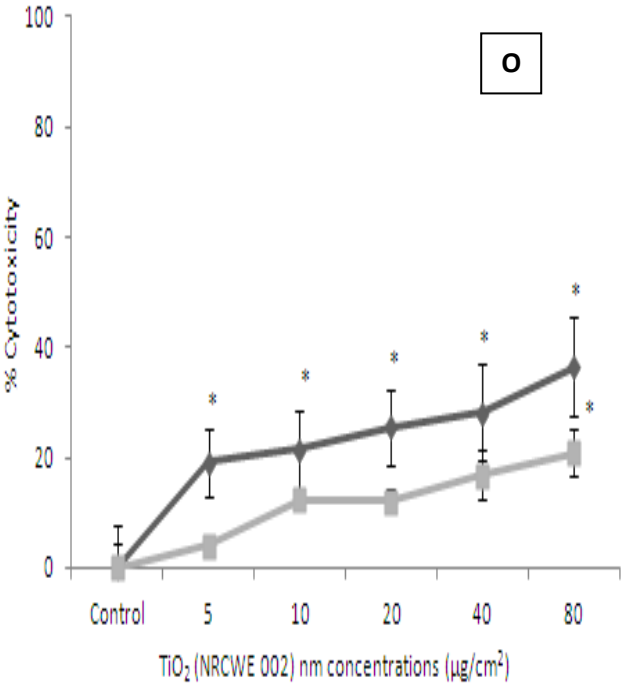
O
% Cytotoxicity
100
80
60
40
20
0
Control
5
10
20
40
80
TiO2 (NRCWE 002) nm concentrations (µg/cm2)

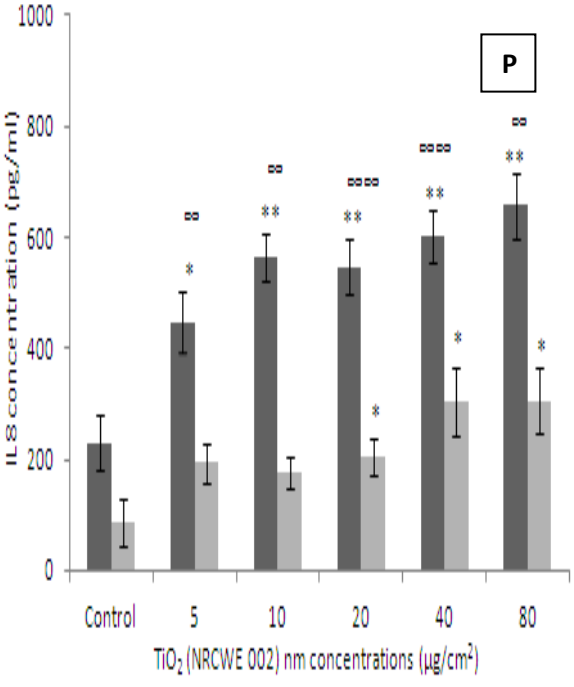
P
IL8 concentration (pg/ml)
1000
800
600
400
200
0
Control
5
10
20
40
80
TiO2 (NRCWE 002) nm concentrations (µg/cm2)

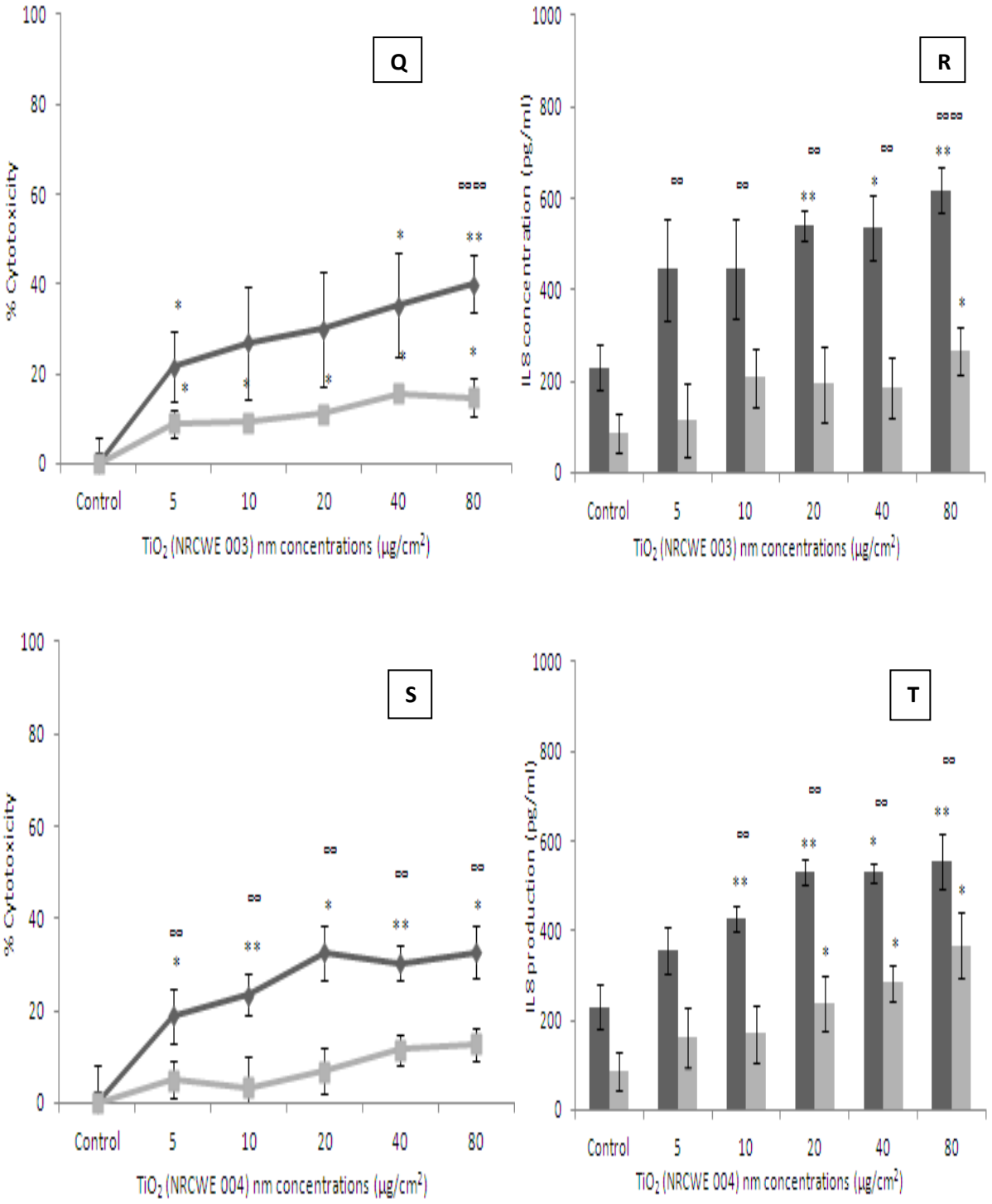

Figure 5.4. The cell viability and induction of IL8 production in C3A cells treated with the ENPRA NMs for 24 hr. Cells pre-treated with the antioxidant Trolox (100 µM, 1 hr) are show in grey, while cells not pre-treated are shown in black. Values represent mean ± SEM (n=3), significance indicated by * = $p<0.05$ and **= $p<0.005$, when nanomaterial treatments are compared to the control. ∞ = $p<0.05$ and ∞∞ $p<0.005$ is representative of significant difference between values signifying absence and presence of Trolox pre-treatment at each given concentration. **A)** NM 101 cytotoxicity **B)** NM 101 IL8 secretion **C)** NM 110 cytotoxicity **D)** NM 110 IL8 secretion **E)** NM 111 cytotoxicity **F)** NM 111 IL8 secretion **G)** NM 300 cytotoxicity **H)** 300 IL8 secretion **I)** NM 400 cytotoxicity **J)** NM 400 IL8 secretion **K)** NM 402 cytotoxicity **L)** NM 402 IL8 secretion **M)** NRCWE 001 cytotoxicity **N)** NRCWE 001 IL8 secretion **O)** NRCWE 002 cytotoxicity **P)** NRCWE 002 IL8 secretion **Q)** NRCWE 003 cytotoxicity **R)** NRCWE 003 IL8 secretion **S)** NRCWE 004 cytotoxicity **T)** NRCWE 004 IL8 secretion.

5.5 DNA damage in C3A cells

In order to investigate the possible DNA damage caused by the panel of nanomaterials, C3A cells were exposed to the NMs for 4 hr. In this study the LC_{20} value for each individual NM plus one concentration above (2x LC_{20}) and one below (0.5x LC_{20}) were chosen (The LC_{50} and LC_{20} values have been previously described) (Chapter 4) (Kermanizadeh, *et al*., 2012c).

DNA damage was most evident following exposure to NM 101 (TiO_2 - 7 nm) and NRCWE 002 (TiO_2 - 10 nm positively charged) (Figure 5.5a, h). There was also a small but significant increase in percentage tail DNA following exposure to seven of the other eight NMs investigated (NRCWE 003 - negatively charged TiO_2 10 nm being the exception) (Figure 5.5i).

Long term 8 week NM 300 (Ag) exposed cells resulted in a small but significant increase in tail moment compared to our cell only control, however there was no significant difference between short and long term exposure to LC_{20} of Ag (Figure 5.6).

Addition of the FPG enzyme to the samples resulted in increased percentage of tail DNA following treatment with the NMs. This indicates that the damage witnessed is partially due to oxidative DNA damage.

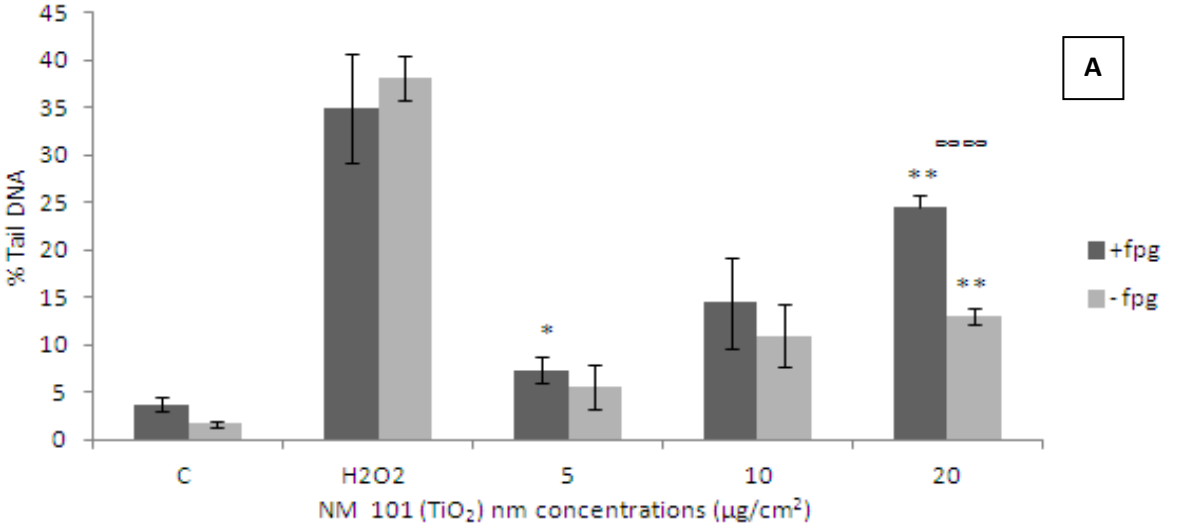
A
% Tail DNA
45
40
35
30
25
20
15
10
5
0
C
H2O2
5
10
20
NM 101 (TiO_2) nm concentrations (µg/cm²)
+fpg
- fpg
*
**
**
====

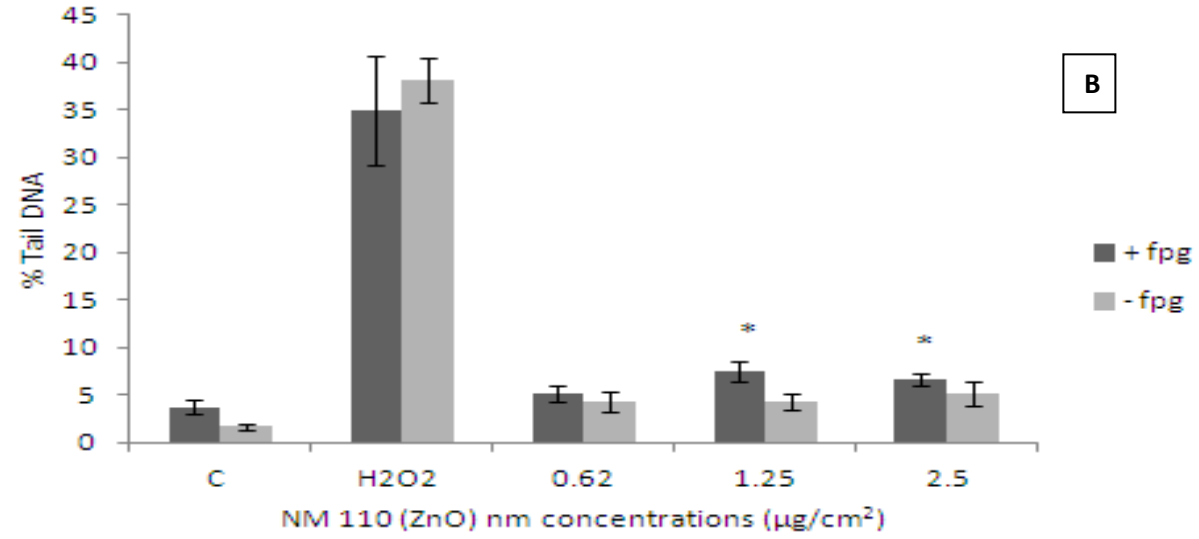
B
% Tail DNA
45
40
35
30
25
20
15
10
5
0
C
H2O2
0.62
1.25
2.5
NM 110 (ZnO) nm concentrations (µg/cm²)
+ fpg
- fpg
*
*

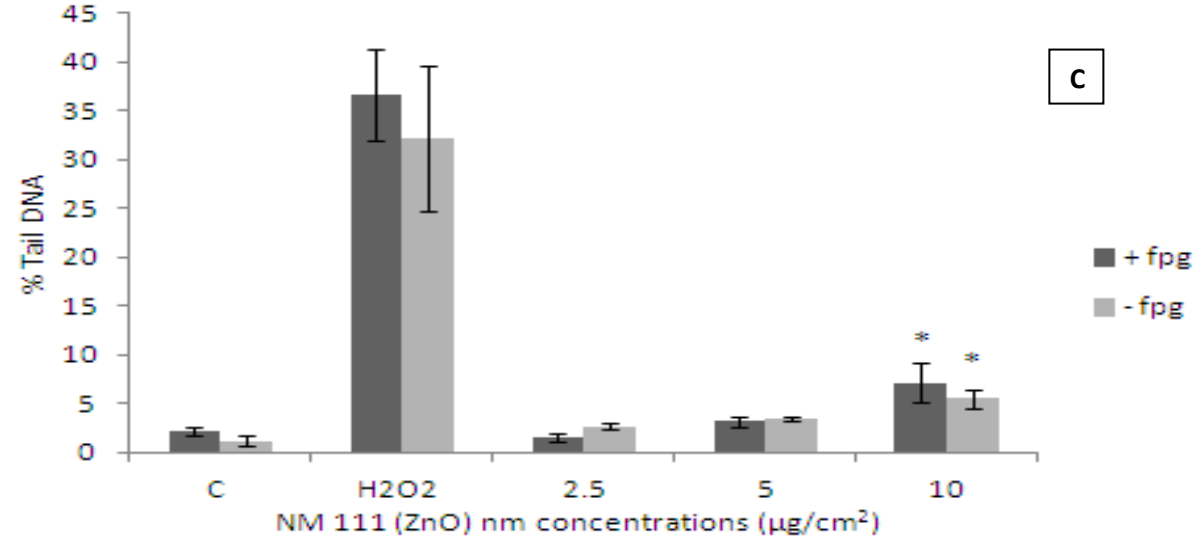
C
% Tail DNA
45
40
35
30
25
20
15
10
5
0
C
H2O2
2.5
5
10
NM 111 (ZnO) nm concentrations (µg/cm²)
+ fpg
- fpg
*
*

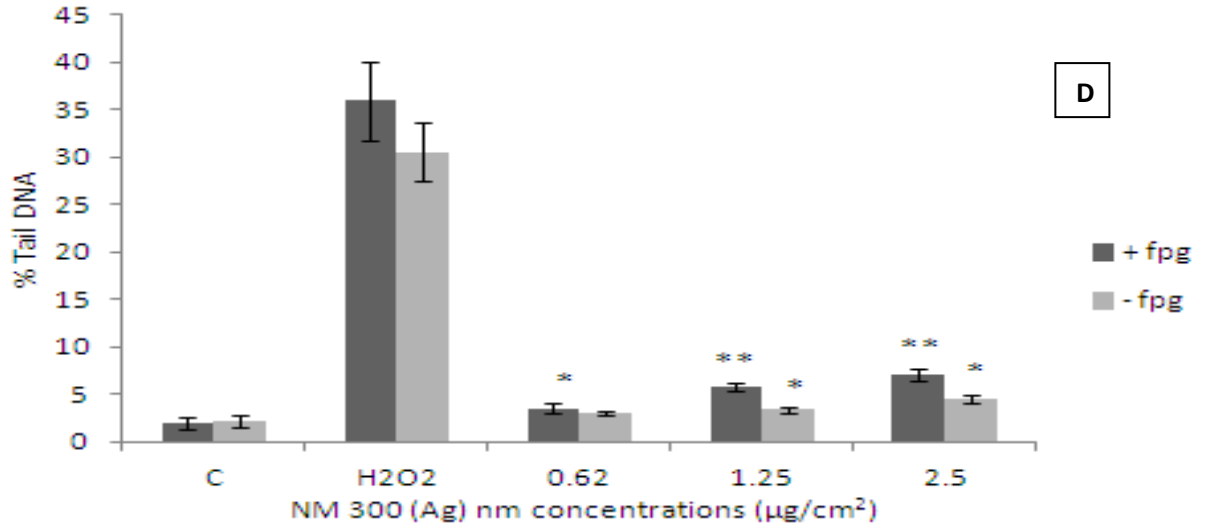
D
% Tail DNA
45
40
35
30
25
20
15
10
5
0
+ fpg
- fpg
C
H2O2
0.62
1.25
2.5
NM 300 (Ag) nm concentrations (µg/cm²)

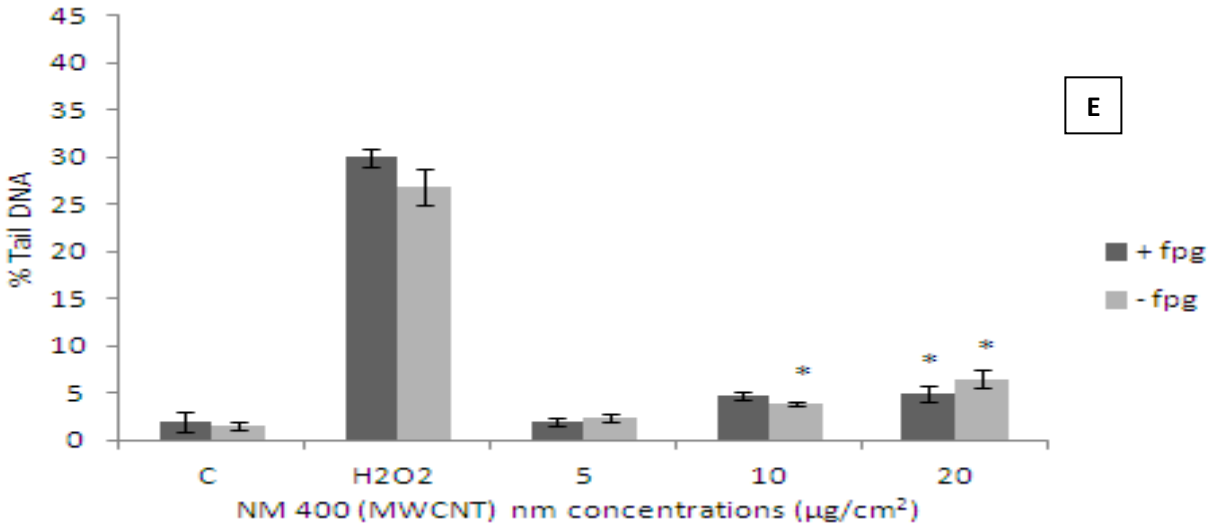
E
% Tail DNA
45
40
35
30
25
20
15
10
5
0
+ fpg
- fpg
C
H2O2
5
10
20
NM 400 (MWCNT) nm concentrations (µg/cm²)

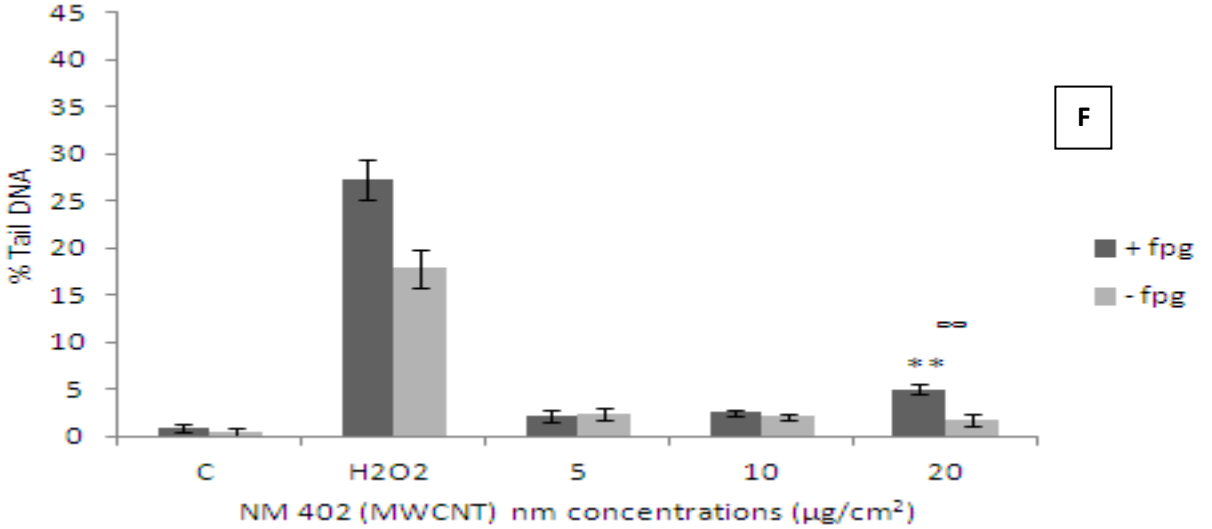
F
% Tail DNA
45
40
35
30
25
20
15
10
5
0
+ fpg
- fpg
C
H2O2
5
10
20
NM 402 (MWCNT) nm concentrations (µg/cm²)

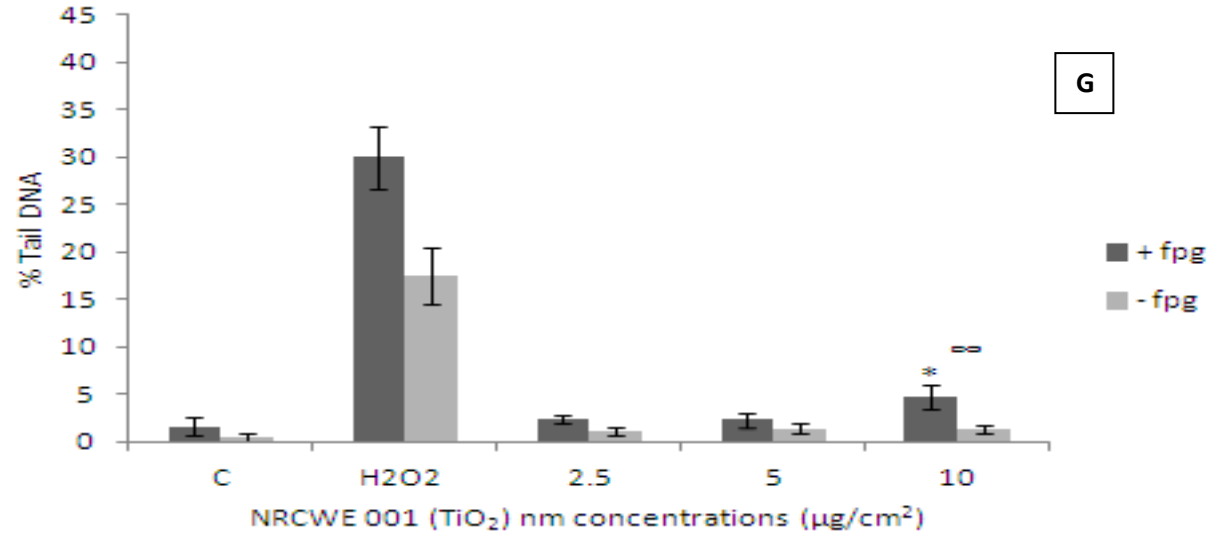
G
% Tail DNA
45
40
35
30
25
20
15
10
5
0
+ fpg
- fpg
C
H2O2
2.5
5
10
NRCWE 001 (TiO2) nm concentrations (µg/cm2)

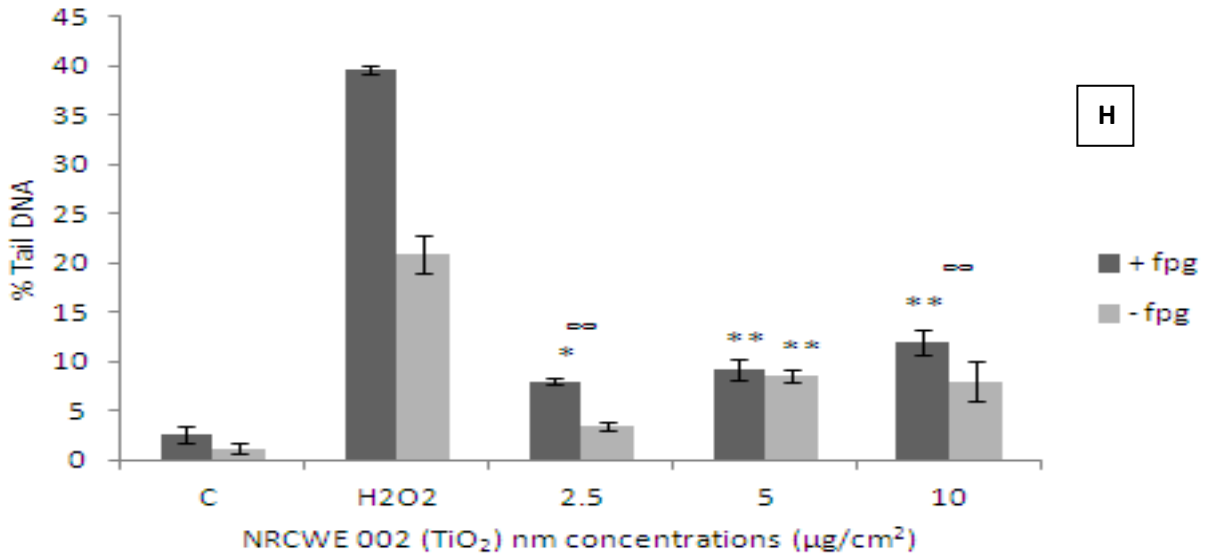
H
% Tail DNA
45
40
35
30
25
20
15
10
5
0
+ fpg
- fpg
C
H2O2
2.5
5
10
NRCWE 002 (TiO2) nm concentrations (µg/cm2)

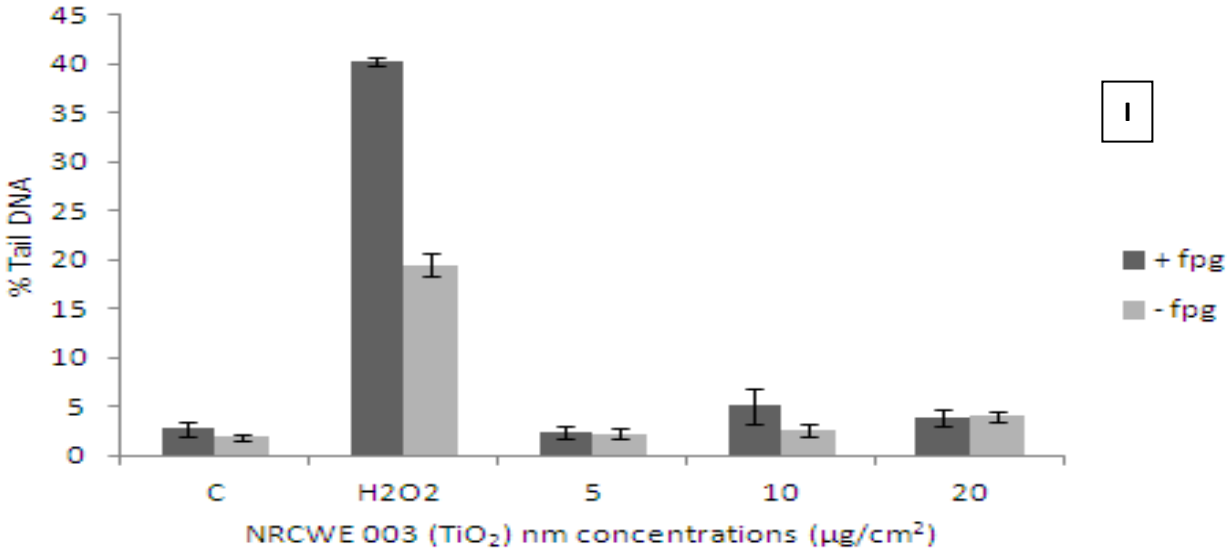
I
% Tail DNA
45
40
35
30
25
20
15
10
5
0
+ fpg
- fpg
C
H2O2
5
10
20
NRCWE 003 (TiO2) nm concentrations (µg/cm2)

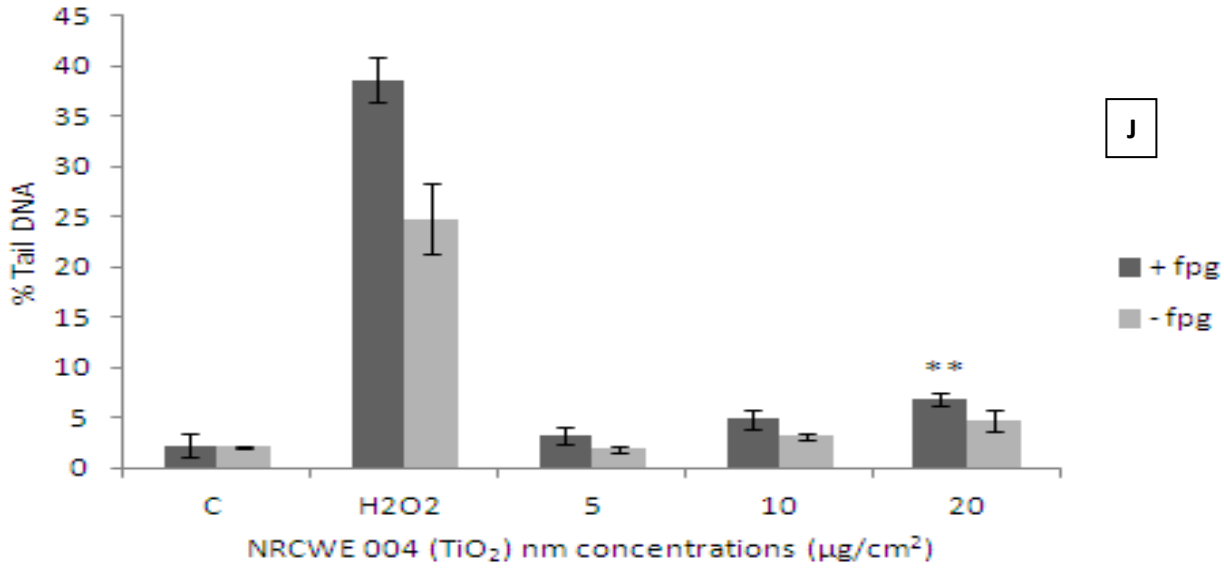

Figure 5.5. DNA damage expressed as percent of tail DNA following exposure of the C3A cells to LC_{20} ± one serial dilution to the ENPRA panel of engineered nanomaterials. The cells were exposed to cell medium (control), 60 µM H_2O_2 or NMs for 4 hr. Values represent mean ± SEM (n=3), significance indicated by * = $p<0.05$ and ** = $p<0.005$, when material treatments are compared to the control. ∞ = $p<0.05$ and ∞∞ $p<0.005$ is representative of significant difference between values signifying absence and presence of FPG enzyme at each given concentration**. A)** NM 101 **B)** NM 110 **C)** NM 111 **D)** NM 300 **E)** NM 400 **F)** NM 402 **G)** NRCWE 001 **H)** NRCWE 002 **I)** NRCWE 003 **J)** NRCWE 004.

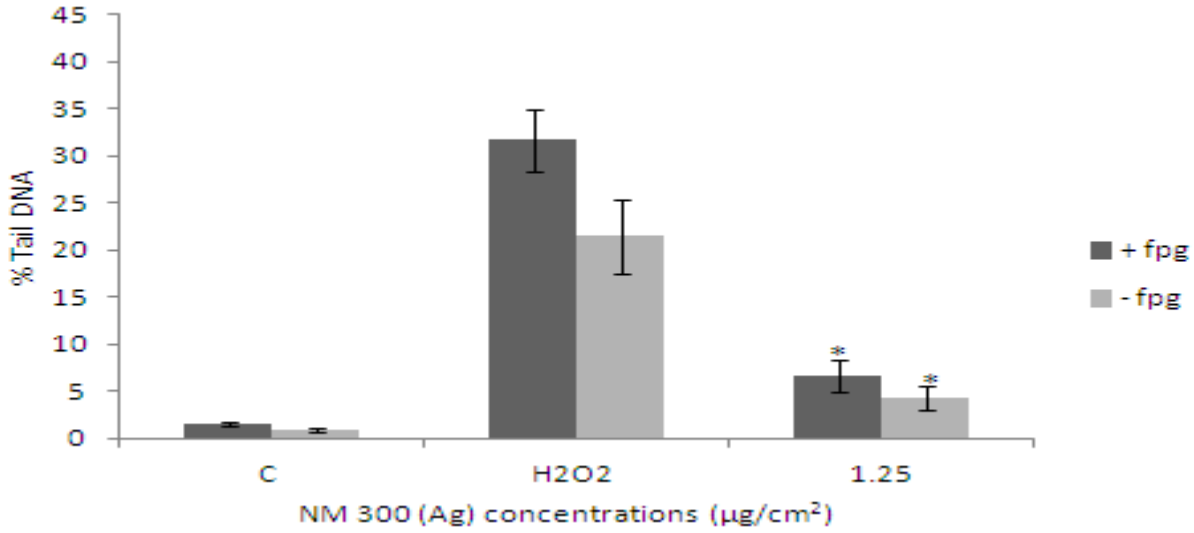

Figure 5.6. DNA damage expressed as percent of tail DNA following exposure of the C3A cells to LC_{20} of silver (NM 300). The cells were exposed to cell medium (control), 60 µM H_2O_2 (for 4 hr) or NMs for a period of 8 weeks. Values represent mean ± SEM (n=3), significance indicated by * = $p<0.05$.

5.6 Discussion

In the previous chapter it was demonstrated that the panel of nanomaterials investigated could be divided into a high toxicity group (two ZnO and one Ag) and a low toxicity group (five TiO_2 and two MWCNTs) according to their ability to induce cytotoxicity in the C3A cell line. The discussion below is therefore structured to allow comparison between the low toxicity and high toxicity materials in order to ascertain whether this pattern is retained across a wider array of sub-lethal endpoints (Table 5.1).

NM	Composition	LC50 (WST-1)	GSH Depletion	Increase in intracellular ROS levels	DNA damage compared to control
NM 101	TiO_2	> 80 µg/cm^2	No	Large	Yes
NM 110	ZnO	5 - 10 µg/cm^2	Yes	None	Yes
NM 111	ZnO	10 - 20 µg/cm^2	Yes	Small	Yes
NM 300	Ag	1.25 - 2.5 µg/cm^2	Yes	None	Yes
NM 400	MWCNT	> 80 µg/cm^2	Yes	Large	Yes
NM 402	MWCNT	> 80 µg/cm^2	Yes	Large	Yes
NRCWE 001	TiO_2	> 80 µg/cm^2	No	Large	Yes
NRCWE 002	TiO_2 (+)	> 80 µg/cm^2	No	Large	Yes
NRCWE 003	TiO_2 (-)	> 80 µg/cm^2	No	Large	No
NRCWE 004	TiO_2	> 80 µg/cm^2	No	Large	Yes

Table 5.1. Summary of the observed effects on C3A hepatocytes following exposure to the ENPRA panel of nanomaterials.

Initially the ability of the chosen NMs to induce glutathione depletion in C3A cells was examined. Exposure to the Ag and the two ZnO NMs resulted in significant GSH depletion following a 24 hr exposure. For these highly toxic NMs glutathione depletion at the higher concentrations might be associated with cell death rather than a specific oxidative stress response. In contrast, MWCNTs were also able to significantly deplete glutathione at doses which did not influence cell viability, suggesting that MWCNTs induced oxidative stress in these cells. The TiO_2 materials had no significant effect on the glutathione content of the cells suggesting that they are unable to induce oxidative stress in liver cells in dark experimental conditions.

Next, the intracellular ROS levels following exposure of the ENPRA panel of NMs was investigated. Interestingly the Ag and uncoated ZnO NMs did not generate detectable intracellular ROS according to the DCFH-DA assay at 24 hr, although small yet significant levels could be detected for coated ZnO (NM 111). This assay is dependent on intact viable cells therefore exposure to highly toxic nanomaterials could result in lower levels of fluorescence from the DCFH-DA assay. Furthermore, investigations into earlier exposure time-points (6 hr) revealed higher levels of DCF fluorescence for all of the NMs tested. We therefore suggest that the DCFH assay is not suitable for investigating the cellular ROS response to highly toxic NMs, or that it should be limited to relatively low concentrations and early time points for such materials.

In contrast a concentration dependant increase in ROS levels following exposure to the low toxicity nanomaterials (five TiO_2 and two MWCNT NMs) was observed indicating firstly that these low toxicity materials are able to generate intracellular ROS and secondly that the assay is suitable for these lower toxicity NMs. It is interesting to note that the ROS production by MWCNT translated into a GSH depletion at 24 hr, but the same was not true for the TiO_2 NMs. Either the cells were sufficiently protected with antioxidant defence mechanisms to prevent GSH depletion by the TiO_2 NM, or a longer time point might be required to assess such an effect. Another explanation for the ROS generation by the MWCNT might be that the iron residues within the nanotubes may contribute to the oxygen species generation (e.g. via Fe^{2+} fenton reaction).

A recent study investigated a rat derived liver cell line (BRL 3A) and 10 nm Ag NMs (up to 50 μg/ml – 24 hr exposure) and reported a significant GSH depletion (Hussain, *et al*., 2005).

In a contradictory study however the effects of silver NMs (220 µg/ml) on primary mice hepatocytes *in vitro* revealed a small increase in intracellular GSH levels subsequent to a 24 hr exposure to the particles (Arora, *et al*., 2004). Studies in which human Chang liver cells were exposed to Ag NMs also induced intracellular ROS generation (Piao, *et al*., 2011) which was contrary to findings in this study. However it is important to note that these finding were after much shorter exposure times (Piao, *et al*., 2011) which could therefore mean that viability of these cells was sufficient to allow ROS to be detected. Exposure of HepG2 cell to a 100 nm ZnO NMs resulted in high toxicity associated with reactive oxygen species and oxidative stress (Akhtar, *et al*., 2012).

We could not identify any studies in which the impacts of MWCNTs on hepatocytes was reported, but intraperitoneal injection of functionalized SWCNTs into Swiss-Webster mice resulted in increased ROS levels within liver cells and enhanced the activities of serum amino-transferases (Patlolla, *et al*., 2011).

In a recent set of trials the use of nanoparticulate TiO_2 (intragastric administration) resulted in mice liver damage with the authors suggesting oxidative stress as the mechanism of cytotoxicity (Wang, *et al*., 2011b). In another study exposure of mice (intragastric administration) to TiO_2 NMs for 60 days resulted in hepatocyte apoptosis associated by increased reactive oxygen species accumulation and decreased stress-related gene expression levels of superoxide dismutase and glutathione peroxidise (Cui, *et al*., 2010). These studies add support to our observations for MWCNT and TiO_2 with respect to ROS production in liver cells.

The lipophilic antioxidant Trolox decreased the Ag and ZnO induced cytotoxicity as well as the ZnO induced IL8 production. With respect to Ag, Trolox appeared to enhance IL8 production although this was not statistically significant. This might seem counter-intuitive, as it could be interpreted as protection of the cells from particle induced cytotoxicity by the antioxidant, thereby enhancing their ability to induce a pro-inflammatory response at doses that were toxic in previous experiments without the addition of Trolox (Chapter 4) (Kermanizadeh, *et al*., 2012c). The pre-treatment of the C3A cells with Trolox prevented the low toxicity nanomaterials from increasing DCF fluorescence, confirming that the DCFH assay was measuring oxidative activity. The pre-treatment with Trolox also resulted in protection against cytotoxicity following exposure to relatively high concentrations of TiO_2

NMs (NRCWE 001, NRCWE 004). In addition, Trolox pre-treatment decreased the IL8 secretion following exposure to these NMs. Taken together these results suggest that ROS play a key role in the up regulation of cytokines in hepatocytes following exposure to ZnO, TiO_2 and the MWCNT NMs.

To our knowledge there have been no nanotoxicological studies that have pre-treated liver cells with Trolox *in vitro*, however Trolox pre-treatment of human macrophages significantly reduced the toxicity of superparamagnetic iron oxide (Lunov, *et al*., 2010) and TiO_2 NMs (Miller, *et al*., 2007). The authors of two other studies in which human monocytes were pre-treated with Trolox before exposure to fine carbon black also noted a decrease in the pro inflammatory cytokine TNF-α (Brown, *et al*., 2002; Brown, *et al*., 2007). Contrary to these findings, pre-treatment with Trolox of J774.A1 macrophages (Clift, *et al*., 2010), PC 12 cells (cell line derived from a pheochromocytoma of the rat adrenal medulla) (Lovric, *et al*., 2005), N9 (murine microglial cell line) (Lovric, *et al*., 2005) followed by exposure to quantum dots did not prevent toxicity or cytokine production by the cells.

We also investigated any possible genotoxic effects following exposure to the NMs at sub-lethal concentrations. Short term exposure (4 hr) of C3A cells to the ENPRA panel of nanomaterials resulted in a small but significant increase in percent tail DNA for nine of the ten NMs investigated (the negatively charged TiO_2 - NRCWE 003 being the exception). Exposure of the C3A cells to LC_{20} of Ag NM for 8 weeks resulted in a marginal yet significant increase in tail moment compared to the control, however there was no significant difference between short and long term exposure to this particular particle. A small but significant increase in DNA damage following exposure to both ZnO and the two MWCNT NMs was also noted. Genotoxicity was most evident following exposure to NM 101 (TiO_2 7 nm) and NRCWE 002 (positively charged TiO_2 10 nm). The relative genotoxicity of the NM panel is therefore strikingly different to their ranking with respect to cytotoxicity. This therefore indicates the importance of assessing sub-lethal effects and the need for further chronic *in vivo* studies to assess the validity of these short term *in vitro* observations.

It is important to emphasis the role of FPG enzyme in the comet assay. The enzyme measures specific oxidative DNA mediated strand breaks so it is not surprising to see increased tail length in the presence of the enzyme following exposure to one of the MWCNTs (NM 402) and three of the TiO_2 NMs (NM 101, NRCWE 001 and NRCWE 002). As seen from the data

in the DCFH-DA assay there was a significant increase in intracellular ROS following exposure of the hepatocytes to these materials. Therefore these findings suggest that ROS plays an important role in the genotoxicity witnessed for the MWCNTs and TiO_2 NM investigated in this study.

In a recent study exposure of human epidermal cell line A431 to TiO_2 resulted in significant oxidative stress related DNA damage (Shukla, *et al*., 2011). Our short-term exposure findings are similar in part to a study in which low concentration exposures of 90 nm TiO_2 NMs to human embryo hepatocytes did not induce DNA breaks or chromosome damage (Shi, *et al*., 2010b). Another study using A549 cells alveolar epithelial cells, HepG2 hepatocytes and NRK-52E kidney cells were exposed to a panel of NMs including TiO_2, Al_2O_3, gold and MWCNTs discovered that genotoxicity was weak and that DNA damage was limited to single-strand beaks and/or alkali-labile sites (Simon, *et al*., 2007).

5.7 Conclusion

In conclusion, utilising this particular *in vitro* hepatocyte model showed that the NM which induced a low cytotoxicity (TiO_2 and MWCNTs), generated intracellular ROS, induced oxidative stress (GSH depletion), and that an oxidative mechanism was involved in both the induction of IL8 protein production and genotoxicity according to the Comet assay. The highly toxic Ag and ZnO NMs appeared to work by different mechanisms. Silver did not generate ROS measurable by the DCFH-DA assay, although pre-treatment with an antioxidant may marginally enhance IL8 production by the hepatocytes suggesting that the toxic mechanisms might be partially mediated by ROS. In addition the data indicates that Ag particles are capable of enhancing a pro-inflammatory response, providing that they are not too toxic.

Chapter Six

Primary human hepatocytes vs. hepatic cell line: suitability for *in vitro* nanotoxicology testing

Based on publication: Kermanizadeh, A, Gaiser BK, Ward MB, Stone V. (2012b). Primary human hepatocytes vs. hepatic cell line – assessing their suitability for *in vitro* nanotoxicology. Nanotoxicology DOI: 10.3109/17435390.2012.734341.

6.1 Aims and chapter outline

The use of hepatocyte cell lines as a replacement for animal models have been heavily criticised mainly due to low expression of metabolism enzymes. This study compares primary human hepatocytes to the C3A cell line and with respect to their response to a panel of nanomaterials.

Here the potential of engineered NMs to induce cytotoxicity, measured by mitochondrial function using the WST-1 assay, and to induce an inflammatory response in the C3A and primary human cells, measured by the release of pro-inflammatory cytokines (IL6, IL8 and TNF-α) was measured. Furthermore albumin was measured following exposure of the cells to the panel of nanomaterials as a good indicator of hepatic functionality. Finally, the interaction of the NMs with the cells was investigated by the use of transmission and scanning electron microscopy (TEM and SEM).

In this study six of the ten NMs in the panel of ENPRA nanomaetrials were utilised (selected as the priority NMs by the ENPRA consortium).

6.2 Characteristics of nanomaterials and exposure media

Investigated nanomaterials were characterised by a combination of analytical techniques in order to infer primary physical and chemical properties useful to understand their toxicological behaviour and described in chapter 4 (Kermanizadeh, *et al*., 2012c). In order to investigate if the nanomaterials behaved differently in William's E medium, the hydrodynamic size distributions of the NMs was measured by DLS after the nanomaterials were dispersed in the complete medium between 1 - 128 µg/ml (Table 6.1).

ENM code	ENM type	Size in MEM (DLS) Ψ	Size in William's E medium (DLS) Ψ
NM 110	ZnO	306	393.3
NM 111	ZnO	313	322.1
NM 300	Ag	114	137.7
NM 400	MWCNT	*	*
NM 402	MWCNT	*	*
NRCWE 002	TiO_2	287	314.9

[$] wet XRD in capillary tube
[£] dried samples
* Not detectable by DLS due to the very large aspect ratio
Ψ Intensity based size average in biological media after 15 mins.

Table 6.1. Main physical and chemical properties of tested NMs in MEM and William's E medium.

6.3 Impact of the selected panel of NMs on C3A and human primary cell viability

From the WST-1 data it was evident that there was a dose dependent decrease in cell viability at 24 hr across the entire nanomaterial panel for both C3A and primary human hepatocytes (Figure 6.1). Overall the toxicity following exposure to the panel of engineered NMs was fairly similar for both the C3A and primary cells, although small differences were witnessed for the uncoated ZnO NM between the cell types which were significant at the higher exposures (Figure 6.1a). An LC_{50} was reached following exposure to Ag (NM 300), uncoated ZnO (NM 110) and coated ZnO (NM 111) after a 24 hr exposure (Figure 6.1a, b and c). All of the TiO_2 and MWCNT NMs were considered to be low toxicity materials as the LC_{50} was not reached after a 24 hr exposure to the C3A and primary cells at the range investigated (Table 6.2).

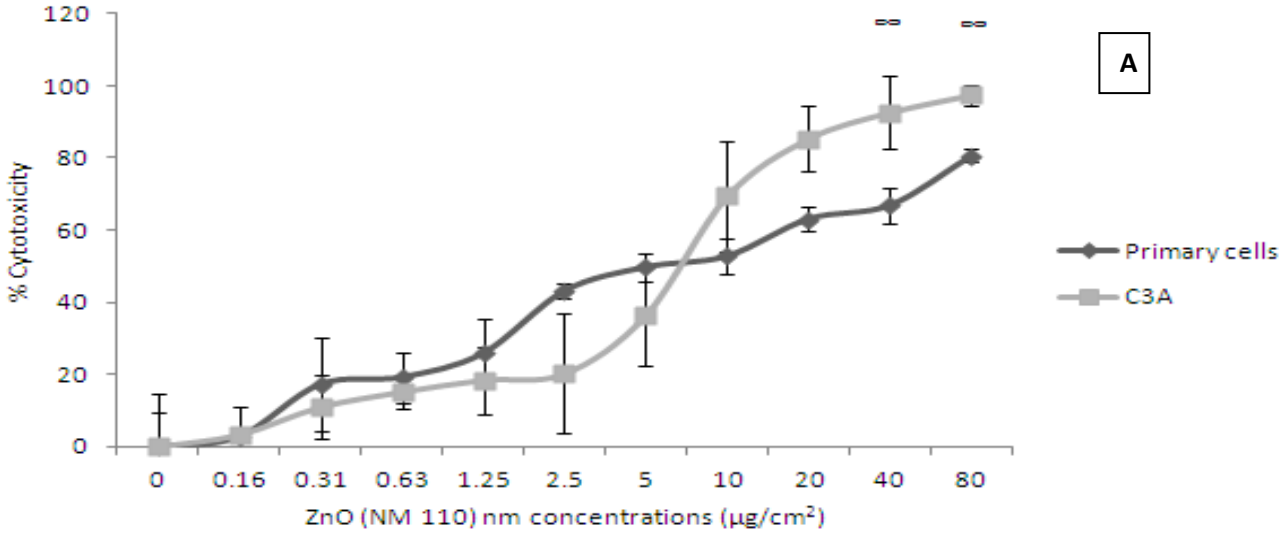
120
100
80
60
40
20
0
% Cytotoxicity
0
0.16
0.31
0.63
1.25
2.5
5
10
20
40
80
ZnO (NM 110) nm concentrations (µg/cm²)
A
Primary cells
C3A

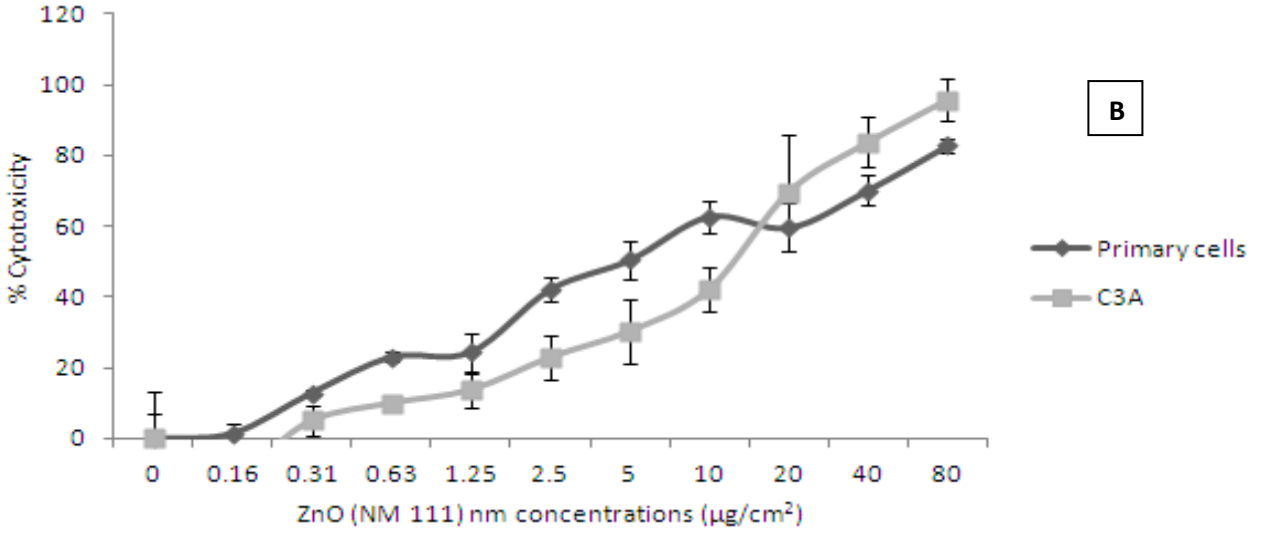
120
100
80
60
40
20
0
% Cytotoxicity
0
0.16
0.31
0.63
1.25
2.5
5
10
20
40
80
ZnO (NM 111) nm concentrations (µg/cm²)
B
Primary cells
C3A

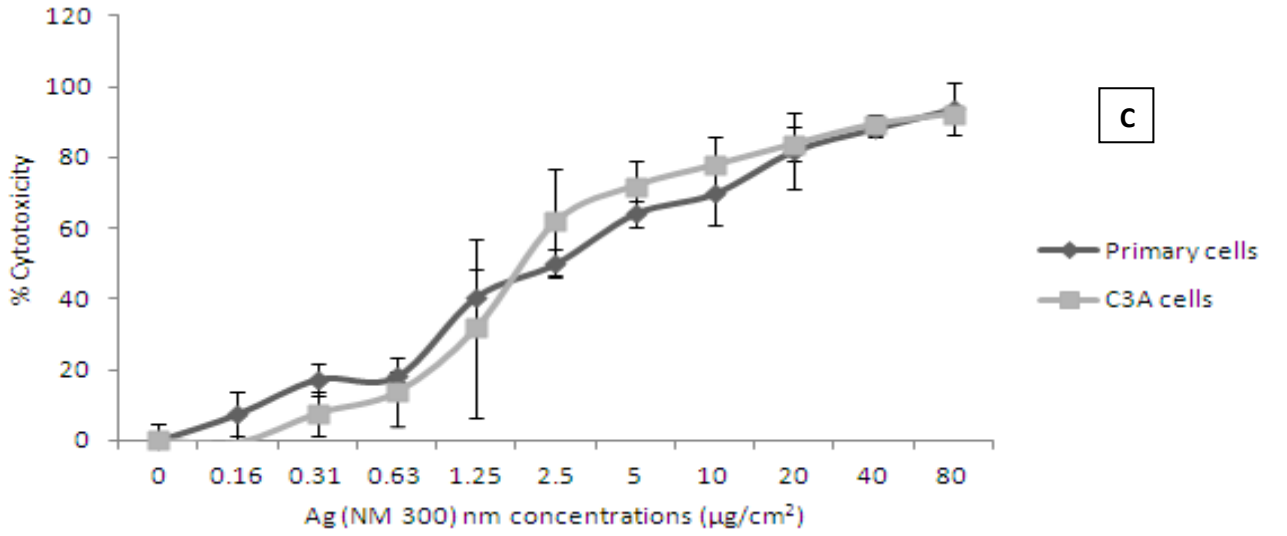
120
100
80
60
40
20
0
% Cytotoxicity
0
0.16
0.31
0.63
1.25
2.5
5
10
20
40
80
Ag (NM 300) nm concentrations (µg/cm²)
C
Primary cells
C3A cells

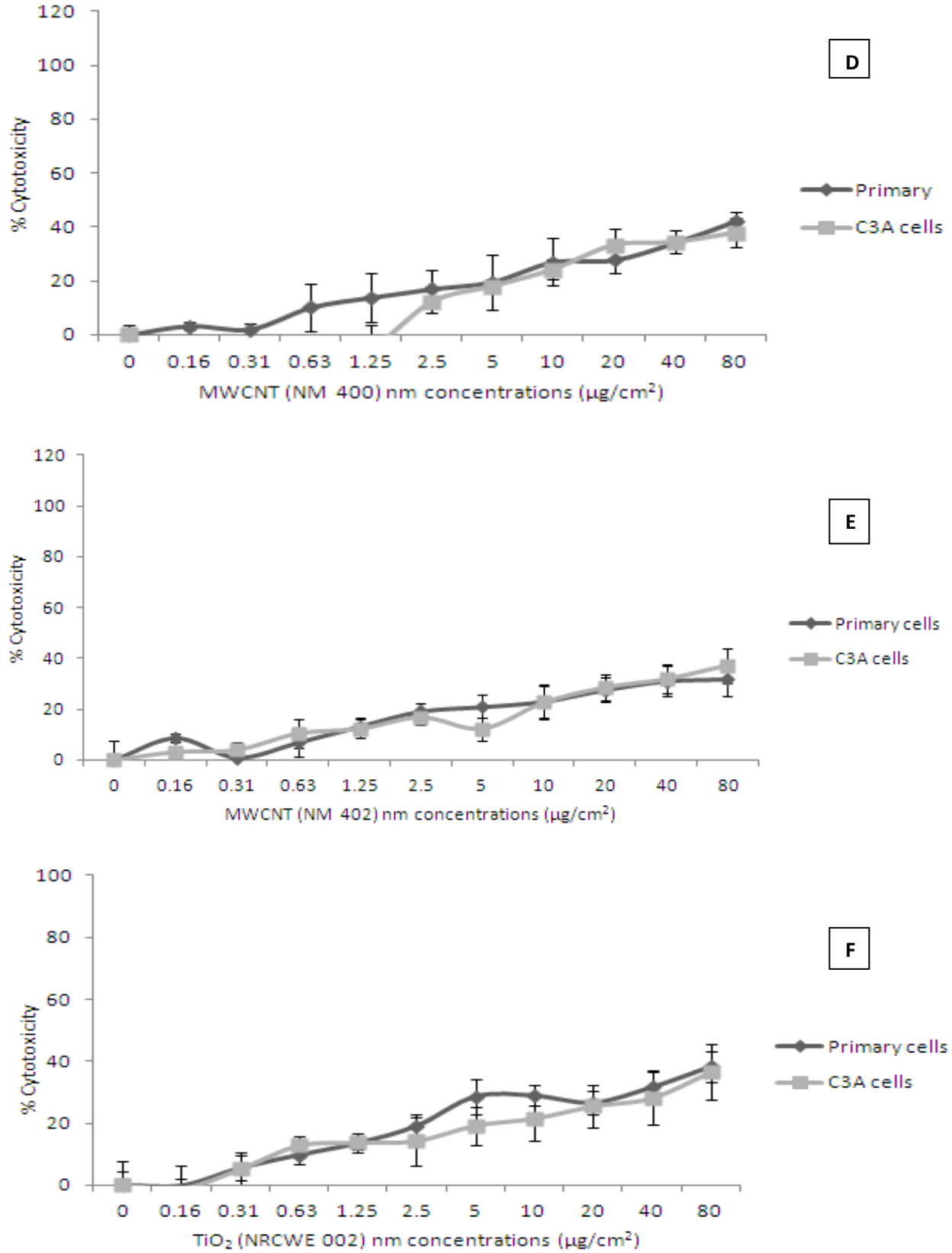

Figure 6.1. Cytotoxicity of C3A cells and human primary hepatocytes in the presence of a panel of engineered nanomaterials. The cells were exposed to cell medium control and NMs for 24 hr with cytotoxicity measured via the WST-1 assay. Values represent mean ± SEM (n=3). **A)** NM 110 **B)** NM 111 **C)** NM 300 **D)** NM 400 **E)** NM 402 **F)** NRCWE 002. Significance difference between C3A and primary cells indicated by ∞ = $p<0.05$.

	C3A - LC_{50} (WST-1), µg/cm^2	**Primary hepatocytes LC_{50} (WST-1), µg/cm^2**
NM 110	LC_{50} between 5 and 10 µg/cm^2	LC_{50} between 5 and 10 µg/cm^2
NM 111	LC_{50} is between 10 and 20 µg/cm^2	LC_{50} around 5 µg/cm^2
NM 300	LC_{50} is between 1.25 and 2.5 µg/cm^2	LC_{50} around 2.5 µg/cm^2
NM 400	LC_{50} not reached up to 80 µg/cm^2	LC_{50} not reached up to 80 µg/cm^2
NM 402	LC_{50} not reached up to 80 µg/cm^2	LC_{50} not reached up to 80 µg/cm^2
NRCWE 002	LC_{50} not reached up to 80 µg/cm^2	LC_{50} not reached up to 80 µg/cm^2

Table 6.2. WST-1 cytotoxicity following 24 hr exposure of C3A hepatocytes and human primary hepatocytes to NM 110 (ZnO - uncoated 100 nm), NM 111 (ZnO - coated 130 nm), NM 300 (Ag - < 20 nm) and NM 400 (MWCNT), NM 402 (MWCNT) and NRCWE 002 (TiO_2 - rutile 10 nm with positive charge) NMs.

6.4 Impact of the engineered NMs on C3A and human hepatocyte IL8 production

Changes in cytokine production as a consequence of NM exposure were assessed within the supernatant of exposed hepatocytes and quantified via ELISA. For the low toxicity TiO_2 and MWCNT samples (NRCWE 002, NM 400 and NM 402) the IL8 production increased in a dose dependent manner, reaching statistical significance compared to the control at high exposure concentrations (Figure 6.2d, e and f). However, in the presence of the highly toxic materials Ag and ZnO (NM 300, NM 110 and NM 111) there was a significant increase in the level of IL8 protein production, followed by a decrease in the amounts of the cytokine produced as the toxicity increased (Figure 6.2a, b and c). A similar pattern of IL8 secretion from both the cell line and primary cells following exposure to the panel of ENPRA NMs was noted. However, there were small but significant differences between the two cell types on certain exposures. These differences included one low exposure for NM 111, two low exposures for NM 300, one exposure for both MWCNTs and the four highest exposures for the TiO_2 NM. Following the exposure to the ZnO and the Ag at these mentioned concentrations IL8 secretion was higher from the primary hepatocytes while exposure to the MWCNT and the TiO_2 at the above mentioned concentrations resulted in greater cytokine production from the C3A cells. The cells treated with LPS produced significant amounts of IL8 (primary cells – 662.3±71.0 pg/ml; C3A cells – 682.5±30.6 pg/ml).

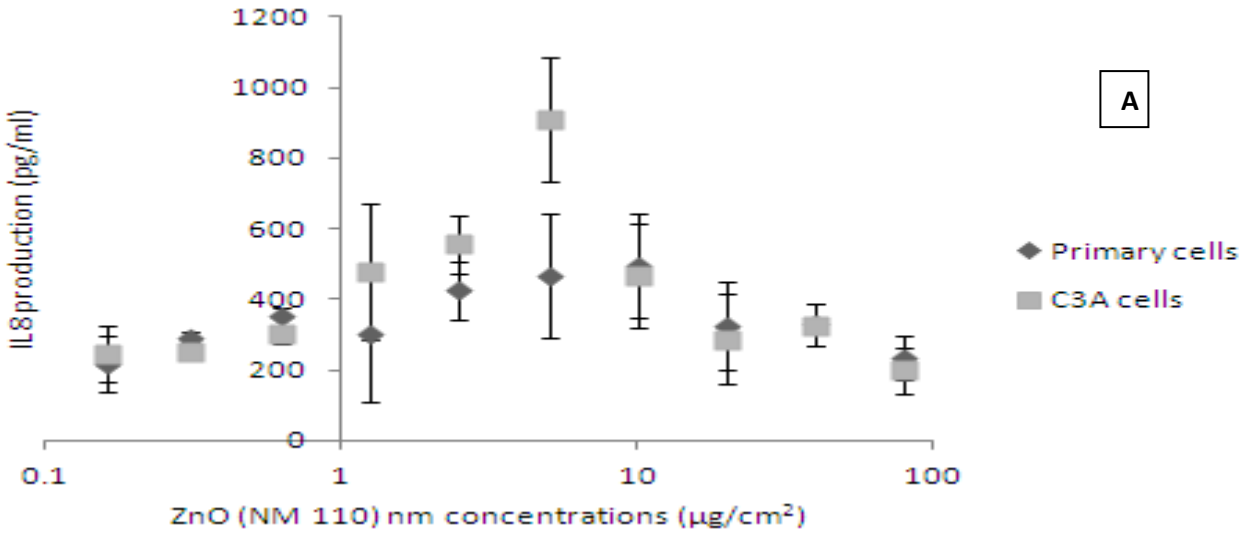
A
IL8 production (pg/ml)
1200
1000
800
600
400
200
0
0.1
1
10
100
ZnO (NM 110) nm concentrations (µg/cm²)
Primary cells
C3A cells

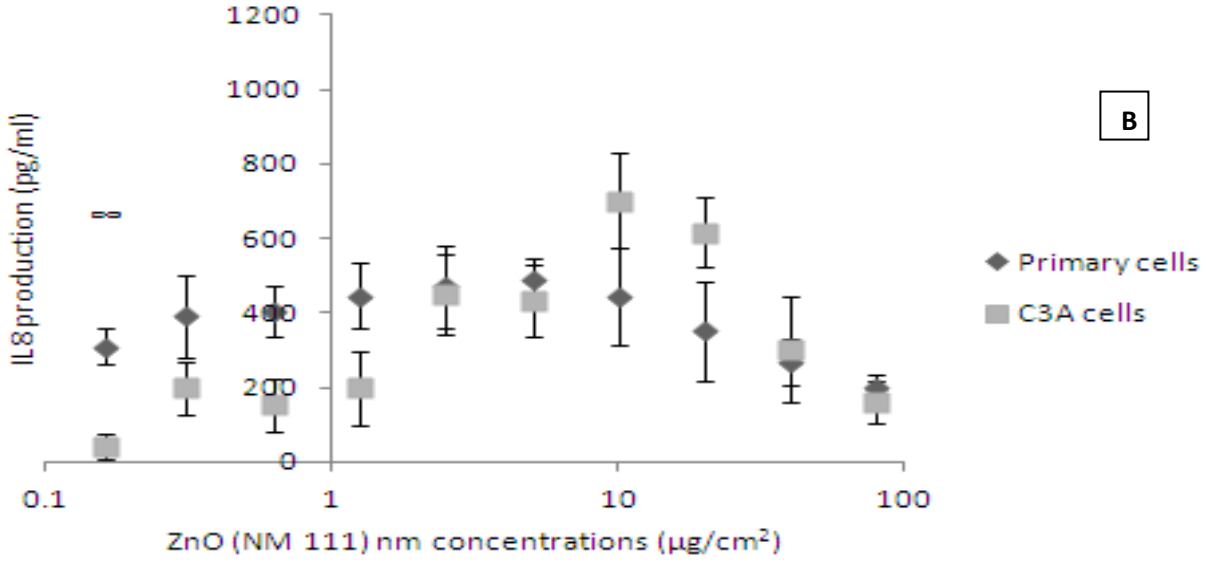
B
IL8 production (pg/ml)
1200
1000
800
600
400
200
0
0.1
1
10
100
ZnO (NM 111) nm concentrations (µg/cm²)
Primary cells
C3A cells

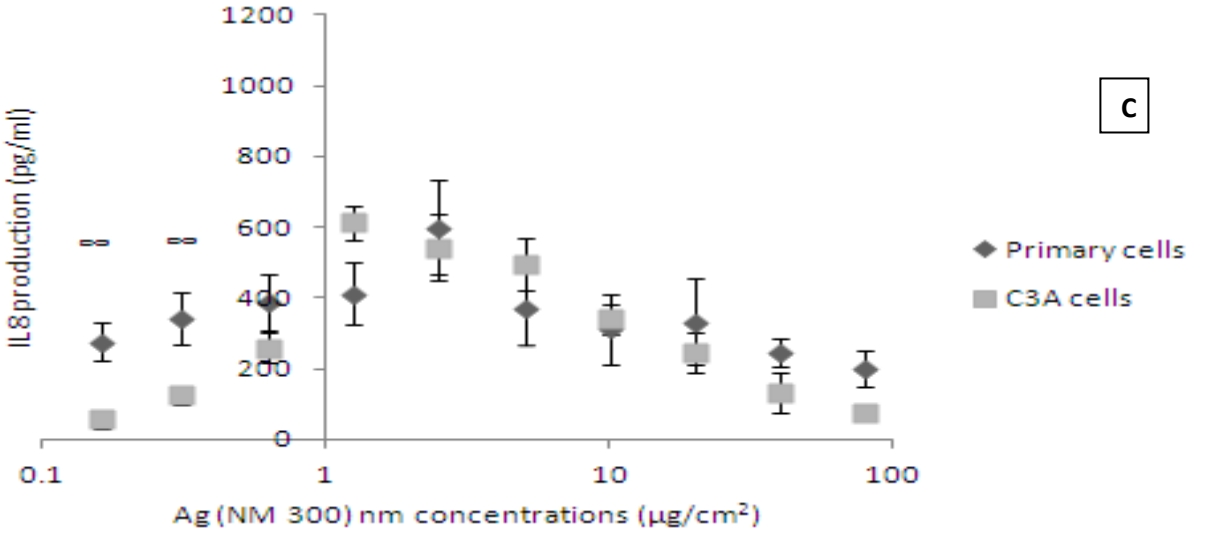
C
IL8 production (pg/ml)
1200
1000
800
600
400
200
0
0.1
1
10
100
Ag (NM 300) nm concentrations (µg/cm²)
Primary cells
C3A cells

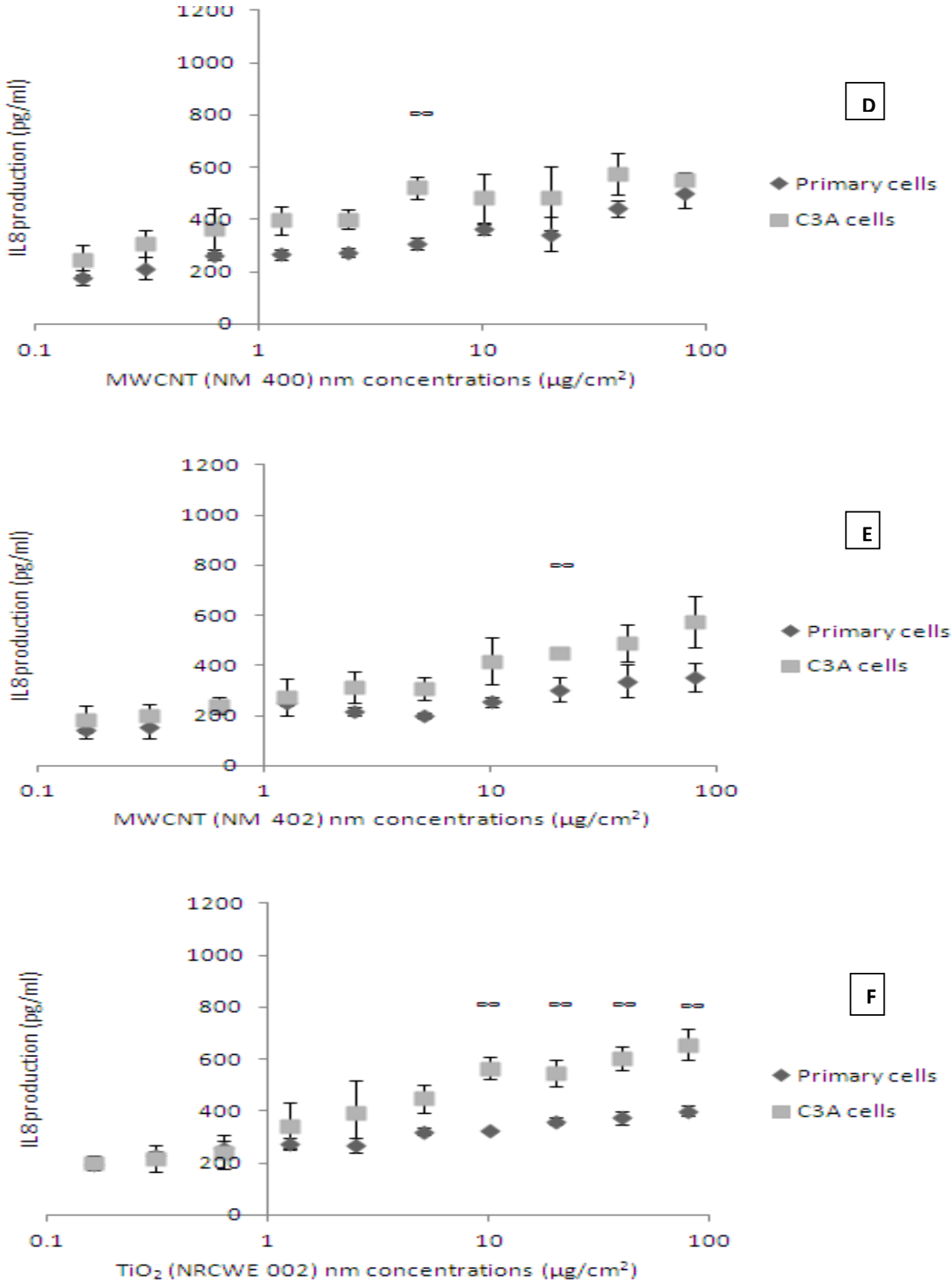

Figure 6.2. IL8 secretion by C3A cells and primary human hepatocytes in the presence of a panel of engineered nanomaterials. The cells were exposed to cell medium control and NMs for 24 hr. IL8 production within cell supernatants was measured by ELISA. Values represent mean ± SEM (n=3). **A)** NM 110 **B)** NM 111 **C)** NM 300 **D)** NM 400 **E)** NM 402 **F)** NRCWE 002. Significance between C3A and primary hepatocytes indicated by ∞ = $p<0.05$.

6.5 Impact of the NMs on C3A and primary hepatocyte in terms of IL6 and TNF-α production

Secretion of IL6 and TNF-α into the supernatant of exposed hepatocytes was quantified using ELISA analysis. There was no significant increase or decrease in the production of IL6 or TNF-α compared to the negative control after the exposure of the C3A cells or primary cells to any of the selected nanomaterials (data not shown). As a positive control both cell types were treated with LPS for 24 hr. This resulted in IL6 production by both cell types (primary hepatocytes 650±250 pg/ml; C3A cells 530±286 pg/ml. LPS treatment of both cell types did not result in any TNF-α production from the hepatocytes above the back ground levels.

6.6 Impact of engineered NMs on albumin production by primary hepatocytes

In order to establish whether any of the NMs affected albumin production, four exposure concentrations were chosen for each material. These concentrations included the LC_{50} and three subsequently lower concentrations for the highly toxic particles (NM 110, NM 111 and NM 300) and four highest concentrations for the low toxicity nanomaterials (80, 40, 20 and 10 $\mu g/cm^2$). There was a significant decrease in levels of albumin secreted at LC_{50} concentrations for the NM 110 ZnO NM (compared to the control) (Figure 6.3a). However, none of the other five NMs were capable of affecting albumin production by primary hepatocytes. As shown in chapter 4 sub-lethal exposures to the nanomaterials did not impact albumin production from C3A cells with the exception of the two ZnO NMs at LC_{50}.

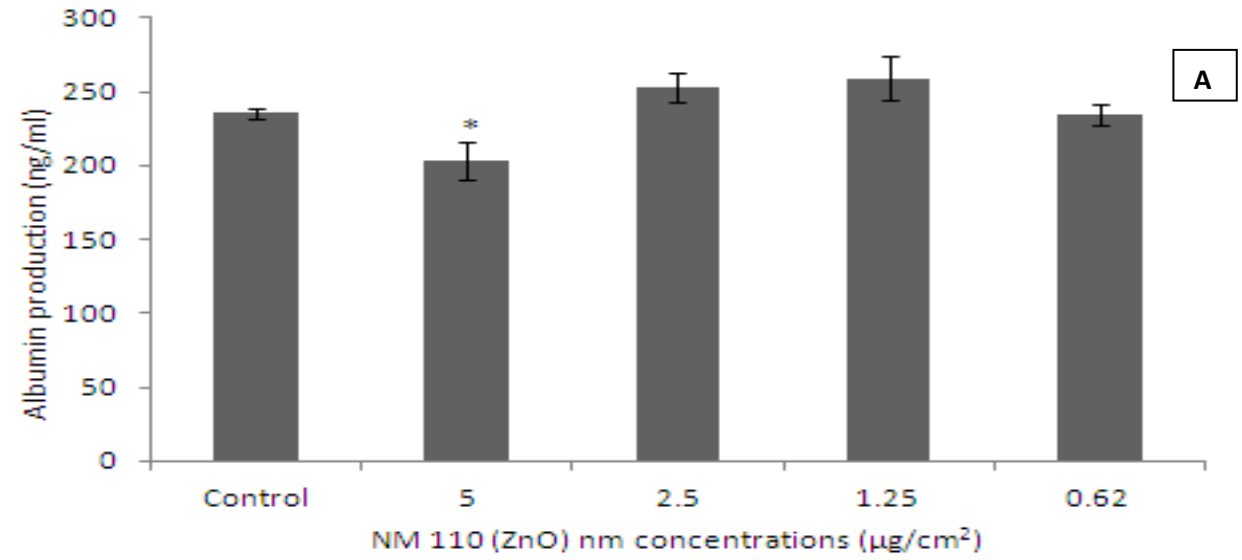
A
Albumin production (ng/ml)
300
250
200
150
100
50
0
*
Control
5
2.5
1.25
0.62
NM 110 (ZnO) nm concentrations (µg/cm²)

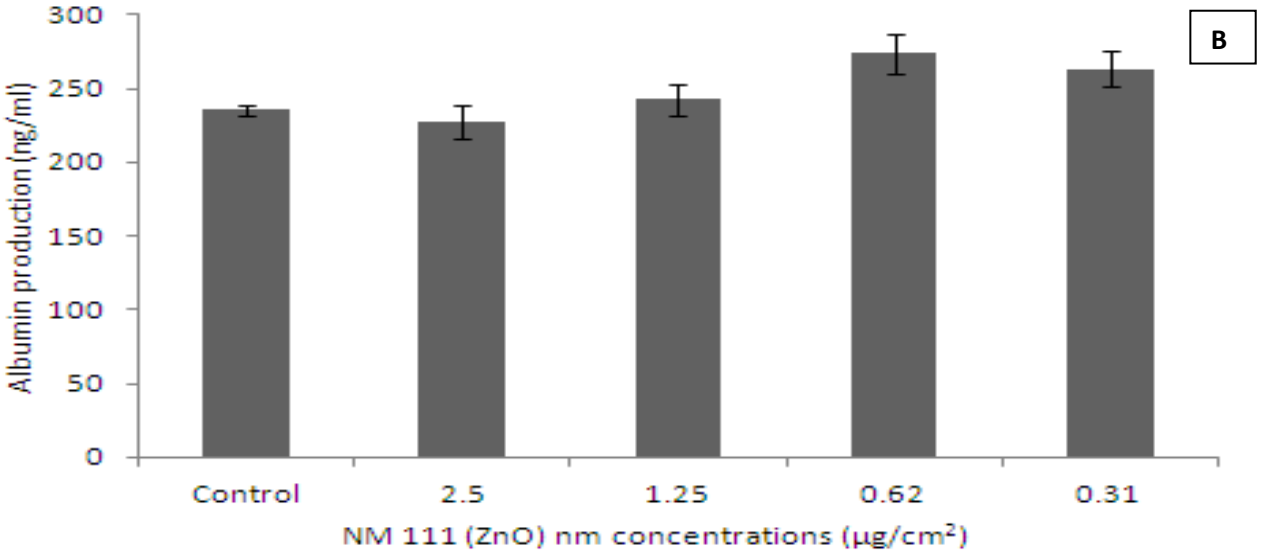
B
Albumin production (ng/ml)
300
250
200
150
100
50
0
Control
2.5
1.25
0.62
0.31
NM 111 (ZnO) nm concentrations (µg/cm²)

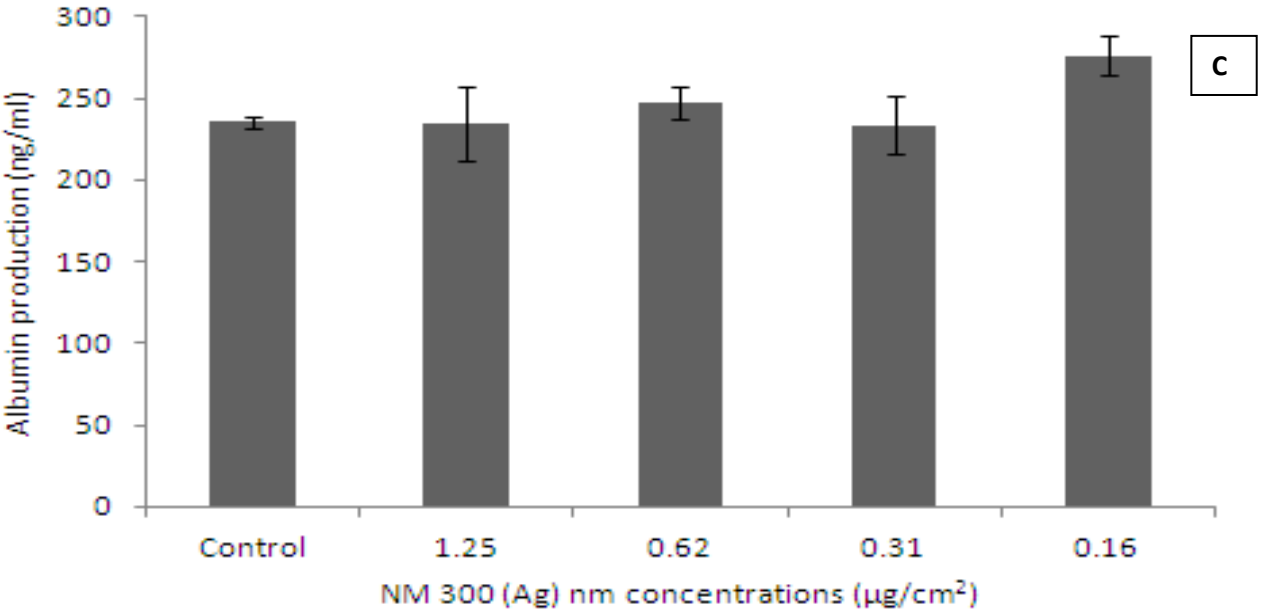
C
Albumin production (ng/ml)
300
250
200
150
100
50
0
Control
1.25
0.62
0.31
0.16
NM 300 (Ag) nm concentrations (µg/cm²)

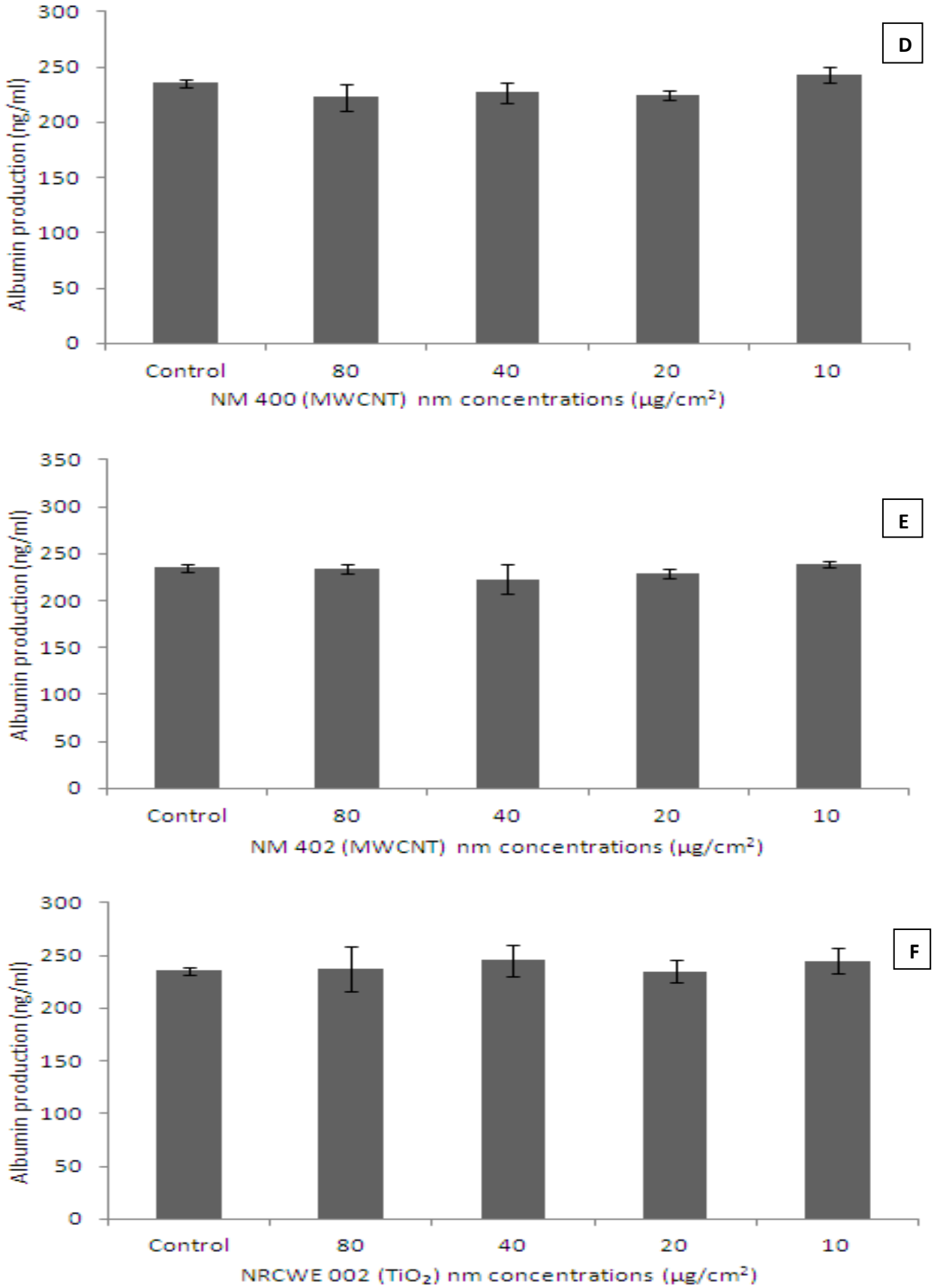

Figure 6.3. Albumin production from primary human hepatocytes following exposure to sub-lethal concentrations of the panel of engineered nanomaterials. Cells were exposed to medium (control) or NMs for 24 hr. Values represent mean ± SEM (n=3), significance indicated by * = $p<0.05$, compared to the control. **A)** NM 110 **B)** NM 111 **C)** NM 300 **D)** NM 400 **E)** NM 402 **F)** NRCWE 002.

6.7 Interaction of cells and the nanomaterials

In order to observe the interaction between the cells and the nanomaterials we utilised TEM (Figures 6.4-10) and SEM (Figures 6.11-17). It was noted that both the C3A cells and primary human cells were capable of uptake of nanomaterials (Figure 6.4-10). This alone was quite an interesting finding as hepatocytes are not intrinsically phagocytic cells. Four of the nanomaterials were observed in the cytoplasm of the investigated cells (NM 300, NM 400, NM 402 and NRCWE 002). Additionally, one of the MWCNT (NM 402) was also found in the nucleus of both the cell line and the primary cells (Figure 6.9). The two ZnO NMs investigated in this study are extremely soluble in the chosen media (Chapter 4) (Kermanizadeh, *et al*., 2012c) and as a result no individual particles were observed, nor was any high local concentration of Zn present for detection via EDX. Therefore only damage caused by these NMs is shown (Figure 6.5 and 6.6).

Furthermore, we investigated the surface interaction of the cells with the NMs utilising SEM. It is evident that the highly toxic NMs (Ag and ZnO) cause relatively large amounts of surface damage to both the C3A and the primary cells (Figures 6.12, 13 and 14). The MWCNT are clearly visible as thin fibres on the surface of the cells and they tended to agglomerate around the cells (Figure 15 and 16). The TiO_2 NMs were evident on the surface of the cells (Figure 6.17). Once again there were no distinguishable differences between the C3A cell line and the primary human hepatocytes.

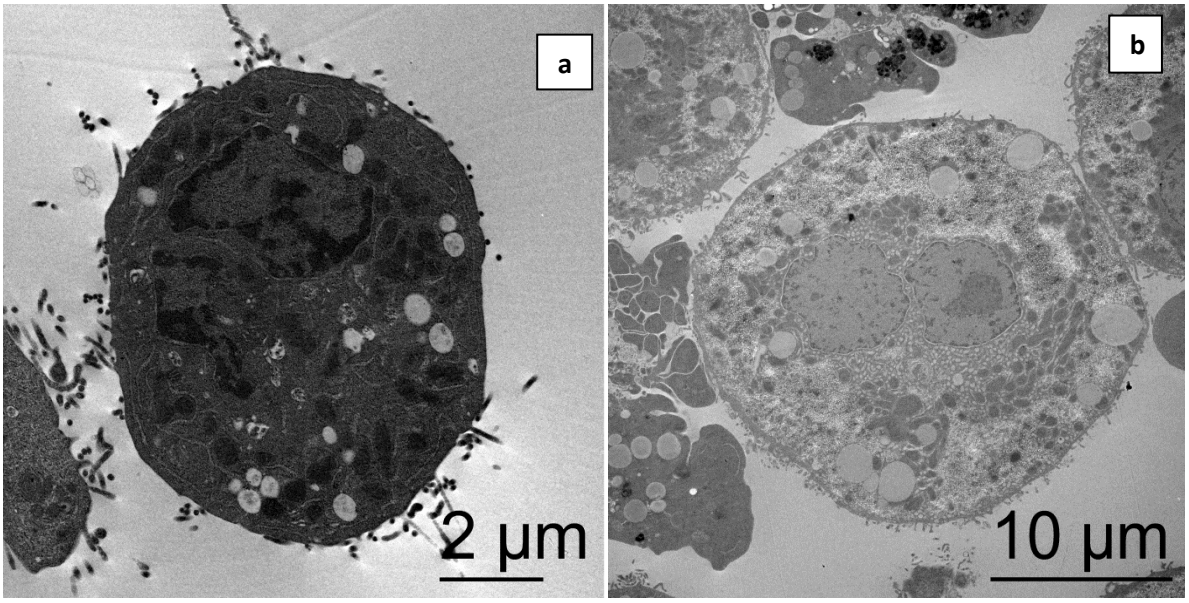

Figure 6.4. TEM images of C3A **(a)** and primary human hepatocytes **(b)** from the control samples.

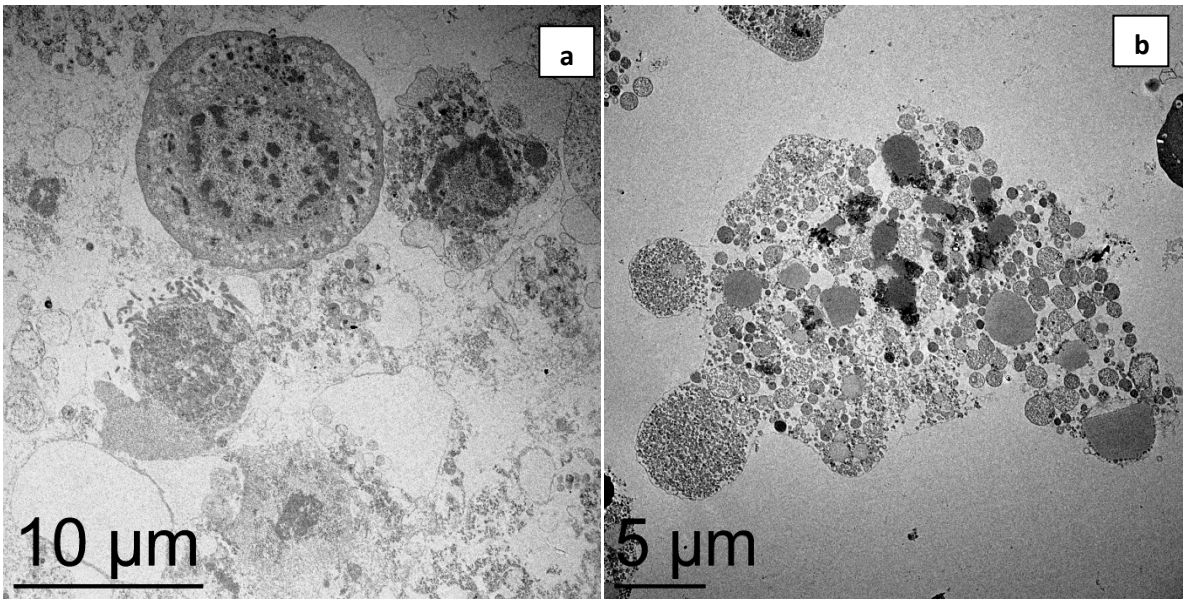

Figure 6.5. TEM images of C3A **(a)** and primary human hepatocytes **(b)** exposed to NM 110 – uncoated ZnO. Cell death is clearly evident in both samples; however no elemental Zn was detected, suggesting complete dissolution within the cell culture medium in the investigated samples.

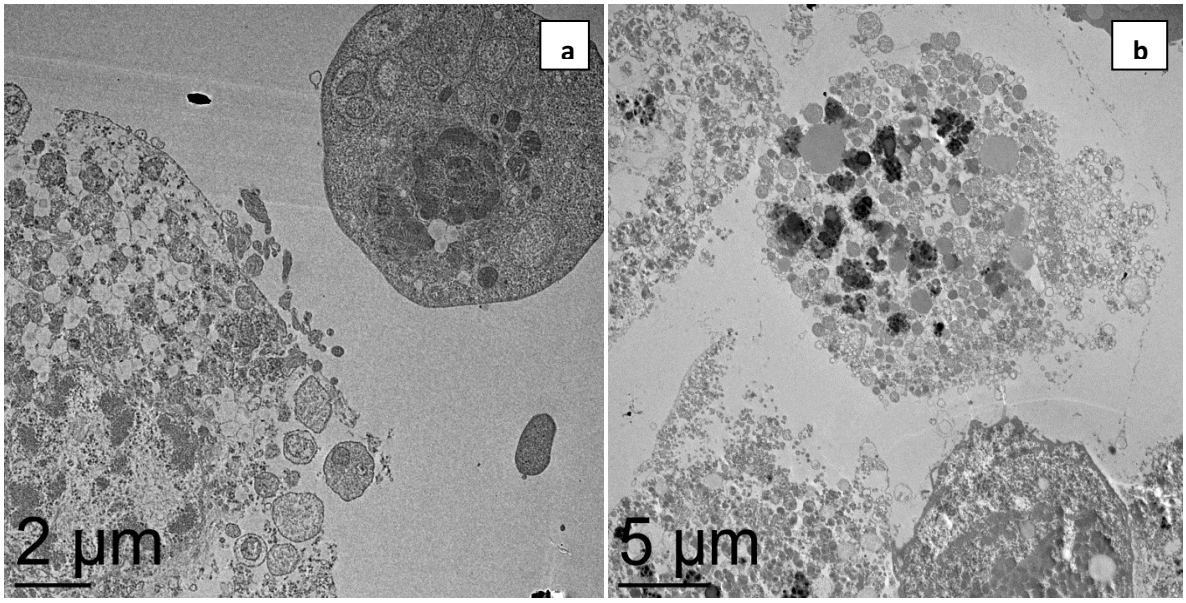

Figure 6.6. TEM images of C3A **(a)** and primary human hepatocytes **(b)** exposed to NM 111 – coated ZnO. Cell death is clearly evident in both samples; however no elemental Zn was detected, suggesting complete dissolution within the cell culture medium in the investigated samples.

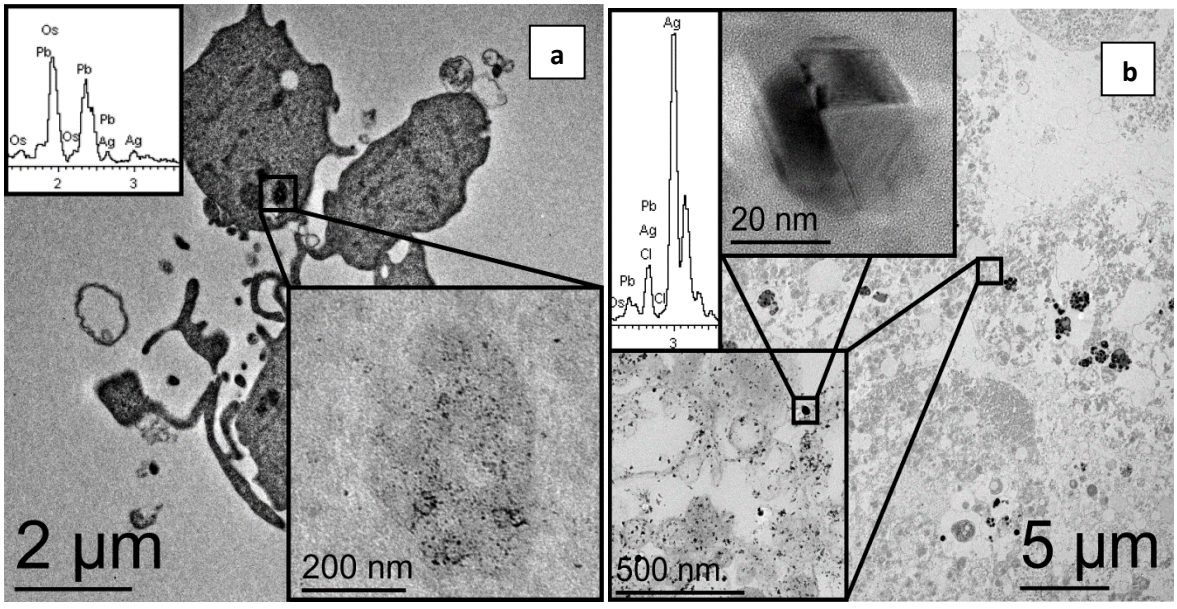

Figure 6.7. TEM images of C3A **(a)** and primary human hepatocytes **(b)** exposed to NM 300 – Ag. Cell damage was observed in both samples, and concentrations of Ag were detected using EDX (spectra inset in **(a)** and **(b)**, with X-ray energy in keV shown on the scale bar). The Ag concentrations existed as both fine dispersed particles (comparable in size and contrast to the heavy metal stain particles) as shown in **(a)**, and also as large defined polycrystalline particles, as shown in **(b)**.

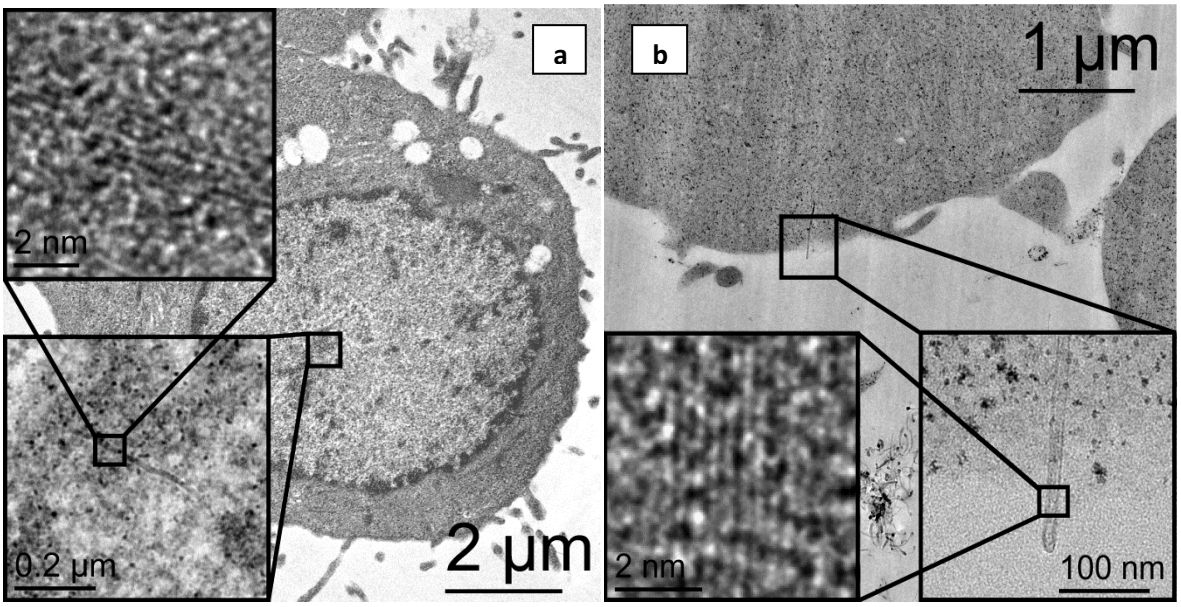

Figure 6.8. TEM images of C3A **(a)** and primary human hepatocytes **(b)** exposed to NM 400 – MWCNT. In both samples MWCNTs were identified throughout the cells. They were easily identified by their long filament-like morphology, and characteristic 0.335 nm (0001) basal plane spacing (see images inset).

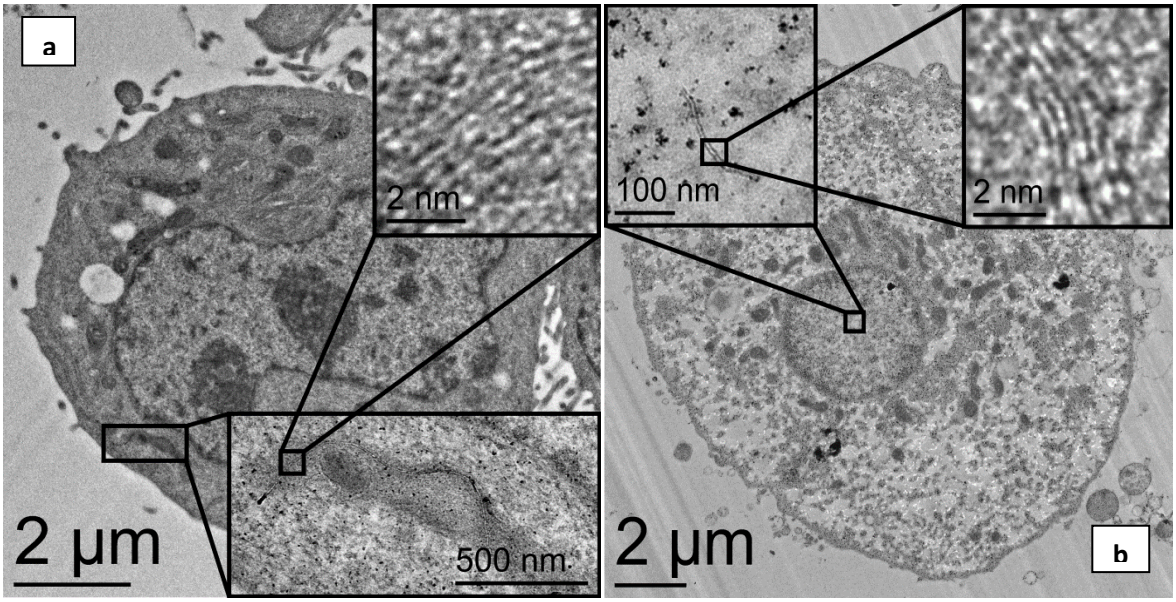

Figure 6.9. TEM images of C3A **(a)** and primary human hepatocytes **(b)** exposed to NM 402 – MWCNT. In both samples MWCNTs were identified throughout the cells. They were easily identified by their long filament-like morphology, and characteristic 0.335 nm (0001) basal plane spacing (see images inset).

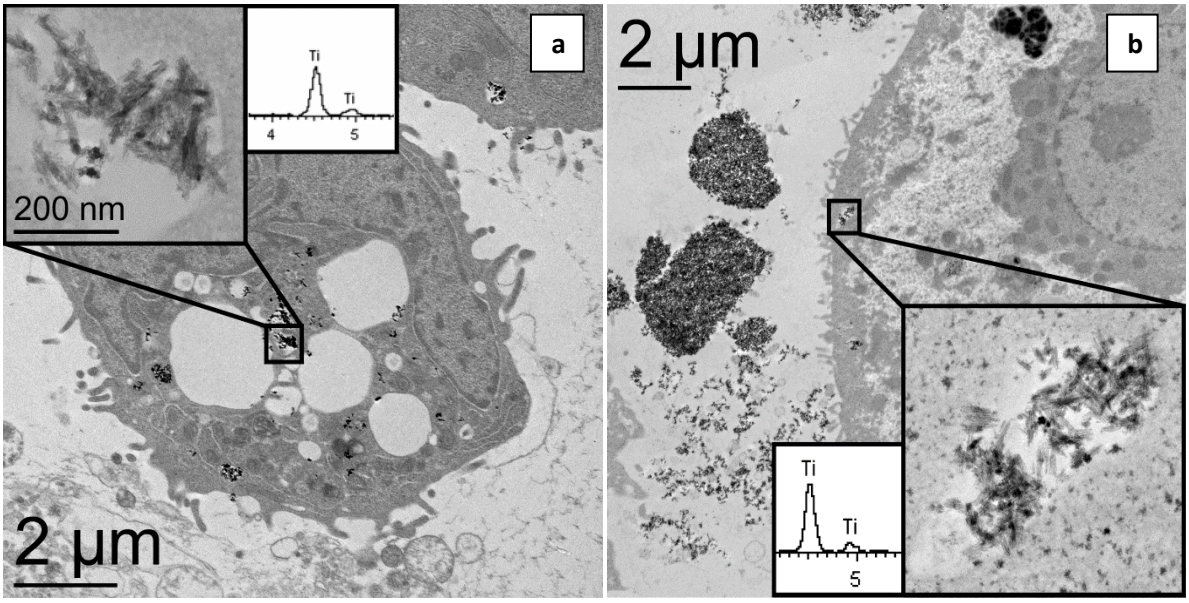

Figure 6.10. TEM images of C3A **(a)** and primary human hepatocytes **(b)** exposed to NRCWE002 – positively charged TiO_2. The strong contrast exhibited by the clusters of needle-like particles makes them clearly visible in both samples. EDX also confirms the particles to be composed from Ti (spectra inset in **(a)** and **(b)**, with X-ray energy in keV shown on the scale bar).

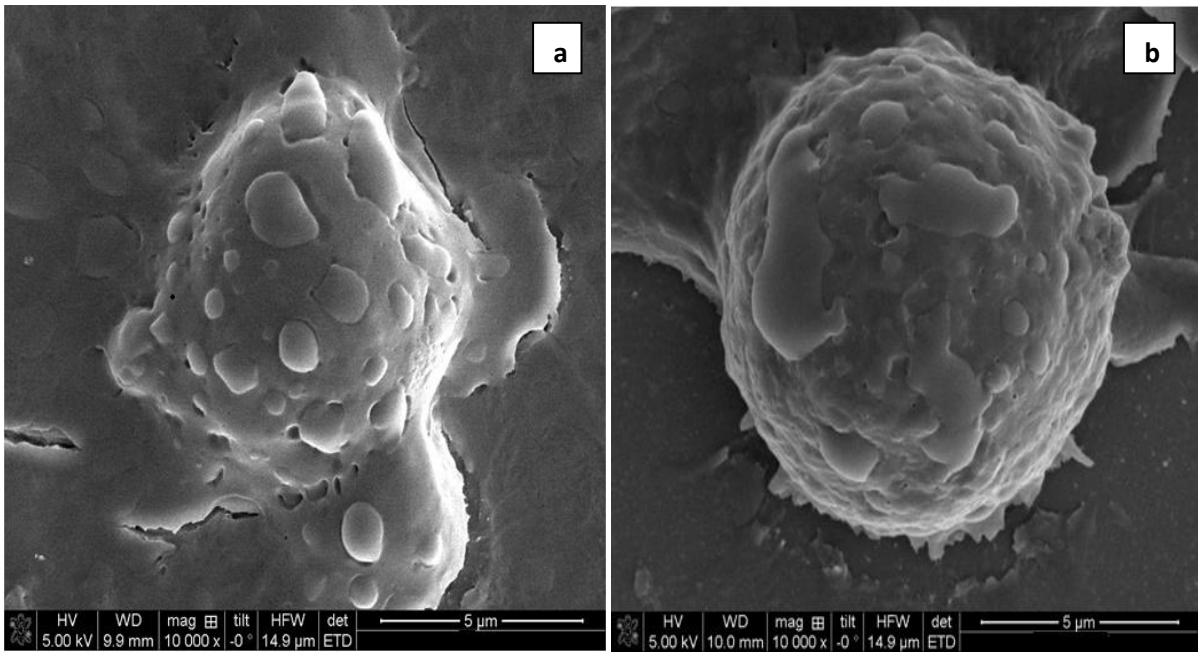

Figure 6.11. Scanning electron microscopy pictures of **a)** C3A and **b)** primary human hepatocytes.

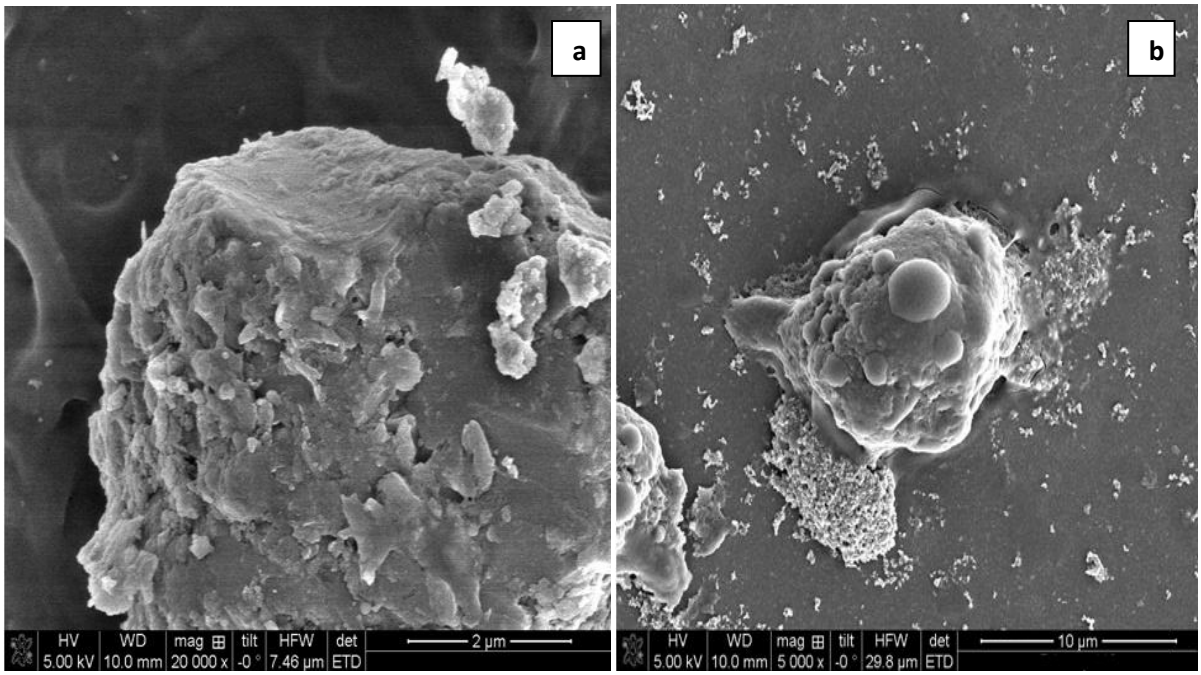

Figure 6.12. Scanning electron microscopy pictures of interaction of ZnO (NM 110) NMs with the cells following a 4 hr exposure **a)** C3A cell **b)** human primary hepatocyte.

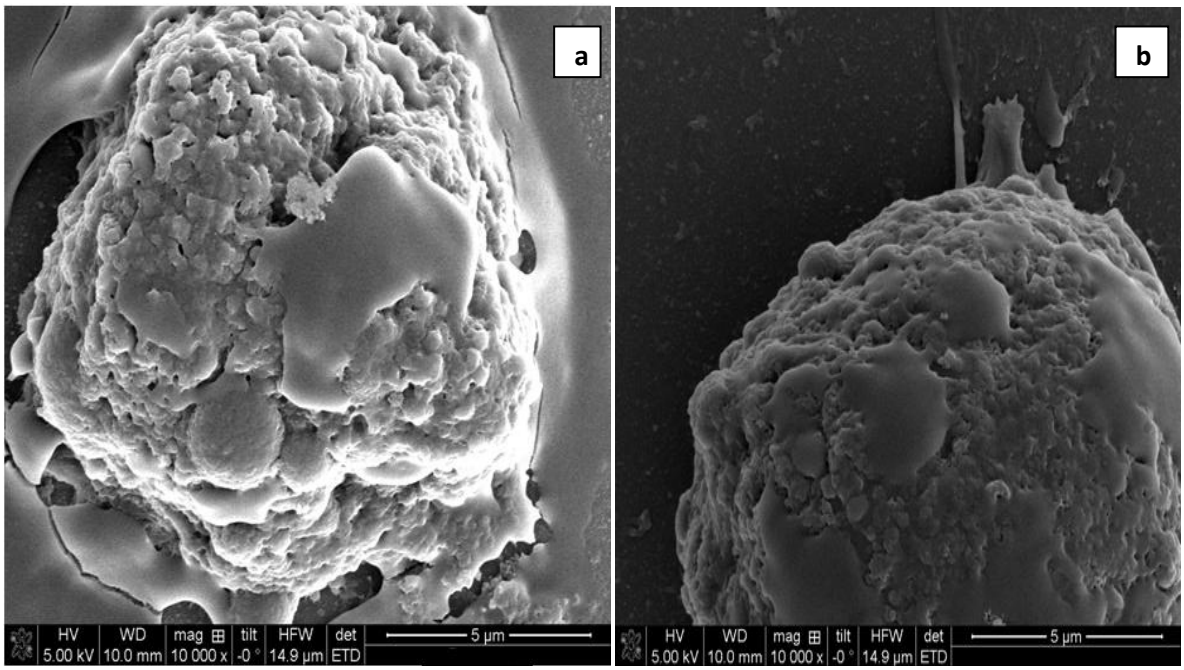

Figure 6.13. Scanning electron microscopy pictures of interaction of ZnO (NM 111) NMs with the cells following a 4 hr exposure **a)** C3A cell **b)** human primary hepatocyte.

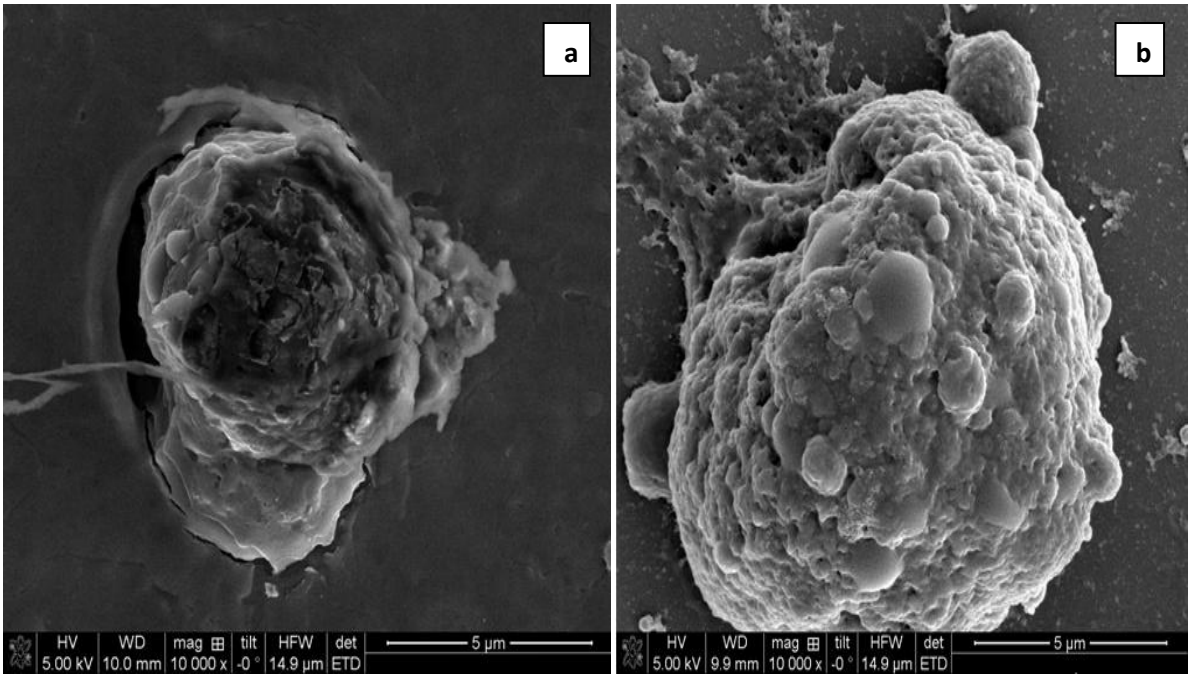

Figure 6.14. Scanning electron microscopy pictures of interaction of Ag (NM 300) NMs with the cells following a 4 hr exposure **a)** C3A cell **b)** human primary hepatocyte.

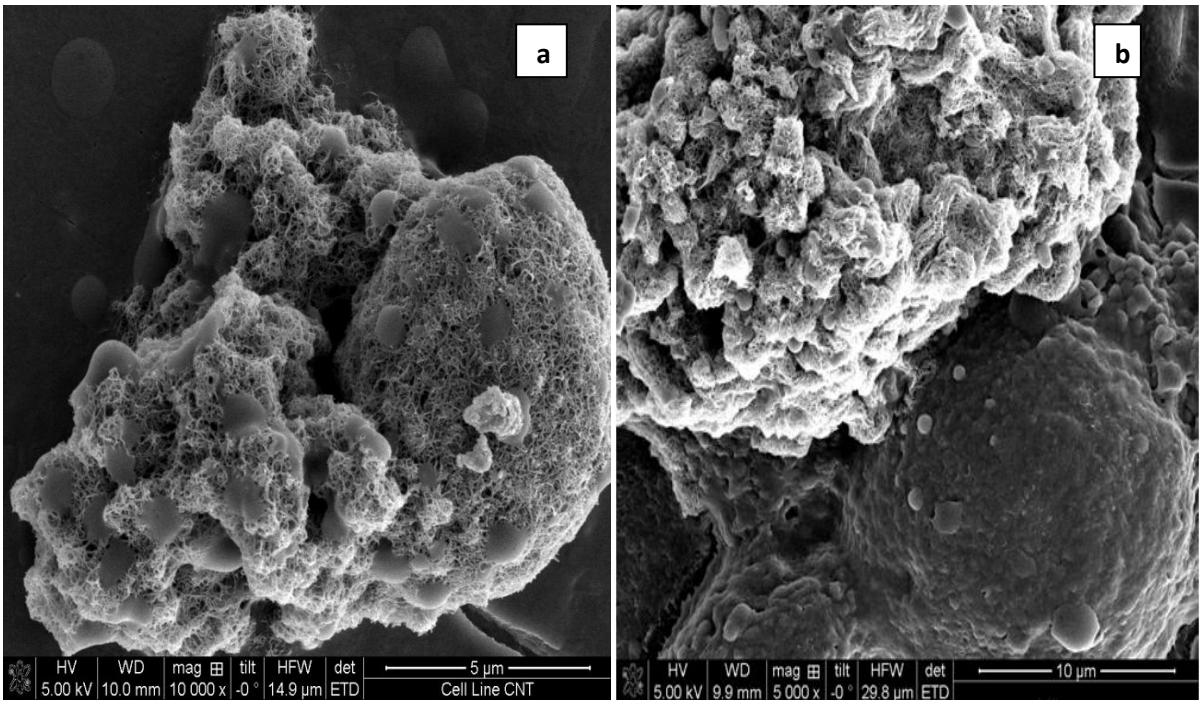

Figure 6.15. Scanning electron microscopy pictures of interaction of MWCNT (NM 400) NMs with the cells following a 4 hr exposure **a)** C3A cell **b)** human primary hepatocyte.

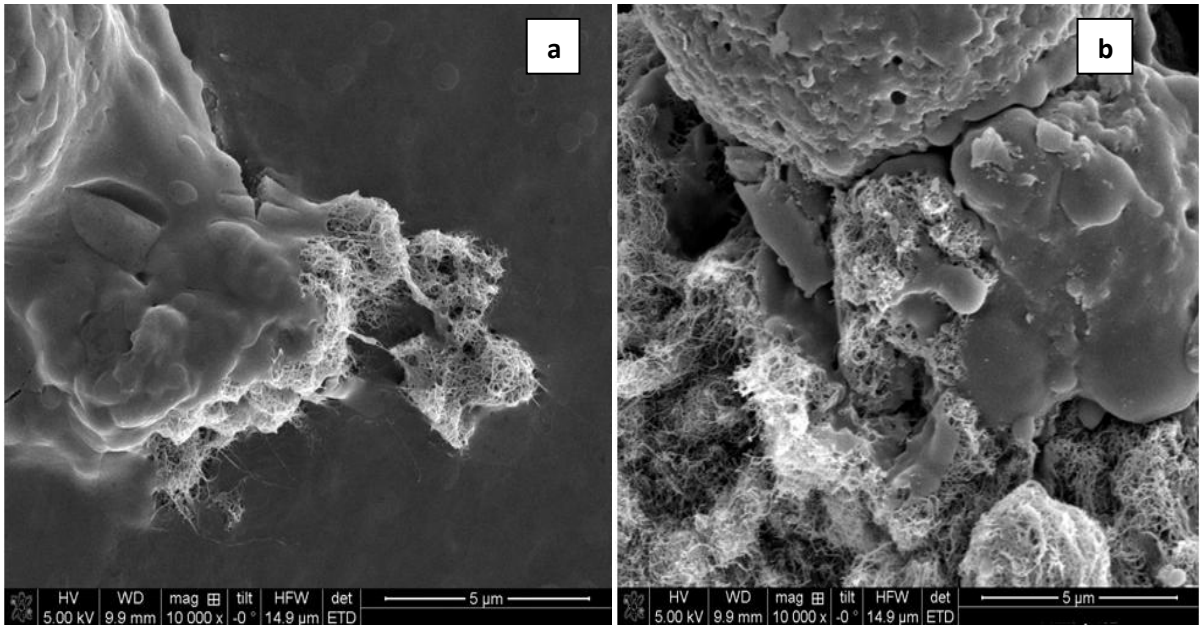

Figure 6.16. Scanning electron microscopy pictures of interaction of MWCNT (NM 402) NMs with the cells following a 4 hr exposure **a)** C3A cell **b)** human primary hepatocyte.

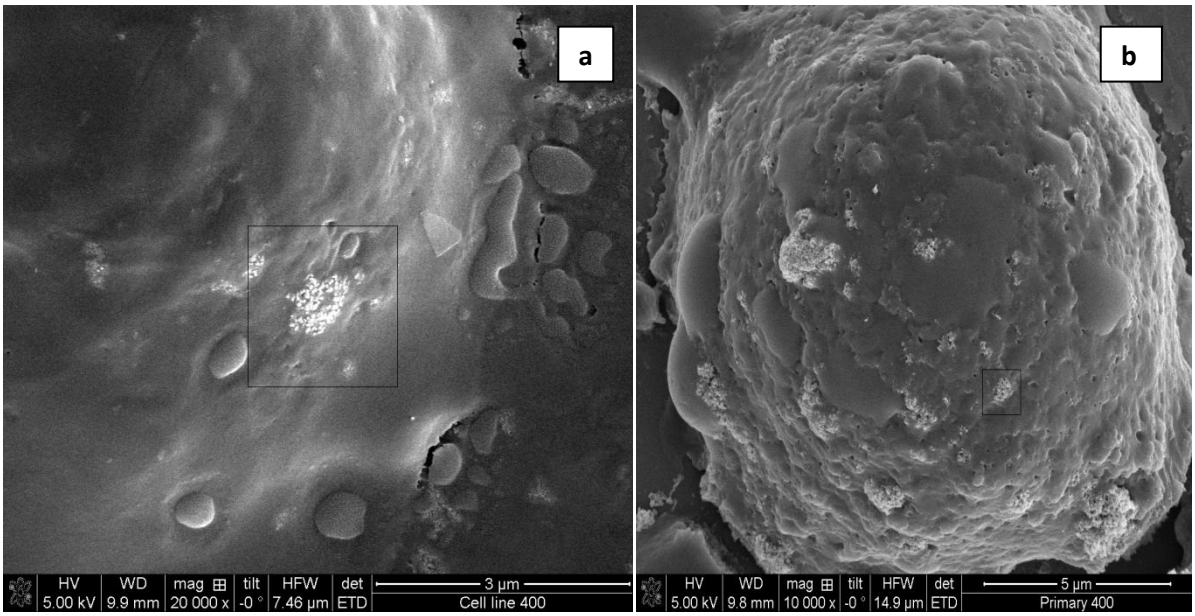

Figure 6.17. Scanning electron microscopy pictures of interaction of TiO_2 (NRCWE 002) NMs with the cells following a 4 hr exposure **a)** C3A cell **b)** human primary hepatocyte.

6.8 Cytochrome P450 levels

Hepatic cytochrome P450 activities (CYP 3A4, 2B4 and 2D6) were simultaneously examined in the C3A cell lines and primary human hepatocytes. Unsurprisingly we found greater levels of CYP450 activity in the untreated primary cells compared to the C3A cell line (Figure 6.18). Furthermore, exposure of the cells to the panel of engineered NMs at the low sub-lethal concentration of 0.31 μg/cm^2 did not affect cytochrome CYP450 levels in either cell type (Figure 6.18).

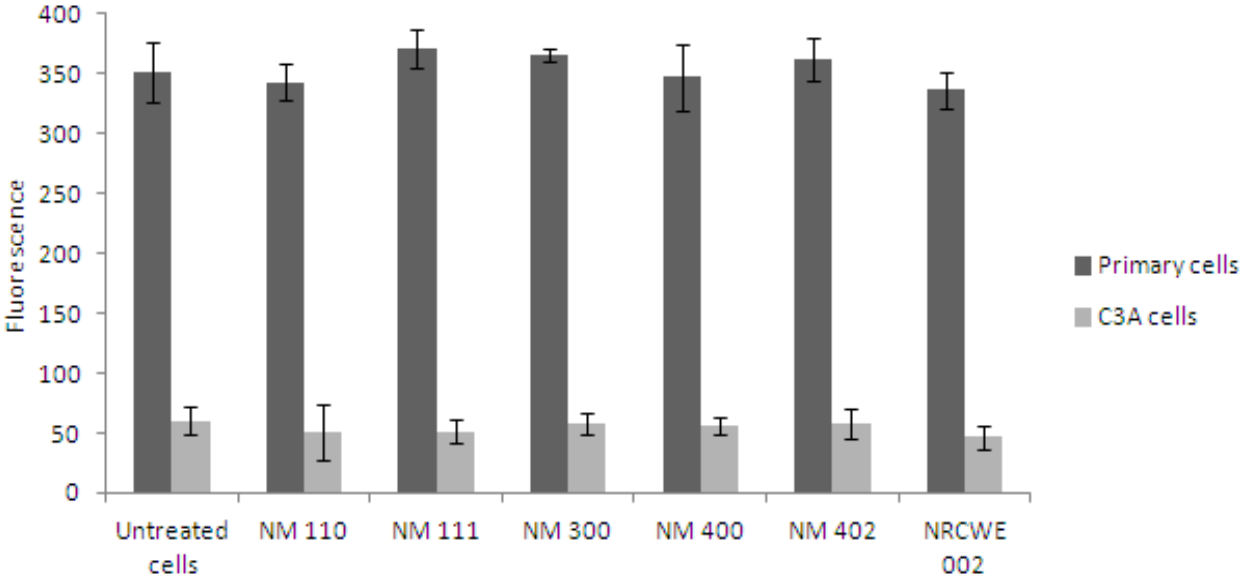

Figure 6.18. Hepatic cytochrome P450 (3A4, 2B4 and 2D6) measured from both untreated primary human hepatocytes and C3A cells. Both cells types were also treated with a sub-lethal concentration of the panel of nanomaterials at 0.31 µg/cm^2 quantified via DetectX® P450 demethylating fluorescent activity kit.

6.9 Discussion

This particular chapter focused on the impacts of the investigated nanomaterial panel on human primary hepatocytes and C3A hepatic cell line with respect to cytotoxicity, pro-inflammatory cytokine production, albumin production and nanomaterial uptake. The data shows that although there are small variations between the primary cells and the cell line, the overall responses are very similar from both cell types following acute exposure (24 hr) to the investigated nanomaterials *in vitro*.

The use of *in vitro* hepatocyte models have been extremely useful in both fundamental research and various application areas. Primary hepatocytes appear as the closest model for the human liver. However, these cells are phenotypically unstable, they can be very expensive and have an extremely limited life span. In addition they exhibit large variability between different human donors (Liguori, *et al*. 2008; Sahi, *et al.* 2010). Hepatocyte cell lines on the other hand are cheap and much easier to maintain. Hence they are often utilised as surrogates for human primary hepatocytes. However their use in absorption, metabolism, excretion and toxicity studies have been questioned as the basal levels of their metabolizing enzymes is greatly reduced compared to primary cells (Hansson, *et al*., 2004).

Similar to previous studies it was found that that the ENPRA panel of NMs panel can be segregated into a low (TiO_2 and MWCNT) and a high toxicity group (Ag and coated and uncoated ZnO) as investigated using the WST-1 assays. The most interesting finding was that the toxicity pattern was similar for both hepatocyte cell types, with the silver NMs being the most toxic followed by the uncoated and the coated ZnO NMs. While the TiO_2 and MWCNTs were not considered as highly cytotoxic to the hepatocytes as the LC_{50} was not reached following a 24 hr exposure. To our knowledge no studies have investigated the NM induced toxicity to primary human hepatocytes however previous studies have shown that ZnO (Sharma, *et al*., 2011) and Ag (Piao, *et al*., 2011) NMs are highly toxic to hepatocyte cell lines *in vitro* while TiO_2 NMs (Wang, *et al*., 2011b) were of relatively low toxicity. Exposure of HepG2 cells to MWCNTs for 48 hr resulted in an LC_{50} of around 40 µg/ml (Anreddy, *et al*., 2011).

IL8 is a chemokine mediating the activation and migration of a wide variety of inflammatory cells including neutrophils into tissue, hence playing a pivotal role in initiation of an

inflammatory response (Puthothu, *et al*., 2006). Both primary hepatocytes and the hepatic cell line produced significant levels of the chemokine following exposure to the nanomaterials. The pattern of cytokine production witnessed was similar for both hepatocyte cell models. Our findings suggest that the *in vitro* hepatocyte nanomaterial-induced inflammation seems to include IL8 production from both the primary and C3A hepatocytes. These particular findings are similar to previous studies in which it has been shown that primary hepatocytes (Wanninger, *et al*., 2009) and hepatocyte cell lines (Delpino, *et al*., 2010) produce IL8 following exposure to foreign antigens. This being said small differences in IL8 secretion was observed following exposure to certain concentrations of five of the NMs investigated in this study. Although statistically significant these distinctions do not influence the conclusions made above. It is also worth noting that it would be impossible to produce identical replication of ELISA results even if the exact same cell type were being utilised.

Furthermore no change in the levels of IL6 or TNF-α compared to the control following exposure of the primary hepatocytes or C3A cells to any of the investigated nanomaterials was noted suggesting that the cytokine production from these cells is limited.

Albumin is the most abundant protein produced from the liver and was quantified as a measure of liver function. Previously it was shown that exposure of C3A cells to the panel of nanomaterials resulted in very little change in the levels of albumin with the exception of the two ZnO NMs at LC_{50} concentrations (Chapter 4) (Kermanizadeh, *et al*., 2012c). In this study exposure of the primary human hepatocytes to sub-lethal levels of the ENPRA NMs once again resulted in a very similar outcome to the results seen with the C3A cell line with one exception. Exposure of the primary cells to one of the ZnO NMs (NM 111) at the LC_{50} did not result in a significant decrease in albumin as previously witnessed. These results suggest that despite varying degrees of cell death, none of the nanomaterials investigated (at sub-lethal concentrations) affected hepatocyte function *in vitro* in terms of albumin production.

Next the interaction of the nanomaterials with both cell types was investigated. Both the primary hepatocytes and the C3A cells were capable of nanomaterial uptake. Four of the nanomaterials were found in the cytoplasm of the cells (Ag – NM 300, TiO_2 - NRCWE 002 and MWCNTs – NM 400 and NM 402), while one of the carbon nanotubes (NM 402) was also observed within the nucleus of the cells. It is important to note however that our TEM

study had its limitations. It was extremely difficult to identify any of the ZnO NMs due to their high solubility in the chosen culture media (Chapter 4) (Kermanizadeh, *et al*., 2012c).

As the SEM and TEM pictures demonstrate cell death is evident following exposure of the hepatocytes to the Ag and two ZnO NMs. Although we suspect apoptosis to be the mechanism of death in this *in vitro* model, this has not been checked or validated so there is a real possibility that other mechanisms could be involved in the liver cells dying.

Apoptosis is a form of programmed cell death in which cells die without release of their intracellular contents (no damage to neighbouring cells). Apoptosis is characterised by appearance of morphological changes including membrane blebbing, chromatin condensation and the fragmentation of the nucleus and externalisation of phosophatidylserine residues (very important in the clearance of apoptotic bodies by phagocytes) (Beere, *et al*., 2001).

Apoptosis is orchestrated by a number of cysteine proteases generally termed as caspases. These proteases are synthesised as inactive precursors that are cleaved in order to become active prior to apoptosis (Ola, *et al*., 2011). Interior caspases contain protein-protein interaction domains or the related death effector domains. Binding of specific adaptor molecules to these domains promotes the activation of the caspase (Ola, *et al*., 2011). Caspase activation is regulated by a number of cytosolic events one of the most important is the formation of the apoptosome (Ola, *et al*., 2011). This complex comprises of several proteins including apoptotic protease activating factor-1 (APAF-1), cytochrome c and procaspase 9 (Ola, *et al*., 2011). The release of cytochrome c from the mitochondria into the cytosol in particular is crucial for both apoptosome formation and caspase activation in response to the apoptotic stimuli (Ola, *et al*., 2011). The APAF-1 complex sequesters procaspase-9, which then autoactivates, recruits and cleaves procaspase-3. Catalytically active caspase-3 is then able to cleave its target substrates to induce apoptosis (Ola, *et al*., 2011). It is important to note that abnormalities in apoptosis can lead to a variety of diseases including cancer and a number of degenerative disorders hence it must be heavily regulated through independent signalling pathways that are initiated either from triggering events within the cell or on its surface (Beere, *et al*., 2001).

As already mentioned cell death can be classified in many ways mostly distinguished as being actively regulated or passive and/or accidental (Beere, *et al*., 2001). Necrosis in contrast to apoptosis is an example of unregulated cell death.

Although a significant proportion of necrotic deaths are passive, recent experimental evidence has emerged that necrosis can also be regulated. The relative proportion of unregulated versus regulated necrotic death is not currently known (Parone, *et al*., 2002). The archetypal features of necrosis are loss of plasma membrane integrity and depletion of cellular ATP (Parone, *et al*., 2002). As a result of this plasma membrane dysfunction, necrotic cells become swollen. There is also swelling of organelles such as the mitochondria. These events result in a general collapse of intracellular homeostasis. In contrast to the clean-up operation that is typical in apoptosis, the release of cellular contents into the extracellular space engenders an inflammatory response in necrosis (Parone, *et al*., 2002). Although the exact mechanisms of necrosis signalling are currently unknown it is believed that two pathways might be responsible for necrosis of a cell. Firstly, necrosis can be mediated by a multi-protein complex including TRADD, RIP1, TRAF2, and cIAP1/2 (i.e. binding of TNF-α receptor 1) (Parone, *et al*., 2002). A second necrosis pathway involves the mitochondrial permeability transition pore (MPTP) in the inner mitochondrial membrane and its regulation by cyclophilin D. The MPTP may be opened by increased Ca^{2+}, oxidative stress or decreased ATP (Parone, *et al*., 2002).

In a contrast to necrosis and apoptosis, autophagy is primarily a survival mechanism. The processs is an intracellular recycling process in which organelles, proteins and lipids are catabolised by lysosomal degradation (Whelan, *et al*., 2010). Autophagy provides cells with amino acids, free fatty acids and energy in times of nutrient shortage. In addition, it serves to regulate protein and organelle abundance and quality. Autophagy can involve a chaperone in which it binds a target protein and escorts it to the lysosome, provides a means for the degradation of the selected proteins (Whelan, *et al*., 2010).

In addition to the above mentioned forms of cell death there are many other mechanisms in which cells die and tissue homeostasis is maintained (e.g. entosis – a viable cell is phagocytosed by a neighbouring cells which then dies (Kroemer, *et al*., 2009), anoikis – cells lose their attachment to neighbouring cells (Kroemer, *et al*., 2009)).

The uptake mechanism of the nanomaterials into the hepatocytes is currently unknown, but since hepatocytes are not phagocytic, the uptake is most likely to be via clathrin mediated endocytosis as witnessed in other cell types (Passagne, *et al*., 2012; Smith, *et al*., 2012; Zhao, *et al*., 2011).

Following an investigation into the surface interaction of the cells with the NMs utilising SEM we noted that the highly toxic NMs (Ag and ZnO) cause large amounts of surface damage to both the C3A and the primary cells, while the TiO_2 and MWCNT were clearly evident on or interacting with the surface of the cells.

The Cytochrome P450 levels for the C3A cell lines and the primary hepatocytes was also examined. Significantly lower levels of CYP450 (3A4, 2B4 and 2D6) activity from the C3A cells compared to their primary counterparts were found. These finding are similar to previous studies in which it has been shown that CYP450 isozymes are intrinsically lower in hepatocyte cell lines compared to primary cells (Wongkajornslip, *et al*., 2012). These findings are not surprising and have been reported elsewhere however it is worth noting that the materials investigated here did not interfere with the metabolic activity of the primary cells at low sub lethal concentrations. Furthermore it seems that CYP450 activity does not play a role in the adverse effects witnessed following exposure of the cells to the panel of engineered nanomaterials.

Finally, reactive oxygen species and oxidative stress have been demonstrated to play a key role in the response of many cell types to a range of NMs (Pichardo, *et al.*, 2012; Shvedova, *et al*., 2012). Therefore it would be interesting to know whether the hepatocyte cell line responds to these materials via a mechanism involving oxidative stress and whether this is comparable to the primary hepatocytes. It was not possible to investigate this question using the primary human hepatocytes due to their extremely high cost, and so we have asked the same question using liver tissue from exposed animals (Chapters 7 and 8).

6.10 Conclusions

This *in vitro* study demonstrated that the C3A cells are a very good model to investigate nanomaterial induced effects on hepatocytes with regards to the end points investigated (cytotoxicity, cytokine secretion, nanonmaterial uptake and functional markers). The results

also suggest that biotransformation enzymes in hepatocytes are not important in terms of determining nanotoxicology. Over all the cell line was found to be extremely useful as a replacement for a primary model for specific studies (on occasions the use of primary cells is often difficult or all together impossible) providing that the limitation for each cell type and experiment is thoroughly understood.

Chapter Seven

Nanomaterial impact on liver antioxidant status and gene expression following administration via the lungs

Based on publications: Gosens I, Kermanizadeh A, Jacobson NR, Stoeger T, Bokkers B, de Jong WH, Stone V, Tran L, Cassee FR. (2013a). Hazard identification of zinc oxide and silver nanomaterials based on acute lung and systemic toxicity in mice. Manuscript in preparation.

Gosens I, Kermanizadeh A, Jacobson NR, Stoeger T, Bokkers B, de Jong WH, Stone V, Tran L, Cassee FR. (2013b). Hazard identification of titanium dioxide and multi-walled carbon nanotubes nanomaterials based on acute lung and systemic toxicity in mice. Manuscript in preparation.

7.1 Aims and chapter outline

To assess the oxidative impact (glutathione depletion) and gene expression (C3, CXCL2, IL6, IL10 and TNF-α) response of mice liver tissue 24 hr following intratracheal exposure via the lungs.

Mice were exposed via intratracheal instillation to the ENPRA NMs (described in section 3.29) before the liver was removed to assess for glutathione content (section 3.17) and the expression of a range of genes (section 3.30).

7.2 Liver glutathione measurements following intratracheal instillation of nanomaterials

Analysis of the changes of total glutathione levels (GSH and GSSG) in mice liver tissue revealed that there was a visible dose-dependent decrease in the antioxidant levels compared to the control tissue across four of the ten investigated NMs; NM 110 (ZnO uncoated), NM 111 (ZnO coated), NM 300 (Ag), and NRCWE 002 (positively charged TiO_2) (Figure 7.1b, c, d and h). The largest depletion was observed following exposure to the coated ZnO and Ag NMs. There was no significant impact on liver glutathione following exposure to the remaining TiO_2 NMs (NM 101, NRCWE 001, NRCWE 003 and NRCWE 004) and MWCNTs (NM 400 and NM 402) (Figure 7.1a, e, f, g, i and j).

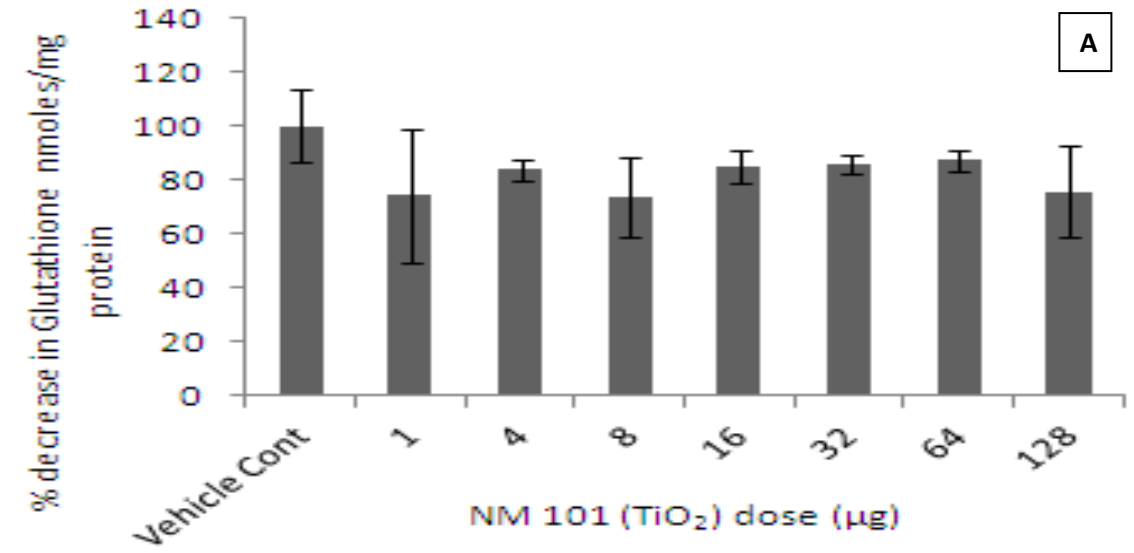
A
% decrease in Glutathione nmoles/mg protein
140
120
100
80
60
40
20
0
Vehicle Cont
1
4
8
16
32
64
128
NM 101 (TiO_2) dose (µg)

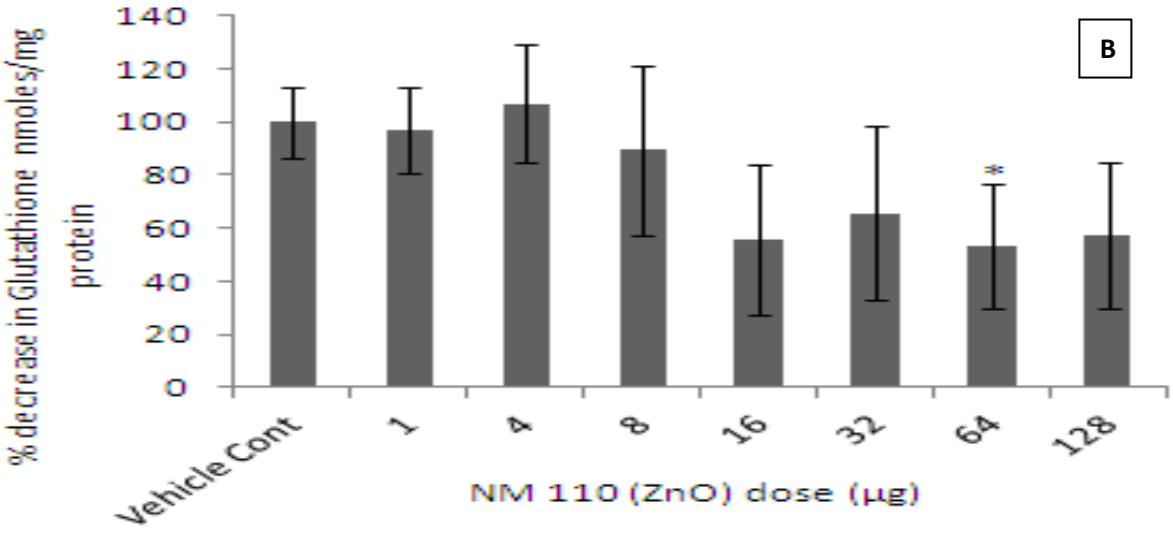
B
% decrease in Glutathione nmoles/mg protein
140
120
100
80
60
40
20
0
*
Vehicle Cont
1
4
8
16
32
64
128
NM 110 (ZnO) dose (µg)

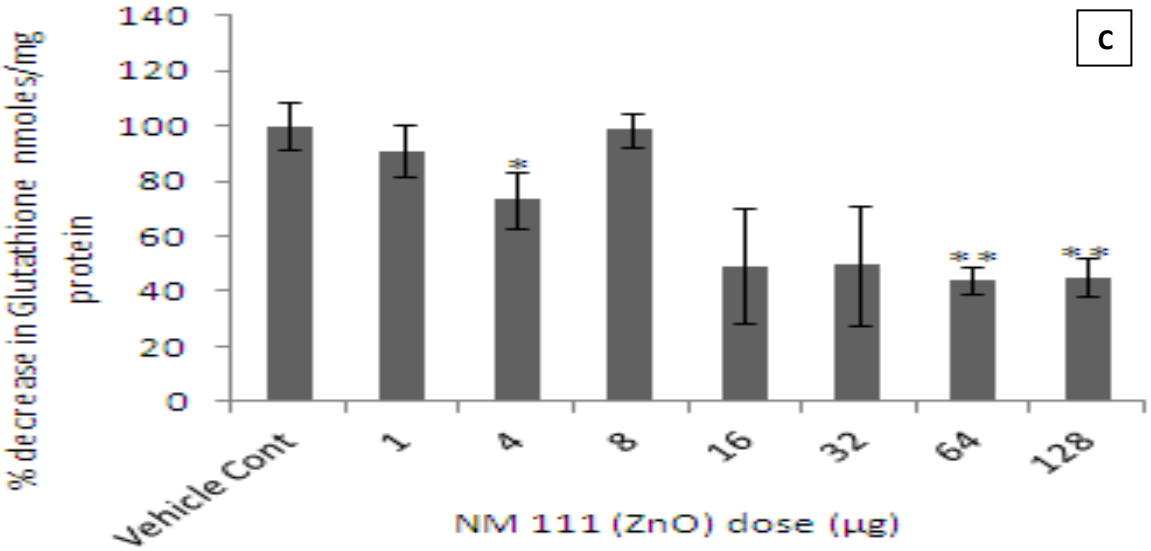
C
% decrease in Glutathione nmoles/mg protein
140
120
100
80
60
40
20
0
*
**
**
Vehicle Cont
1
4
8
16
32
64
128
NM 111 (ZnO) dose (µg)

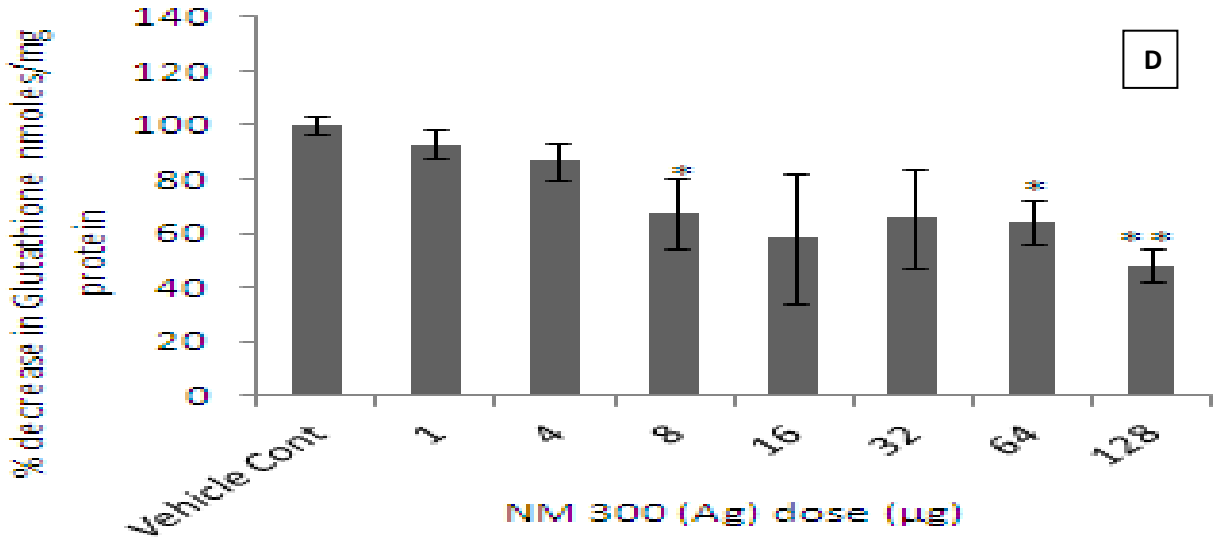
D
% decrease in Glutathione nmoles/mg protein
140
120
100
80
60
40
20
0
Vehicle Cont
1
4
8
16
32
64
128
NM 300 (Ag) dose (µg)

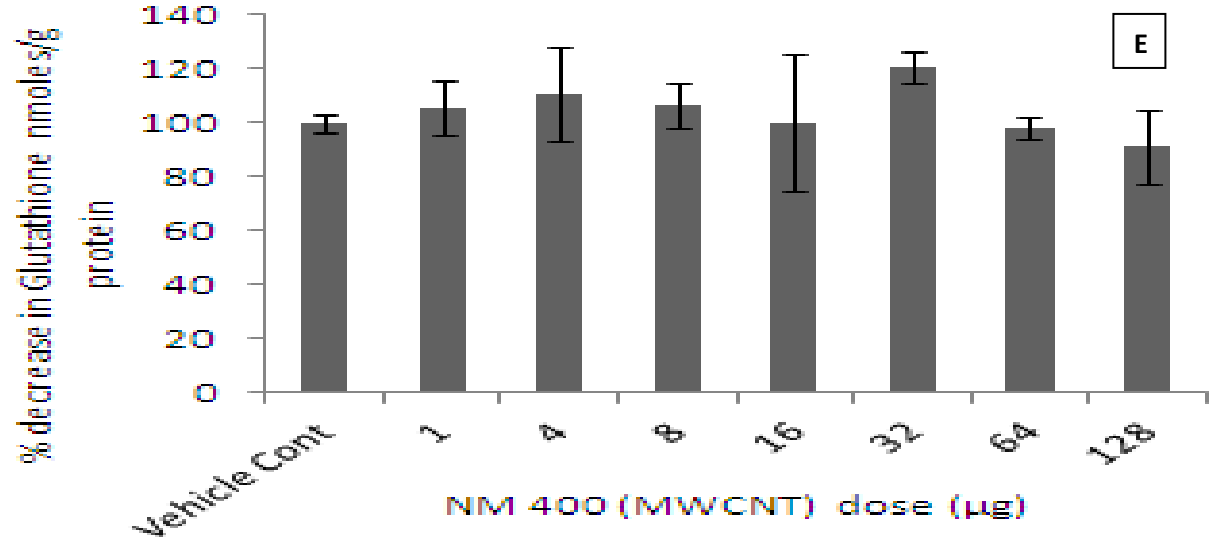
E
% decrease in Glutathione nmoles/g protein
140
120
100
80
60
40
20
0
Vehicle Cont
1
4
8
16
32
64
128
NM 400 (MWCNT) dose (µg)

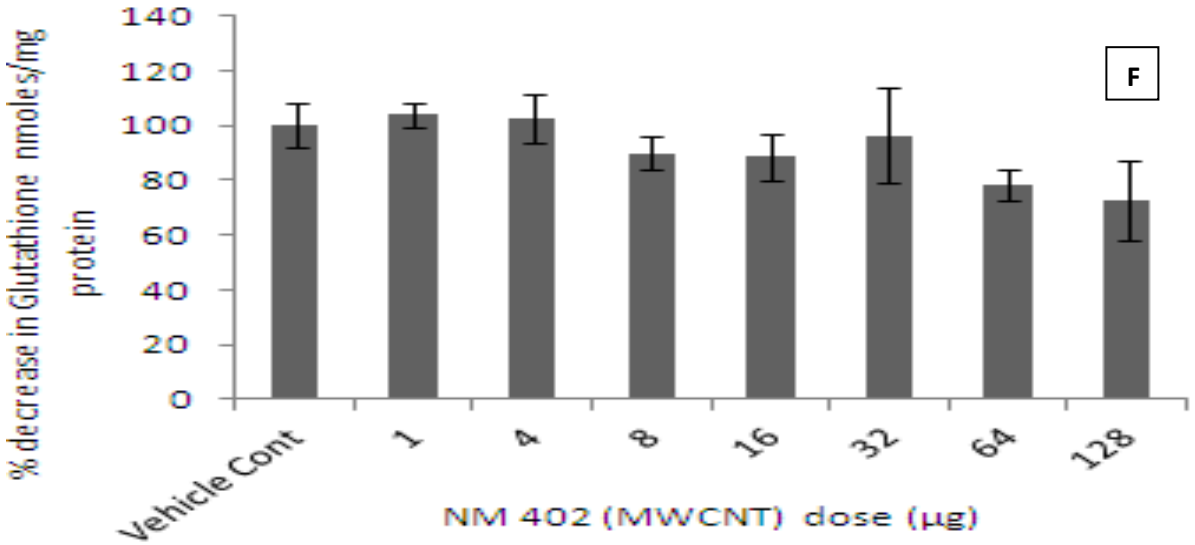
F
% decrease in Glutathione nmoles/mg protein
140
120
100
80
60
40
20
0
Vehicle Cont
1
4
8
16
32
64
128
NM 402 (MWCNT) dose (µg)

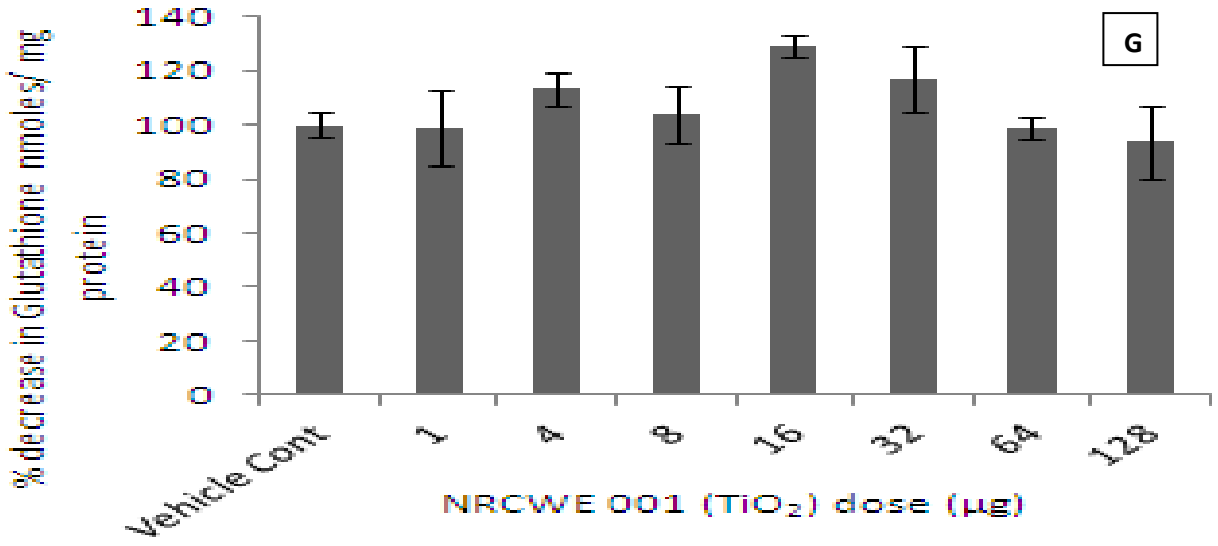
G
% decrease in Glutathione nmoles/ mg protein
140
120
100
80
60
40
20
0
Vehicle Cont
1
4
8
16
32
64
128
NRCWE 001 (TiO2) dose (µg)

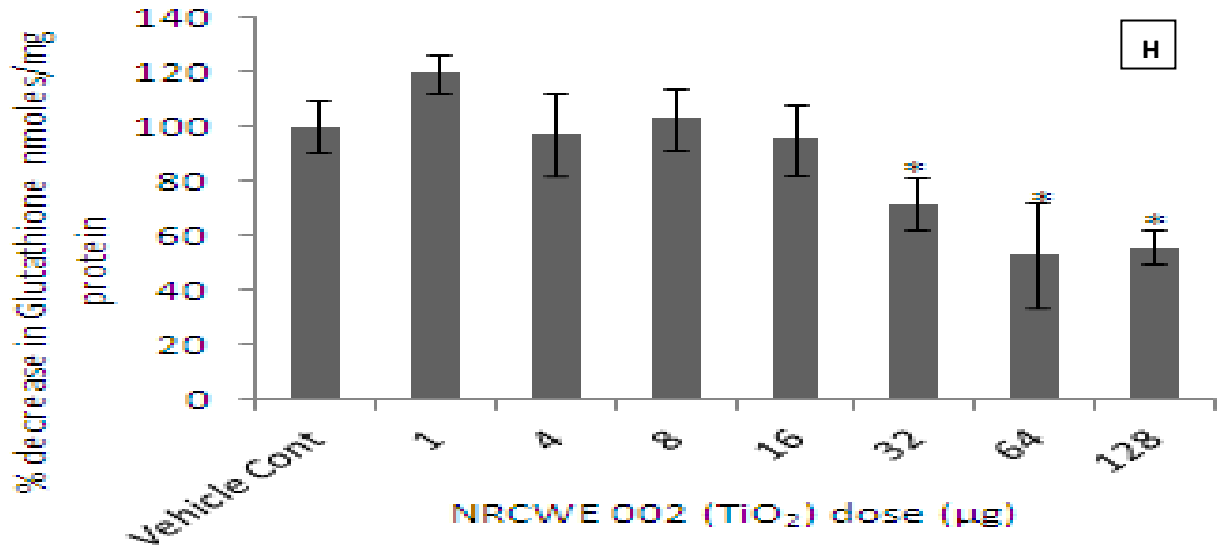
H
% decrease in Glutathione nmoles/mg protein
140
120
100
80
60
40
20
0
*
*
*
Vehicle Cont
1
4
8
16
32
64
128
NRCWE 002 (TiO2) dose (µg)

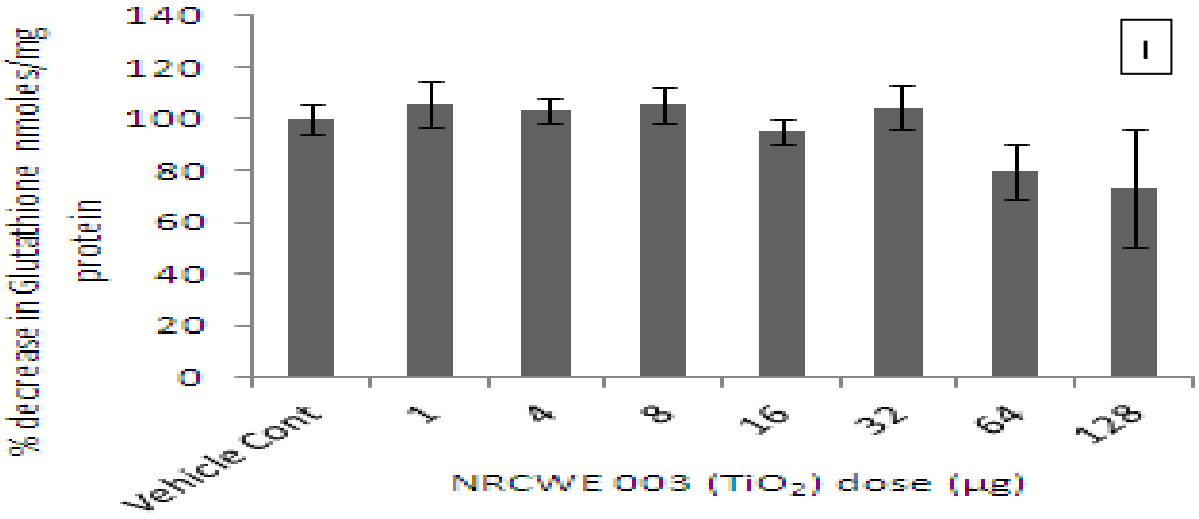
I
% decrease in Glutathione nmoles/mg protein
140
120
100
80
60
40
20
0
Vehicle Cont
1
4
8
16
32
64
128
NRCWE 003 (TiO2) dose (µg)

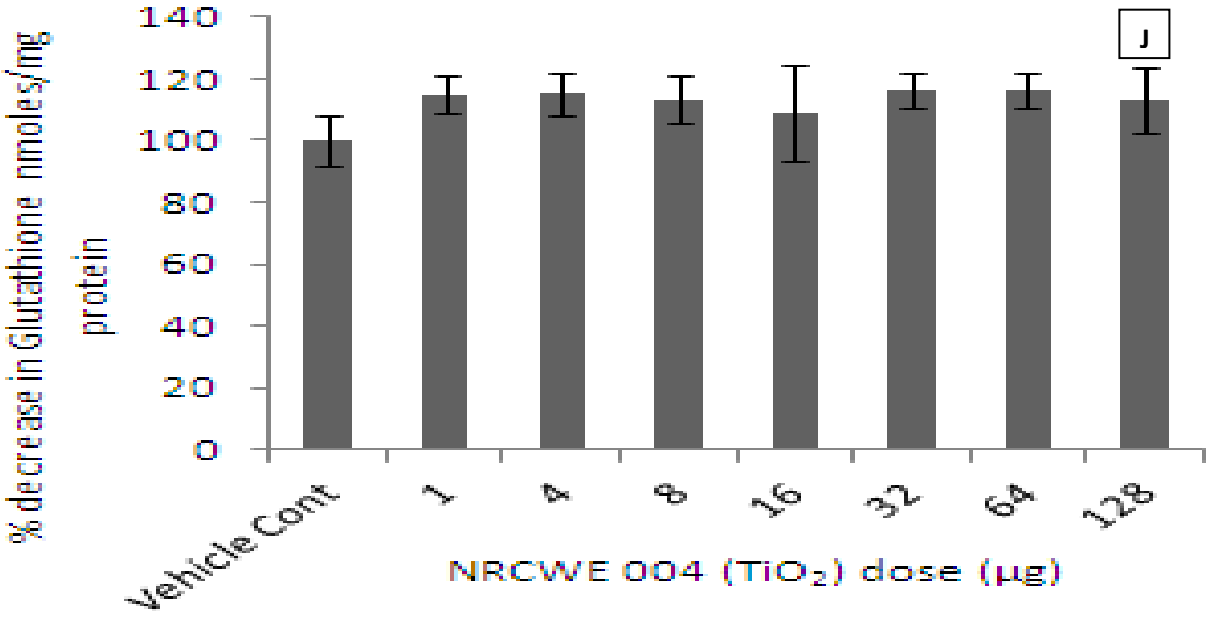

Figure 7.1. Effects of NM intratracheal instillation (24 hr) on the total glutathione content of mouse liver tissue. Values represent means ± SEM (n=3), significance indicated by * = $p<0.05$ and ** = $p<0.005$, when NM treatments are compared to the control. **A)** NM 101 **B)** NM 110 **C)** NM 111 **D)** NM 300 **E)** NM 400 **F)** NM 402 **G)** NRCWE 001 **H)** NRCWE 002 **I)** NRCWE 003 **J)** NRCWE 004.

7.3 mRNA expression in mice liver following IT exposure of NMs

Analysis of mRNA expression in livers of mice 24 hr post intratracheal instillation showed a decrease in C3 following exposure to NM 101, NM 110, NM 111, NM 300, NRCWE 001 and NRCWE 002 (Table 7.1). There was no large change in the levels of CXCL2 following exposure to the ENPRA nanomaterials (Table 7.2). an increase in the IL6 mRNA following exposure to NM 110, NM 111, NM 300, NRCWE 001, NRCWE 002, NRCWE 003 and NRCWE 004 was noted (Table 7.3). The largest and most significant change of all the genes investigated was an increase in IL10 following exposure to NM 101, NM 110, NM 111, NM 300, NRCWE 001, NRCWE 002, NRCWE 003 and NRCWE 004 (Table 7.4). Finally no significant change in TNF-α gene expression was observed following exposure to any of the nanomaterials investigated (Table 7.5).

NM	1	8	32	64	128
NM 101	++++	0	-	---	--
NM 110	---	--	--	-	-
NM 111	---	--	----	--	0
NM 300	0	0	--	--	---
NM 400	0	0	0	0	0
NM 402	0	0	0	0	0
NRCWE 001	0	+	0	--	--
NRCWE 002	0	---	0	--	-
NRCWE 003	0	0	0	0	--
NRCWE 004	0	0	0	0	0

Table 7.1. mRNA expression of complement component 3 in C57/BL6 mice liver. The animals were exposed to increasing doses of NMs via the lungs. The animals were dissected 24 hr after exposure and the mRNA expression was analysed by real time PCR with B2m utilised as an endogenous control. – or + is representative of 50% change, -- or ++ is representative of 75% change, --- or +++ is representative of 100% change and ---- or ++++ is representative of ≥ 200% change. (n=3)
Doses - µg per animal

NM	1	8	32	64	128
NM 101	0	-	-	0	0
NM 110	--	--	0	--	0
NM 111	-	-	--	--	0
NM 300	0	0	0	0	0
NM 400	0	0	0	0	0
NM 402	0	0	0	0	0
NRCWE 001	++	0	0	0	0
NRCWE 002	+	0	0	0	0
NRCWE 003	0	0	0	0	0
NRCWE 004	0	0	0	0	0

Table 7.2. mRNA expression of CXCL2 in C57/BL6 mice liver. The animals were exposed to increasing doses of NMs via the lungs. The animals were dissected 24 hr after exposure and the mRNA expression was analysed by real time PCR with B2m utilised as an endogenous control. – or + is representative of 50% change, -- or ++ is representative of 75% change, --- or +++ is representative of 100% change and ---- or ++++ is representative of ≥ 200% change. (n=3)
Doses - µg per animal

NM	1	8	32	64	128
NM 101	0	0	0	0	++
NM 110	--	--	0	-	0
NM 111	-	+	0	0	+
NM 300	-	0	++	++	++
NM 400	0	0	0	0	0
NM 402	0	0	0	0	0
NRCWE 001	0	++	++	++++	++++
NRCWE 002	0	++	++	++++	++++
NRCWE 003	0	++	++	++++	++++
NRCWE 004	0	0	0	0	++

Table 7.3. mRNA expression of IL6 in C57/BL6 mice liver. The animals were exposed to increasing doses of NMs via the lungs. The animals were dissected 24 hr after exposure and the mRNA expression was analysed by real time PCR with B2m utilised as an endogenous control. – or + is representative of 50% change, -- or ++ is representative of 75% change, --- or +++ is representative of 100% change and ---- or ++++ is representative of ≥ 200% change. (n=3)
Doses - µg per animal

NM	1	8	32	64	128
NM 101	----	0	0	0	++++
NM 110	++++	++++	++++	++++	++++
NM 111	+	0	++++	0	++++
NM 300	++	0	+++	++	++++
NM 400	0	0	0	0	0
NM 402	0	0	0	0	0
NRCWE 001	0	0	++	+++	++++
NRCWE 002	0	0	0	+	++
NRCWE 003	0	0	++	+++	++++
NRCWE 004	0	+	+	++	+++

Table 7.4. mRNA expression of IL10 in C57/BL6 mice liver. The animals were exposed to increasing doses of NMs via the lungs. The animals were dissected 24 hr after exposure and the mRNA expression was analysed by real time PCR with B2m utilised as an endogenous control. – or + is representative of 50% change, -- or ++ is representative of 75% change, --- or +++ is representative of 100% change and ---- or ++++ is representative of ≥ 200% change. (n=3)
Doses - µg per animal

NM	1	8	32	64	128
NM 101	0	0	0	0	0
NM 110	0	-	0	0	0
NM 111	0	--	--	0	0
NM 300	--	0	0	0	0
NM 400	0	0	0	0	0
NM 402	0	0	0	0	0
NRCWE 001	0	0	0	0	0
NRCWE 002	0	0	0	0	0
NRCWE 003	0	0	0	0	0
NRCWE 004	0	0	0	0	0

Table 7.5. mRNA expression of TNF-α in C57/BL6 mice liver. The animals were exposed to increasing doses of NMs via the lungs. The animals were dissected 24 hr after exposure and the mRNA expression was analysed by real time PCR with B2m utilised as an endogenous control. – or + is representative of 50% change, -- or ++ is representative of 75% change, --- or +++ is representative of 100% change and ---- or ++++ is representative of ≥ 200% change. (n=3)
Doses - µg per animal

7.4 Discussion

This study shows the intratracheally instilled Ag, ZnO and positively charged TiO_2 result in acute distal effects on the liver that involved oxidative stress (glutathione depletion), while exposure to all nanomaterials with the exception of the MWCNT result in changes in gene expression in the liver.

To our knowledge this is the first time that distal effects relating to toxicity or oxidative stress in the liver have been demonstrated following exposure via the lung. This is not a uniform effect induced by all NMs, but instead it is limited to the highly toxic Ag (NM 300) and ZnO NMs (NM 110, NM 111) and the positively charged TiO_2 (NRCWE 002) (Chapter 4). These *in vivo* effects are reflected to some extent using the C3A cells, where five of the tested NMs also induced glutathione depletion (Chapter 5) (Kermanizadeh, *et al*., 2012a).

It is important to note that our investigation into glutathione depletion following intratracheal instillation of the ENPRA NMs had limitations which have to be taken into account when interpreting the findings. Firstly, the source of glutathione is unknown in the *in vivo* assays as the measurements could be potentially from any number of cell populations within the liver and not just the hepatocytes as is the case for the *in vitro* experiments. This could be an important factor as 20-25% of the organ is composed of non parenchymal cells (Kmiec, 2001). Secondly, there were some differences between the levels of intracellular glutathione between the vehicle control animals for each nanomaterial. Hence the levels of glutathione depletion observed in our experiments are only comparable to the control group for each nanomaterial and not uniform for all treatments.

Few studies have investigated the effects of Ag, ZnO, TiO_2 or MWCNT on GSH depletion within the liver *in vivo* or *in vitro*, however in a recent study Sprague Dawley rats were exposed to 10 nm cerium oxide NMs via a single dose intratracheal instillation. The authors discovered an array of adverse effects in the liver (Nalabotu, *et al*., 2011). In another study the cellular redox state of a human liver cell line (HL7702) was investigated (Gao, *et al*., 2011). The authors demonstrate a clear decrease in intracellular GSH levels after exposure to 8 nm gold nanoparticles for 24 hr (Gao, *et al*., 2011). The use of a rat derived liver cell line (BRL 3A) and 10 nm Ag NMs (up to 50 μg/ml – 24 hr exposure) also resulted in significant GSH depletion (Hussain, *et al*., 2005). In a contradictory study however the effects of silver

NMs on primary mice hepatocytes *in vitro* revealed a small increase in intracellular GSH levels subsequent to 24 hr exposure to the NMs (Arora *et al*., 2009).

The *in vivo* and *in vitro* assays therefore produced comparable results for the Ag and ZnO nanomaterials, but there were differences for the TiO_2 (for which the *in vivo* system was more sensitive) and MWCNT (for which the *in vitro* system was more sensitive). The difference following MWCNT exposure may be related to the shape and size of carbon nanotubes compared to the nanoparticles. Since the MWCNTs examined had lengths in the μm-range, it is possible that their translocation into the bloodstream, and subsequent exposure of the liver, is relatively lower in comparison to the smaller NMs. The difference for the positive TiO_2 particles is less easy to explain. Positively charged particles have been demonstrated to penetrate cellular barriers more readily than uncharged or negatively charged particles (Orthmann, *et al*., 2010), and to be more cytotoxic *in vitro* (Salomon, *et al*., 2011). However, the positive TiO_2 particles in this study were not considered to be highly toxic in the C3A cell line. Something relating to the respiratory route of exposure might have imparted a characteristic to the particles that enhanced their toxicity. Perhaps coating the particles with lung lining fluid (LLF) could influence their impact on the liver cells. Other studies conducted within our research group have demonstrated that LLF can modulate the cytotoxicity and pro-inflammatory nature of gold and silica nanomaterials to hepatocytes and macrophages (Brown, *et al*., 2013a and b). Alternatively the positively charged TiO_2 may have induced a localised response in the lung generating a response that impacted on the liver.

Next it was shown that 24 hr exposure of ENPRA nanomaterials (with the exception of two MWCNTs) via the lungs affects gene expression in the liver - with a decrease in C3 and an increase in IL6 and IL10 mRNA levels most evident. The data in this study suggest that the overall response in the liver is anti-inflammatory, hence tolerance is the mechanism of response in the organ following exposure to these NMs. To our knowledge studies into gene expression in the liver following exposure of nanomaterials via the lungs are limited in number. However in a recent study a significant hepatic response was witnessed in the offspring of rats exposed to carbon black at mRNA level (Jackson, *et al*., 2012). The genes investigated in this study, their role in the liver and possible consequences of the route of exposure of nanomaterials are comprehensively discussed in chapter 8.

7.5 Conclusions

In conclusion, this study shows that instilled Ag, ZnO and positively charged TiO_2 result in distal effects on the liver in the form of oxidative stress. Furthermore all NMs with the exception of the two MWCNTs instilled via the lungs caused changes in gene expression in the liver in varying degrees. In the *in vitro* C3A cell line similar results were generated (GSH depletion), with two exceptions, positively charged TiO_2 (NRECWE 002) and the MWCNTs (NM 400 and NM 402). The animal model was more sensitive to the positive TiO_2, while the cell line was more sensitive to the MWCNTs, while we observed differences in the mechanism of action and response to antioxidants depending on the toxicity of the NMs applied.

Chapter Eight

Evaluating the impact of the engineered nanomaterials in the liver following exposure via an intravenous route – the role of polymorphonuclear leukocytes, antioxidant status and gene expression in the organ

Based on publication: Kermanizadeh A, Brown DM, Hutchison G, Stone V. (2013a). Engineered nanomaterial impact in the liver following exposure via an intravenous route – the role of polymorphonuclear leukocytes and gene expression in the organ. Nanomedicine and Nanotechnology 4: 157. DOI:10.4172/2157-7439.1000157.

8.1 Aims and chapter outline

In previous chapters it was demonstrated that the panel of engineered nanomaterials investigated could be divided into a high toxicity group and a low toxicity group according to their ability to induce cytotoxicity in the C3A cell line (Kermanizadeh, *et al*., 2012c), primary human hepatocytes (Kermanizadeh, *et al*., 2012b), primary rat co-cultures of hepatocytes and Kupffer cells (Filippi, *et al*., manuscript in preparation) and renal cells (Kermanizadeh, *et al*., 2013b). Hence six nanomaterials were chosen - three of which were shown to be highly toxic (Ag and two ZnO NMs) and three that were relatively low toxic (positively charged TiO_2 and two MWCNTs) in the *in vitro* systems.

The aim of this study was to investigate the potential for NMs to induce neutrophil influx in the liver. We investigated the role of neutrophils by looking at the influx of these cells into the liver following IV exposure (large percentage of NMs reach the liver very quickly) of mice to a panel of NMs. Furthermore the changes in the expression of C3, IL6, CXCL2, IL10, TNF-α, Fas ligand, albumin and intracellular adhesion molecule 1 (ICAM-1) in the liver following nanomaterial exposure to gain a better understanding of how the organ responds following a NM (NM 110, NM 111, NM 300, NM 400, NM 402 and NRCWE 002) challenge were investigated. Finally we examined the total glutathione (GSH and GSSG) levels in the liver to ascertain any changes in the organ's antioxidant status following IV exposure to the NMs.

8.2 Myeloperoxidase quantification in liver tissue

MPO is a lysosomal protein stored in granules of all granulocytes, and hence it is found in largest quantities in neutrophils. In order to quantify PMN infiltration into the liver we measured MPO in the tissue samples. A modest but statistically significant increase in MPO in the liver as early as 6 hr following intravenous injection of four of the six NMs (NM 110, NM 300, NM 400 and NRCWE 002) was noted (Figure 8.1) ($p<0.05$). MPO content of the liver tissue had subsided back to control levels by 48 hr (all NMs) (Figure 8.2). Multiple doses of Ag and TiO_2 NMs (one high and one low toxicity materials) did not enhance the MPO up-regulation further (Figure 8.3).

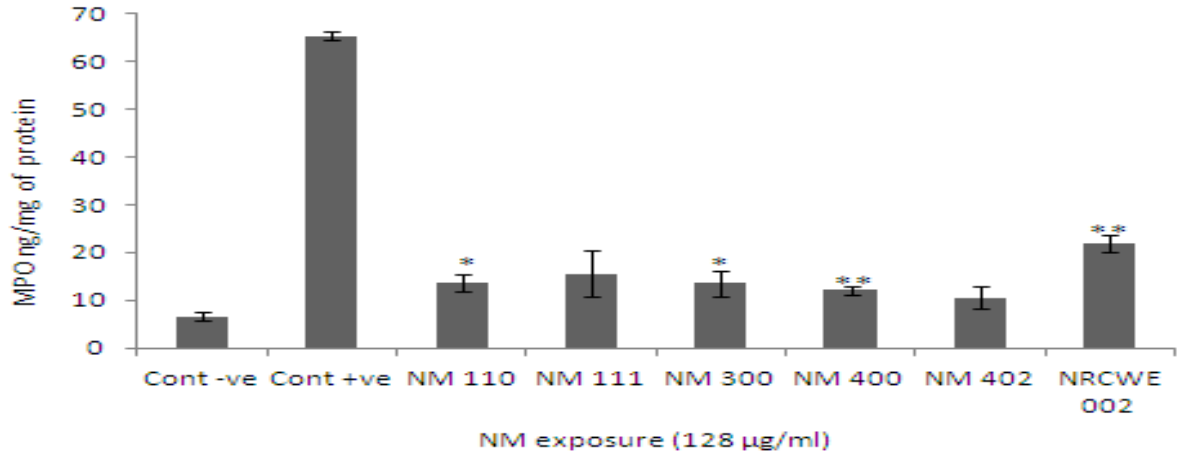

Figure 8.1. MPO measured in the liver tissue following 6 hr IV exposure to 100 µl 128 µg/ml of the panel of NMs (NM 110 – ZnO uncoated; NM 111 – ZnO coated; NM 300 – Ag; NM 400 – MWCNT; NM 402 MWCNT; NRCWE 002 – positively charged TiO_2. A positive control of LPS (50 µl - 100 µg/ml) was also employed. The negative control is representative of animals injected with 100 µl of PBS. (n=3±SEM) * P<0.05, ** P<0.005 compared to negative control.

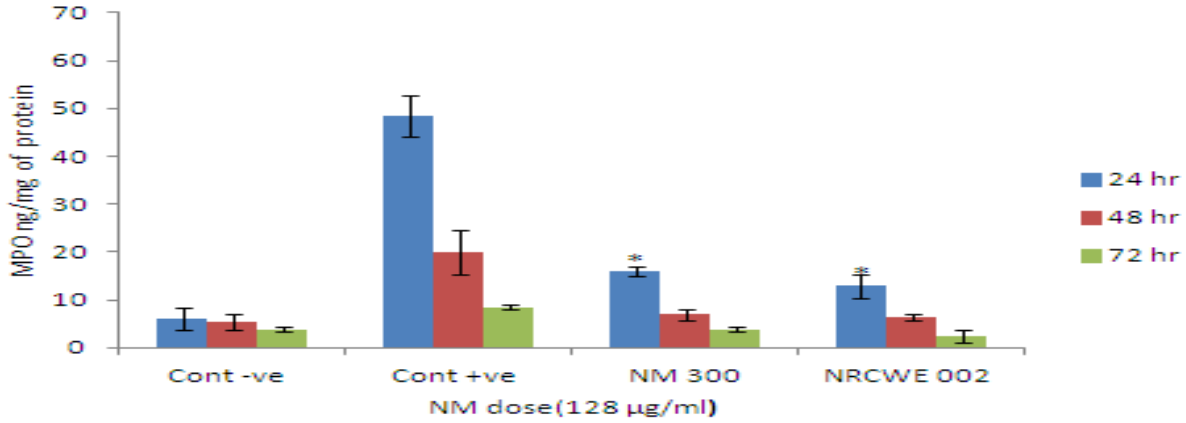

Figure 8.2. MPO measured in the liver following 24, 48 and 72 hr exposure to 100 µl of 128 µg/ml the NM 300 – Ag and NRCWE 002 – positively charged TiO_2. A positive control of LPS (50 µl - 100 µg/ml) was also employed. The negative control is representative of animals injected with 100 µl of PBS. (n=3±SEM) * P<0.05, ** P<0.005compared to negative control.

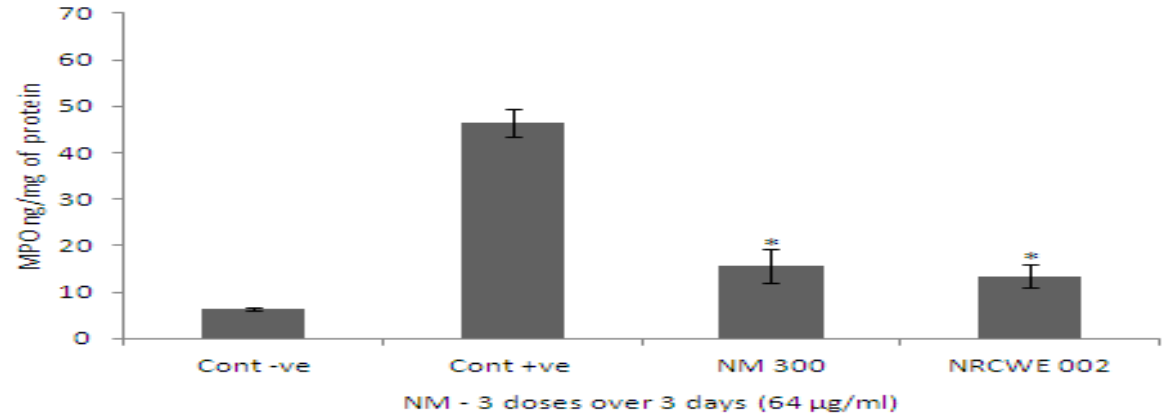

Figure 8.3. MPO measured in the liver following 3 repeated doses of NMs over three days (3 doses of 100 µl of 64 µg/ml every 24 hr). The animals were dissected 72 hr following the initial dose. The negative control is representative of animals injected with three doses of 100 µl of PBS while the positive control animals were injected with three doses of LPS (50 µl - 50 µg/ml per injection). (n=3±SEM) * P<0.05, ** P<0.005compared to negative control.

8.3 Immunohistochemistry

As already mentioned MPO is found in all granulocytes including basophils and eosinophils all be it in smaller quantities compared to neutrophils. Therefore to ascertain whether the increase in MPO witnessed previously (Figure 8.1, 2 and 3) was indeed associated with neutrophils, the tissues were labelled using a specific neutrophil cell surface marker (Ly-6B.2). Staining of the sections showed neutrophils in the tissues exposed to the positive control and the nanomaterials 6 hr post exposure which were not evident in the negative control (Figure 8.4). Furthermore the relative numbers of neutrophils stained in the tissues were comparable to results obtained from the MPO experiments for the time course in that the staining decreased with time (Figure 8.5). Multiple dose experiments also reflected the MPO results, in that repeated exposures did not further enhance the neutrophil influx into the tissue (Figure 8.6).

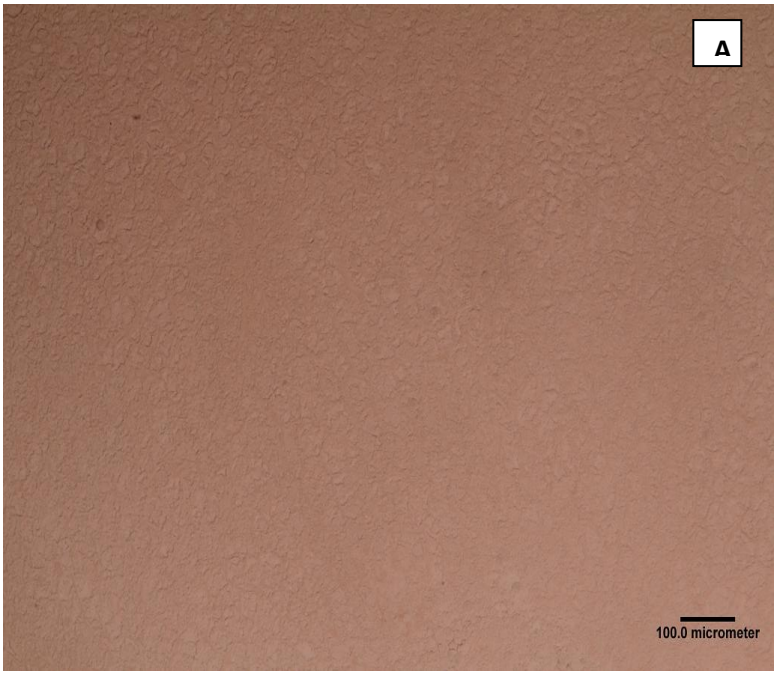
A
100.0 micrometer

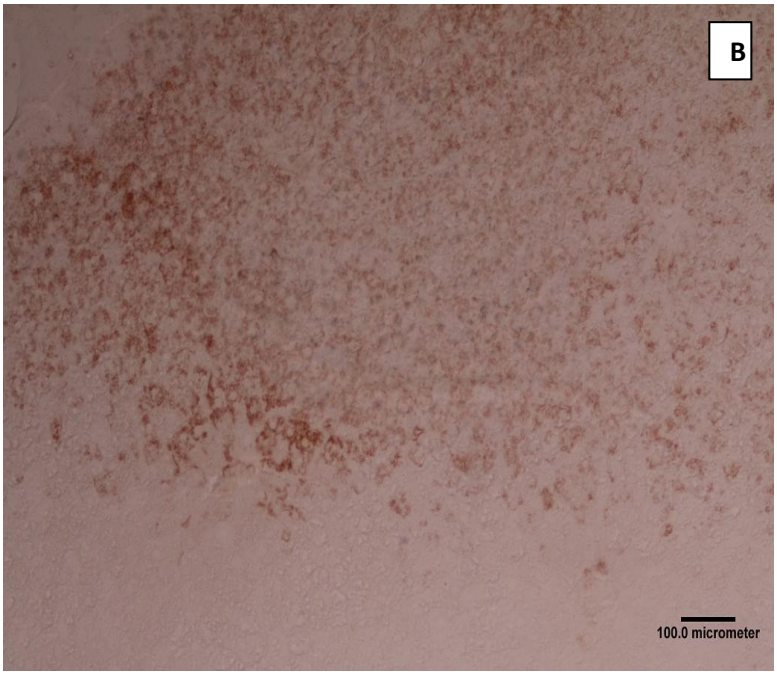
B
100.0 micrometer

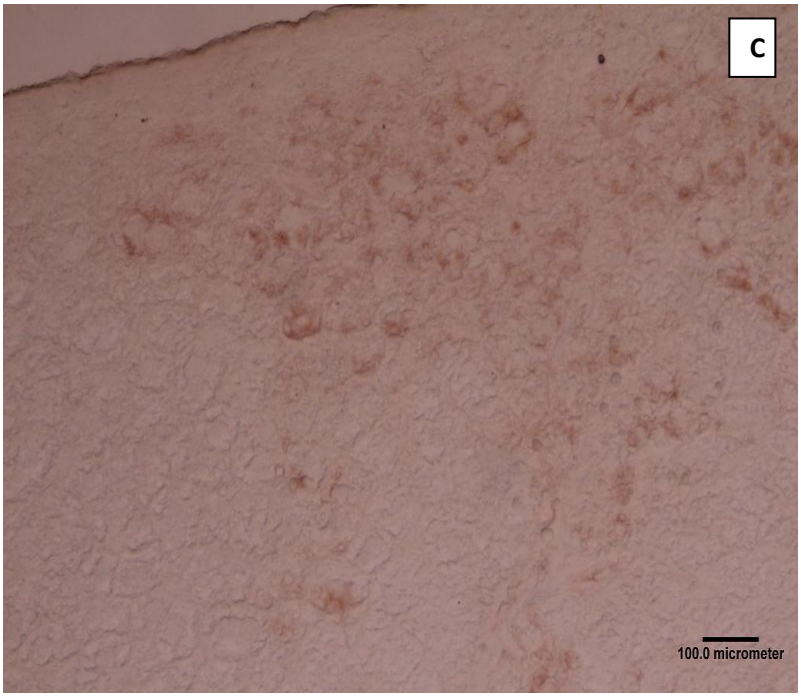
C
100.0 micrometer

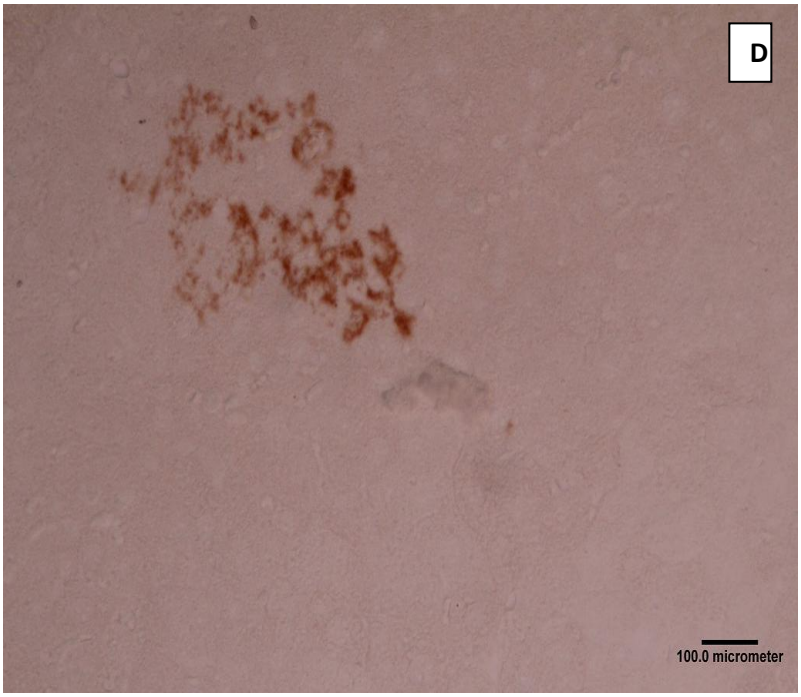
D
100.0 micrometer

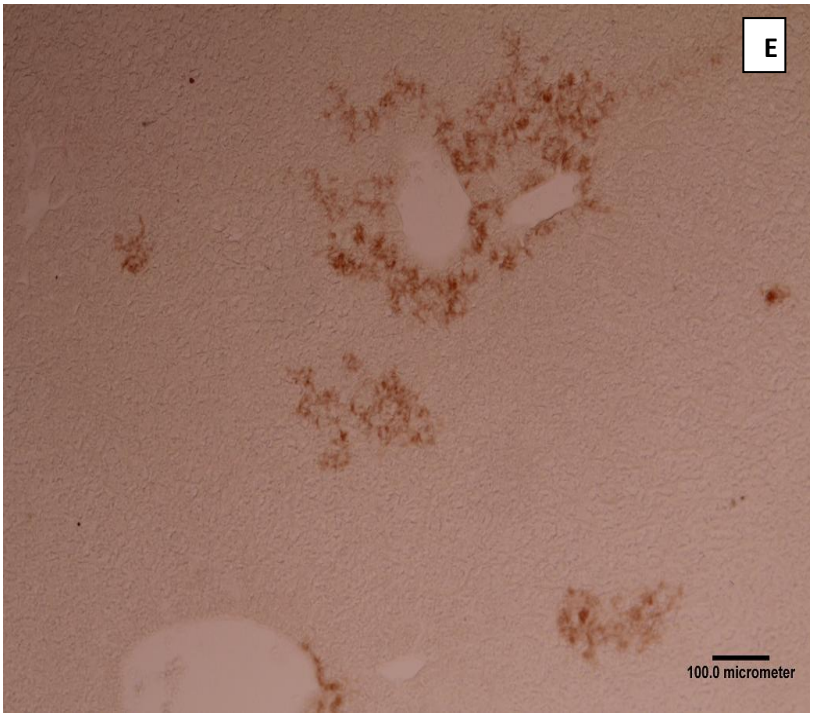
E
100.0 micrometer

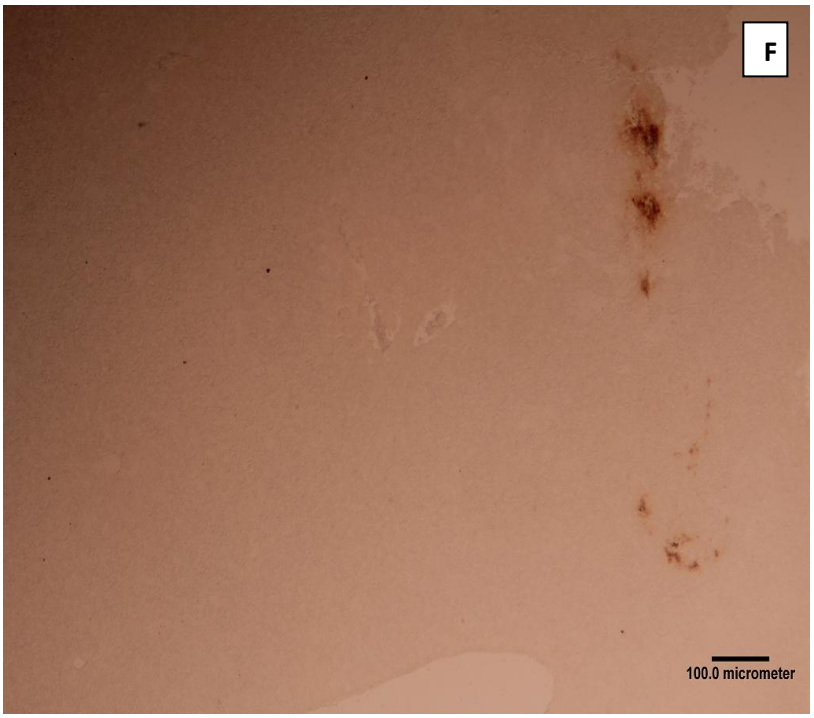
F
100.0 micrometer

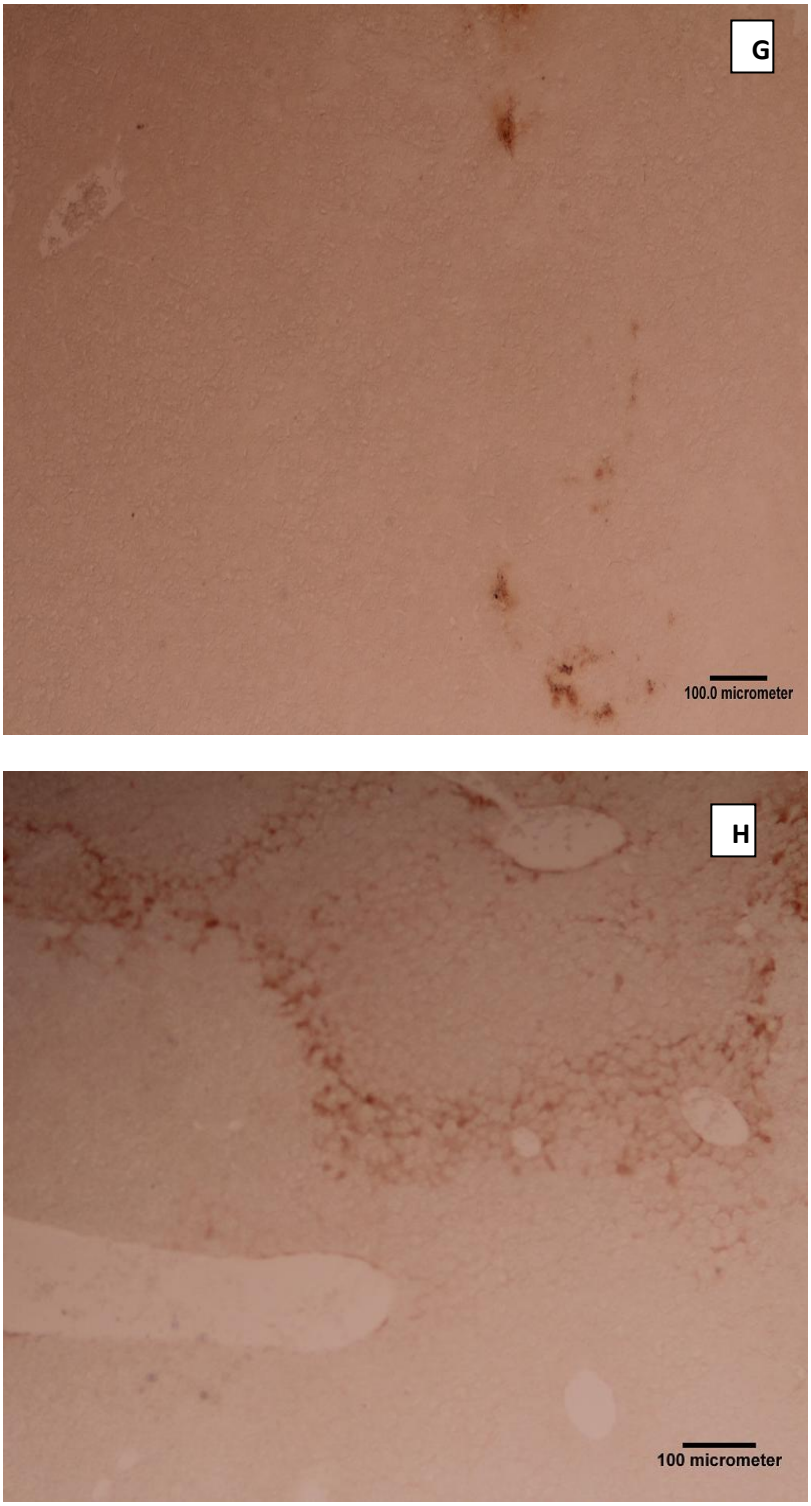

Figure 8.4. Ly6B.2 staining of mouse liver tissue by immunohistochemistry 6 hr post intravenous exposure to ENPRA panel of engineered nanomaterials (100 µl - 128 µg/ml of NMs). A positive control of LPS (50 µl - 100 µg/ml) was also employed. The negative control is representative of animals injected with 100 µl of PBS. **A)** PBS **B)** LPS **C)** NM 110 **D)** NM 111 **E)** NM 300 **F)** NM 400 **G)** NM 402 **H)** NRCWE 002.

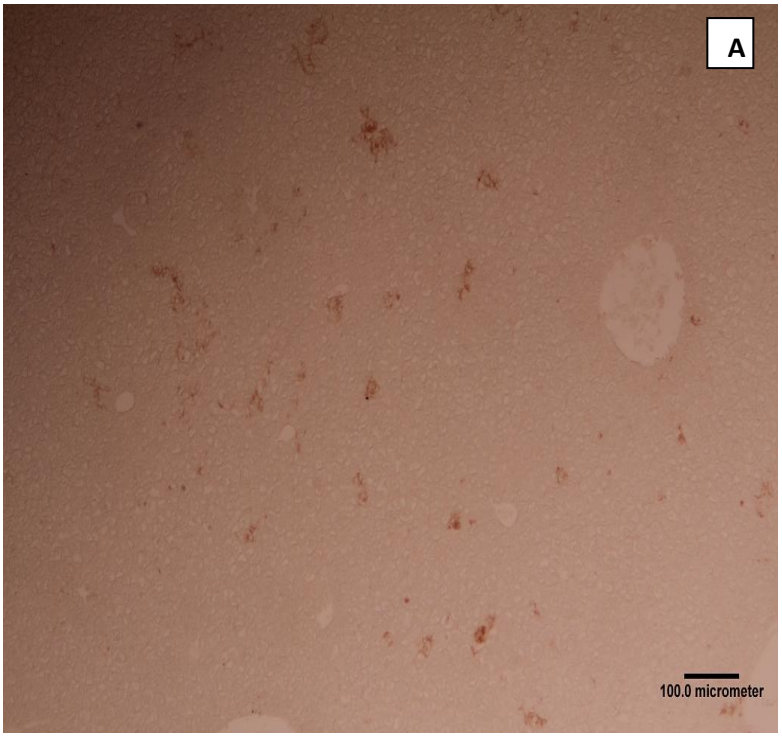
A
100.0 micrometer

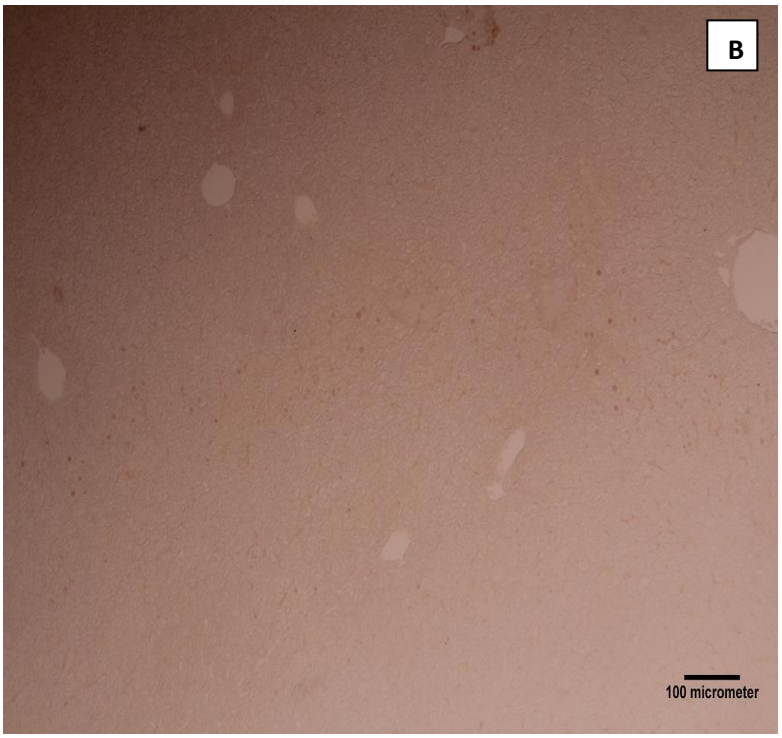
B
100 micrometer

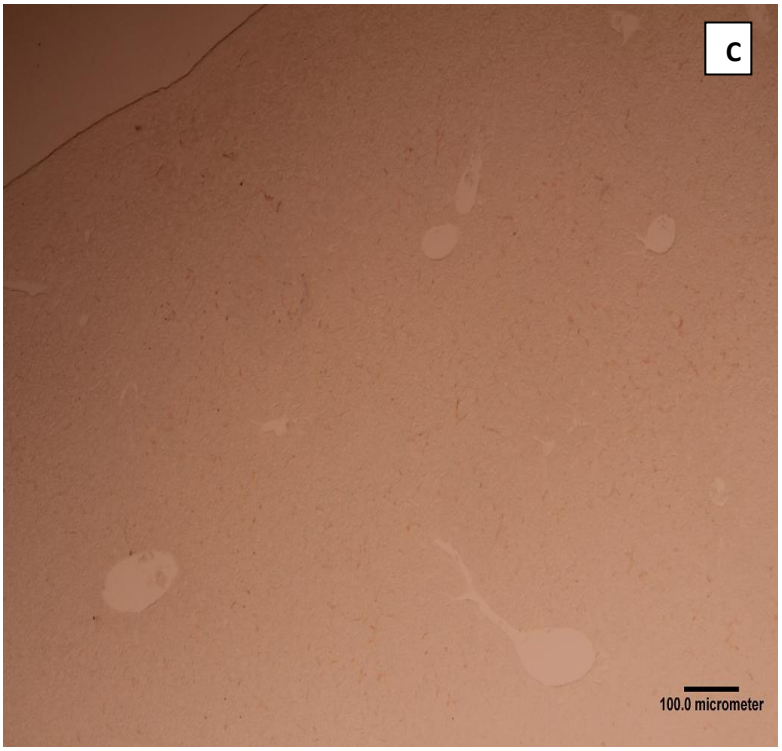
C
100.0 micrometer

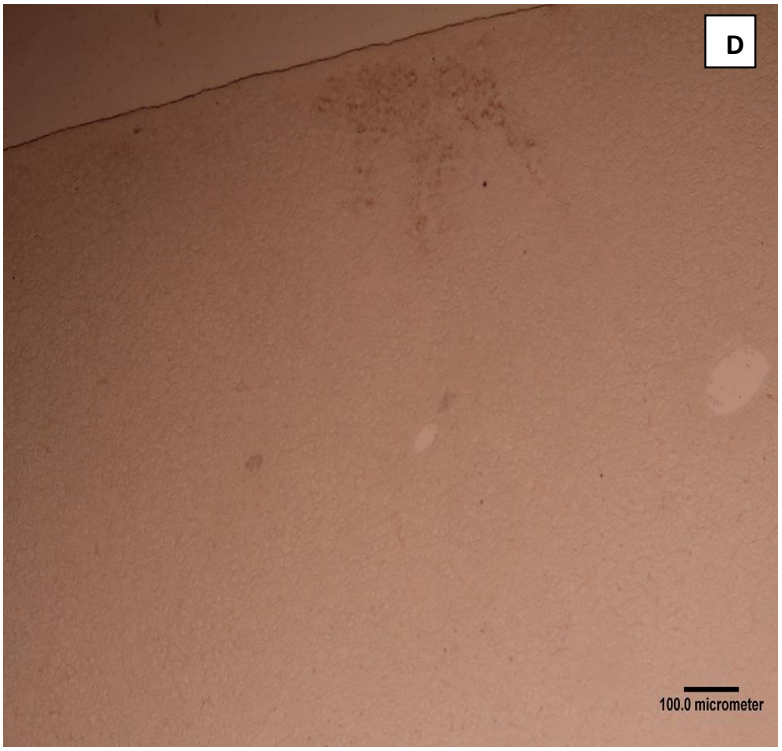
D
100.0 micrometer

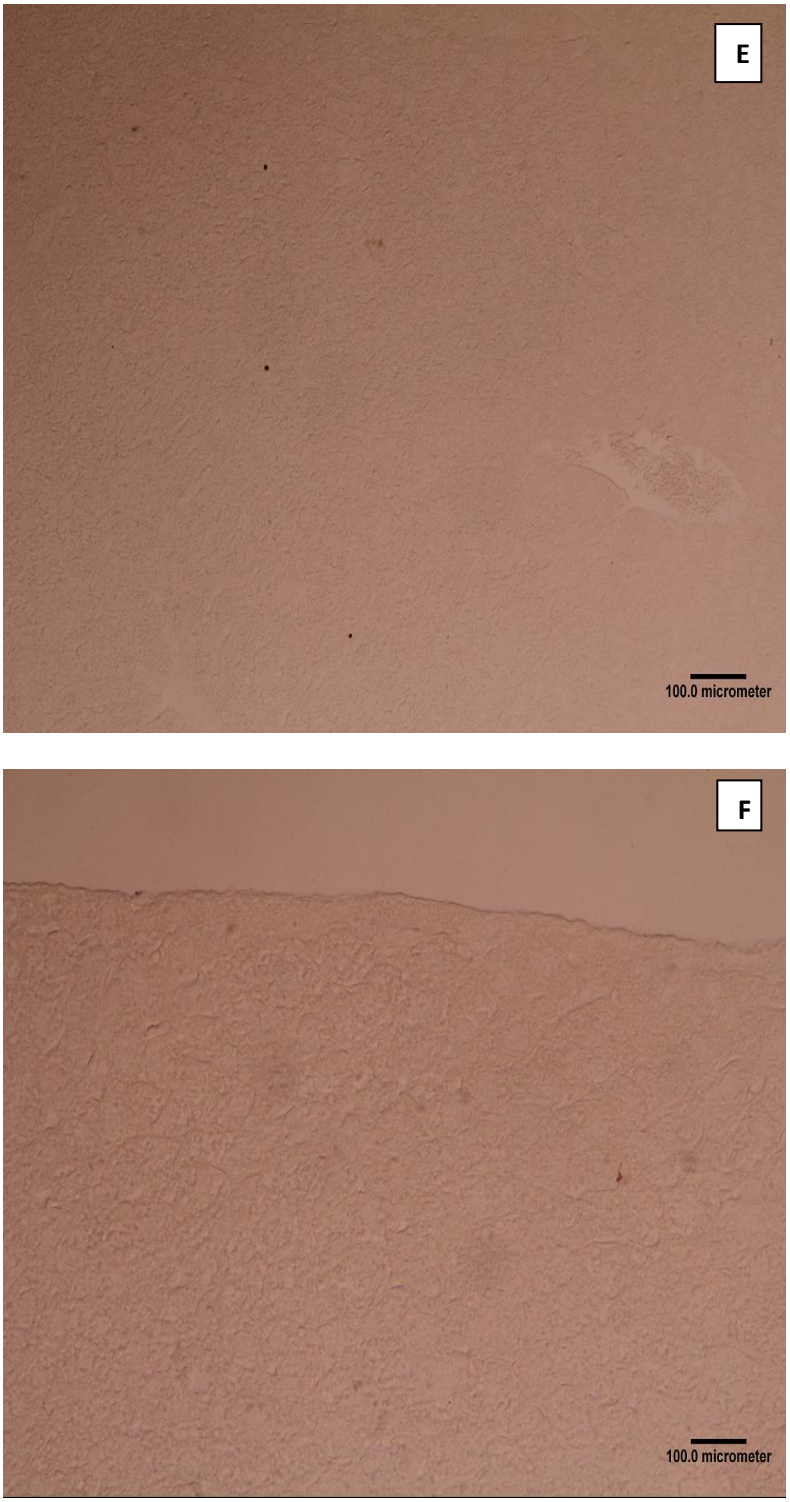

Figure 8.5. Ly6B.2 staining of mouse liver tissue by immunohistochemistry representing samples from animals 24, 48 or 72 hr post intravenous exposure to ENPRA panel of engineered nanomaterials (100 µl - 128 µg/ml of NMs). **A)** NM 300 – 24 hr **B)** NRCWE 002 – 24 hr **C)** NM 300 – 48 hr **D)** NRCWE 002 – 48 hr **E)** NM 300 – 72 hr **F)** NRCWE 002 – 72 hr.

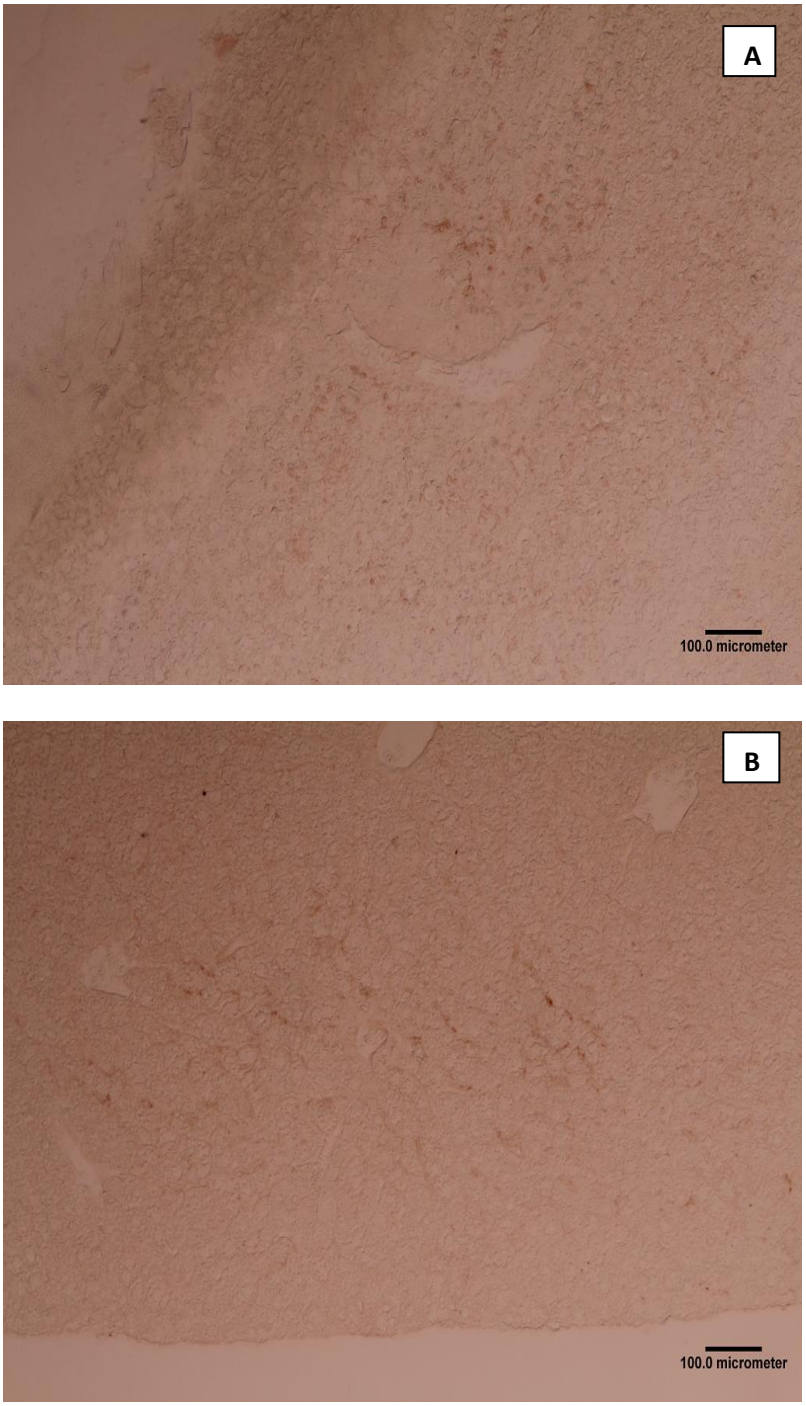

Figure 8.6. Ly6B.2 staining of mouse liver tissue by immunohistochemistry following three repeated doses over three days (3 doses of 100 µl of 64 µg/ml of NMs every 24 hr). The animals were dissected 72 hr following the initial dose. **A)** NM 300 **B)** NRCWE 002.

8.4 Liver glutathione measurements following intravenous injection of nanomaterials

Analysis of the changes of total glutathione levels in mice liver tissue revealed no significant changes 24 hr following a intravenous exposure to 100 µl of 128 µg/ml of the Ag (NM 300) or positively charged TiO_2 (NRCWE 002) nanomaterials (Figure 8.7).

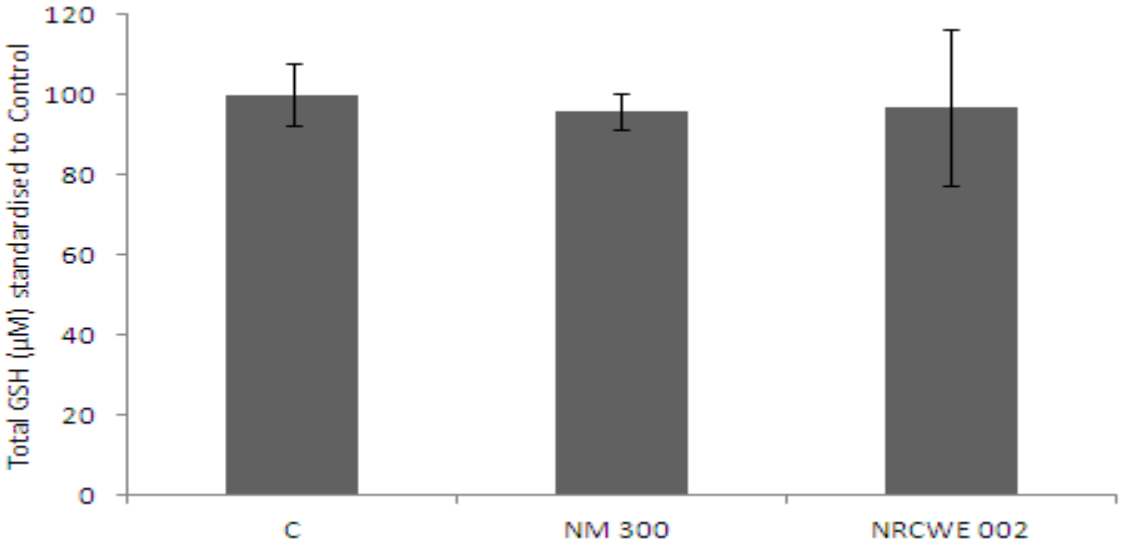

Figure 8.7. Effects of NM exposure on total glutathione levels in liver tissue. The animals were exposed to the nanomaterials via an intravenous route - 100 µl of 128 µg/ml of the Ag (NM 300) or positively charged TiO_2 (NRCWE 002) for a period of 24 hr before dissection and the removal of the liver. The negative control group of animal received 100 µl of PBS. (n=3±SEM)

8.5 mRNA expression in mice liver following intravenous exposure of NMs

Analysis of mRNA expression in mice liver 6 hr after intravenous injection of 100 µl of 128 µg/ml of panel of nanomaterials showed a decrease in C3 following exposure to ZnO (NM 110 and NM 111), MWCNT (NM 400 and NM 402) (Table 8.1). A decrease in IL6 mRNA levels following exposure to ZnO (NM 110, NM 111) and Ag NMs (NM 300) (Table 8.1). Increases in IL10 was witnessed following exposure to ZnO (NM 110) and TiO_2 (NRCWE 002) (Table 8.1) was observed. Finally a large increase in CXCL2 was witnessed following exposure to NM 110. No significant changes were detected in the expression of albumin, TNF-α, Fas ligand or ICAM-1 following treatment with any of the nanomaterials (Table 8.1).

Repeated exposure of the C57/BL6 mice to three doses of the Ag (NM 300) and positively charged TiO_2 (NRCWE 002) nanomaterials resulted in a large increase in IL10 levels while smaller yet significant decreases in C3 and ICAM-1 mRNA were noted following exposure to both NMs (Table 8.2).

Finally, the animals were exposed to a single dose of 100 µl of 64 µg/ml of the Ag and positively charged TiO_2 NMs by injection via the lateral tail vein. The animals were dissected 24 hr, 48 hr and 72 hr after the initial injection. We found that in all instances the increase or decrease in mRNA was most evident after the 24 hr exposure. For all the genes investigated in this study resolution to control levels had occurred 72 hr post exposure (Tables 8.3 and 4).

Gene Expression	NM 110	NM 111	NM 300	NM 400	NM 402	NRCWE 002
IL6	----	-	----	0	0	0
IL10	++	0	0	0	+	++++
C3	-	--	--	-	--	0
CXCL2	++++	0	0	0	0	0
TNF-α	0	0	0	0	0	0
Fas ligand	0	0	0	0	0	0
ICAM-1	0	0	0	0	0	0
Albumin	0	0	0	0	0	0

Table 8.1. mRNA expression of inflammatory cytokines and receptors, FasL and albumin in C57/BL6 mice liver. The animals were exposed to 100 µl of 128 µg/ml of panel of nanomaterials for 6 hr by injection via the lateral tail vein. mRNA expression was analysed by real time PCR with B2m utilised as an endogenous control. – or + is representative of 50% change, -- or ++ is representative of 75% change, --- or +++ is representative of 100% change and ---- or ++++ is representative of ≥ 200% change. (n=3)

Gene Expression	NM 300	NRCWE 002
IL6	0	0
IL10	++++	++++
C3	--	--
CXCL2	0	0
TNF-α	+	0
Fas Ligand	0	0
ICAM-1	--	--
Albumin	0	0

Table 8.2. mRNA expression of inflammatory cytokines and receptors, FasL and albumin in C57/BL6 mice liver. The animals were exposed three times (0 hr, 24 hr and 48 hr) to 100 µl of 64 µg/ml of the Ag (NM 300) and the positively charged TiO_2 NM (NRCWE 002) by injection via the lateral tail vein. The animals were dissected 72 hr after the first injection and the mRNA expression was analysed by real time PCR with B2m utilised as an endogenous control. – or + is representative of 50% change, -- or ++ is representative of 75% change, --- or +++ is representative of 100% change and ---- or ++++ is representative of ≥ 200% change. (n=3)

Gene Expression (NM 300)	Day 1	Day 2	Day 3
IL6	++	+	0
IL10	++++	++	0
C3	--	-	0
CXCL2	0	0	0
TNF-α	0	0	0
Fas Ligand	++	0	0
ICAM-1	++	0	0
Albumin	0	0	0

Table 8.3. mRNA expression of inflammatory cytokines and receptors, FasL and albumin in C57/BL6 mice liver. The animals were exposed to a single dose of 100 µl of 128 µg/ml of the Ag NM (NM 300) by injection via the lateral tail vein. The animals were dissected 24 hr, 48 hr and 72 hr after the initial injection and the mRNA expression was analysed by real time PCR with B2m utilised as an endogenous control. – or + is representative of 50% change, -- or ++ is representative of 75% change, --- or +++ is representative of 100% change and ---- or ++++ is representative of ≥ 200% change. (n=3)

Gene Expression (NRCWE 002)	Day 1	Day 2	Day 3
IL6	0	0	0
IL10	++++	++++	0
C3	--	0	0
CXCL2	0	0	0
TNF-α	0	0	0
Fas Ligand	++	0	0
ICAM-1	++	0	0
Albumin	0	0	0

Table 8.4. mRNA expression of inflammatory cytokines and receptors, FasL and albumin in C57/BL6 mice liver. The animals were exposed to a single dose of 100 µl of 128 µg/ml of the TiO_2 NM (NRCWE 002) by injection via the lateral tail vein. The animals were dissected 24 hr, 48 hr and 72 hr after the initial injection and the mRNA expression was analysed by real time PCR with B2m utilised as an endogenous control. – or + is representative of 50% change, -- or ++ is representative of 75% change, --- or +++ is representative of 100% change and ---- or ++++ is representative of $\geq$ 200% change. (n=3)

8.6 Discussion

Numerous studies have demonstrated that NMs entering the body via the lungs, ingestion or direct injection accumulate in the liver (Chen, *et al*., 1999; Diesen, *et al*., 2009; Sadauskas, *et al*., 2009b). In previous studies it has been shown that hepatocytes are capable of producing potent neutrophil chemoattractants (human – IL8) (Delpino, *et al*., 2010; Kermanizadeh, *et al*., 2012a; b and c) (rat - CINC-3) (Ding, *et al*., 2008; Filippi, *et al*., manuscript in preparation) following exposure to foreign materials or disease models. We therefore investigated neutrophil infiltration into the liver following intravenous exposure of mice to a panel of engineered nanomaterials.

Here it was shown that all six NMs (NM 110, NM 111, NM 300, NM 400, NM 402 and NRCWE 002) were able to induce a neutrophil influx into the liver as early as 6 hr post IV injection. It is extremely important to note that the doses which the animals were exposed to were very low doses mirroring realistic possible human (i.e. less than 15 µg of nanomaterials per animal) - suggesting neutrophils are involved in the organs immunity to the foreign nanomaterials. To our knowledge the role of neutrophils in the liver following nanomaterial exposure has not been addressed previously however it has been shown that neutrophils can accumulate within hepatic microvasculature following an increase in inflammatory mediators such as TNF-α, IL1, MIP-2, and PAF (Bajt, *et al*., 2001; Ramaiah, *et al*., 2007). Furthermore in a recent study an increase in numbers of neutrophils in the liver of BALB/c mice was observed during casein induced anaphylaxis (Krishnamurthy, *et al*., 2012).

It appears that the neutrophils are only involved in the initial phases of the immune response against the NMs. The initial increase of neutrophil numbers in tissue was resolved by 48 hr post exposure. It is possible that after the initial infiltration of the neutrophils into the tissue the resident macrophages (Kupffer cells) take over the immune response to the nanomaterials. It was also very interesting to note that repeated doses of the nanomaterials did not result in further accumulation of the polymorphonuclear leukocytes into the tissue suggesting once again that after their role in initiating the immune response in the liver the neutrophils play no further part in the maintenance or the continuation of the inflammatory response.

It has been shown that the most common neutrophil mediated response in the liver is governed by the adhesion of the cells to hepatocytes (via ICAM-1 binding Mac-1) (Bautista, 2002; Ramaiah, *et al*., 2007). This adhesion triggers the formation of reactive oxygen species (ROS) by NADPH oxidase and release of proteases through the degranulation of the PMNs. This process could lead to neutrophilic hepatitis characterised by self aggravating mechanisms resulting in chronic disease (Bautista, 2002). However a prolonged neutrophil response does not happen following exposure to the nanomaterials utilised in this study. As already mentioned the neutrophils decrease in number with time after the initial exposure. In addition the up-regulation of ICAM-1 mRNA was only noted after the 24 hr and had returned to normal background levels 48 hr post IV NM exposure.

Next it was noted that there was no significant impact on liver total glutathione following IV exposure of the mice to the Ag or positively charged TiO_2 NMs after 24 hr. These findings are contradictory to our previous studies in which both materials were shown to deplete total GSH in the liver following intratracheal instillation (IT) into the lungs (Chapter 7) (Gosens, *et al.,* 2013a and b - manuscript in preparation) and in a hepatocyte cell line model (Chapter 5) (Kermanizadeh, *et al*., 2012a) after a 24 hr time point. One explanation for this could be that the doses administrated within this study are just not high enough to induce an effect on the antioxidant levels in the liver (these particular doses were chosen to mirror realistic exposure scenarios). It is also possible that 24 hr is too long for the analysis of the antioxidant status in the liver. It has been shown that MWCNT/Fe_3O_4 NM reached the liver as early as 2 hr following intravenous exposure (Wu, *et al*., 2011), while single walled carbon nanotubes injected into mice were found in the liver after 3 hr (McDevitt, *et al*., 2007). Hence it is possible that following this small NM challenge any antioxidant fluctuation could have taken place at earlier time points, with the cells being able to recover after 24 hr. The third hypothesis for the differences between the IT and IV routes is that passage through the lungs might impart a specific toxicity to the NMs that results in an impact on the liver. This may involve either the formation of a specific protein corona on the NM surface derived from the lung lining fluid or a humoral mediated effect initiated by cells in the lung.

Next the expression of a range of genes related to inflammation, oxidative stress and apoptosis was analysed in livers of mice exposed to the panel of engineered nanomaterials. Analysis of mRNA expression in mice livers 6 hr after intravenous injection of panel of nanomaterials resulted in a decrease in C3 following exposure to ZnO (NM 110 and NM

111), Ag (NM 300) and MWCNT (NM 400 and NM 402) NMs. Repeated exposure of the mice to three doses of the Ag (NM 300) and positively charged TiO_2 (NRCWE 002) nanomaterials also resulted in small yet significant decrease in C3. Complement component 3 is one of the most abundant and important protein in the complement cascade. C3 activation is essential for all the functions of the complement system. It is crucial in promoting phagocytosis, supporting the local immune response against foreign agents and instructing the adaptive immune responses to select the appropriate antigens for any eventual antibody response (Sahu, *et al*., 2002). Moreover C3 might be capable of interaction with the coagulation system and contributing to pro-coagulation and ultimately a prothrombotic state (Hertle, *et al*., 2012). The decrease in C3 expression might suggest that exposure to low doses of NMs in this study results in overall tolerance in the liver rather than a fully developed immune response.

Furthermore there was a decrease in IL6 mRNA levels following exposure to the ZnO and Ag NMs after 6 hr of exposure. IL6 is a multifunctional cytokine that acts on a number of cell types including B and T lymphocytes, hepatocytes, hematopoietic progenitor cells and neuronal cells (Kishimoto, *et al*., 1995). Under different circumstances the cytokine can be both pro and anti-inflammatory. In the liver IL6 is a potent inducer of acute phase proteins which are in most part pro-inflammatory proteins (including C reactive protein, complement factors and serum amyloid A) (Poli, *et al*., 1989). Once again the decrease in IL6 expression suggests that exposure to low doses of these NMs results in tolerance in the liver.

IL10 is a multifunctional cytokine with diverse effects on a wide range of hemopoietic cells. The cytokine's principle function is to terminate inflammatory responses (Moore, *et al*., 2001). IL10 also regulates growth or differentiation of B and T lymphocytes, NK cells, mast cells, most granulocytes, dendritic cells, keratinocytes, and endothelial cells (Mocellin, *et al.,* 2004). IL10 also plays a key role in differentiation of regulatory T cells, which figure prominently and importantly in the control of immune responses and developing a tolerant immune state (Mocellin, *et al.,* 2004). Analysis of IL10 mRNA showed an increase following exposure to exposure to NM 110, NM 300, NM 402 and NRCWE 002. The increase in IL10 mRNA was the largest and the most significant of all the genes investigated in this study once again suggesting tolerance as being the overall response in the organ following acute low exposure to NMs.

CXCL2 also known as macrophage inflammatory protein 2 alpha (MIP-2) is a chemokine secreted from a number of cells in particular monocytes and macrophages (Zamjahn, *et al*., 2011). MIP-2 is a potent chemoattractant for neutrophils and hematopoetic stem cells (Zamjahn, *et al*., 2011). A large increase in CXCL2 was witnessed following exposure to NM 110 (uncoated ZnO) following 6 hr exposure. It is important to note that increases compared to base levels of CXCL2 were also witnessed following the 6 hr exposure to other nanomaterials however due to large fluctuations in the control group of animals these changes could not be regarded as significant. Up regulation of CXCL2 could be associated with the short term acute recruitment of neutrophils into the liver.

No significant changes were detected in the expression of albumin, TNF-α, Fas ligand or ICAM-1 following 6 hr of any of the nanomaterials utilised in this study. The fact that there was no change in the levels of TNF-α would again suggest that there is no significant pro-inflammatory response following exposure to the NMs. FasL (also referred to as CD95L) is a homotrimeric type II transmembrane protein signalling through trimerisation with CD95 on the target cells leading to death by apoptosis (McIntyre., 2012). The findings here would suggest that there is no apoptosis following exposure to these particular nanomaterials and time points however it is very possible that FasL might be up-regulated at later time points in relation of PMN clearance from the organ. Finally there was no change in albumin gene expression suggesting that the NM challenge at these low doses does not affect liver function. Repeated exposure of the C57/BL6 mice to three doses of the Ag (NM 300) and positively charged (NRCWE 002) nanomaterials again resulted in large increases in IL10 levels while smaller yet significant decreases in C3 and ICAM-1 mRNA were noted following exposure to both NMs. ICAM-1 (intracellular adhesion molecule 1) is a molecule involved in attraction and adhesion of inflammatory cells to endothelial and epithelial cells, and its soluble form, sICAM-1, is linked to activation of these cells in pathological responses (Yang, *et al*., 2005). It is up-regulated in liver associated diseases such as in hepatitis C (Yang, *et al*., 2005). As already mentioned binding of ICAM-1 to Mac-1 on hepatocytes is crucial to neutrophil mediated response in the liver. The overall decrease in ICAM-1 mRNA suggests that neutrophils are not involved at the latter stages of the liver immunity despite fresh foreign nanomaterial challenges.

Finally, a group of animals were exposed to a single dose of 100 µl of 64 µg/ml of the Ag and positively charged TiO_2 NMs. The animals were dissected 24 hr, 48 hr and 72 hr after the

initial injection. We found that in all instances the changes in mRNA were most evident after the 24 hr exposure. These alterations resolved and all the genes investigated returned to background levels after 72 hr post exposure.

It is important to state that this study has some limitations. It might be important to look at earlier time points to gain a better understanding of the role of neutrophils in the liver following a NM challenge. We would suggest investigating early time points could be advantageous into gaining a better insight into the antioxidant status of liver tissue following intravenous nanomaterial exposure. Future studies might include the utilisation of microarray analysis for a more comprehensive gene expression profile in the liver. Any potential changes in a large number of genes including the likes of the cytochrome P450 family, heat shock proteins and IL1 family of proteins could be invaluable indicators of NM impact on the liver.

8.7 Conclusions

Overall the findings in this study seem to suggest that intravenous exposure of mice to the ENPRA panel of engineered nanomaterials results in acute effects in the liver. However the low doses used here are not sufficient to cause any long term inflammation or damage to the liver tissue. Any changes that were observed after 24 hr post exposure in terms of leukocyte infiltration into the tissue, antioxidant status and changes in gene expression related to inflammation, oxidative stress and apoptosis had resolved 72 hr post exposure.

Chapter Nine

The role of Kupffer cells in the hepatic response to nanomaterials

Based on publication: Filippi C, Kermanizadeh A, Stone V. (2013). Kupffer cell contribution to the hepatic response to nanomaterials – Manuscript in preparation.

9.1 Aims and chapter outline

In previous chapter it has been shown that the ENPRA panel of NMs chosen for this study affect a hepatocyte cell line (Chapters 4 and 5) and human primary hepatopcytes (Chapter 6). In this chapter we are investigating the role of resident liver macrophages (Kupffer cells) co-cultured with hepatocytes in an attempt to gain a better understanding of the liver response following exposure to engineered nanomaterials. The liver cells were thoroughly characterised before different end-points including cytotoxicity, intracellular glutathione levels and in particular cytokine secretion were measured.

Primary rat liver cells were isolated as described in section 3.23. The isolated cells were characterised by Dr Celine Filippi. The primary cell preparation was enriched for Kupffer cells using the protocol described in (section 3.25). The primary co-culture and the enriched Kupffer cell populations were exposed to NM 110, NM 111, NM 300, NM 400, NM 402 and NRCWE 002 with viability, cytokine secretion and antioxidant depletion quantified.

9.2 Characteristics of nanomaterials and exposure media

A list of the measured physical and chemical properties of selected nanomaterials was previously described (Chapter 4) (Kermanizadeh, *et al*., 2012c). In order to investigate if the nanomaterials behaved differently in HepatoZYME medium compared to C3A complete medium, the hydrodynamic size distributions of the NMs was measured by DLS after the nanomaterials were dispersed in this medium between 1 - 128 µg/ml (Table 9.1).

ENM code	ENM type	Manufacturer Size [nm]	Known coating	Size in HepatoZYME (DLS) Ψ
NM110	ZnO	100	none	134.9
NM111	ZnO	130	Trie-othoxy-capry-lsilane 130	149.9
NM300	Ag	< 20	Polyoxylaurat-Tween 20	34.0
NM400	MWCNT	-	none	*
NM402	MWCNT	-	none	*
NRCWE 002	TiO_2	10	Positive charged	128.0

* Not detectable by DLS due to the very large aspect ratio
Ψ Intensity based size average in biological media after 15 mins.

Table 9.1. Physical and chemical properties of tested ENMs in HepatoZyme medium.

9.3 Liver cell characterisation

All the cells utilised in this study were from the second pass (section 3.23) and had a viability of over 90%. The characterisation work was carried out by Dr Celine Filippi and described in detail in Filippi, *et al*., 2013 (including percentage of endothelial cells present in each fraction). The fraction of cells used in subsequent toxicity studies will be termed the primary liver cell culture. This fraction was further purified by MACS column.

Briefly, we noted that Kupffer cell enrichment resulted in an increased in liver macrophages numbers from 3% to 30-40% (Figure 9.1). This preparation is termed the kupffer cell enriched liver cell culture.

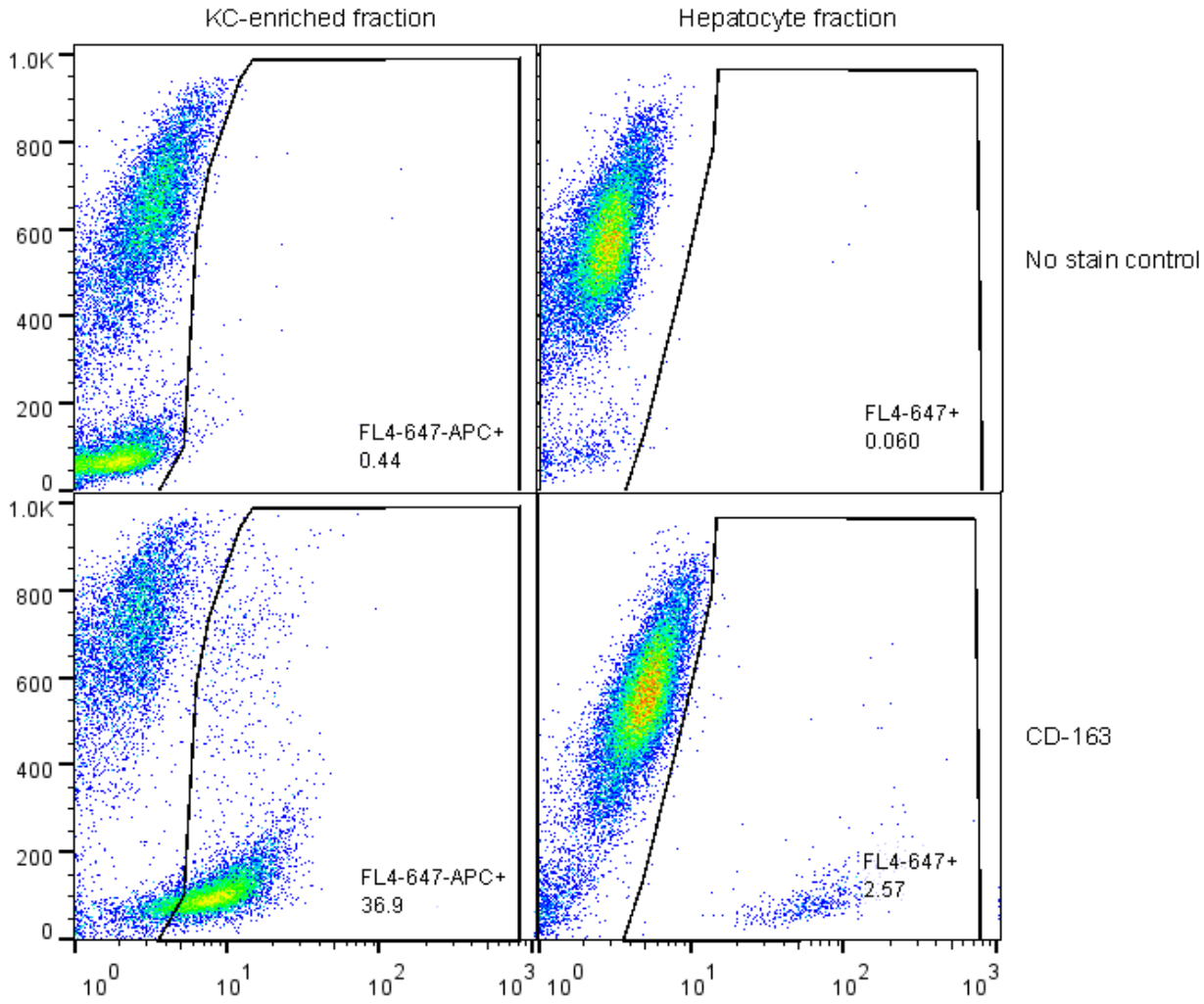

Figure 9.1. Flow cytometry images representative of Kupffer cells numbers prior and post enrichment using the MACS magnetic column. CD163 was used to specifically target and select Kupffer cells.

9.4 Impact of the selected panel of NMs on the primary liver cell co-culture viability

From the WST-1 data it is evident that following exposure of the primary liver cell co-culture to the ENPRA NMs there was a dose dependent decrease in cell viability at 24 hr across the entire nanomaterial panel (Figure 9.2). The two ZnO (NM 110 and NM 111) and the Ag (NM 300) NMs were highly toxic with an LC_{50} reached after a 24 hr exposure (Figure 9.2a, b and c). While the TiO_2 (NRCWE 002) and MWCNT (NM 400 and 402) NMs were considered to be low toxicity materials as the LC_{50} was not reached after a 24 hr exposure (Figure 9.2d, e and f).

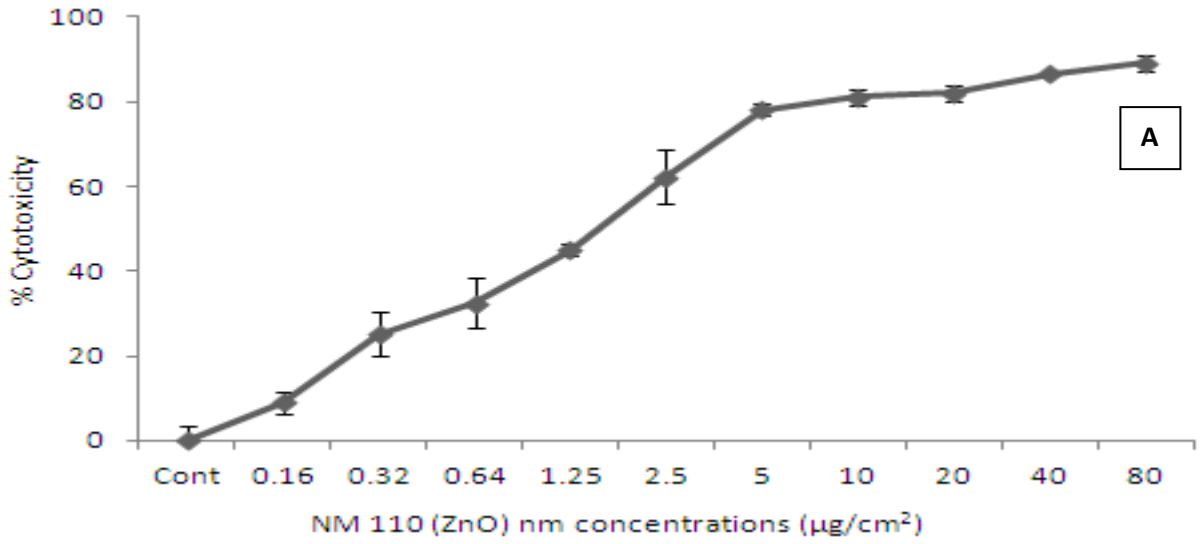
100
80
60
40
20
0
% Cytotoxicity
A
Cont
0.16
0.32
0.64
1.25
2.5
5
10
20
40
80
NM 110 (ZnO) nm concentrations (µg/cm²)

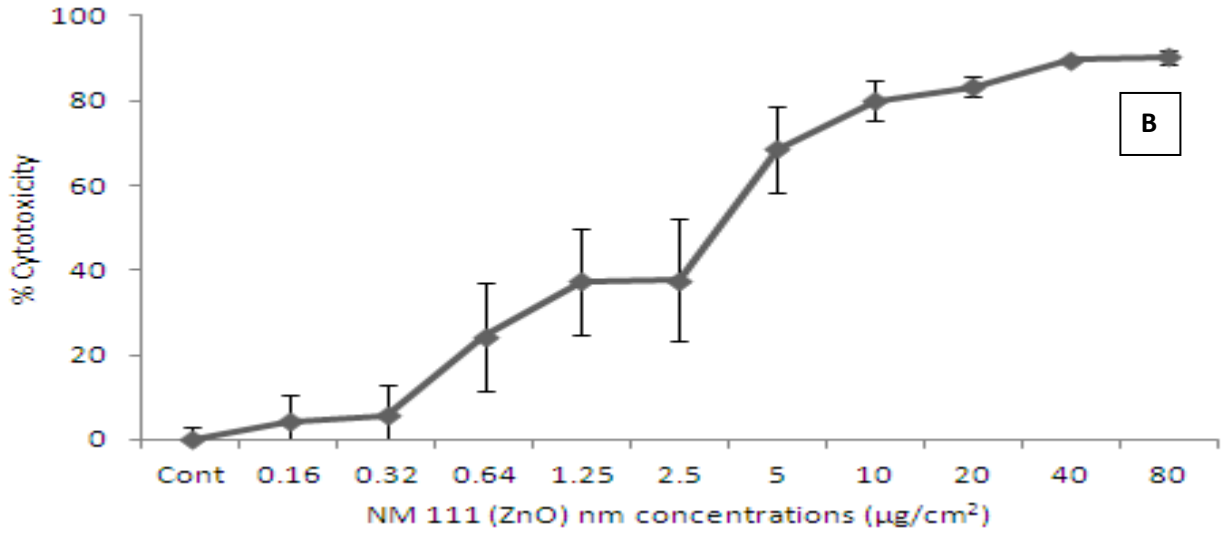
100
80
60
40
20
0
% Cytotoxicity
B
Cont
0.16
0.32
0.64
1.25
2.5
5
10
20
40
80
NM 111 (ZnO) nm concentrations (µg/cm²)

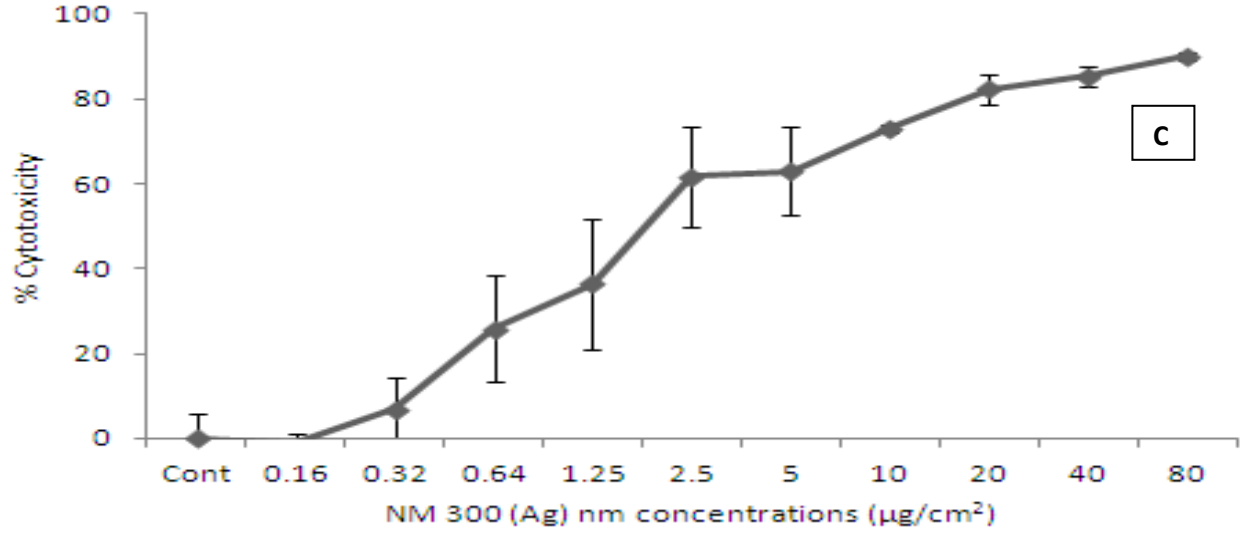
100
80
60
40
20
0
% Cytotoxicity
C
Cont
0.16
0.32
0.64
1.25
2.5
5
10
20
40
80
NM 300 (Ag) nm concentrations (µg/cm²)

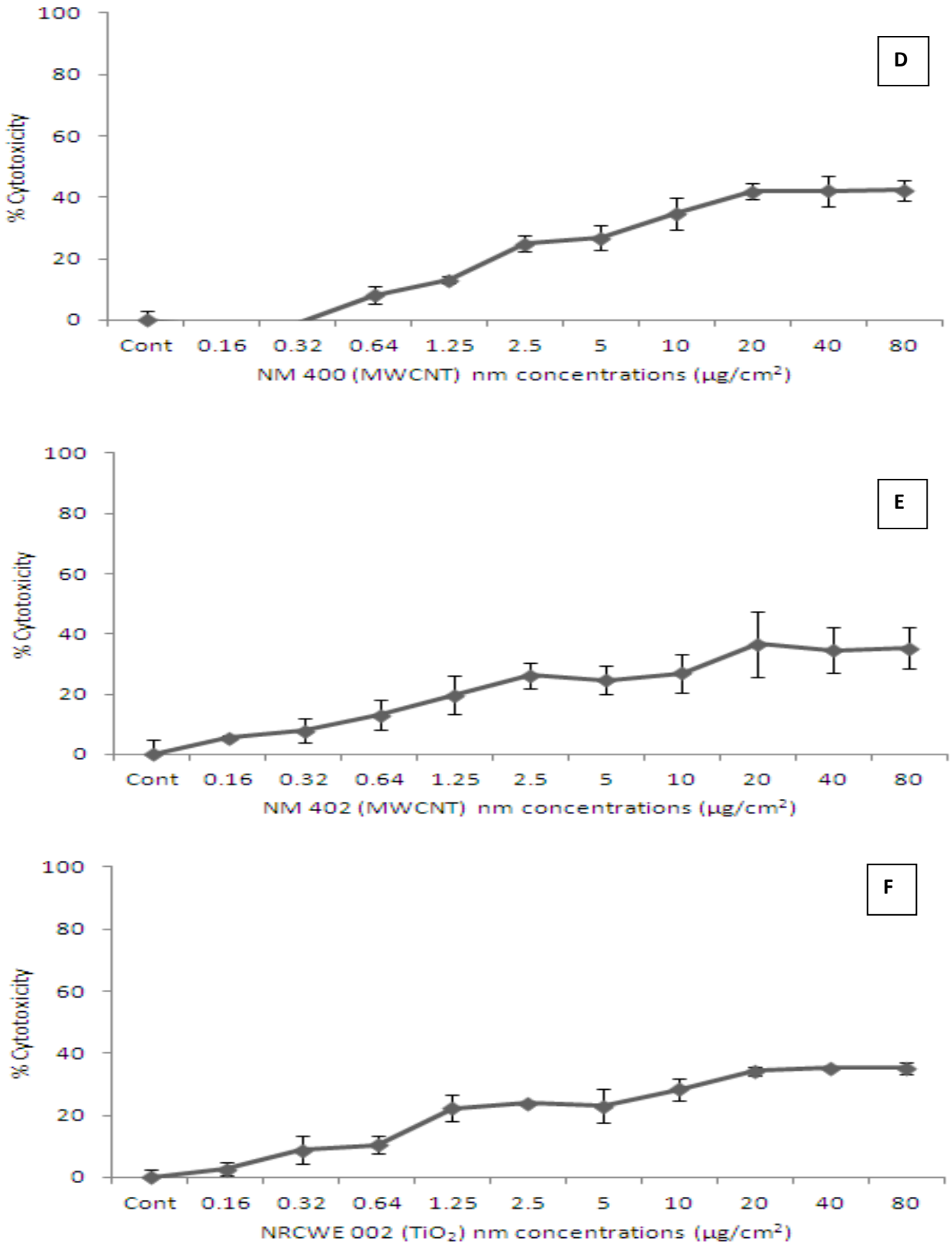

Figure 9.2. Cytotoxicity following exposure to a panel of engineered nanomaterials to the co-culture of primary rat liver cells before Kupffer cell enrichment. The cells were exposed to cell medium (control)/medium and NMs for 24 hr with cytotoxicity measured via WST-1 assay. **A)** NM 110 **B)** NM 111 **C)** NM 300 **D)** NM 400 **E)** NM 402 **F)** NRCWE 002.

9.5 Impact of the engineered NMs on cytokine secretion from the liver cells before Kupffer cell enrichment

Changes in cytokine production as a consequence of NM exposure to the standard primary hepatocye culture (without enrichment) were assessed within the supernatant of exposed liver cells and was quantified via FACSArray and ELISA. We found a dose dependent increase in the levels of TNF-α and IL10 from the liver cells with statistical significance being reached at the higher concentrations of all NMs (Figure 9.3a and b). For the low toxicity TiO_2 and MWCNT samples (NM 400, NM 402 and NRCWE 002) the CINC-3 production increased in a dose dependent manner, reaching statistical significance compared to the control at high exposure concentrations (Figure 9.3c). However, in the presence of the highly toxic particles Ag and ZnO (NM 110, NM 111 and NM 300) there was a significant increase in the level of CINC-3 protein production that peaked around the LC_{50} values, followed by a decrease in the amounts of the cytokine produced as the toxicity increased (Figure 9.3a, b and c). Additionally we found no change in the levels of IL6 or IFN-γ (a cytokine that has crucial importance in macrophage activation so we regarded it as being important with regards to the role of liver Kupffer cells) secreted from these cells following the 24 hr exposure to any of the selected NMs (data not shown).

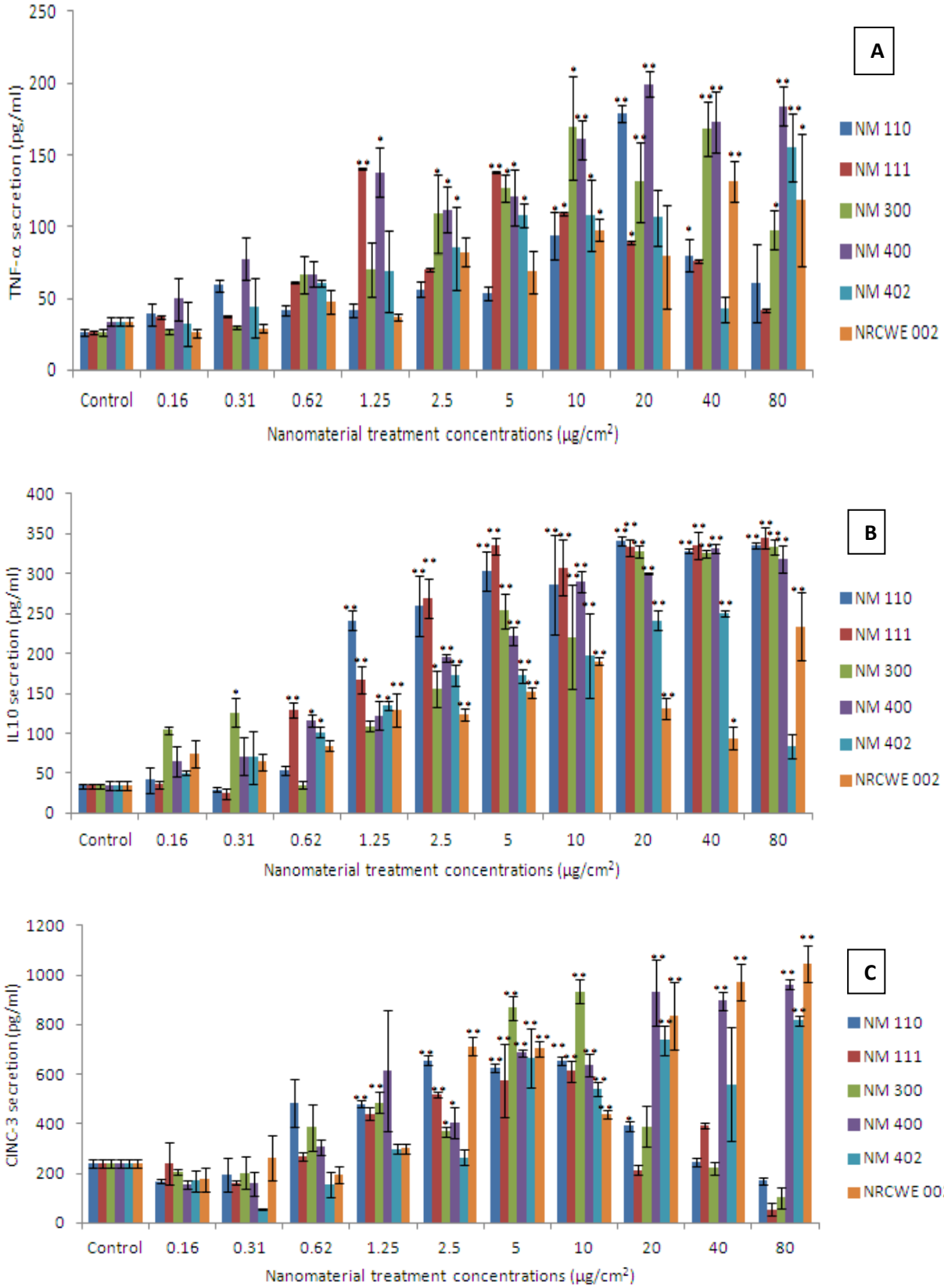

Figure 9.3. Cytokine secretion by primary liver co-culture cells following exposure to the panel of engineered nanomaterials. The cells were exposed to the NMs for 24 hr with cytokine secretion measured utilising the FACS array and ELISA. Values represent mean ± SEM (n=3), significance indicated by * = $p<0.05$ and ** = $p<0.005$, when material treatments are compared to the control. **A)** TNF-α **B)** IL10 **C)** CINC-3.

9.6 Impact of the engineered NMs on cytokine secretion from the liver cells after Kupffer cell enrichment

Liver cells harvested from the Sprague Dawley rats were put through a magnetic bead based cell purification system as described in section 3.24. This typically increased the Kupffer cell content from 3% to 40% of the cell suspension (Section 9.4). The cells were then treated with three concentrations (0.32, 5 and 40 $\mu g/cm^2$) of the highly toxic Ag and the low toxicity positively charged TiO_2. The changes in cytokine production from the Kupffer enriched cells in terms of TNF-α, IFN-γ, IL6, IL10 and CINC-3 were measured and compared to those obtained from cells without the macrophage enrichment (section 9.5).

A dose dependent increase in the levels of TNF-α and IL10 from the Kupffer cell enriched liver cells following exposure of the silver NMs was found. Exposure of the cells to NRCWE 002 (TiO_2) also resulted in significant TNF-α, IL10 and IL6 (Figure 9.4 and 5). There was no change in the levels of IFN- γ produced from the cells relative to the Kupffer cell enrichment (data not shown).

Comparison of the cytokine profiles from cells before and after Kupffer cell enrichment were not as different as expected. There was a significant increase in TNF-α and IL6 levels from Kupffer cell enriched liver cells following exposure to the NMs (Figure 9.6 and 7). IL10 and CINC-3 secretion on the other hand was decreased with some of these alterations significant between the two groups (Figure 9.6 and 7).

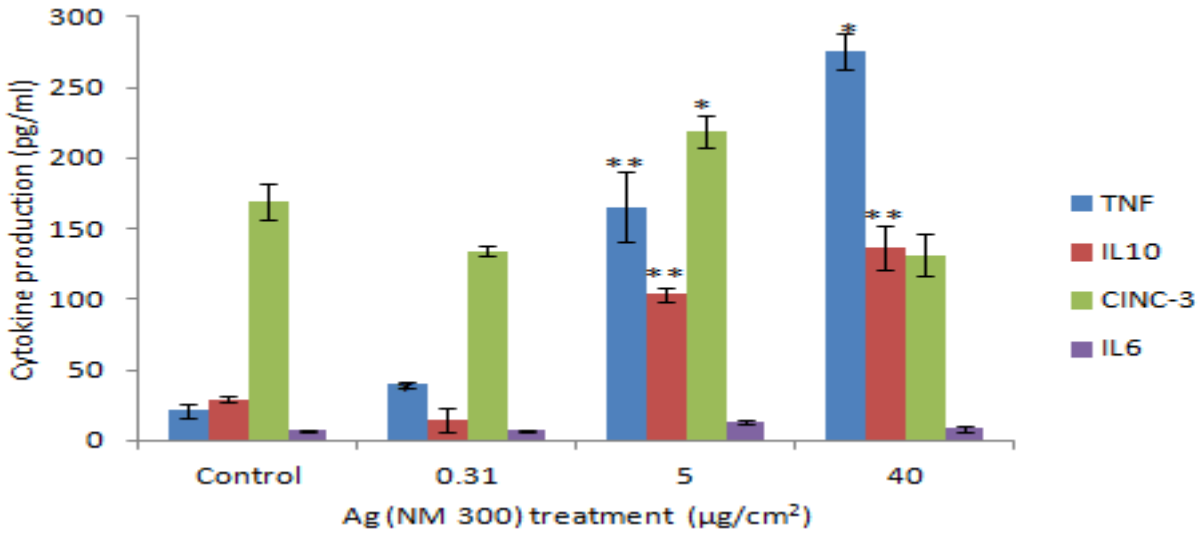

Figure 9.4. Cytokine secretion by rat liver cells (KC enriched) exposed to NM 300. The cells were exposed to the NMs for 24 hr with cytokine secretion measured utilising the FACS array and ELISA. Values represent mean ± SEM (n=3), significance indicated by * = $p<0.05$ and ** = $p<0.005$, when material treatments are compared to the control.

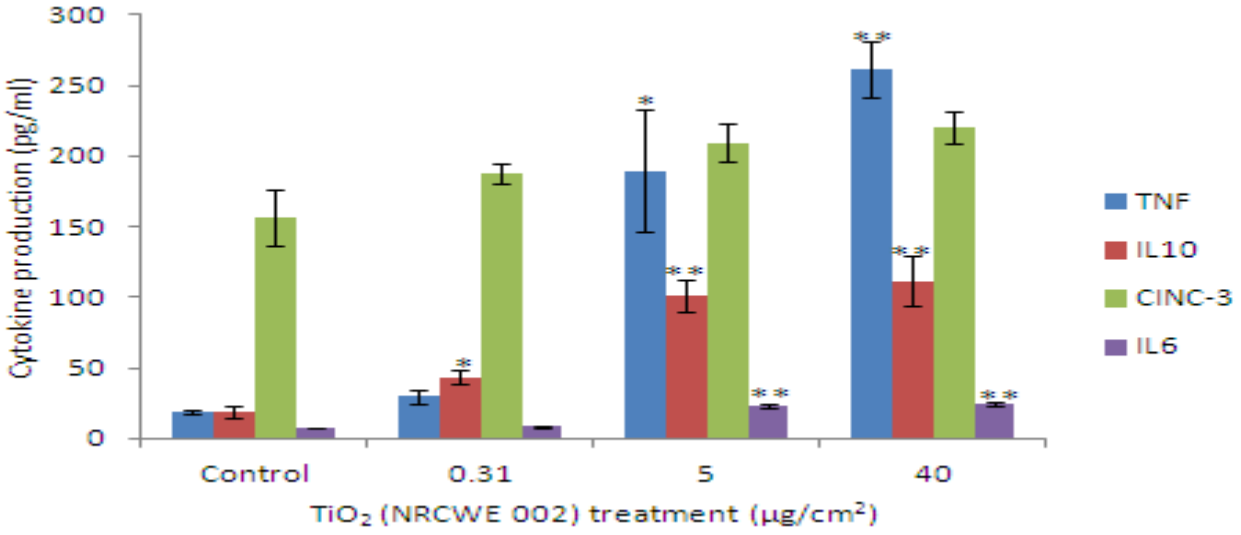

Figure 9.5. Cytokine secretion by rat liver cells (KC enriched) exposed to NRCWE 002. The cells were exposed to the NMs for 24 hr with cytokine secretion measured utilising the FACS array and ELISA. Values represent mean ± SEM (n=3), significance indicated by * = $p<0.05$ and ** = $p<0.005$, when material treatments are compared to the control.

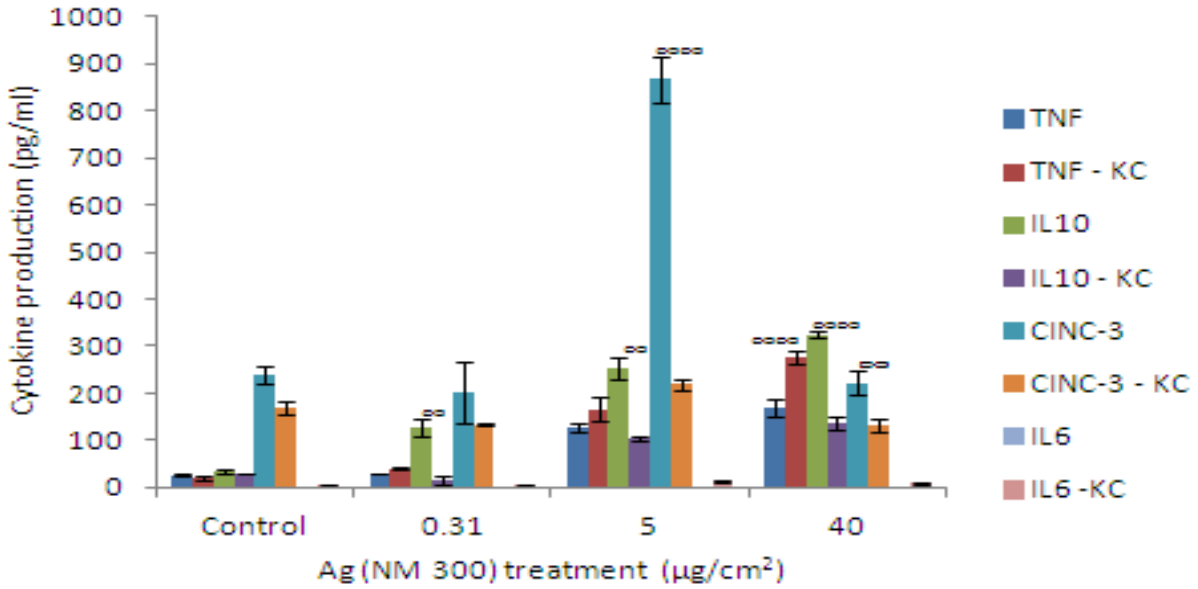

Figure 9.6. Cytokine secretion by rat liver cells before and after Kupffer cell enrichment exposed to NM 300. The cells were exposed to the NMs for 24 hr with cytokine secretion measured utilising the FACS array and ELISA. Values represent mean ± SEM (n=3), ∞ = $p<0.05$ and ∞∞ $p<0.005$ is representative of significant difference between values before and after Kupffer cell (KC) enrichment.

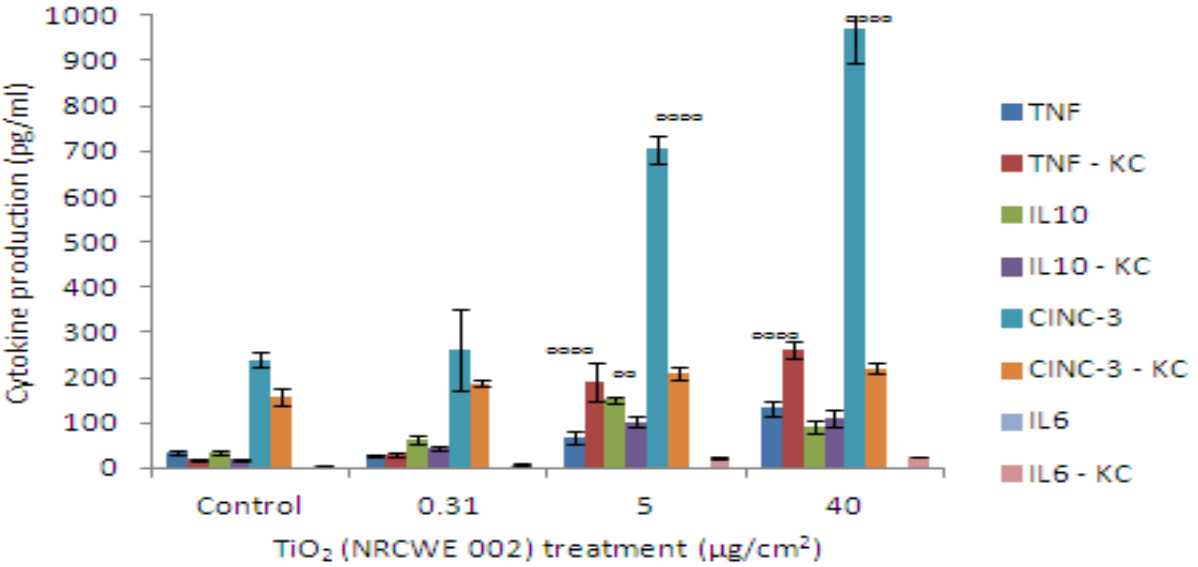

Figure 9.7. Cytokine secretion by rat liver cells before and after Kupffer cell enrichment exposed to NRCWE 002. The cells were exposed to the NMs for 24 hr with cytokine secretion measured utilising the FACS array and ELISA. Values represent mean ± SEM (n=3), ∞ = $p<0.05$ and ∞∞ $p<0.005$ is representative of significant difference between values before and after Kupffer cell (KC) enrichment.

9.7 Impact of the nanomaterials on depletion of total GSH in primary rat liver cells

Analysis of the total glutathione contents of the liver cells (without Kupffer cell enrichment) revealed a dose dependant GSH depletion compared to the control cells at 24 hr following exposure to the highly toxic NMs with these effects most evident as the higher doses (Ag and the two ZnO NMs) (Figure 9.8a, b and c). Also a small but significant decrease following exposure to one of the MWCNT (NM 400) was found (Figure 9.8d). While there was no significant change in intracellular total GSH content following exposure to the other two NMs (NM 402 and NRCWE 002) (Figure 9.8e and f).

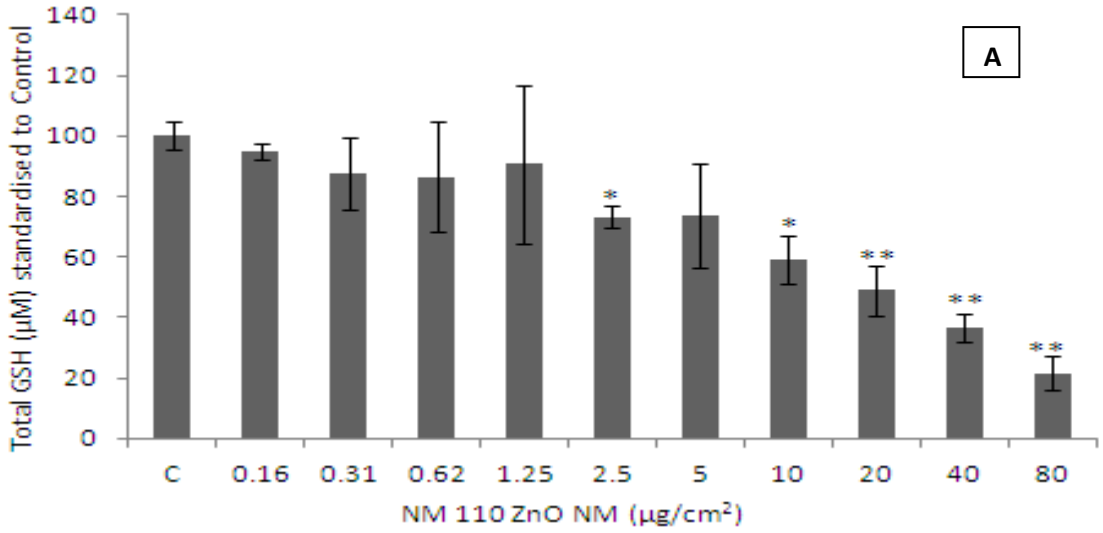
A
Total GSH (µM) standardised to Control
140
120
100
80
60
40
20
0
C
0.16
0.31
0.62
1.25
2.5
5
10
20
40
80
NM 110 ZnO NM (µg/cm²)

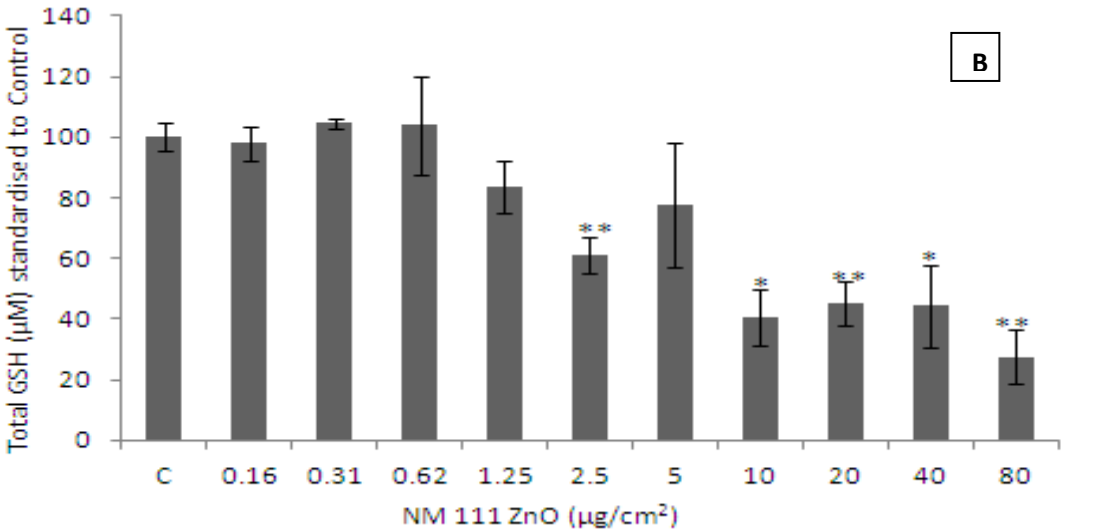
B
Total GSH (µM) standardised to Control
140
120
100
80
60
40
20
0
C
0.16
0.31
0.62
1.25
2.5
5
10
20
40
80
NM 111 ZnO (µg/cm²)

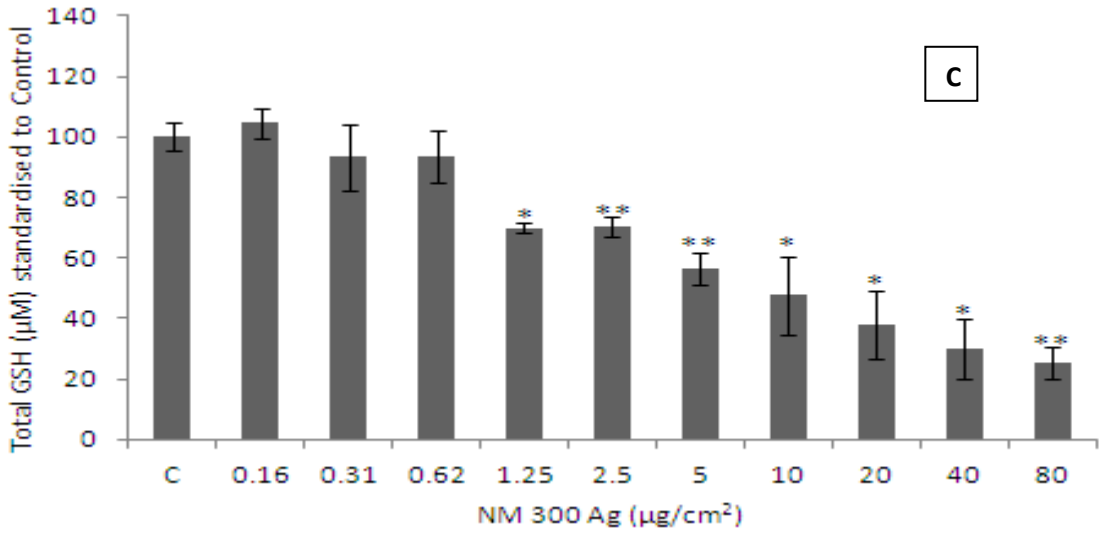
C
Total GSH (µM) standardised to Control
140
120
100
80
60
40
20
0
C
0.16
0.31
0.62
1.25
2.5
5
10
20
40
80
NM 300 Ag (µg/cm²)

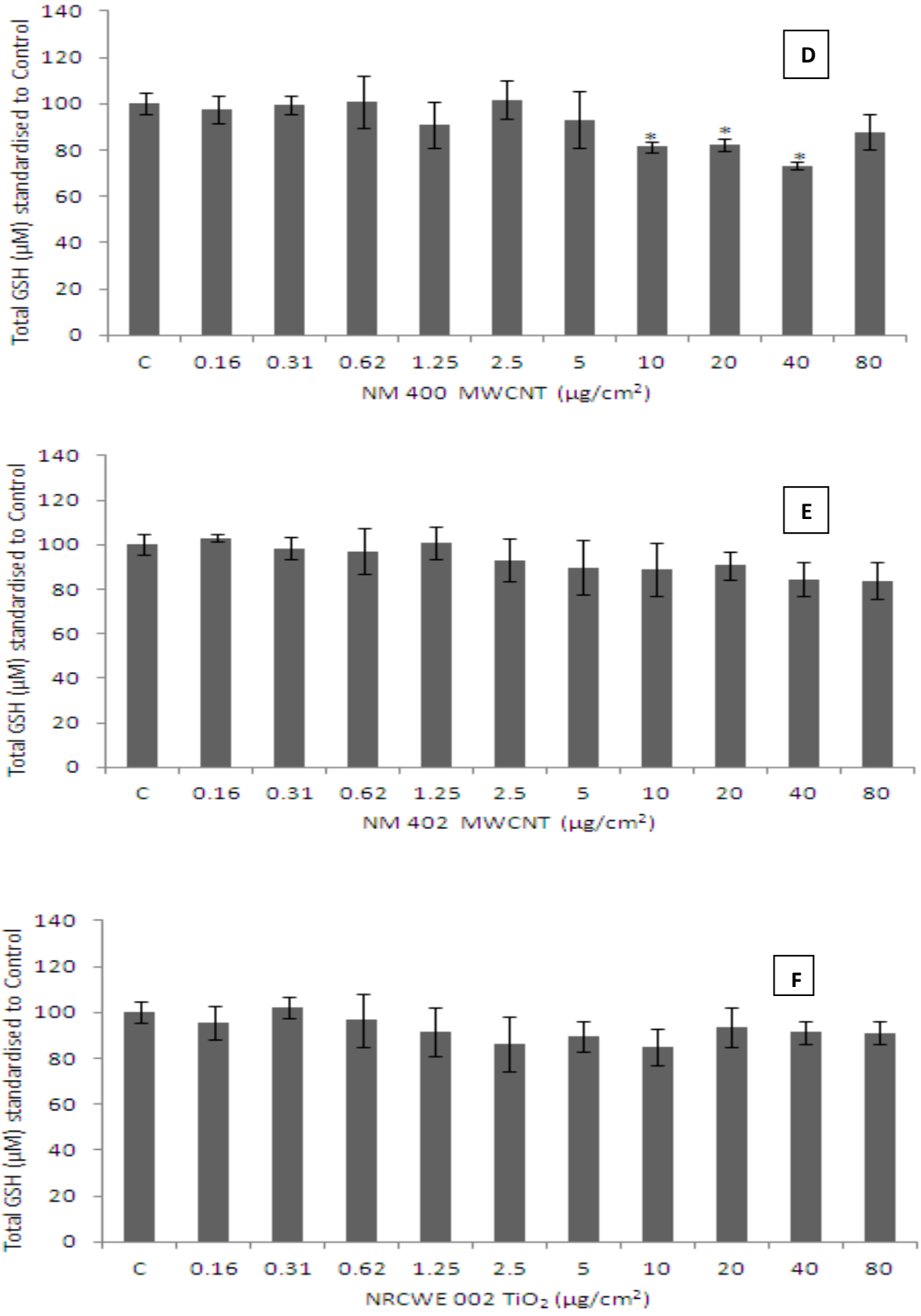

Figure 9.8. Effects of NM exposure on total glutathione levels in primary rat liver co-culture (before Kupffer cell enrichment). The cells were exposed to cell medium (control), and increasing concentrations of selected NMs for 24 hr. Values represent mean ± SEM (n=3), significance indicated by * = $p<0.05$ and ** = $p<0.005$ compared to the control. **A)** NM 110 **B)** NM 111 **C)** NM 300 **D)** NM 400 **E)** NM 402 **F)** NRCWE 002.

9.8 Discussion

As already mentioned NMs entering the blood stream will accumulate within the liver (Chen, *et al*., 1999; Diesen, *et al*., 2009; Sadauskas, *et al*., 2009b). In previous chapters we have looked at how the ENPRA NMs affect liver hepatocytes (Chapter 4, 5 and 6). However, to gain a more accurate representation of how NMs impact on the liver as a whole, incorporation of other cell types in the test system is a necessity. In this chapter the focus was on the liver resident macrophages. Kupffer cells represent the largest portion of resident tissue macrophages in any organ and constitute up to 25% of the total cell populations of a healthy liver (Seki, *et al*., 2011).

Kupffer cells are indispensible in the liver immunity against gut derived antigens and are known to produce a large array of cytokines including IL1, IL6, IL12 and TNF-α but to name a few which can further activate hepatic T cells, in turn activating phagocytosis and cytokine production by Kupffer cells in a positive feedback loop (Bottcher, *et al*., 2011; Seki, *et al*., 2011). However it is believed that Kupffer cells in a non diseased liver are in a constant semi activated state and are crucial in maintaining organ tolerance to food antigens in everyday life (Bottcher, *et al*., 2011). Hence the liver offers a unique scenario in which the resident macrophages can both initiate an immune response or play an active role in retaining an immnuno tolerant state (Bottcher, *et al*., 2011; Nemeth, *et al*., 2009).

Here, the acute exposure of co-culture of primary liver cells to the priority ENPRA NMs resulted in similar cytotoxicity outcome as previously witnessed in the C3A cell line (Chapter 4), primary human hepatocytes (Chapter 6) and HK-2 cell line (Chapter 10). The NMs were segregated into a high toxicity group (the Ag - NM 300) and the two ZnO - NM 110, NM 111 and a low toxicity groups (TiO_2 - NRCWE 002 and MWCNT - NM 400 and NM 402). These findings are not very surprising because the Kupffer cells only formed 3% of the overall population with the hepatocytes still constructing the majority of the cells.

We investigated the cytokine secretion from the primary liver co-culture before and after Kupffer cell enrichment following a 24 hr exposure to the panel of NMs in terms of TNF-α, CINC-3, IL10, IL6 and IFN-γ release from the cells. Interestingly exposure of the co-culture with the 3% Kupffer cell population to the ENPRA NMs resulted in a completely different cytokine profile as previously perceived following hepatocyte only exposures (Chapters 4, 5

and 6). Incorporation of macrophages into the *in vitro* system resulted in a dose dependant release of significant amounts of TNF-α and IL10. There was also substantial secretion of the chemokine CINC-3 (rat equivalent of human IL8) with the same pattern of release as detected for the human hepatocytes models (increase up to the LC_{50} with a gradual drop at the higher most cytotoxic concentration for the highly toxic NMs, while a dose dependant increase was observed for the low toxicity NMs). A very important observation from all co-culture data was the high levels of IL10 being released from the cells. It is possible that IL10 acts as antagonistic against the pro-inflammatory cytokines.

Furthermore no change in the levels of IL6 or IFN-γ compared to the control following exposure of the liver co-culture to any of the investigated nanomaterials was found. The hypothesis is that the Kupffer cell (or potentially any other cytokine producing cells) numbers were not high enough for the secretion of these cytokines.

Next it was shown that the use of a MACS magnetic column is an effective method of enriching liver Kupffer cells. A typical increase in macrophage numbers from 3% to around 40% was observed. To our knowledge this the first time the column is utilised for liver cell enrichment, however the column is frequently used for positive selection of numerous immune cells (Grutzkau, *et al*., 2010). Interestingly the positively selected cells were healthy and viable once they had passed through the column, hence we suggest that the MACS column can be beneficial in Kupffer selection and isolation. However a disadvantage of this system is that the number of the positively selected cells is not very high.

The cytokine analysis of the enriched co-culture population of cells showed significantly higher secretion of TNF-α from the cells, while IL10 and CINC-3 levels had appreciably dropped. We also observed small amounts of IL6 produced from the cells while no IFN-γ was detectable following exposure to any of the NMs in this study. Before any conclusion can be drawn from this data it is important that the limitation of the study is acknowledged. As the liver is composed of more than two cell types it is impossible to pin point which cells are synthesising the cytokines. Although great effort was taken into characterising each cell population it is impossible to completely eliminate all the undesired cell types from the population hence the conclusions made here are based on the theory that the co-culture is principally composed of two cell types (namely hepatocytes and Kupffer cells).

This data suggests that Kupffer cells secrete IL6 and TNF-α following exposure of these NMs. Although other cells in the liver (i.e. endothelial cells (Crisp., 2009)) are capable of cytokine production. Additionally it appears that the principle source of IL10 and CINC-3 is paranchymal cells although it has been shown that Kupffer cells are also capable of producing small levels of IL10 under certain conditions (Tiegs, *et al*., 2009). Once again there was no IFN-γ secreted from the Kupffer cell enriched population. It has been shown that NKT cells and lymphocytes are the main source of IFN-γ production within the liver (Shono, *et al*., 2011) indicating that either these cells were not present in large enough numbers for the cytokine to be detected or exposure to these NMs does not result in IFN-γ secretion from the cells.

In future experiments will include the complete depletion of liver Kupffer cells will be attempted and whole tissue ELISAs inducted to resolve the unanswered queries in this study.

Finally, the ability of the chosen NMs to induce glutathione depletion in the co-culture of the primary liver cells was tested. Exposure to the Ag, two ZnO NMs and one of the MWCNTs (NM 400) resulted in significant GSH depletion following a 24 hr exposure. Similar to the depletion observed in the hepatocyte cell line the GSH reduction following exposure to the highly toxic NMs could be attributed to cell death rather than a specific oxidative stress response. In contrast, MWCNTs were also able to significantly deplete glutathione at doses which were not considered as highly cytotoxic, suggesting that MWCNTs induced oxidative stress in these cells. The TiO_2 NMs had no significant effect on the glutathione content of the liver co-culture. Similarly to the toxicity data the GSH depletion observations in the co-culture model was comparable to the antioxidant levels with the hepatocytes models described previously (Chapter 5) suggesting incorporation of 3% resident macrophages does not play a major role in this *in vitro* oxidative stress model following exposure of the ENPRA NMs.

9.9 Conclusions

It appears that Kupffer cells are crucial in the overall liver response to NMs that reach the organ. Data from the last two chapters allows to hypothesis that neutrophils are the organs first line of defence against NMs, however the resident macrophages take over the immune response after this initial short lived influx. These macrophages secrete a variety of cytokines

which orchestrate the nature of the response. The high levels of IL10 in the *in vitro* system (primary liver co-culture) and IL10 mRNA in the *in vivo* systems (liver tissue following IT and IV exposure of NMs) would suggest that tolerance is favoured over immunity however this can be easily distorted in disease models (animals or humans) or long tem repeated exposure to NMs (even at very small doses).

Chapter Ten

In vitro assessment of panel of engineered NMs following exposure of a human renal cell line in terms of cytotoxicity, pro-inflammatory response, oxidative stress and genotoxicity

Based on publication: Kermanizadeh A, Vranic S, Boland S, Moreau K, Squiban AB, Gaiser BK, Andrzejczuk LA, Stone V. (2013b). An *in vitro* assessment of panel of engineered nanomaterials using a human renal cell line: Cytotoxicity, pro-inflammatory response, oxidative stress and genotoxicity - Submitted to BMC Nephrology.

10.1 Aims and chapter outline

To investigate the effcts on the human renal proximal tubule epithelial cells (HK-2) treated with the panel of engineered nanomaterials in terms of cytotoxicity (WST-1), pro-inflammatory cytokine secretion (IL6, IL8, TNF-α and MCP-1), intracellular reactive oxygen species (HE oxidation assay) and genotoxicity (FPG modified comet assay).

10.2 Characteristics of nanomaterials and exposure media

Investigated nanomaterials were characterised by a combination of analytical techniques in order to infer primary physical and chemical properties useful to understand their toxicological behaviour. A list of the measured physical and chemical properties is described (Table 10.1). In order to investigate if the nanomaterials behaved differently in K-SFM or complete RPMI, the hydrodynamic size distributions of the NMs dispersed in the two media was measured between a 1 - 128 µg/ml concentration range by dynamic light scattering (DLS) (Table 10.1). It is widely accepted that DLS is not a suitable method of ascertaining the size of carbon nanotubes (due to the fact that the machine measures size based on the principle that particles are spherical and well dispersed), hence we examined how the two MWCNTs behave in our two chosen media utilising light microscopy. We found that the MWCNTs agglomerated into larger clusters in the complete RPMI which contained higher levels of FCS in comparison to the K-SFM (data not shown).

ENM code	ENM type	Phase	Known coating	Size in K-SFM (DLS) Ψ	Size in complete RPMI (DLS) Ψ
NM 101	TiO_2	Anatase	none	221	358
NM 110	ZnO	Zincite	none	393	453.6
NM 111	ZnO	Zincite	Trieothoxy-capryl-silane 130	332	362.4
NM 300	Ag	-	Polyoxylaurat-Tween 20	87	51.59
NM 400	MWCNT	-	none	*	*
NM 402	MWCNT	-	none	*	*
NRCWE 001	TiO_2	Rutile	none	349	337.5
NRCWE 002	TiO_2	Rutile	Positive charge	314	378.8
NRCWE 003	TiO_2	Rutile	Negative charge	384	423.6
NRCWE 004	TiO_2	Rutile	none	396	482.6

* Not detectable by DLS due to the very large aspect ratio
Ψ Intensity based size average in biological media after 15 mins.

Table 10.1. Physical and chemical properties of tested ENMs in K-SFM and complete RPMI.

10.3 Impact of the selected panel of NMs on HK-2 cell viability

Our toxicity data show a dose dependent decrease in cell viability at 24 hr across the entire nanomaterial panel (Table 10.2). The Ag and the two ZnO NMs were shown to be highly toxic (NM 110 LC_{50} 2.5 µg/cm^2 – K-SFM, LC_{50} 0.64 µg/cm^2 – complete RPMI; NM 111 LC_{50} 2.5 µg/cm^2 – K-SFM, LC_{50} 1.25 µg/cm^2 – complete RPMI; NM 300 10 µg/cm^2 – K-SFM, LC_{50} 5 µg/cm^2 – complete RPMI) after a 24 hr exposure. All of the TiO_2 and MWCNT NMs were considered to be low toxicity materials as the LC_{50} was not reached after a 24 hr exposure to the HK-2 cells at the range investigated. We observed slightly higher toxicity (not significant) to the cells in complete RPMI exposed to the Ag and ZnO NMs. The toxicity of the ENPRA dispersants namely NM 300 dispersant termed (NM 300 DIS) and 0.5% ethanol in complete medium was also investigated. No cytotoxicity of either dispersant to the HK-2 cells (data not shown) so we conclude that all observed toxicity is due to exposure to the NMs investigated was found. LC_{20} are shown as these values were utilised for the FPG modified comet assay (Table 10.2).

NM	K-SFM		Complete RPMI	
	LC_{20}	LC_{50}	LC_{20}	LC_{50}
NM 101	Not reached up to 80 μg/cm^2	Not reached up to 80 μg/cm^2	80 μg/cm^2	Not reached up to 80 μg/cm^2
NM 110	0.64 μg/cm^2	2.5 μg/cm^2	0.64 μg/cm^2	Between 0.32 – 0.64 μg/cm^2
NM 111	Between 0.64 – 1.25 μg/cm^2	2.5 μg/cm^2	Between 0.32 – 0.64 μg/cm^2	Between 0.64 – 1.25 μg/cm^2
NM 300	1.25 μg/cm^2	10 μg/cm^2	1.25 μg/cm^2	Between 2.5 – 5 μg/cm^2
NM 400	2.5 μg/cm^2	Not reached up to 80 μg/cm^2	20 μg/cm^2	Not reached up to 80 μg/cm^2
NM 402	Between 2.5 – 5 μg/cm^2	Not reached up to 80 μg/cm^2	20 μg/cm^2	Not reached up to 80 μg/cm^2
NRCWE 001	40 μg/cm^2	Not reached up to 80 μg/cm^2	Between 40 – 80 μg/cm^2	Not reached up to 80 μg/cm^2
NRCWE 002	20 μg/cm^2	Not reached up to 80 μg/cm^2	Not reached up to 80 μg/cm^2	Not reached up to 80 μg/cm^2
NRCWE 003	Between 40 – 80 μg/cm^2	Not reached up to 80 μg/cm^2	Not reached up to 80 μg/cm^2	Not reached up to 80 μg/cm^2
NRCWE 004	40 μg/cm^2	Not reached up to 80 μg/cm^2	Not reached up to 80 μg/cm^2	Not reached up to 80 μg/cm^2

Table 10.2. Cytotoxicity following exposure of the HK-2 cells in two different media to a panel of engineered nanomaterials. The cells were exposed to the NM for 24 hr with cytotoxicity measured via WST-1 assay.

10.4 Cytokine secretion by HK-2 cells following exposure to the panel of NMs

Changes in cytokine production as a consequence of NM exposure were assessed within the supernatant of exposed renal cells and quantified via FACS Array. We found a dose dependent (exposure to sub-lethal concentrations of the NMs) increase in the levels of IL8 and IL6 from the kidney cells with statistical significance being reached at the higher concentrations following exposure to nine of the ten nanomaterials (TiO_2 - NM 101 being the exception) (Figure 10.1a). Additionally we found no change in the levels of MCP-1 or TNF-α secreted from the HK-2 cells following the 24 hr exposure to any of the selected NMs (data not shown).

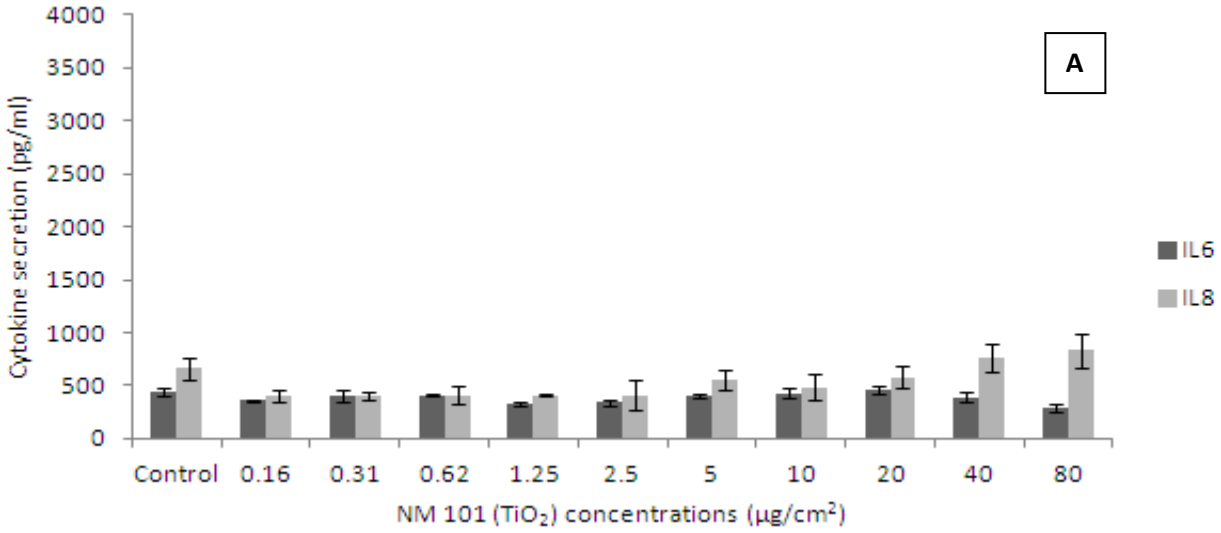
A
Cytokine secretion (pg/ml)
4000
3500
3000
2500
2000
1500
1000
500
0
Control
0.16
0.31
0.62
1.25
2.5
5
10
20
40
80
NM 101 (TiO_2) concentrations (µg/cm²)
IL6
IL8

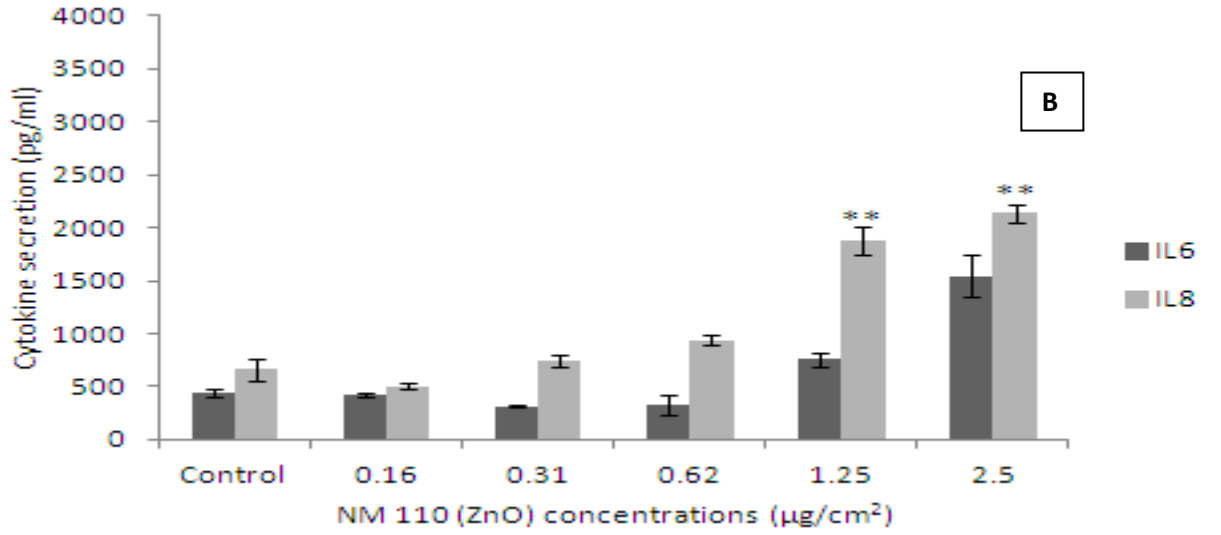
B
Cytokine secretion (pg/ml)
4000
3500
3000
2500
2000
1500
1000
500
0
**
**
Control
0.16
0.31
0.62
1.25
2.5
NM 110 (ZnO) concentrations (µg/cm²)
IL6
IL8

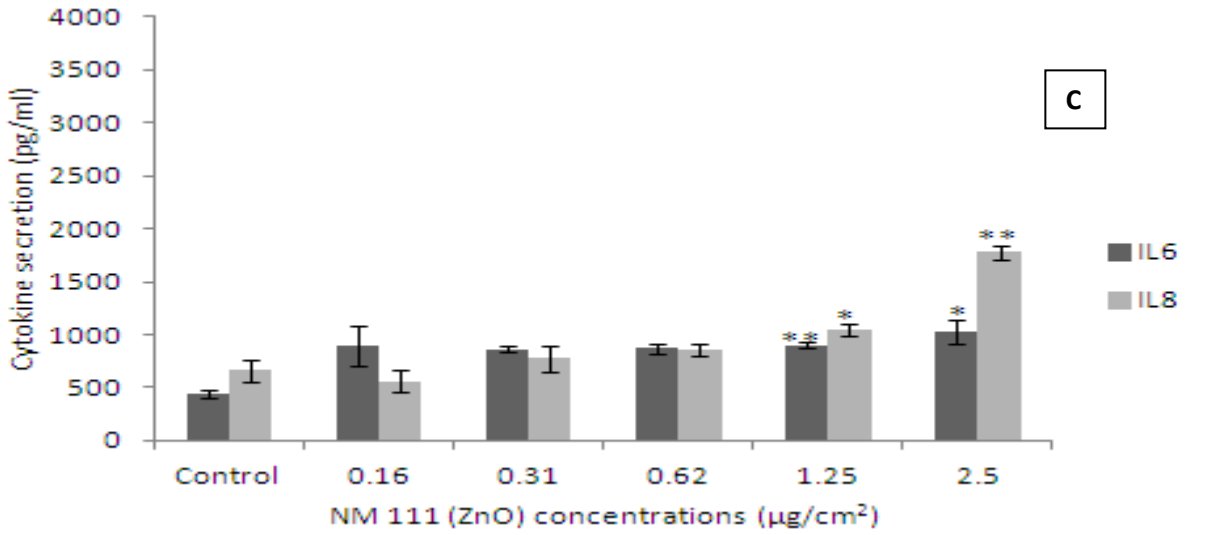
C
Cytokine secretion (pg/ml)
4000
3500
3000
2500
2000
1500
1000
500
0
**
*
*
**
Control
0.16
0.31
0.62
1.25
2.5
NM 111 (ZnO) concentrations (µg/cm²)
IL6
IL8

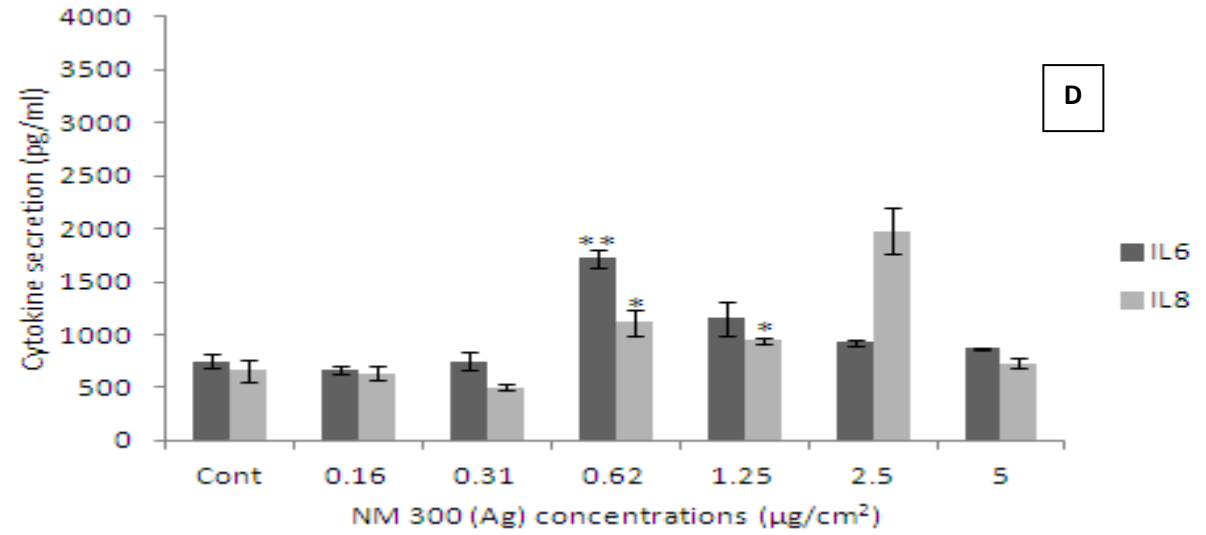
D
Cytokine secretion (pg/ml)
4000
3500
3000
2500
2000
1500
1000
500
0
Cont
0.16
0.31
0.62
1.25
2.5
5
NM 300 (Ag) concentrations (µg/cm²)
IL6
IL8

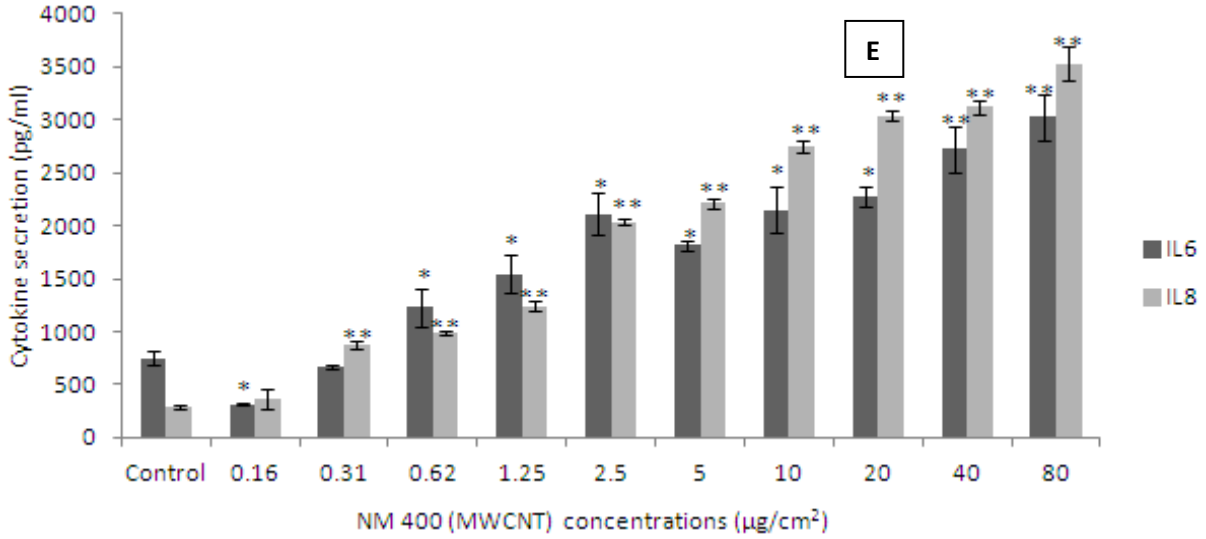
E
Cytokine secretion (pg/ml)
4000
3500
3000
2500
2000
1500
1000
500
0
Control
0.16
0.31
0.62
1.25
2.5
5
10
20
40
80
NM 400 (MWCNT) concentrations (µg/cm²)
IL6
IL8

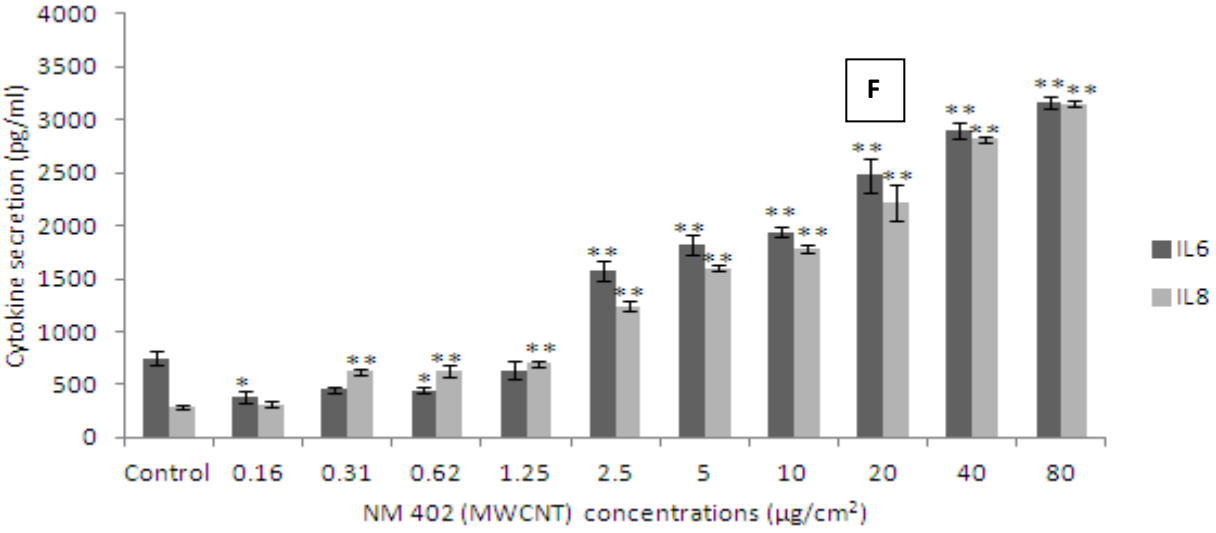
F
Cytokine secretion (pg/ml)
4000
3500
3000
2500
2000
1500
1000
500
0
Control
0.16
0.31
0.62
1.25
2.5
5
10
20
40
80
NM 402 (MWCNT) concentrations (µg/cm²)
IL6
IL8

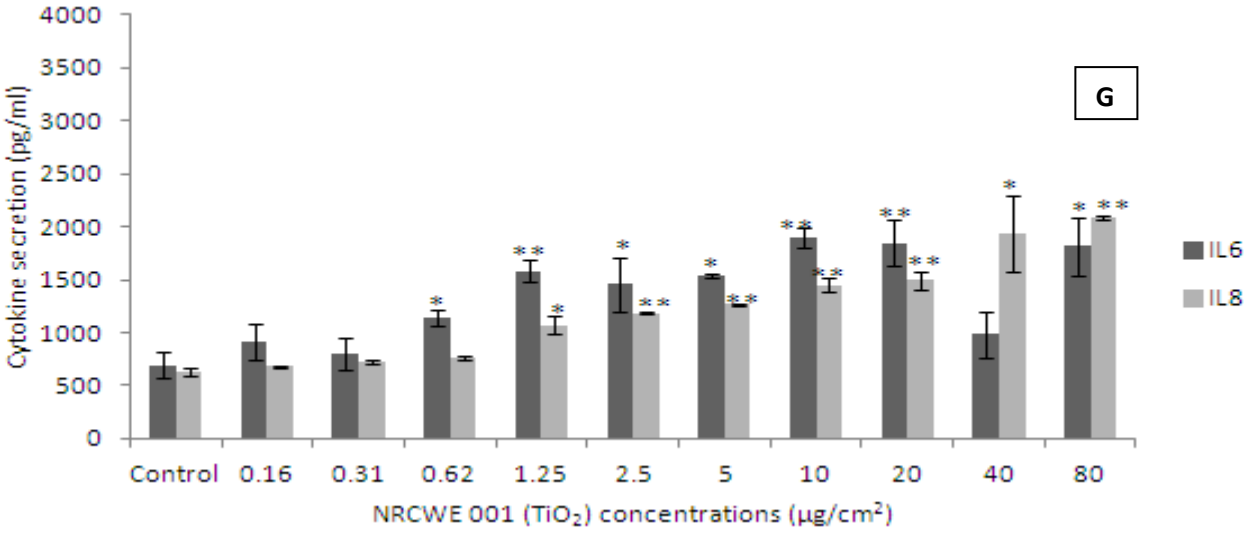
G
Cytokine secretion (pg/ml)
4000
3500
3000
2500
2000
1500
1000
500
0
IL6
IL8
Control
0.16
0.31
0.62
1.25
2.5
5
10
20
40
80
NRCWE 001 (TiO2) concentrations (µg/cm2)

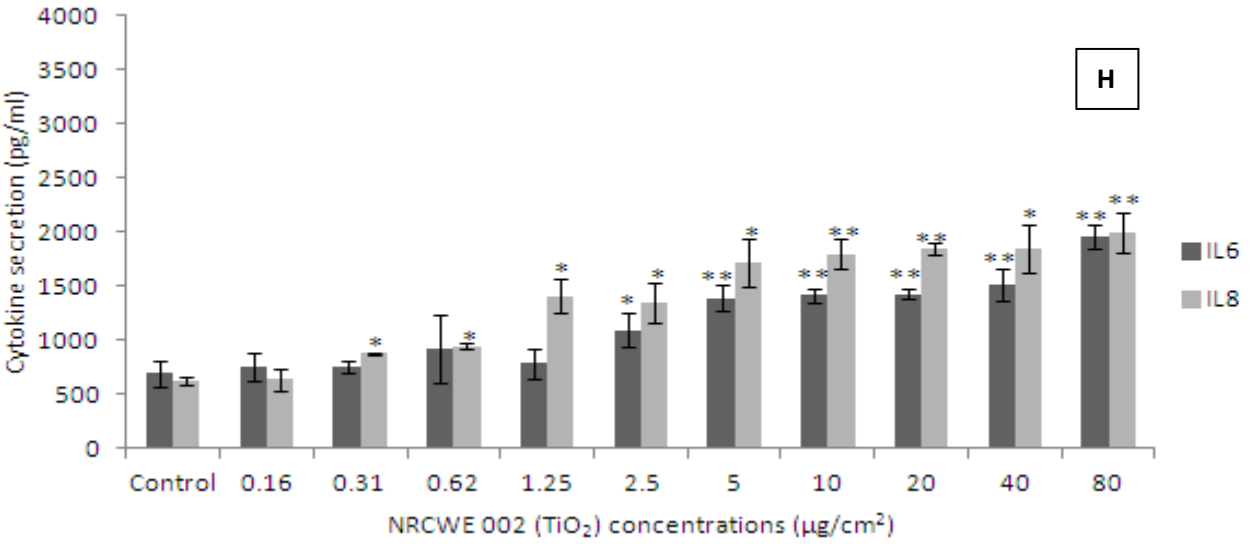
H
Cytokine secretion (pg/ml)
4000
3500
3000
2500
2000
1500
1000
500
0
IL6
IL8
Control
0.16
0.31
0.62
1.25
2.5
5
10
20
40
80
NRCWE 002 (TiO2) concentrations (µg/cm2)

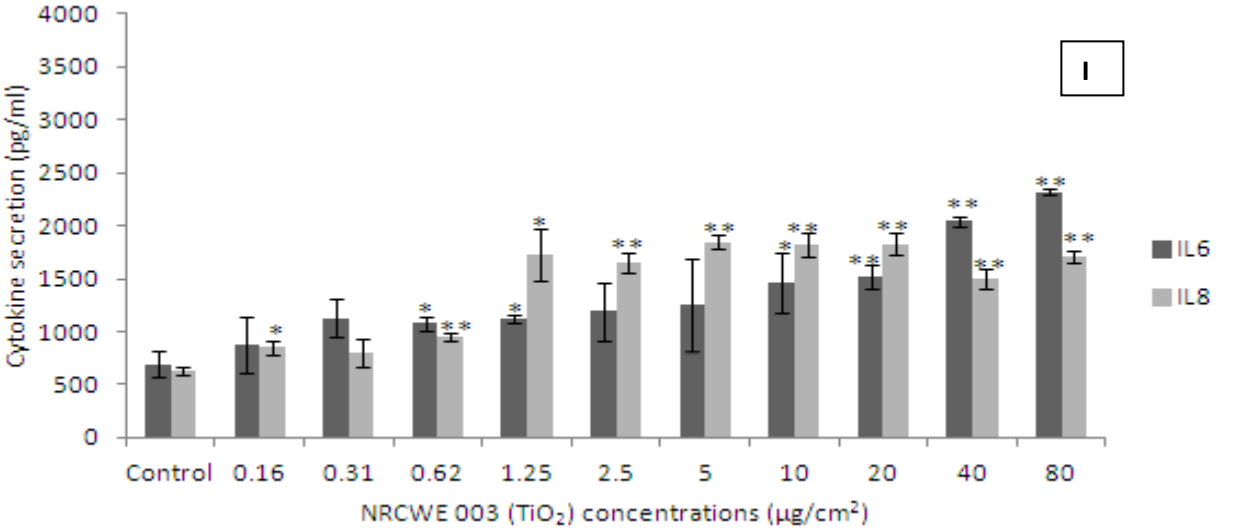
I
Cytokine secretion (pg/ml)
4000
3500
3000
2500
2000
1500
1000
500
0
IL6
IL8
Control
0.16
0.31
0.62
1.25
2.5
5
10
20
40
80
NRCWE 003 (TiO2) concentrations (µg/cm2)

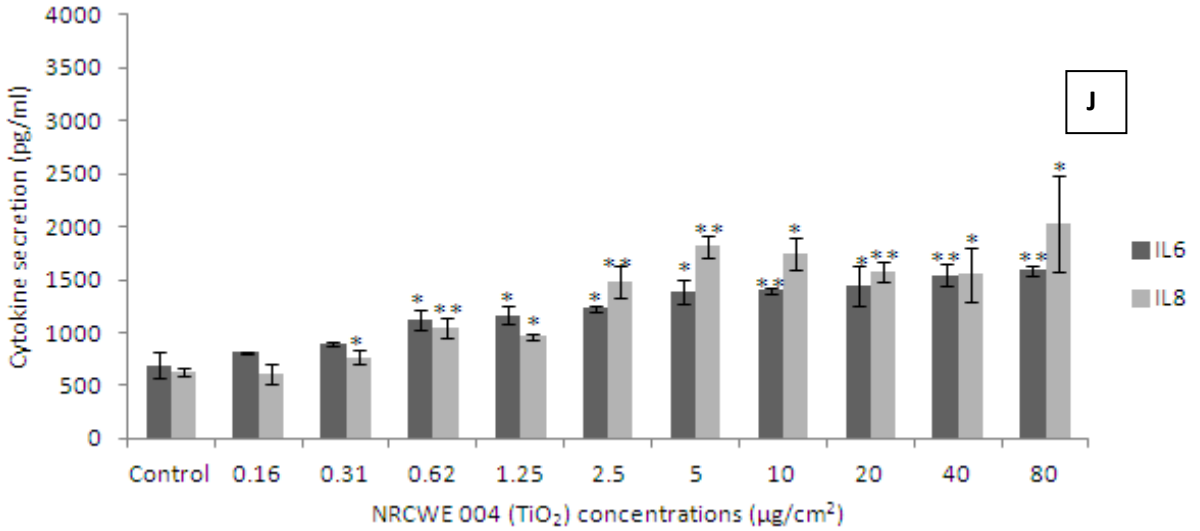

Figure 10.1. IL6 (black bars) and IL8 (grey bars) production by HK-2 cells following exposure to the panel of engineered nanomaterials. The cells were exposed to the sub-lethal concentrations of the NMs for 24 hr with cytokine secretion measured utilising the FACS array. Values represent mean ± SEM (n=3), significance indicated by * = $p<0.05$ and **= $p<0.005$, when material treatments are compared to the control. **A)** NM 101 **B)** NM 110 **C)** NM 111 **D)** NM 300 **E)** NM 400 **F)** NM 402 **G)** NRCWE 001 **H)** NRCWE 002 **I)** NRCWE 003 **J)** NRCWE 004.

10.5 HE Oxidation

This work was carried out by partners in Paris. Briefly, a significant increase in HE positive cells following exposure to ZnO and Ag NMs. A very small yet significant increase was also observed to all the TiO_2 NM with the exception of NRCWE 003. However no change in intracellular reactive oxygen species was noted following exposure to either of the MWCNTs (data not shown).

10.6 DNA damage in the HK-2 cells

In order to investigate the possible DNA damage caused by the panel of nanomaterials, HK-2 cells were exposed to the NMs for 4 hr. In this study we chose the LC_{20} value for each individual NM plus one concentration above (2x LC_{20}) and one below (0.5x LC_{20}). We observed that DNA damage was most evident following exposure to NM 300 (Ag) and NRCWE 002 (TiO_2 - 10 nm positively charged) (Figure 10.2c, h). We also noted a small but significant increase in the percentage of tail DNA following exposure to five of the other eight NMs investigated (ZnO - NM 111, NRCWE 001 and 003 TiO_2 NMs being the exception) (Figure 10.2).

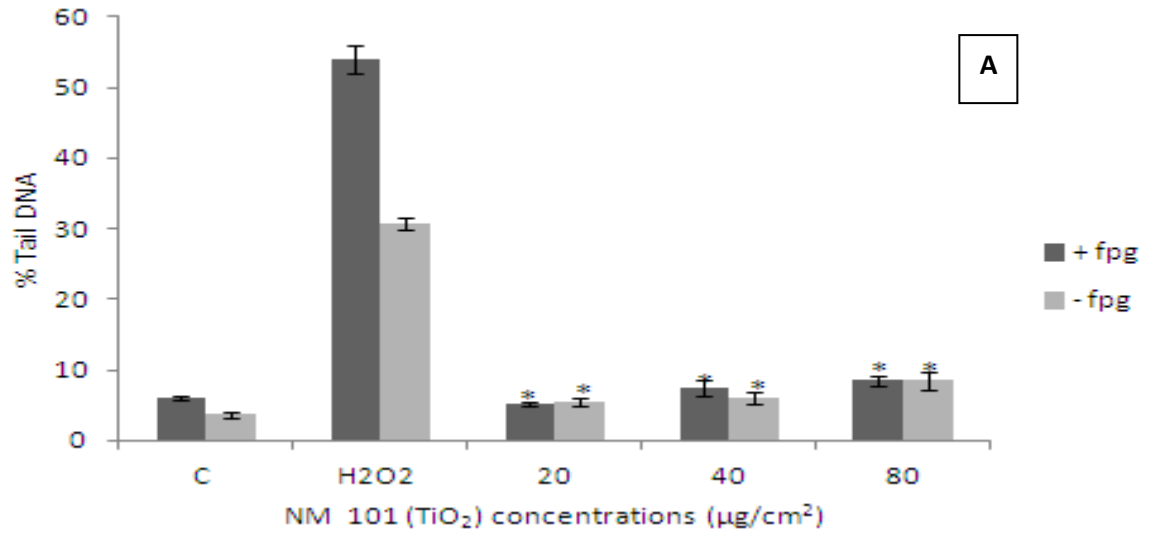
A
% Tail DNA
60
50
40
30
20
10
0
C
H2O2
20
40
80
NM 101 (TiO_2) concentrations (µg/cm²)
+ fpg
- fpg

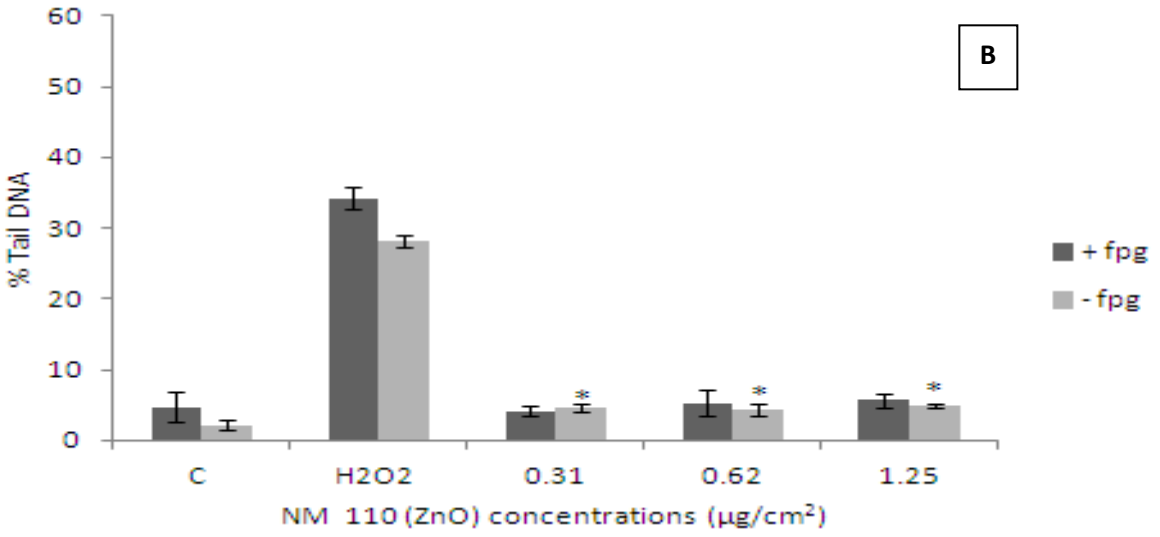
B
% Tail DNA
60
50
40
30
20
10
0
C
H2O2
0.31
0.62
1.25
NM 110 (ZnO) concentrations (µg/cm²)
+ fpg
- fpg

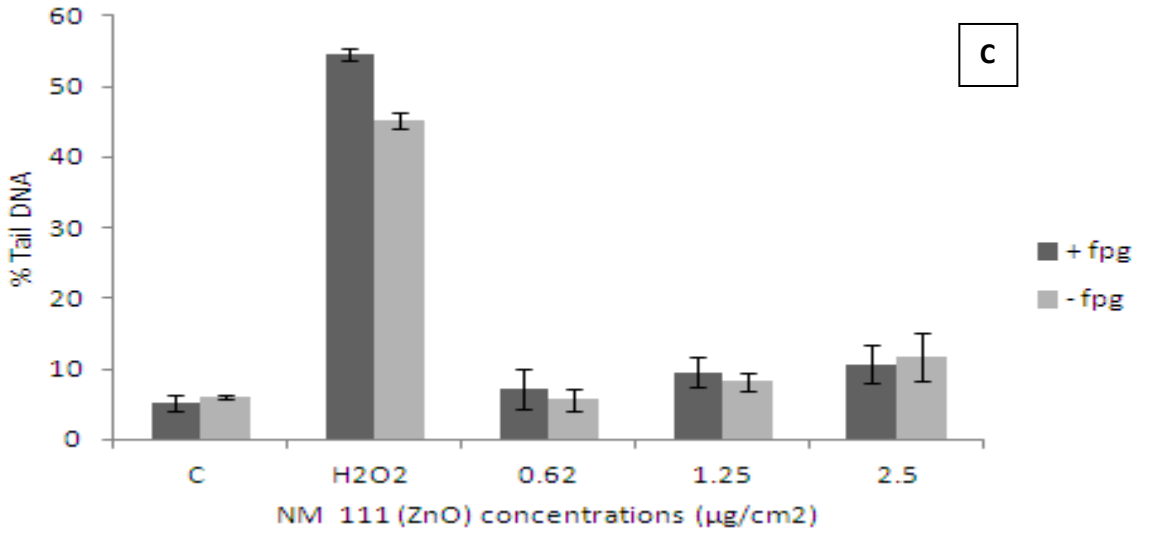
C
% Tail DNA
60
50
40
30
20
10
0
C
H2O2
0.62
1.25
2.5
NM 111 (ZnO) concentrations (µg/cm2)
+ fpg
- fpg

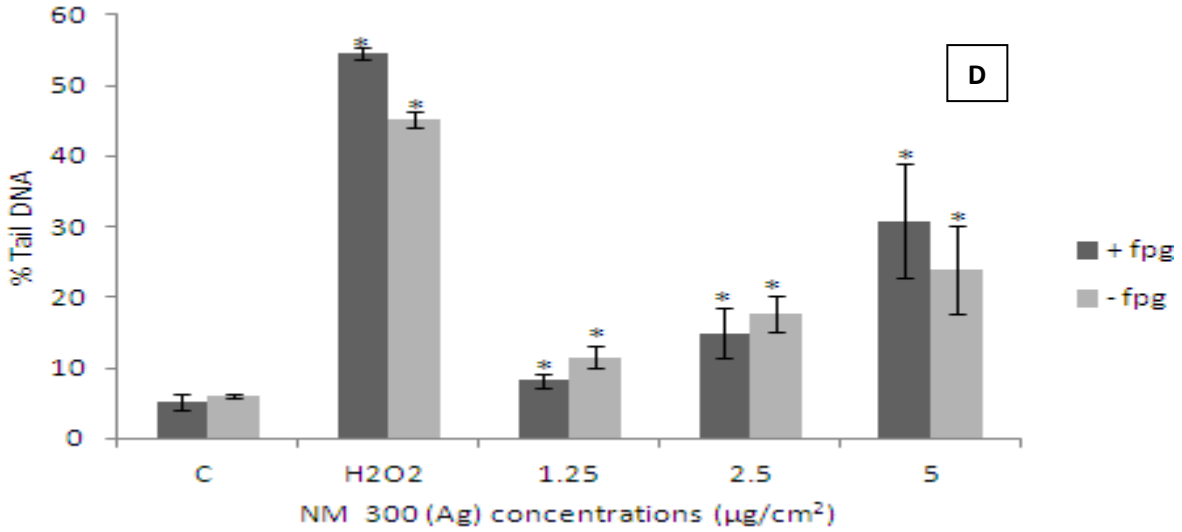
D
% Tail DNA
60
50
40
30
20
10
0
C
H2O2
1.25
2.5
5
NM 300 (Ag) concentrations (µg/cm²)
+ fpg
- fpg

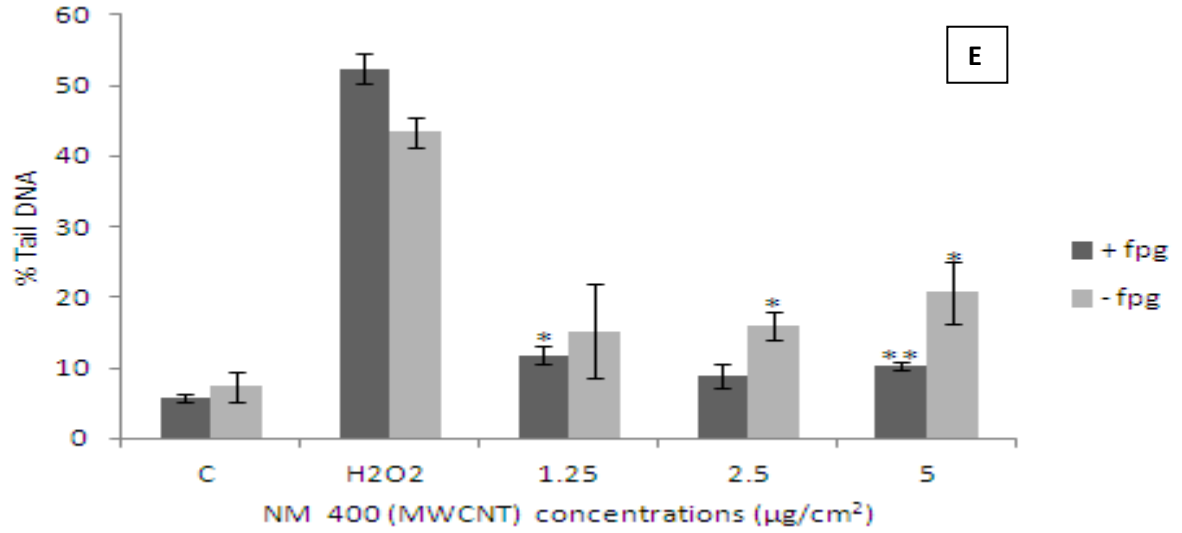
E
% Tail DNA
60
50
40
30
20
10
0
C
H2O2
1.25
2.5
5
NM 400 (MWCNT) concentrations (µg/cm²)
+ fpg
- fpg

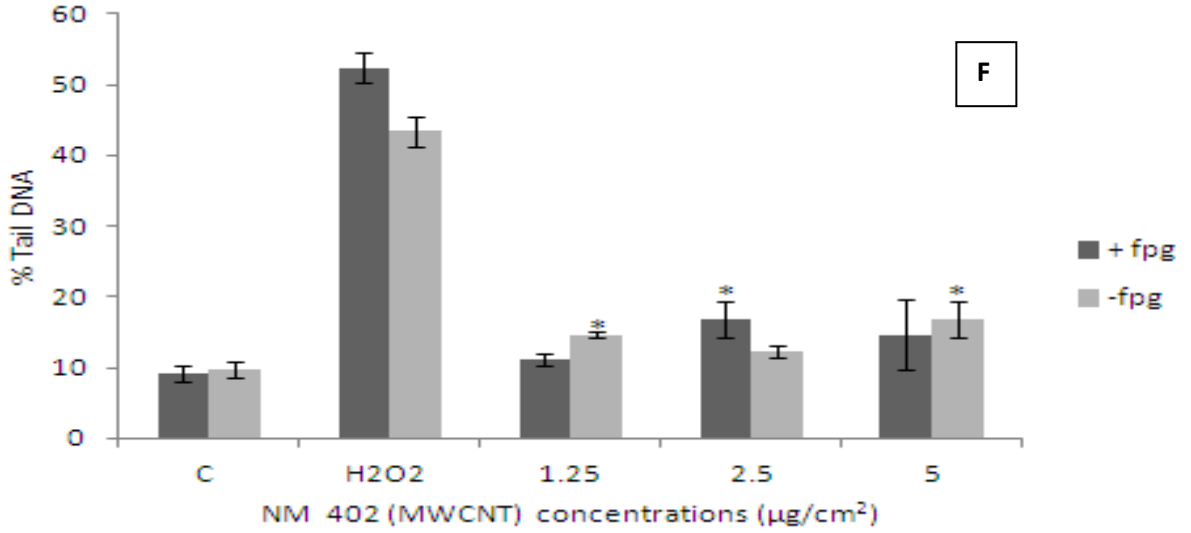
F
% Tail DNA
60
50
40
30
20
10
0
C
H2O2
1.25
2.5
5
NM 402 (MWCNT) concentrations (µg/cm²)
+ fpg
-fpg

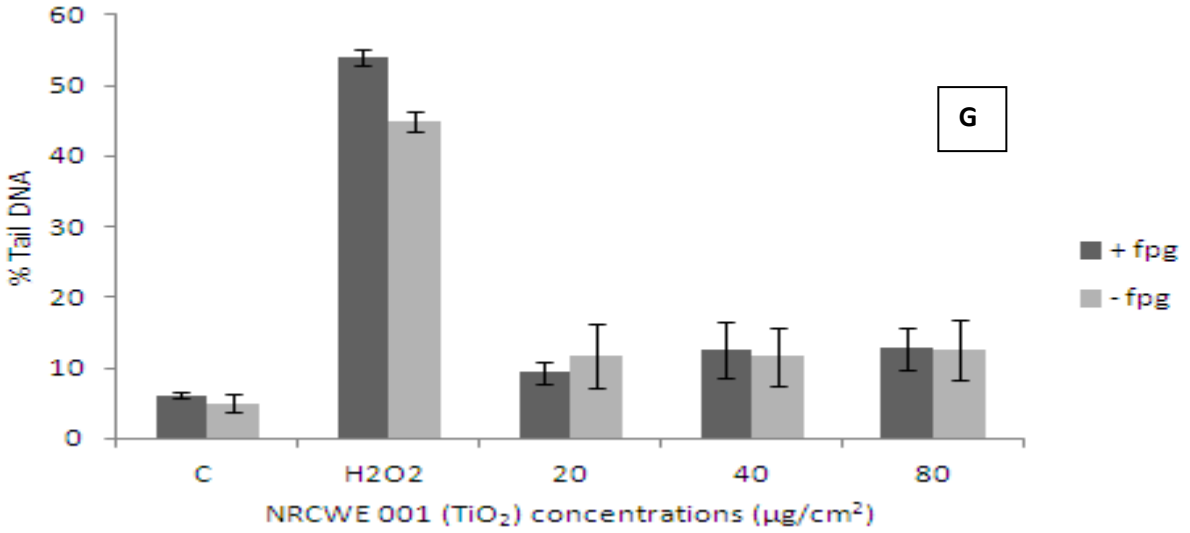
G
% Tail DNA
60
50
40
30
20
10
0
C
H2O2
20
40
80
NRCWE 001 (TiO2) concentrations (µg/cm2)
+ fpg
- fpg

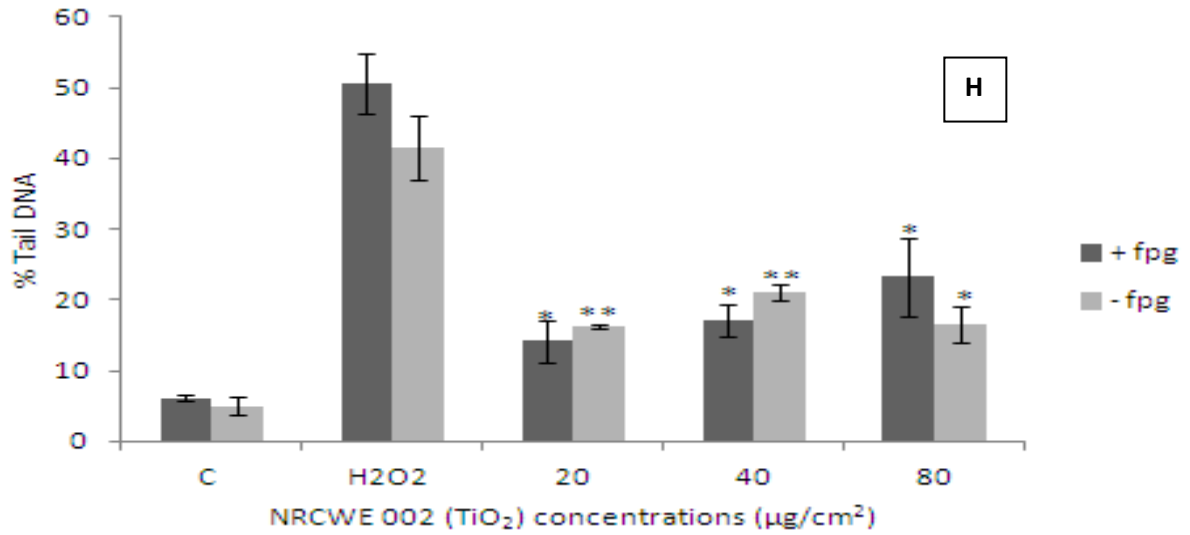
H
% Tail DNA
60
50
40
30
20
10
0
C
H2O2
20
40
80
NRCWE 002 (TiO2) concentrations (µg/cm2)
+ fpg
- fpg

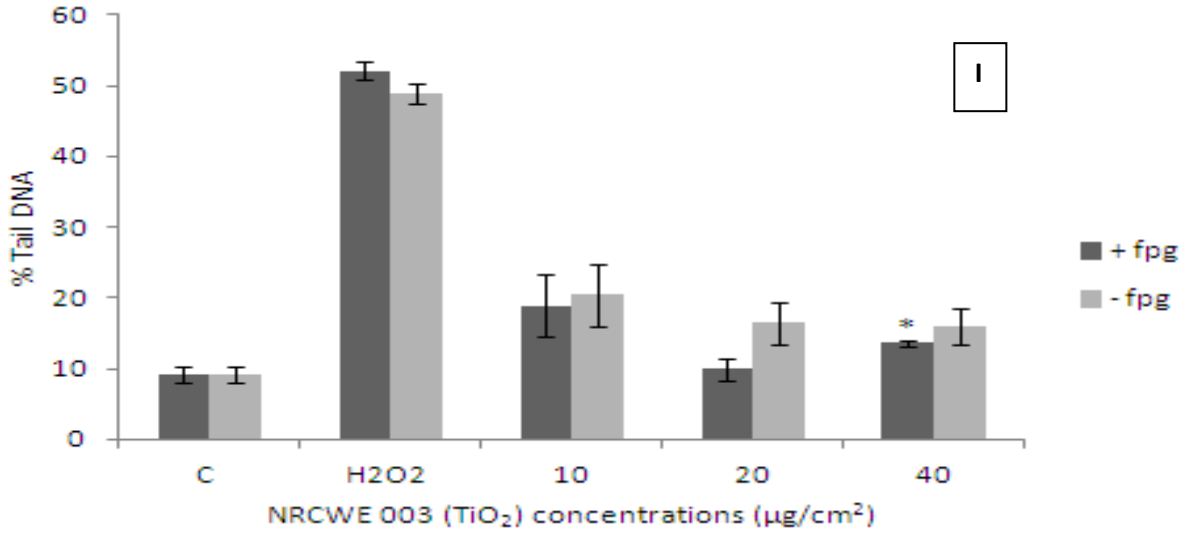
I
% Tail DNA
60
50
40
30
20
10
0
C
H2O2
10
20
40
NRCWE 003 (TiO2) concentrations (µg/cm2)
+ fpg
- fpg

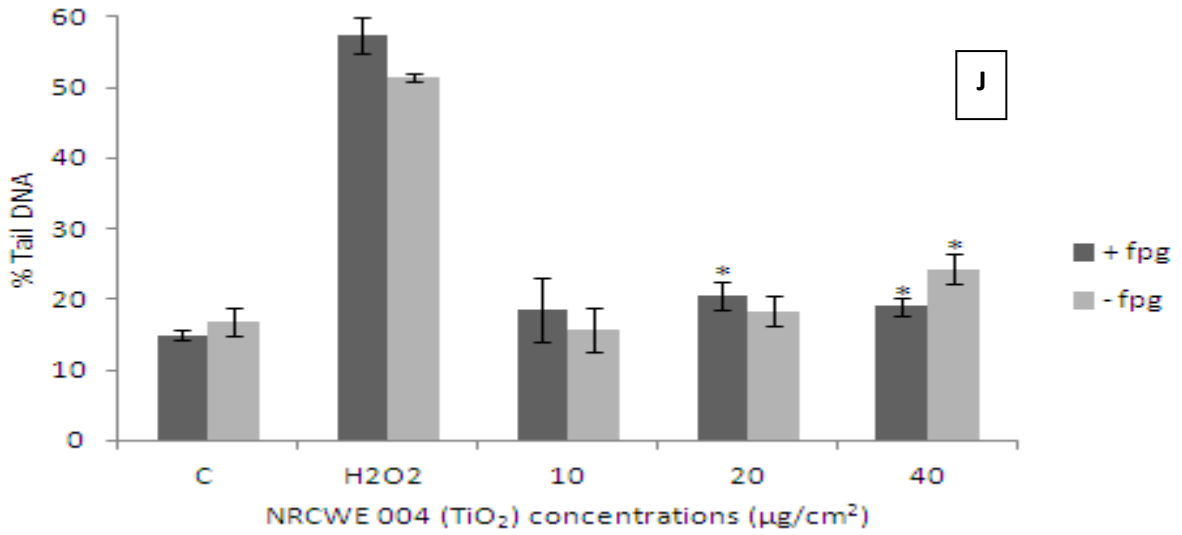

Figure 10.2. DNA damage expressed as percent of tail DNA following exposure of the HK-2 cells to LC_{20} ± one serial dilution to the ENPRA panel of engineered nanomaterials. The cells were exposed to cell medium (control), 60 µM H_2O_2 and NMs for 4 hr. Values represent mean ± SEM (n=3), significance indicated by * = $p<0.05$ and ** = $p<0.005$, when material treatments are compared to the control. **A)** NM 101 **B)** NM 110 **C)** NM 111 **D)** NM 300 **E)** NM 400 **F)** NM 402 **G)** NRCWE 001 **H)** NRCWE 002 **I)** NRCWE 003 **J)** NRCWE 004.

10.7 Discussion

To date human kidneys have received relatively little attention in terms of nanotoxicological studies. Due to high blood supply level and ability to concentrate toxins, this organ could be potentially affected by any nanomaterial that reaches the circulatory system. During active or passive transport of molecules and during re-absorption across the nephral proximal tubule, this part of the nephron may be at high risk of potential damage from NMs. It has been shown previously that the proximal renal tubule is more susceptible to gold NM toxicity than the distal tubule (Abdelhalim, *et al*., 2011). In a recent study it was shown that a high concentration of orally administrated Ag NMs accumulated in kidney tissues at a higher wet mass than any other organ (Kim, *et al*., 2010). This observation suggests that kidneys are important organs in clearing the NMs from the mammalian system and at potential risk of being damaged by NM exposure. Hence we have chosen an immortalized proximal tubule epithelial cell line from adult human kidney (HK-2) as a well differentiated cell line representing an alternative to primary kidney cells (Ryan, *et al*., 1994). This study has focused on the impacts of the investigated panel of nanomaterials on cell cytotoxicity, pro-inflammatory cytokine production, intracellular ROS and DNA damage.

Here we have shown that following acute *in vitro* exposure of the cells to the panel of the NMs, they can be segregated into a low (TiO_2 and MWCNT) and a high toxicity group (Ag and coated and uncoated ZnO) (Table 10.1). This complements our previous data for a hepatocyte cell line (Chapters 4 and 5) and primary human hepatocytes (Chapter 6) and rat liver co-culture (Chapter 9). We observed slightly higher toxicity (not significant) to the cells in RPMI-FCS exposed to the Ag and ZnO NMs (higher amounts of protein within the media compared to the K-SFM) utilised in this study. One theory offering an explanation for this could be that the serum interaction with the NMs might make the materials more bio-available to the cells. It is also possible that the cells might be healthier in the K-SFM compared to RPMI with FCS under the conditions in this study.

We noted that the Ag NM (NM 300) was highly toxic to the HK-2 cells (LC_{50} between 2.5 - 10 μg/cm^2). To our knowledge no study has investigated the toxicity of Ag nanomaterials and human kidney cells *in vitro* however a number of studies have demonstrated that Ag NMs can be highly toxic in other organs and systems both *in vivo* and *in vitro* (Gaiser, *et al*., 2012; Kermanizadeh, *et al*, 2012c; Kim, *et al*., 2011c). Oxidative stress is often proposed as a

mechanism of toxicity (Piao, 2011; Kim, *et al*., 2011). Our HE oxidation data show an increase in intracellular ROS levels following exposure to the NM 300. Furthermore we noted that there was an increase in IL6 and IL8 levels following exposure of the cells to the Ag NMs (highest release at intermediated doses – suggesting cytotoxicity inhibits cytokine production at the highest doses), as well as a significant increase in genotoxicity following exposure to sub-lethal concentrations of the nanomaterial. This indicates that Ag NMs are highly genotoxic to human kidney cells. So far a number of other studies have confirmed dose dependent DNA damage after Ag NM treatment to a liver cell line (Kermanizadeh, *et al.,* 2012a) or genotoxicity in testicular cells (Asare, *et al.,* 2012).

Next we have shown that the two ZnO NMs were highly toxic (with the LC_{50} around 0.64 - 2.5 µg/cm^2) to the renal cells. Our findings are similar to a previous study in which HK-2 cells were shown to be highly susceptible to exposure to ZnO NMs (LC_{50} - 2.4 µg/cm^2) (Pujalté, *et al.,* 2011). The toxicity was associated with increased intracellular ROS production which is very similar to our findings here (Pujalté, *et al.,* 2011). We chose sub-lethal concentrations based on data obtained from our cytotoxicity assays. Notably, exposure to the NM 110 zinc oxide NMs showed a small but significant increase in percentage of tail damage however no significant genotoxicity was witnessed following exposure to NM 111. It is possible that the 4 hr exposure time for genotoxicity was not sufficient to cause larger effects from the two ZnO NMs in this study. Next, we noted a dose dependant increase in IL6 and IL8 secretion from the cells following NM exposure. It has been shown previously that there is an increase of these pro-inflammatory mediators from the kidney following exposure to various antigens (Shing, *et al*., 2011; Dudas, *et al.,* 2011). In a similar theme exposure of human embryonic kidney cell line HEK 293 to 100 nm ZnO NMs resulted in up-regulation of IL6 and IL8 genes from the cells *in vitro* (Dua, *et al.,* 2011).

We had previously shown that the two ZnO NMs used in this study are highly soluble (40-50%) while less than 1% of Ag (NM 300) was soluble after 24 hr of incubation in complete medium (Chapter 4). Therefore there is a real possibility that the high toxicity (all be much smaller amount of DNA damage) of the two ZnO materials are in part due to the release of ions, with this scenario being very unlikely following exposure to the Ag NMs.

It has been shown previously that in sufficient doses TiO_2 can cause damage to cells and tissue (Chen, *et al*., 2008; Hu, *et al*., 2011; Jin, *et al*., 2008). Furthermore other studies have

shown that after translocation from the primary site of exposure, the TiO_2 NMs can induce oxidative stress - mediated toxicity in many cell types by producing large amounts of free radicals (Jin, *et al*., 2008; Kang, *et al*., 2008; Wang, *et al*., 2007). In this study we found all five TiO_2 were of relatively low toxicity to the HK-2 cells (LC_{50} was not reached in the presence of any of the NMs up to 80 $\mu g/cm^2$) with only small increases of oxidative stress presenting cells following exposure to four of the five TiO_2 NMs. Our findings are similar to a previous study in which exposure of HK-2 cells to a 12 nm TiO_2 resulted in low toxicity (Pujalte, *et al*., 2011). Similarly, in a study using Caco2 cells it was found that there was low cytotoxicity following 24 hr exposure to TiO_2 NMs (Jin, *et al*., 2008). In addition the data presented here indicate that relatively high TiO_2 exposure concentrations can induce production of the pro-inflammatory cytokine IL6 and IL8. In a recent study exposure of mice to 6 nm TiO_2 NM via an intragastric route promoted the expression of IL2, IL4, IL6, IL8, IL10, IL18, IL1-β, TGF-β and IFN-γ from the kidney (Gui, *et al*., 2011). Furthermore exposure of C3A cell line *in vitro* also resulted in IL8 secretion at high TiO_2 concentrations (Kermanizadeh, *et al*., 2012c; Monteiller, *et al*., 2007). Finally we show a significant increase in genotoxicity following a 4 hr exposure to two of the five TiO_2 NMs investigated in this study (NM 101 and NRCWE 004). Our findings are similar to a recent study in which exposure of Cos-1 monkey kidney fibroblasts to TiO_2 NMs resulted in significant DNA damage as measured via the comet assay (Magdolenova, *et al*., 2012).

We found that the MWCNTs tested were relatively non-toxic to the HK-2 cells at the times and concentrations tested. The toxicity of MWCNTs is widely documented, with adverse effects observed in pulmonary (Ji, *et al*., 2009), hepatic (Kermanizadeh, *et al*. 2012c), renal (Barillet, *et al*., 2010), dermal cells (Kishore, *et al*., 2009) as well as monocyte (De Nicola, *et al*., 2009) and macrophage cells (Hirano, *et al*., 2008). It has been shown that exposure of NRK-52E cells (an *in vitro* renal model) to MWCNT resulted in low toxicity (LC_{25} following 24 hr exposure) (Simon, *et al*., 2008) which is similar to our findings in this study. Exposure of the HK-2 cells to the two MWCNTs in this study resulted in a dose dependant increase in both IL6 and IL8 following a 24 hr exposure. Our findings are similar to a recent study in which exposure of HEK 293 cells to two types of MWCNTs (80 and 150 nm) resulted in increased production of IL8 (Reddy, *et al*., 2010). The HE oxidation assay showed no intracellular ROS following exposure to either of two MWCNTs. This is contradictory to findings from Reddy and colleagues in which cytotoxicity was associated with oxidative stress (Reddy, *et al*., 2010). Finally we show that short term (4 hr) exposure of the HK-2 cells

to the two carbon nanotubes at sub-lethal concentrations resulted in significant DNA damage. Barillet *et al* also witnessed small but significant genotoxicity following exposure of NRK-52E cells to 100 nm MWCNT which is similar to our findings in this study (Barillet, *et al*., 2010).

Finally no TNF-α or MCP-1 production was observed following exposure to ENPRA panel of NMs. It has been shown that under certain disease models that kidney cells produce TNF-α (Zuo, *et al*., 2011) and MCP-1 (Wittlinger, *et al*., 2010; Zehnder, *et al*., 2008). Here we show that exposure to these particular nanomaterials even at very high (in some cases cytotoxic) doses are not sufficient for MCP-1 or TNF-α secretion from the cells.

10.8 Conclusions

This *in vitro* renal model demonstrated that ZnO and Ag NMs were consistently more potent with respect to cytotoxicity, cytokine production (IL6 and IL8) and intracellular reactive oxygen species production. In comparison the MWCNT and TiO_2 nanomaterials investigated revealed relatively lower toxicity. We noted that short term sub-lethal exposure to eight of the ten nanomaterials (coated ZnO and 10 nm TiO_2 NMs being the exception) resulted in DNA damage to the cells (most evident following exposure to the Ag, 10 nm positively charged TiO_2 and 94 nm TiO_2).

Chapter Eleven

General Discussion

11.1 Summary of findings in this study

This thesis was able to demonstrate the ability of the human C3A cell line to distinguish between different NM in terms of cytotoxicity and sub-lethal effects. The relevance of this data was supported by the comparable data obtained from primary human and rodent hepatocytes with regards to a number of relevant investigated end points. While most or all of the NMs were able to induce glutathione depletion and IL8 protein production in this *in vitro* system, this reflected the hepatic response following instillation for only a sub-population of the nanomaterials. This suggests that the *in vitro* system is useful but not sufficient as currently used to predict *in vivo* hepatic responses following inhalation. The *in vitro* system provided a false positive for MWCNT which might be explained by a lack of translocation of MWCNT from the lung due to agglomeration of particle shape. The *in vitro* system provided a false negative for positively charged TiO_2 NMs which might be explained by the ability of positively charged materials to more efficiently penetrate cell barriers compared to neutral or negatively charged materials (Roblegg, *et al*., 2012). In addition, the positively charged TiO_2 may have acquired a coating from the lung that rendered them more active than if suspended in serum. Alternatively the positively charged materials, because of their ability to penetrate lung cells might have induced a humoral or neural stimulus to active a hepatic response.

The dose response data generated by this study correlated well with the different partners across Europe for the ENPRA project and clearly demonstrated that despite the use of different cell lines, media and different systems (pulmonary, cardio-vascular, hepatic, renal and developmental) that the NMs can be divided into a highly toxic (Ag and ZnO) and low toxicity (TiO_2 and MWCNT) group with respect to cytotoxicity *in vitro*. This data allowed for the identification of a sub-lethal dose range for each target system to investigate the molecular/cellular mechanism driving the toxicity of the NMs chosen in this study.

The next important observation made in this project was the fact that in addition to the cytotoxicity observations, that sub-lethal exposure of the nanomaterials were not without effect in terms of oxidative, pro-inflammatory, genotoxic effects and gene expression. There appears to be differences between the cell types with respect to their sensitivities to the sub-lethal effects of the materials and differences between each NM. These differences in toxicity and the sub-lethal effects between each nanomaterial could be attributed to their physicochemical characteristics. As discussed previously the solubility of NMs is extremely

important in the associated toxicity (Kwok, *et al*., 2012). Therefore an unqualified understanding of the dissolution kinetics of partially soluble compounds in both the test material preparation and in the cell media is crucial for further understanding of the toxicology of these nanomaterials.

Another explanation for material toxicity and reactive oxygen species generation might be contaminants in the materials i.e. iron residues within the nanotubes in study may contribute to their toxicity (e.g. via Fe^{2+} fenton reaction).

Next is the importance of presence or the absence of proteins in the test system contributing to the toxicity of NMs. Some nanomaterials can adsorb proteins and form a protein corona (Montes-Burgos, *et al*., 2010) which could influence uptake and fate of the NM. It is believed that the amount and the nature of protein could and does influence the toxicity of the NM in question (Brown, *et al*., 2013a; McCormack, *et al*., 2012).

A deeper analysis of the data in other work packages of the ENPRA project is required to pick out a more detailed picture of how the NM properties relate to their impacts on different cell types.

We also show that neutrophils and Kupffer cells are very important in the overall immune response of the organ following low acute dose exposure to these particular engineered NMs. We also believed that these NMs at the low doses administered cause a toleregenic response which is in all probability IL10 orchestrated.

11.2 *In vitro* vs. *in vivo* systems and limitations

The potential of NMs to translocate to the liver is a realistic prospect (Nalabotu, *et al*., 2011; Nemmar, *et al*., 2001). Therefore there is a necessity that the threat of nanomaterial exposure to normal liver function is thoroughly investigated. In this study the toxicity of the NMs to the liver was assessed using both *in vitro* and *in vivo* models. The use of primary cells and tissues were critical to determine if the response witnessed in the *in vitro* systems was indeed mirrored and representative of cells *in vivo*.

Through this study and numerous other experiments elsewhere major advances have been made in identifying the potential nanotoxicological effects on the liver, however there are still large gaps in what is needed to fully understand the adverse effects of realistic NM exposure.

Very few studies have attempted to make a direct comparison between *in vitro* and *in vivo* liver models. However this European funded project (ENPRA) has investigated the toxicity of a panel NMs to the liver, assessed using a hepatocyte cell line, primary human hepatocytes and liver tissues to determine if the response witnessed in the *in vitro* systems was indeed mirrored and representative of cells *in vivo*. The results show that there are some comparisons between certain end points of a hepatocyte cell line (C3A), primary human hepatocytes and primary mice and rat liver cells to the ENPRA NMs (Table 1) (not the case for all end points and NMs – e.g. instilled Ag, ZnO and positively charged TiO_2 result in distal effects on the liver in the form of oxidative stress. In the C3A cell line similar results were generated, with two exceptions, positively charged TiO_2 and the two MWCNTs. The animal model was more sensitive to the positive TiO_2, while the cell line was more sensitive to the MWCNTs).

End point	C3A cells	Primary human hepatocytes	Rat liver tissue	Mice liver tissue
Cytotoxicity	YES	YES	NA	NA
Antioxidant depletion	YES	NA	YES	NO (IV exposure) / YES (IT exposure)
Changes in gene expression	YES	NA	YES	YES
DNA damage	YES	NA	NA	NO
Cytokine production	YES	YES	NA	NA
NM Uptake	YES	YES	YES	YES
Functional markers	YES	YES	NO	NA

Table 11.1. General similarities for certain investigated end points between test systems in the ENPRA projects (responses were not uniform for all NMs – table offers a simplified summary).

It is often very difficult to make a direct comparison between *in vitro* and *in vivo* tissue responses. At best, *in vitro* findings can act as an indicator of possible *in vivo* responses. One

principle reason for this is that the comparisons between the systems are rarely like with like, i.e. cytotoxicity in an *in vitro* system is not inflammation *in vivo*, and using doses that would cause liver cells to die *in vivo* would be unethical and, in addition, disguise any sub-lethal effects. The limitations continue as an organ is never comprised of only a single cell type, and cross-talk between both different cell types and different organs is essential to responding to a toxic challenge *in vivo*. Sophisticated new *in vitro* models such as three-dimensional culture, tissue slices and fluidic models as used in the InLiveTox have been developed in order to improve *in vitro* risk assessment of any number of substances, with a view to reducing, refining and replacing animal studies.

In an *in vitro* system, soluble NMs remain trapped in the well, whereas soluble material constituents can disperse in an *in vivo* model. Likewise, many NMs can be removed from the site of deposition by macrophages and other phagocytes and excreted via a number of different routes. As already mentioned it is very unlikely that any NM will reach the liver without a protein coating which will no doubt influence its overall toxicity to the organ. It is often very difficult to reproduce the exact protein corona in any *in vitro* studies, however the route of exposure and translocation can be used to inform the preparation and dispersion of nanomaterials.

Overall, although some attempts have been made to improve *in vitro* testing systems (i.e. InLiveTox project) the use of animal models are still in all probability the most reliable representation of a whole organ/body response to foreign materials i.e. NMs. This being said, the high cost and ethical implications of any *in vivo* study must be considered.

The findings obtained in this study will provide hazard data for the ENPRA panel of nanomaterials that will be used for risk assessment purposes conducted by partners within the project to hopefully determine any health implications associated with these NMs. Finally the knowledge of the extent of NM exposure is imperative as this will impact on their toxicity, as risk is dictated by the hazard associated with the extent of NM exposure.

11.3 Risk assessment and future studies

As with many toxicological studies it would be very interesting to investigate some of the endpoints in more detail to provide further verification of the findings within this study. Of particular importance would be an investigation into ROS levels within the hepatocytes utilising a more suitable method than the one used in this study i.e. HE oxidation assay (the DCFH-DA assay requires viable intact cells, therefore is not entirely suitable for highly cytotoxic NMs). To fully validate the findings in this study it would be interesting to investigate the primary human hepatocyte response to these materials in order to establish the mechanism of toxicity and whether this is comparable to the hepatocyte cell line. It was not possible to investigate this question using the primary human hepatocytes due to their extremely high cost. The ENPRA nanomaterials were found within the hepatocytes hence identifying the mechanisms of uptake and fate of these NMs would be extremely interesting and warrant further investigation. The use of fluorescent non toxic NMs would allow for a better understanding of the potential role of endocytosis by hepatocytes (Johnston, *et al*., 2010). Investigations into the role of bile in elimination of these nanomaterials, as well as accumulation and localisation of ENPRA NMs within organelles of the cells would also be fascinating (Johnston, *et al*., 2010).

Evaluating the impact of the nanomaterial exposure on hepatocytes could be expanded upon. Hepatocytes are polarized epithelial cells that fulfil a lot of different tasks to contribute to the liver physiology such as storage of glycogen, lipid and serum protein synthesis, biotransformation, bile secretion, as well as detoxification of xenobiotics by phase I and phase II metabolic pathways. It would be interesting to investigate markers of differentiated hepatocytes (especially in the primary model) to gain a better understanding of NM modification of liver function.

In this study it was revealed that several materials were able to compromise cell vitality and it is of great interest to determine the mechanism by which this cell death occurs specifically via necrosis (premature cell death) or apoptosis (programmed cell death). One assay that would have been utilised if time was not an issue is the Annexin V Propidium iodide assay.

Taking into account the financial and time restraints of this project all the avenues in the *in vivo* experiments were exhausted however there are a few questions that could still be

addressed. Firstly it would be interesting to investigate earlier time points following intravenous exposure of nanomaterials. Although we looked at mRNA levels following IT and IV exposure of animals to NMs, to gain a more accurate and comprehensive of gene expression profile in the liver the utilisation of microarray analysis would be greatly advantageous.

All of the experiments in this study were carried out after acute exposures, with the longest exposure time being 72 hr. It would be very interesting to repeat the *in vivo* experiments after long term exposure to the NMs. In all probability any nanomaterial mediated adverse effects to humans would be following small, yet multiple dose exposures, therefore long term exposure of animals would give more accurate representation of any potential human health issues.

In this study we showed that Kupffer cells play a crucial role in the liver immunity in response to the ENPRA panel of nanomaterials. However we did not manage to isolate a pure population of Kupffer cells. An effective approach that could be pursued in the future would be the complete depletion of the liver macrophage population utilising Clodrosome (liposomal clodronate) (Chen, *et al*., 2012; Niebel, *et al*., 2012). Comparisons made between models in which the Kupffer cells have been depleted and wild type animals will allow to better demonstrate the role of liver macrophages in the immune response of the liver against NMs.

Finally, the rheological behaviour of ENPRA NMs and interactions with human blood proteins would be very interesting. An investigation of NM interaction with blood is imperative in gaining a better understanding of NM toxicity to the liver (for a NM to have any impact on the liver it must pass through blood).

As a note a suggestion for any future study design might to reduce the number of nanomaterials utilised in the study as this would allow for a more realistic and detailed investigation into the mechanism of the NM toxicity.

With the advances in the fields of nanotechnology and nanomedicine, the potential for public and occupational exposure is likely to increase, so that there is an urgent necessity to consider the possibility of any detrimental health consequences associated with this increased

exposure to nanomaterials. This can be achieved in the form of a critical risk assessment. Engineered nanomaterials are manufactured from a diverse group of substances and can have a very diverse range of physicochemical characteristics such as size, shape, surface charge, surface reactivity, crystalline phase, polarity, solubility or impurities, hence a varied range of materials with different characteristics need to be evaluated for a comprehensive toxicity profile allowing for structure activity relationships to be generated. Likewise, standardisation of methods such as particle preparation and exposure conditions are essential to be able to compare studies carried out in different laboratories and ensure that any differences in toxicological responses are due to the materials only and not the methodology.

Therefore one of the most important reasons for conducting nanotoxicological studies is to provide a knowledge base towards assessing the risks associated with realistic NM exposures. The findings obtained in such studies should provide hazard data for the nanomaterials that will be used for risk assessment purposes and determine any health implications associated with these NMs. For this purpose there are areas in liver nanotoxicology in which knowledge is severely lacking

To our knowledge there have been very few studies if any that have investigated the effects of nanomaterials on the liver following inhalation exposure (in all reality the most prominent route of nanomaterial exposure). It is important to note that inhalation and instillation are not always comparable, since for example the deposition patterns of the particles in the lung can vary between the two methods. Adverse effects observed following an IT exposure might not necessarily be seen following an inhalation study.

One of the most important paradigms of risk assessment is exposure. From the literature it is evident that there is a clear lack of studies in which low realistic relevant exposure scenarios have been employed that can be used for risk assessment purposes concentrating on the liver. There is a real need for long term studies in which animals are exposed to low and repeated doses of different NMs via different routes (i.e. inhalation, ingestion and intravenous routes). This will be the only way a realistic and reliable liver risk assessment model can be formulated.

References

Abdelhalim MAK, Jarrar BM. (2011). The appearance of renal cells cytoplasm degeneration and nuclear destruction might be an indication of GNPs toxicity. Lipids in Health and Disease 10, 147-153.

Acalovschi M, Buzas C, Radu C, Grigorescu M. (2009). Hepatitis C infection is a risk factor for gallstone disease: a prospective hospital-based study of patients with chronic viral C hepatitis. Journal of Viral Hepatitis 16, 860-866.

Aitken RJ, Chaudhry MQ, Boxall AB, Hull M. (2006). Manufacture and use of nanomaterials: current status in the UK and global trends. Occupational Medicine 56, 300-306.

Akhtar MJ, Ahamed A, Kumar S, Khan MAM, Ahmad J, Alrokayan SA. (2012) Zinc oxide nanoparticles selectively induce apoptosis in human cancer cells through reactive oxygen species. International Journal of Nanomedicine 7, 845-857.

Al-Nasiry S, Geusens N, Hanssens M, Luyten C, Pijnenborg R. (2007). The use of Alamarblue assay for quantitative analysis of viability, migration and invasion of choriocarcinoma cells. Human Reproduction 22, 1304-1309.

Anreddy RNR, Devarakonda RK, Vurimindi H, Yellu NR. (2011). *In vitro* cytotoxicity of carbon nanoparticles against HepG32 cells. Latin American Journal of Pharmacy 30, 177-180.

Arora S, Jain J, Rajwade JM, Paknikar KM. (2009). Interactions of silver nanoparticles with primary mouse fibroblasts and liver cells. Toxicology and Applied Pharmacology 236, 310-318.

Asare N, Instanes C, Sandberg WJ, Refsnes M, Schwarze P, Kruszewski M, Brunborg G. (2012). Cytotoxic and genotoxic effects of silver nanoparticles in testicular cells. Toxicology 291, 65-72.

Avedisian CT, Cavicchi RE, McEuen PL, Zhou X. (2009). Nanoparticles for cancer treatment: role of heat transfer. Annals of New York Academy of Sciences 1161, 62-73.

Baffy G. (2009). Kupffer cells in non-alcoholic fatty liver disease: the emerging view. Journal of Hepatology 51, 212-223.

Bajt ML, Farhood A, Jaeschke H. (2001). Effects of CXC chemokines on neutrophil activation and sequestration in hepatic vasculature. American Journal of Physiology: Gastrointestinal and liver Physiology 281, 1188-1195.

Banerjee R. (2001). Liposomes: applications in medicine. Journal of Biomaterial Applications 16, 3-21.

Baniyash M. (2006). Chronic inflammation, immunosuppressant and cancer: New insights and outlook. Seminars in Cancer Biology 16, 80-88.

Barillet S, Simon-Deckers A, Herlin-Boime N, Mayne-L'Hermite M, Reynaud C, Cassio D, Gouget B, Carriere M. (2010). Toxicological consequences of TiO_2, SiC nanoparticles and multi-walled carbon nanotubes exposure in several mammalian cell types: an *in vitro* study. Journal of Nanoparticle Research 12, 61-73.

Bautista A. (2002). Netrophilic infiltration in alcoholic hepatitis. Alcohol 27, 17-21.

Beere HM, Green DR. (2001). Stress management – heat shock protein-70 and the regulation of apoptosis. Trends in Cell Biology 11, 6-10.

Beliveau-Carey G, Cheung CW, Cohen S, Brusilow S, Raijman L. (1993). Regulation of urea and citrulline synthesis under physiological conditions. Biochemical Journal 292, 241–247.

Benn TM, Westerhoff P. (2008). Nanoparticle silver released into water from commercially available sock fabrics. Environmental Science and Technology 42, 4133-4139.

Berry JP, Arnoux B, Stanislas G, Galle P, Chretien J. (1977). A microanalytic study of particle transport across the alveoli: Role of blood platelets. Biomed Central 27, 354-357.

Beutler B. (2004). Innate immunity: an overview. Molecular Immunology 40, 845-859.

Birlouez-Aragon I, Tessier FJ. (2003). Antioxidant vitamins and degenerative pathologies. A review of vitamin C. The Journal of Nutrition, Health and Aging 7, 103-109.

Black S, Kushner I, Samols D. (2004). C reactive protein. The Journal of Biological Chemistry 279, 48487-48490.

Bottcher JP, Knolle PA, Stabenow D. (2011). Mechanisms Balancing Tolerance and Immunity in the Liver. Digestive Diseases 29, 384-390.

Boyle TJ, Bunge SD, Alam TM, Holland GP, Headley TJ, Avilucea G. (2005). Cadmium Amido Alkoxide and Alkoxide Precursors for the Synthesis of Nanocrystalline CdE (E = S, Se, Te). Inorganic Chemistry 44, 1309-1318.

Brody AR, Hill LH, Warheit DB. (1985). Induction of early alveolar injury by inhaled asbestos and silica. Federation Proceedings 44, 2596-2601.

Brown DM, Donaldson K, Brom PJ, Schins P, Dehnhardt M, Gilmour P, Jiminez LA, Stone V. (2004). Calcium and ROS mediated activation of transcription factors and TNF-α cytokine gene expression in macrophages exposed to ultrafine particles. American Journal of Lung Physiology 286, 344-353.

Brown DM, Hutchison L, Donaldson K, Stone V. (2007). The effects of PM_{10} particles and oxidative stress on macrophages and lung epithelial cells: modulating the effects of calcium signalling antagonists. American Journal of Lung Physiology 292, 1444-1451.

Brown DM, Johnston H, Gubbins E, Stone V. (2013a). Cytotoxicity and cytokine release in rat hepatocytes and macrophages exposed to gold nanoparticles – effect of biological dispersion media or corona. Manuscript in preparation.

Brown DM, Johnston H, Gubbins E, Stone V. (2013b). Size and surface charge effects of silica nanoparticles on J774 cells are influenced by the dispersant medium. Manuscript in preparation.

Brunauer PH, Emmet H, Teller E. (1938). Adsorption of gases in multi-molecular layers. Journal of American Chemical Society 60, 309-315.

Buzea C, Pacheco II, Robbie K. (2007). Nanomaterials and nanoparticles: Sources and toxicity. Biointerpahses 2, 18-67.

Carlson C, Hussain SM, Schrand AM, Braydich-Stolle LK, Hess KL, Jones RL, Schlager JJ. (2008). Unique cellular interaction of silver nanoparticles: Size-dependent generation of reactive oxygen species. Journal of Physical Chemistry 112, 13608-13619.

Carneiro LA, Magalhaes JG, Tattoli L, Philpott DJ, Travassos LH. (2008). NOD-like proteins in inflammation and disease. Journal of Pathology 214, 136-148.

Carreo JS, Yilmaz MI, Lindholm B, Stenvinkel P. (2008). Cytokine dysregulation in chronic kidney disease: How can we treat it? Blood Purification 26, 291-299.

Cartiera MS, Johnson KM, Rajendran V, Caplan MJ. (2009). The uptake and intracellular fate of PGLA nanoparticles in epithelial cells. Biomaterials 30, 2790-2798.

Caruthers SD, Wickline SA, Lanza GM. (2007). Nanotechnological applications in medicine. Current Opinion in Biotechnology 18, 26-30.

Chappell MA, Miller LF, George AJ, Pettway BA, Prince CL, Porter BE, Bednar AJ, Seiter JM, Kennedy AJ. (2011). Simultaneous dispersion-dissolution behaviour of concentrated silver nanoparticle suspensions in the presence of model organic solutes. Chmosphere 84, 1108-1116.

Chen BX, Wilson SR, das M, Coughlin DJ, Erlanger BF, Erlanger BF. (1998). Antigenicity of fullerenes: antibodies specific for fullerenes and their characteristics. Proceedings of National Academy of Sciences of the United States of America 95, 10809-10813.

Chen C, Zhang P, Hou X, Chai Z. (1999). Sub-cellular distribution of selenium and Se-containing proteins in human liver. Biochemica et Biophysica Acta-General Subjects 1427, 205-215.

Chen E, Ruvalcaba M, Araujo L, Chapman R, Chin WC. (2008a). Ultrafine titanium dioxide nanoparticles induce cell death in human bronchial epithelial cells. Journal of Experimental Nanoscience 3, 171-183.

Chen LL, Ye HY, Zhao XL, Miao Q, Li YM, Hu RM. (2012). Selective depletion of hepatic Kupffer cells significantly alleviated hepatosteatosis and intrahepatic inflammation induced by high fat diet. Hepato-Gastroenterology 59, 1208-1212.

Chen X, Schluesener HJ. (2008b). Nanosilver: A nanoproduct in medical application. Toxicology Letters 176, 1-12.

Chen Z, Meng H, Xing G, Chen C, Zhao Y, Jia G, Wang T, Yuan H, Ye C, Zhao F, Chai Z, Zhu C, Fang X, Ma B, Wan L. (2006). Acute toxicological effects of copper nanoparticles *in vivo*. Toxicology Letters 163, 109-120.

Chuang YH, Lan RY, Gershwin ME. (2009). The immunopathology of human biliary cell epithelium. Seminars in Immunopathology 31, 323-331.

Clift MJ, Boyles MS, Brown DM, Stone V. (2010). An investigation into the potential for different surface coated quantum dots to cause oxidative stress and affect macrophage cell signalling *in vitro*. Nanotoxicology 4, 139-149.

Cohen MP. (2003). Intervention strategies to prevent pathogenetic effects of glycated albumin. Archives of Biochemistry and Biophysics 419, 25–30.

Coussens LM, Werb Z. (2002). Inflammation and cancer. Nature 420, 860-866.

Crisp IN. (2007). The liver as a lymphoid organ. Annual review of Immunology 27, 147-163.

Crosera M, Bovenzi M, Maina G, Adami G, Zanette C, Florio C, Filon Larese F. (2009). Nanoparticle dermal absorption and toxicity: a review of the literature. International archives of Occupational and Environmental Health 82, 1043-1055.

Cui Y, Gong X, Duan Y, Li N, Hu R, Liu H, Hong M, Zhou M, Wang L, Wang H, Hong F. (2010). Hepatocyte apoptosis and its molecular mechanisms in mice caused by titanium dioxide nanoparticles. Journal of Hazardous Materials 183, 874-880

Delpino MV, Barrionuevo P, Scian R, Fossati CA, Balsi PC. (2010). Brucella-infected hepatocytes mediate potentially tissue-damaging immune responses. Journal of Hepatology: 53, 145-54.

Deng X, Luan Q, Chen W, Wang Y, Wy M, Zhang H, Jiao Z. (2009). Nanosized zinc oxide paticles induce neural stem cell apoptosis. Nanotechnology 20, 1-7.

De Nicola M, Nuccitelli S, Gattia DM, Traversa E, Magrini A, Bergamaschi A, Ghibelli L. (2009). Effects of carbon nanotubes on human monocytes. Natural compounds and their role in apoptotic cell signalling pathways 1171, 600-605.

Diesen DL, Kuo PC. (2009). Nitric Oxide and redox regulation in the liver: Part I. General considerations and redox Biology in Hepatitis. Journal of Surgical Research 162, 95-109.

Donaldson K, Aitken R, Tran L, Stone V, Duffein R, Forrest G, Alexander A. (2006). Carbon nanotubes: a review of their properties in relation to pulmonary toxicology and workplace safety. Toxicological Sciences 92, 5-22.

Donaldson K, Macnee W. (1998). The Mechanism of lung injury caused by PM10. Issues in Environmental Science and Technology 10, 21-32.

Donldson K, Murphy F, Schinwald A, Duffin R, Poland CA. (2011). Identifying the pulmonary hazard of high aspect ratio nanoparticles to enable their safety-by-design. Nanomedicine 6, 143-156.

Donaldson K, Tran CL. (2002). Inflammation caused by particles. Inhalation Toxicology 14, 4-27.

Dong BW, Liang P, Yu XL, Zeng XQ, Wang PJ, Su L, Wang XD, Xin H, Li S. (1998). Sonographically guided microwave coagulation treatment of liver cancer: an experimental and clinical study. American Journal of Roentgenology 171, 449-454.

Drake PL, Hazlewood KJ. (2005). Exposure-related health effects of silver and silver compounds: a review. Annals of Occupational Hygiene 49, 575-585.

Dreher KL. (2004). Health and environmental impact of nanotechnology: Toxicological assessment of manufactured nanoparticles. Toxicological Sciences 77, 3-5.

Dua P, Chaudhari KN, Lee CH, Chaudhari NK, Hong SW, Yu JS, Kim S, Lee DK. (2011). Evaluation of toxicity and gene expression changes triggered by oxide nanoparticles. Bulletin of Korean Chemical society 32, 2051-2057.

Dubrovinsky LS, Dubrovinskaia NA, Swamy V, Muscat J, Harrison NM, Ahuja R, Holm B, Johansson B. (2001). Materials science: The hardest known oxide. Nature 410, 653-654.

Du Clos TW, Mold C. (2004). C-reactive protein: an activator of innate immunity and a modulator of adaptive immunity. Immunological Research 30, 261-277.

Dudas PL, Sague SL, Elloso MM, Farrell FX. (2011). Proinflammtory/Profibiotc effects of interlukin 17A on human proximal tubule epithelium. Nephron Experimental Nephrology 117, 114-123.

Edwards-Jones V. (2009). The benefits of silver in hygiene, personal care and healthcare. Letters in Applied Microbiology 49, 147-152.

Ellinger-Ziegelbauer H, Pauluhn J. (2009). Pulmonary toxicity of multi-walled carbon nanotubes (Baytubes(R)) relative to alpha-quartz following a single 6 h inhalation exposure of rats and a 3 months post-exposure period. Toxicology 266, 16-29.

Eom HJ, Choi J. (2009). Oxidative stress of CeO_2 nanoparticles via p38 - Nrf2 signalling pathway in human bronchial epithelial cell, Beas-2B. Toxicology Letters 187, 77-83.

European Union official recommendation – Nanomaterials. – Accessed – 3-3-2012 http://eur-lex.europa.eu/LexUriServ/LexUriServ.do?uri=OJ:L:2011:275:0038:0040:EN:PDF.

Fabrega J, Luoma SN, Tyler CR, Galloway TS, Lead R. (2011). Silver nanoparticles: behaviour and effects in the aquatic environment. Environment International 37, 517-531.

Fainboim L, Chernavsky A, Paladino N, Flores AC, Arruvito L. (2007). Cytokines and chronic liver disease. Cytokine and Growth Factor Reviews 18, 143-157.

Ferin J, Oberdorster G, Penny DP, Soderholm SC, Gelein R, Piper HC. (1990). Increased pulmonary toxicity of ultrafine particles? Particle clearance, translocation, morphology. Journal of Aerosol Science 21, 381-384.

Ferin J, Oberdorster G, Penny DP. (1992). Pulmonary retention of ultrafine and fine particles in rats. American Journal of Respiratory Cell and Molecular Biology 6, 535-542.

Fernandez-Martinez AB, Jimenez MIA, Cazana FJL. (2012). Retionic acid increases hypoxia-inducible factor-1 alpha through intracrine prostaglandin E-2 signalling in renal proximal tubular cells HK-2. Biochemica et Biophysica Acta - Molecular and Cell Biology of Lipids 4, 672-683.

Ferrari M. (2005). Cancer nanotechnology: opportunities and challenges. Nature Review Cancer 9, 343-346.

Filippi C, Kermanizadeh A, Stone V. (2013). Kupffer cell contribution to the hepatic response to nanomaterials – manuscript in preparation.

Fischer NO, Verma A, Goodman CM, Simard JM, Rotello VM. (2003). Reversible "irreversible" inhibition of chymotrypsin using nanoparticle receptors. Journal of American Chemical Society 125, 13387-13391.

Fitzgerald JP, Nayak B, Shanmugasundaram K, Friedrichs W, Sudarshan S, Eid AA, De Napoli T, Parekh DJ, Gorin Y, Block K. (2012). Nox4 mediated renal cell carcinoma cell invasion through hypoxia-induced interleukin 6 and 8 production. Plos One 7, e30712.

Foldbjerg R, Dang DA, Autrup H. (2011). Cytotoxicity and genotoxicity of silver nanoparticles in human lung cancer line, A549. Archives of Toxicology 85, 743-750.

Gabay C, Kushner I. (1999). Acute-phase proteins and other systemic responses to inflammation. The New England Journal of Medicine 340, 448-454.

Gaiser BK, Biswas A, Rosenkranz P, Jepson MA, Lead JR, Stone V, Tyler CR, Fernandes, TR. (2011). Effects of silver and cerum oxide micro and nano sized particles on Daphnia magna. Journal of Environmental Monitoring 13, 1227-1235.

Gaiser BK, Fernandes TF, Jepson MA, Lead JR, Tylor CR, Baalousha M, Biswas A, Britton GJ, Cole PA, Johnston BD, Ju-Nam Y, Rosenkranz P, Scown TM, Stone V. (2012). Interspecies comparison on the uptake and toxicity of silver and cerium dioxide nanoparticles. Environmental Toxicology and Chemistry 31, 144-154.

Gao W, Csu K, Jib L, Tang B. (2011). Effect of gold nanoparticles on glutathione depletion-induced hydrogen peroxide generation and apoptosis in HL7702 cells. Toxicology Letters 205, 86-95.

Gekle M. (2005). Renal tubule albumin transport. Annual Review of Physiology 67, 573-594.

Gilmour PS, Ziesenis A, Morrison ER, Vickers MA, Drost EA, Ford I, Karg E, Mossa C, Schroeppel A, Ferron GA, Heyder J, Greaves M, MacNee W, Donaldson K. (2004). Pulmonary and systemic effects of short-term inhalation exposure to ultrafine carbon black particles. Toxicology and Applied Pharmacology 195, 35-44.

Glantzounis GK, Salacinski HJ, Yang W, Davidson BR, Seifalian AM. (2005). The contemporary role of antioxidant therapy in attenuating liver ischemia reperfusion injury: a review. Liver Transplantation 11, 1031-1047.

Gojovo A, Guo B, Kota RS, Rutledge JC, Kennedy IM, Barakat AI. (2007). Induction of inflammation in vascular endothelial cells by metal oxide nanoparticles: effect of particle composition. Environmental Health Perspectives 115, 403-409.

Gosens I, Kermanizadeh A, Jacobson NR, Stoeger T, Bokkers B, de Jong WH, Stone V, Tran L, Cassee FR. (2013a). Hazard identification of zinc oxide and silver nanomaterials based on acute lung and systemic toxicity in mice. Manuscript in preparation.

Gosens I, Kermanizadeh A, Jacobson NR, Stoeger T, Bokkers B, de Jong WH, Stone V, Tran L, Cassee FR. (2013b). Hazard identification of titanium dioxide and multi-walled carbon nanotubes nanomaterials based on acute lung and systemic toxicity in mice. Manuscript in preparation.

Grill AE, Johnston NW, Sadhukha T, Panyam J. (2009). Reversible "irreversible" inhibition of chymotrypsin using nanoparticle receptors. Journal of American Chemical Society: Recent Patents on Drug Delivery and Formulation 3, 137-142.

Grutzkau A, Radbruch A. (2010). Small but mighty: How the MACS – technology based on nanosized supermagnetic particles helped to analyze the immune system within the last 20 years. Chemistry parts A77, 643-647.

Guengerich FP. (2001). Common and uncommon cytochrome P450 reactions related to metabolism and chemical toxicity. Chemical Research in Toxicology 14, 611-650.

Gui S, Zhang Z, Zheng L, Cui Y, Liu X, Li N, Sang X, Sun Q, Gao G, Cheng Z, Wang L, Tang M, Hong F. (2011). Molecular mechanism of kidney injury of mice caused by exposure to titanium dioxide nanoparticles. Journal of Hazardous Materials 195, 365-370.

Gutsch A, Muhlenweg H, Krumerm H. (2005). Tailor-made nanoparticles via gas-phase synthesis. Small 1, 1-46.

Hagens WI, Oomen AG, de Jong WH, Casee FR, Sips AJAM. (2007). What do we (need to) know about the linetic properties od nanoparticles in the body? Regulatory Toxicology and Pharmacology 49, 217-229.

Hamerman JA, Ogasawara K, Lanier LL. (2005). NK cells in innate immunity. Current Opinions in Immunology 17, 29-35.

Hamilton Jr RF, Thakur SA, Holian A. (2008). Silica binding and toxicity in alveolar macrophages. Free Radical Biology 44, 1246-1258.

Handy RD, Owen R, Valsami-Jones E. (2008). The ecotoxicology of nanoparticles and nanomaterials: current status, knowledge gaps, challenges, and future needs. Ecotoxicology 17, 315-325.

Hansson PK, Asztely AK, Clapham JC, Schreyer SA. (2004). Glucose and fatty acid metabolism in McA-RH7777 hepatoma cells vs. rat primary hepatocytes: responsiveness to nutrient availability. Biochemica *et* Biophysica Acta 1684, 54-62.

Hardman R. (2006). A toxicologic review of quantum dots: toxicity depends on physicochemical and environmental factors. Environmental Health Perspectives 114, 165-172.

Häussinger D, Lamers WH, Moorman AFM. (1993). Metabolism of amino acids and ammonia. Enzyme 46, 72–93.

Häussinger D, Schliess F. (2008). Pathogenetic mechanisms of hepatic encephalopathy. Gut 57, 1156-1165.

Hertle E, van Greevenbroek MMJ, Stehouwer CDA. (2012). Complement C3: an emerging risk factor in cardiometabolic disease. Diabetologica 55, 881-884.

Heyder J, Gebhart J, Rudolf G, Schiller CF, Stahloffen W. (1986). Deposition of particles in the human respiratory tract in the size range 0.005-15 μm. Journal of aerosol science 17, 811-825.

Hirano S, Kanno S, Furuyama A. (2008). Multi-walled carbon nanotubes injure the plasma membrane of macrophages. Toxicology and Applied Pharmacology 232, 244-251.

Hirano S. (2009). A current overview of health effect research on nanoparticles. Environmental Health and Preventative Medicine 14, 223-225.

Hoet PHM, Hohlfeld IB, Salata O. (2004). Nanaoparticles – known and unknown health risks. Journal of Nanobiotechnology 2, 12-27.

Hu RP, Zheng L, Zhang T, Gao GD, Cui YL, Cheng Z, Cheng J, Hong MM, Tang M, Hong FS. (2011). Molecular mechanism of hippocampal apoptosis of mice following exposure to titanium dioxide nanoparticles. Journal of Hazardous Materials 191, 32-40.

Huang C, Bonroy K, Reekmans G, Laureyn W, Verhaegen K, De Vlaminck I, Lagae L, Borghs G. (2009). Localized surface plasmon resonance biosensor integrated with microfluidic chip. Biomedical Microdevices 4, 893-901.

Huang Z, Zheng X, Yan D, Yin G, Liao X, Kang Y, Yao Y, Huang D, Hao B. (2008). Toxicological effect of ZnO nanoparticles based on bacteria. Langmuir 24, 4140-4144.

Hussain SM, Hes KL, Gearhart JM, Geiss KT, Schlager JJ. (2005). *In vitro* toxicity of nanoparticles in BRL3A rat liver cells. Toxicology *in vitro* 19, 975-983.

Jackson P, Hougaard KS, Vogel U, Wu DM, Casavant L, Willliams A, Wade M, Yauk CL, Wallin H, Halappanavar S. (2012). Exposure of pregnant mice to carbon black by intratracheal instillation: Toxicogenomic effects in dams and offspring. Mutation Research – Genetic Toxicology and Environmental Mutagenesis 745, 73-83.

Jacobsen NR, Pojano G, Wallin H, Jensen KA. (2010). Nanomaterial dispersion protocol for toxicological studies in ENPRA. Internal ENPRA Project Report. The National Research Centre for the Working Environment. 6 pp.

Jaeschke H, Hasegawa T. (2006). Role of neutrophils in acute inflammatory liver injury. Liver International 26, 912-919.

Jaitovich A, Bartorello AM. (2009). Salt, Na^+, K^+ - ATPase and hypertension. Life Sciences 86, 73-78.

Jani P, Halbert GW, Langridge J, Florence AT. (1990). Nanoparticle uptake by the rat gastrointestinal mucosa: quantisation and particle size dependency. Journal of Pharmacy and Pharmacology 42, 821-826.

Janssen YM, van Houten B, Borm PJ, Mossman BT. (1993). Cell and tissue responses to oxidative damage. Laboratory investigation 69, 261-274.

Jensen KA, Bilaničová D, Birkedal R, Pojana G, Marcomini A, Wallin H, Jacobsen NR. Optimization and evaluation of a generic nanoparticle dispersion protocol for *in vitro* and *in vivo* toxicity testing using serum-water. Manuscript in preparation.

Ji Z, Zhang D, Li L, Shen X, deng X, Dong L, Wu M, Liu Y. (2009). The hepatotoxicity of multi-walled carbon nanotubes in mice. Nanotechnology 20, article no: 445101.

Jia G, Wang H, Yan L, Wang X, Pei R, Yan T. (2005). Cytotoxicity of carbon nanomaterials: single-wall nanotube, multi-wall nanotube, and fullerene. Environmental Science and Technology 39, 1378-1383.

Jin CY, Zhu BS, Wang XF, Lu QH. (2008). Cytotoxicity of Titanium dioxide nanoparticles in mouse fibroblast cells. Chemical Research in Toxicology 21, 1871-1877.

Johnston HJ, Semmler-Behnke M, Brown DM, Kreyling W, Tran L, Stone V. (2009). Evaluating the uptake and intracellular fate of polystyrene nanoparticles by primary and hepatocyte cell lines *in vitro*. Toxicology and Applied Pharmacology 242, 66-78.

Kalyanaraman B. (2011). Oxidative chemistry of florescent dyes: implications in the detection of reactive oxygen and nitrogen species. Biochemical Society Transactions 39, 1221-1225.

Kanel G, Korula J. (2005). Atlas of liver pathology. Saunders 2nd Edition., USA.

Kang KJ. (2002). Mechanism of hepatic ischemia/reperfusion injury and protection against reperfusion injury. Transplantation Proceedings 34, 2659-2661.

Kang SJ, Kim BM, Lee YJ, Chung HW. (2008). Titanium dioxide nanoparticles trigger p53-mediated damage response in peripheral blood lymphocytes. Environmental and Molecular Mutagenesis 49, 399-405.

Karczewski M, Karczewski J, Poniedzialek B, Wiktorowicz K, Glyda M. (2009). Cytometric analysis of TH1/TH2 cytokines in the urine of patients undergoing kidney transplantation. Annals of Transplantation 14, 25-28.

Kawata K, Osawa M, Okabe S. (2009). *In vitro* toxicity of silver nanoparticles at noncytotoxic doses to HepG2 human hepatoma cells. Environmental Science and Technology 43, 6046–6051.

Kegan VE, Tyurina YY, Tyruin VA, Konduru NV, Potapovich AI, Osipov AN, Kisin ER, Schwegler-Berry D, Mercer R, Castranova V, Shevadova AA. (2006). Direct and indirect effects of single walled carbon nanotubeson RAW 264.7 macrophages: role of iron. Toxicology Letters 165, 88-100.

Kermanizadeh A, Brown DM, Hutchison G, Stone V. (2013a). Engineered nanomaterial impact in the liver following exposure via an intravenous route – the role of polymorphonuclear leukocytes and gene expression in the organ. Nanomedicine and Nanotechnology 4: 157. DOI:10.4172/2157-7439.1000157.

Kermanizadeh A, Gaiser BK, Hutchison GR, Stone V. (2012a). An *in vitro* liver model – assessing oxidative stress and genotoxicity following exposure of hepatocytes to a panel of engineered nanoparticles. Particle and Fibre Toxicology DOI:10.1186/1743-8977-9-28.

Kermanizadeh A, Gaiser BK, Ward MB, Stone V. (2012b). Primary human hepatocytes vs. hepatic cell line – assessing their suitability for *in vitro* nanotoxicology. Nanotoxicology DOI: 10.3109/17435390.2012.734341.

Kermanizadeh A, Pojana G, Gaiser BK, Birkedal R, Bilaničová D, Wallin H, Jensen KA, Sellergren B, Hutchison GR, Marcomini A, Stone V. (2012c). *In vitro* assessment of engineered nanomaterials using C3A cells: Cytotoxicity, pro-inflammatory cytokines and function markers. Nanotoxicology DOI: 10.3109/17435390.2011.653416.

Kermanizadeh A, Vranic S, Boland S, Moreau K, Squiban AB, Gaiser BK, Andrzejczuk LA, Stone V. (2013b). An *in vitro* assessment of panel of engineered nanomaterials using a human renal cell line: Cytotoxicity, pro-inflammatory response, oxidative stress and genotoxicity. Submitted to BMC Nephrology.

Kim BS, Park IK, Hoshiba T, Jiang HL, Choi YJ, Akaike Y, Cho CS. (2011a). Design of artificial extracellular matrices for tissue engineering. Progress in Polymer Science 36: 238-268.

Kim HR, Kim MJ, Lee SY, Oh SM, Chung KH. (2011b). Genotoxic effects of silver nanoparticles stimulated by oxidative stress in human bronchial epithelial (BEAS-2B) cells. Mutation Research- Genetic Toxicology and Environmental Mutagenesis 726, 129-135.

Kim J, Kim S, Lee S. (2011c). Differentiation of the toxicities of silver nanoparticles and silver ions to the Japanese medaka (Oryzias latipes) and the cladoceran Daphnia magna. Nanotoxicology 5: 208-214.

Kim JS, Yoon TJ, Yu KN, Kim BG, Park SJ, Kim HW, Lee KH, Park SB, Lee JK, Cho MH. (2006). Toxicity and tissue distribution of magnetic nanoparticles in mice. Toxicological Sciences 89, 338-347.

Kim YS, Song MY, Park JD, Song KS, Ryu HR, Chung YH, Chang HK, Lee JH, Oh KH, Kelman BJ, Hwang IK, Yu IJ. (2010). Subchronic oral toxicity of silver nanoparticles. Particle and Fibre Toxicology 7, 20-31.

Kishimoto T, Akira S, Narazaki M, Taga T. (1995). Interleukin 6 family of cytokines and gp 130. Blood 86, 1243-1254.

Kishore AS, Surekha P, Murthy PB. (2009). Assessment of the dermal and ocular irritation potential of multi-walled carbon nanotubes by using *in vitro* and *in vivo* methods. Toxicology Letters 191, 268-274.

Kmiec Z. (2001). Co-operation of liver cells in health and disease. Advances in Anatomy, Embryology and Cell Biology 161, 1-151.

Koeneman BA, Zhang Y, Westerhoff P, Chen Y, Crittenden JC, Capco DG. (2010). Toxicity and cellular responses of intestinal cells exposed to titanium dioxide. Cell Biology and Toxicology 26, 225-238.

Krishnamurphy D, Starkl P, Szalai K, Roth-Walter F, Diesner SC, Mittlboeck, M, Mannhalter C, Untersmayr E, Jensen-Jarolim E. (2012). Monitoring neutrophils and platelets during casein-induced anaphylaxis in an experimental BALB/c mouse model. Clinical and Experimental allergy: Journal of the British Society for Allergy and clinical Immunology 42, 1119-1128.

Kroemer G, Galluzzi L, Vandenabeele P, Abrams J, Alnemri ES, Baehrecke EH, Blagosklonny MV, El-Deiry WS, Golstein P, Green DR, Hengartner M, Knight RA, Kumar S, Lipton SA, Malorni W, Nunez G, Peter ME, Tschopp J, Yuan J, Piacentini M, Zhivotovsky B, Melino G. (2009). Classification of cell death: recommendations of nomenclature committee on cell death 2009. Cell Death and Differentiation 16, 3-11.

Kwok KWH, Auffan M, Badireddy AR, Nelson CM, Wiesner MR, Chilkoti AL, Marinakos SM, Hinton DE. (2012). Uptake of silver nanoparticles and toxicity of early life stages of Japanese medaka (Oryzias latipes): Effect of coating materials. Aquatic toxicology 120, 59-66.

Lakshminarasimhan N, Kim W, Choi W. (2008). Effect of agglomerated state on the photocatalytic hydrogen production with in situ agglomeration of colloidal TiO_2 nanoparticles. Journal of Physical Chemistry 112, 20451-20457.

Lam CW, James JT, McCluskey R, Hunter RL. (2003). Pulmonary toxicity of single wall carbon nanotubes in mice 7 and 90 days after intratracheal instillation. Toxicological Sciences 77, 117-125.

L'azou B, Jorly J, On D, Sellier E, Moisan F, Fleury-Feith J, Cambar J, Brochard P, Ohayon-Courtes C. (2008). *In vitro* effects of nanoparticles on renal cells. Particle and Fibre Toxicology 5, 22-36.

Lee WB, Weng CH, Cheng FY, Yeh CH, Lei HY, Lee GB. (2009). Biomedical microdevices synthesis of iron oxide nanoparticles using a microfluidic system. Biomedical Microdevices 11, 161-171.

Lieber CS. (1997). Role of oxidative stress and antioxidant therapy in alcoholic and non alcoholic liver diseases. Advances in Pharmacology 38, 601-628.

Liguori MJ, Blomme EAG, Waring JF. (2008). Trovafloxacin induced gene expression changes in liver derived in vitro systems: Comaprison of primary human hepatocytes to HepG2 cells. Drug Metabolism and Disposition 36, 223-233.

Lines MG. (2008). Nanomaterials for practical functional uses. Journal of Alloys and Compounds 449, 242-245.

Liu ZC, Zhou QL, Liu ZQ, Li XZ, Zuo XX, Tang R. (2012). Tumour necrosis factor like weak inducer of apoptosis (TWEAK) mediates p38 mitogen activated protein kinase activation and signal transduction in peripheral blood mononuclear cells from patients with lupus nephritis. Inflammation 35, 935-943.

Lovric J, Bazzi HS, Cuie Y, Fortin GR, Winnik FM, Maysinger D. (2005). Differences in sub-cellular distribution and toxicity of green and red emitting CdTe quantum dots. Journal of Molecular Medicine., 83 377-385.

Lunov O, Syrovets T, Buchele B, Jiang XE, Rocker C, Tron K, Nienhaus GU, Walther P, Mailander V, Landfester K, Simmet T. (2010). The effects of carboxydextran-coated supermagnetic iron oxide nanoparticles on c-Jun N-terminal kinase-mediated apoptosis in human macrophages. Biomaterials 31, 5063-5071.

Luo X, Li W, Bird N, Chin SW, Hill NA, Johnson AG. (2007). On the mechanical behaviour of the human biliary system. World Journal of Gastroenterology 13, 1384-1392.

Ma LL, Zhao JF, Wang J, Liu J, Duan YM, Liu HT, Li N, Yan JY, Ruan J, Wang H, Hing SF. (2009). The acute liver injury in mice caused by Nano-Anatase TiO_2. Nanoscle research Letters 4, 1275-1285.

Madolenova Z, Bilanicova D, Pojana G, Fjellsbo LM, Hudecova A, Hasplove K, Marcomini, A, Dusinska M. (2012). Impact of agglomeration and different dispersions of titanium dioxide nanoparticles on the human related *in vitro* cytotoxicity and genotoxicity. Journal of Environmental Monitoring 14, 455-464.

Mailander V, Landfester K. (2009). Interaction of nanoparticles with cells. Biomacromolecules 10, 2379-2400.

Mamalis AG. (2006). Recent advances in nanotechnology. Journal of Materials and Processing Technology 181, 52-58.

Martindale JL, Holbrook NJ. (2002). Cellular response to oxidative stress: Signalling for suicide and survival. Journal of Cellular Physiology 192, 1-15.

Matsumoto K, Fukuda N, Abe M, Fujita T. (2010). Dendritic cells and macrophages in kidney disease. Clinical and Experimental Nephrology 14, 1-11.

Maynard MA. (2007). Nanotechnology: The next big thing, or much ado about nothing? The Annals of Occupational Hygiene 51, 1-12.

Mazzola L. (2003). Commercialising nanotechnology. Nature Biotechnology 21, 1137-1143.

McCormack TJ, Clark RJ, Dang MKM, Ma GB, Kelly JA, Veinot JGC, Goss GG. (2012). Inhibition of enzyme activity by nanomaterials: Potential and implications for nanotoxicity testing. Nanotoxicology 6, 514-525.

McDevitt MR, Chattopadhyay D, Jaggi JS, Finn RD, ZanzonicoPB, Villa C, Rey D, Mendenhall J, Batt CA, Njardarson JT, Schienberg DA. (2007). PET imaging of soluble Yttrium-86-labelled Carbon nanotubes in mice. PLoS ONE 2, e907.

McIntyre TM. (2012). Bioactive activity truncated phospholipids in inflammation and apoptosis: Formation, targets and inactivation. Biochimica et biophysica acta 1818, 2456-2464.

McWilliam S, Riorden A. (2010). How to use: C- reactive protein. Archives of disease in childhood 95, 55-58.

Meena R, Paulraj R. (2012). Oxidative stress mediated cytotoxicity of TiO_2 nano anatse in liver and kidney of Wister rats. Toxicological and Environmental Chemistry 94, 146-163.

Miller TJ, Knapton A, Adeyemo O, Noory LS, Weaver JL, Hanig JP, Honchel R, Zhang J, Espandiari P, Benedick MF, Umbreit TH, Tomazic-Jezic VJ, Sadrieh N. (2007). Toxicology of Titanium dioxide (TiO_2) nanoparticles: *in vitro* and *in vivo* evaluation of macrophage uptake of TiO_2. The Journal of the Federation of American Societies for Experimental Biology 6, 812-814.

Mingoia RT, Nabb DL, Yang CH, Han X. (2007). Primary culture of rat hepatocytes in 96 well plates: Effects of extracellular matrix configuration on cytochrome P450 enzyme activity and inducibility and its application *in vitro* cytotoxicity screening. Toxicology *in vitro* 21: 165-173.

Mitchell LA, Gao J, Wal RV, Gigliotti A, Burchiel SW, McDonald JD. (2007). Pulmonary and systemic immune response to inhaled multi-walled carbon nanotubes. Toxicological Sciences 10, 203-214.

Mocellin S, Panelli MC, Wang E, Nagorsen D, Marincola FM. (2004). The dual role of IL10. Trends in Immunology 24, 36-43.

Moore KW, Malefyt R, Coffman RL, O'Garra A. (2001). Interluekin-10 and the interluekin-10 receptor. Annual Review of Immunology 19, 683-765.

Monteiller C, Tran L, MacNee W, Faux S, Jones A, Miller B, Donaldson K. (2007). The pro-inflammatory effects of low toxicity low solubility particles, nanoparticles and fine particles, on epithelial cells *in vitro*: the role of surface area. Occupational and Environmental Medicine 64: 609-615.

Montes-Burgos I, Walcyzk D, Hole P, Smith J, Lynch I, Dawaon K. (2010). Characterisation of nanoparticle size and state prior to nanotoxicological studies. Journal of Nanoparticle Research 12, 47-53.

Morris SM. (2002). Regulation of enzymes of the urea cycle and arginine metabolism. Annual Review of Nutrition 22, 87–105.

Mossman B, Landersman J. (1983). Importance of oxygen free radicals in asbestos-induced injury to airway epithelial cells. Chest 83, 50-51.

Mossman B, Marsh J, Shatos M. (1986). Alteration of superoxide dismutase activity in tracheal epithelial cells by asbestos and inhibition of cytotixicity by anti-oxidants. Laboratory Investigation 54, 204-212.

Muhlfeld C, Gehr P, Rothen-Rutishauser B. (2008). Translocation and cellular entering mechanisms of nanoparticles in the respiratory tract. Swiss Medical Weekly 138, 387-391.

Muller RH, Keck CM. (2004). Drug delivery to the brain – realisation by novel drug carriers. Journal of Neuroscience and nanotechnology 207, 221-231.

Murphy FA, Schinwald A, Poland CA, Donaldson K. (2012). The mechanism of pleural inflammation by long carbon nanotubes: interaction of long fibres with macrophages stimulates them to amplify pro-inflammatory responses in mesothelial cells, Particle and Fibre Toxicology DOI. 10.1186/1743-8977-9-8.

Murr LE, Bang JJ, Esquivel PA, Lopez DA. (2004). Carbon nanotubes, nanocrystal forms, and complex nanoparticle aggregates in common fuel gas combustion sources and ambient air. Journal of Nanoparticle Research 6, 241-251.

Nafee N, Schneider M, Schaefer UF, Lehr C. (2009). Relevance of the colloidal stability of chitosan/ PLGA nanoparticles on their cytotoxicity profile. Pharmaceutical Nanotechnology 381, 130-139.

Nagayama S, Ogawara K, Fukuoka Y, Higaki K, Kimura T. (2001). Time-dependent changes in opsonin amount associated on nanoparticles alter their hepatic uptake characteristics. International Journal of Pharmaceutics 342, 215-221.

Nalabotu SK, Madhukar BK, Triest WE, Ma JY, Manne NDPK, Katta A, Addagarla HS, Rice KM, Blough ER. (2011). Intratracheal instillation of cerium oxide nanoparticles induces hepatic toxicity in Sprague-Dawley rats. International Journal of Nanomedicine 6, 2327-2335.

Nel A, Xia T, Madler L, Li N. (2006). Toxic potential of materials at the nanolevel. Science 311, 622-627.

Nemeth E, Baird AW, O'Farrelly C. (2009). Microanatomy of the liver immune system. Seminars in Immunopathology 31, 333-343.

Nemmer A, Vanibilleion H, Hoylaerts MF, Hoet PH, Verbruggen A, Nemery A. (2001). Passage of intratracheally instilled ultrafine particles from the lung into the systemic circulation in hamster. American Journal of Respiratory and Critical Care Medicine 164, 1665-1668.

Niebel W, Walkenbach K, Beduneau A, Pellequer Y, Lamprecht A. (2012). Nanopraticle-based clodronate delivery mitigates murine experimental colitis. Journal of Controlled Release 160, 659-665.

Nohl H, Gille L, Kozlov A, Staniek K. (2003). Are mitochondria a spontaneous and permanent source of reactive oxygen species? Redox Report 8, 135-141.

Nohynek GJ, Dufour EK, Roberts MS. (2008). Nanotechnology, Cosmetics and the Skin: Is There a Health Risk? Skin Pharmacology and Physiology 21, 136-149.

Oberdorster G, Feerin J, Finklestein J, Wade P, Corson N. (1990). Increased pulmonary toxicity of ultrafine particles? Lung lavage studies. Journal of Aerosol Sciences 21, 384-387.

Oberdorster G, Maynard A, Donaldson K, Castranova V, Fitzpatrick J, Ausman K, Carter J, Karn B, Kreyling W, Lai D, Olin S, Monteiro-Riviere N, Warheit D, Yang H. (2005). Principles for characterizing the potential human health effects from exposure to nanomaterials: elements of a screening strategy. Particle and Fibre Toxicology 2, DOI: 10.1186/1743-8977-2-8.

Oberdorster G, Stone V, Donaldson K. (2007). Toxicology of nanoparticles: A historical perspective. Nanotoxicology 1, 2-25.

Ola MS, Nawaz M, Ahsan H. (2011). Role of Bcl-2 family proteins in the regulation of apoptosis. Molecular and Cellular Biochemistry 351, 41-58.

Olde Damink S, Deutz N, Dejong C, Soeters PB, Jalan R. (2002). Interorgan ammonia metabolism in liver failure. Neurochemistry International 41, 177–188.

Park EJ, Park K. (2009). Oxidative stress and pro-inflammatory responses induced by silica nanoparticles *in vivo* and *in vitro*. Toxicology Letters 184, 18-25.

Park EJ, Yi J, Kim Y, Choi K, Park K. (2010). Silver nanoparticles induce cytotoxicity by a Trojan-horse type mechanism. Toxicology *In Vitro* 24, 872–878.

Park MVDZ, Neigh AM, Vermeulen JP, de la Fonteyne LJJ, Verharen HW, Briede JJ, van Loveren H, de Jong WH. (2011). The effects of particle size on the cytotoxicity, inflammation, developmental toxicity and genotoxicity of silver nanoparticles. Biomaterials-ahead of press.

Parone PA, Martinou JJC. (2002). Mitochondria: regulating the inevitable. Biochimie 84, 105-111.

Passagne I, Morille M, Rousset M, Pujalte I, L'azou B. (2012). Implication of oxidative stress in size-dependant toxicity of silica nanoparticles in kidney cells. Toxicology 299, 112-124.

Patlolla A, McGinnis B, Tchounwou P. (2011). Biochemical and histopathological evaluation of functionalized single-walled carbon nanotubes in Swiss-Webster mice. Journal of Applied Toxicology 31, 75-83.

Peters TJ. (1996). All about albumin. Academic Press San Diego P7.

Petkovic J, Zegura B, Stevanovic M, Drnovsek N, Uskokovic D, Novak S, Filipic M. (2011). DNA damage and alterations in expression of DNA damage responsive genes induced by TiO_2 nanoparticles in human hepatoma HepG2 cells. Nanotoxicology 5, 341-353.

Piao MJ, Kang KA, Lee IK, Kim HS, Kim S, Choi JY, Choi J, Hyun JW. (2011). Silver nanoparticles induce oxidative cell damage in human liver cells through inhibition of reduced glutathione and induction of mitochondrial involved apoptosis. Toxicology Letters 201, 92-100.

Pichardo S, Gutierrez-Praena D, Puerto M, Sanchez E, Grilo A, Camean AM, Jos A. (2012). Oxidative stress responses to carboxylic acid functionalized single wall carbon nanotubes on the human intestinal cell line Caco-2. Toxicology *in vitro* – ahead of print.

Pisanic II TR, Blackwell JD, Shubayev VI, Finones RR, Jin S. (2007). Nanotoxicity of iron oxide nanoparticle internalization in growing neurons. Biomaterials 28, 2572-2581.

Poland CA, Duffin R, Kinloch I, Maynard A, Wallace WA, Seaton A, Stone V, Brown S, Macnee W, Donaldson K. (2008). Carbon nanotubes introduced into the abdominal cavity of mice show asbestos-like pathogenicity in a pilot study. Nature nanotechnology 3, 423-428.

Poli V, Cortese R. (1989). Interleukin 6 induces a liver specific nuclear protein that binds to the promoter of acute phase genes. Proceeding of the National Academy of Sciences 86, 8202-8206.

Pujalté I, Passagne I, Brouillaud B, Tréguer M, Durand E, Ohayon-Courtès C, L'Azou B. (2011). Cytotoxicity and oxidative stress induced by different metallic nanoparticles on human kidney cells. Particle and Fibre Toxicology 8, 10-26.

Puthothu B, Krueger M, Heinze J, Forster J, Heinzmann A. (2006). Impact of IL8 and IL8-receptor alpha polymorphisms on the genetics of bronchial asthma and severe RSV infections. Clinical and Molecular Allergy 4, 2-8.

Quinlan GJ, Martin GS, Evans TW. (2005). Albumin: biochemical properties and therapeutic potential. Hepatology 41, 1211–1219.

Racine-Samson L, Scoazec JY, D'Errico A, Fiorentino M, Christa L, Moreau A, Roda C, Grigioni WF, Feldman G. (1996). The metabolic organization of the adult human liver: a comparative study of normal, fibrotic, and cirrhotic liver tissue. Hepatology 24, 104–113.

Ramaiah SK, Jaeschke H. (2007). Role of neutrophils in the pathogenesis of acute inflammatory liver injury. Toxicologic Pathology 35, 456-766.

Raven PH, Johnson GB, Losos JB, Mason KA, Singer SR. (2008). Biology. Eighth edition - McGraw Hill International, 1030.

Ravenzwaay B, Leibold E. (2004). A comparison between *in vitro* rat and human and *in vivo* skin penetration studies. Human and Experimental Toxicology 23, 412-430.

Reddy ARN, Reddy YN, Krishna DR, Himabindu V. (2010). Multi walled carbon nanotubes induce oxidative stress and cytotoxicity in human embryonic kidney (HEK293) cells. Toxicology 272, 11-16.

Reich PB, Hungate BA, Luo YQ. (2006). Carbon-nitrogen interactions in terrestrial ecosystems in response to rising atmospheric carbon dioxide. Annual review of Ecology Evolution and Systematics 37, 611-636.

Rhee SG, Chang TS, Jeong W, Kang D. (2010). Methods for detection and measurement of Hydrogen peroxide inside and outside of cells. Molecules and Cells 29, 539-549.

Robblegg E, Frohlich E, Meindl C, Teubl B, Zaversky M, Zimmer A. (2012). Evaluation of a physiological *in vitro* systems to study the transport of nanoparticles through the buccal mucosa. Nanotoxicology 6, 399-413.

Roberts M, Reiss M, Monger G. (2000). Advanced Biology. Nelson Publishing, 280.

Roche M, Rondeau P, Singh NR, Tarnus E, Bourdon E. (2008). The antioxidant properties of serum albumin. FEBS Letters 582, 1783-1787.

Roduner E. (2006). Size matters: Why nanomaterials are different. Chemical Society Reviews 35, 583-592.

Roselli M, Finamore A, Garaguso I, Britti MS, Mengheri E. (2003). Zinc oxide protects cultured enterocytes from the damage induced by Escherichia coli. Journal of Nutrition 133, 4077-4082.

Rothen-Rutishauser BM, Schurch S, Haenni B, Kapp N, Gehr P. (2006). Interaction of fine particles and nanoparticles with red blood cells visualised with advanced microscopic techniques. Environmental Science and Technology 40, 4353-4359.

Saad B, Frei K, Scholl FA, Fontana A, Maier P. (1995). Hepatocyte-derived interleukin-6 and tumor-necrosis factor alpha mediate the lipopolysaccharide-induced acute-phase response and nitric oxide release by cultured rat hepatocytes. European Journal of Chemistry 229, 349-355.

Sadauskas E, Danscher G, Stoltenberg M, Vogel U, Larsen A, Wallin H. (2009a). Protracted elimination of gold nanoparticles from mouse liver. Nanomedicine 5, 162-169.

Sadauskas E, Jacobson NR, Danscher G, Soltenberg M, Larsen A, Kreyling W, Wallin H. (2009b). Bio-disruption of gold nanoparticles in mouse lung following intratracheal instillation. Chemistry Central Journal 3: 16-23.

Sadauskas E, Wallin H, Stoltenberg M, Vogel U, Doering P, Larsen A, Danscher G. (2007). Kupffer cells are central in the removal of nanoparticles from the organism. Particle and Fibre Toxicology 4, 10-17.

Sahi J, Grepper S, Smith C. (2010). Hepatocytes as a tool in drug metabolism, transport and safety evaluations in drug discovery. Current Drug Discovery Technologies 7, 188-198.

Sahu A, Lambris JD. (2002). Structure and biology of complent protein C3, a connecting link between the innate and acquired immunity. Immunological reviews 180, 35-48.

Saini S, Edelman PR, Sharma P, Li W, Mayo-Smith W, Slater GJ, Eisenberg PJ, Hahn PF. (1995). Blood-pool MR contrast material for detection and characterisation of focal hepatic lesions: initial clinical experience with ultra small superparamagnetic iron oxide (AMI-227). American Journal of Roentgenology 164, 1147-1152.

Salomon JJ, Ehrhardt C. (2011). Nanoparticles attenuate P-glycoprotein/MDR1 function in A549 human alveolar epithelial cells. European Journal of Pharmaceutics and Biopharmaceutics 77, 392-397.

Sanders S, Barnett A, Correa-Valez I, Coulthard M, Doust J. (2008). Systematic review of the diagnostic accuracy of C reactive protein to detect bacterial infection in non hospitalized infants and children with fever. The Journal of Paediatrics 153, 570-574.

Sandhiya S, Dkhar SA, Surendiran A. (2009). Emerging trends of nanomedicine - an overview. Fundamental and Clinical Pharmacology 23, 263-269.

Sands JM. (2003). Mammalian urea transporters. Annual Review of Physiology 65, 543–566.
Schubert D, Dargusch R, Raitano J, Chan SW. (2006). Cerium and Yttrium Oxide nanoparticles are neuroprotective. Biochemical and Biophysical Research Communications 342, 86-91.

Scott A, Khan KM, Cook JL, Duronio V. (2004). What is Inflammation? Are we ready to move beyond Celsius? British Journal of Sports Medicine 38, 248-249.

Seki S, Nakashima H, Nakashima M, Kinoshita M. (2011). Antitumor immunity produced by the liver Kupffer cells, NK cells, NKT cells, and CD8 CD122 T cells. Clinical and Developmental Immunology 2011, 868345.

Semmler-Behnke M, Wolfgang KG, Lipka J, Fertsch S, Wenk A, Takeneka S, Schmid G, Brandau W. (2008). Bio-distribution of 1.4 and 18 nm gold particles in rats. Small 12, 2108-2111.

Senft AP, Dalton TP, Shertzer HG. (2000). Determining Glutathione and Glutathione Disulfide using the fluorescence probe *o*-Phthalaldehyde. Analytical Biochemistry 280, 80-86.

Sharma V, Anderson D, Dhawan A. (2011). Zinc Oxide Nanoparticles induce Oxidative stress and Genotoxicity in Human Liver Cells (HepG2). Journal of Biomedical Nanotechnology 7, 98-99.

Sharma V, Anderson D, Dhawan A. (2012a). Zinc oxide nanoparticles induce oxidative DNA damage and ROS-triggered mitochondria mediated apoptosis in human liver cells (HepG2). Apoptosis 17, 852-870.

Sharma V, Singh P, Pandey AK, Dhawan A. (2012b). Induction of oxidative stress, DNA damage and apoptosis in mouse liver after sub-acute oral exposure to zinc oxide nanoparticles. Mutation Research - Genetic Toxicology and Environmental Mutagenesis 745, 84-91.

Shi XL, Gu JY, Han B, Xu HY, Fang LA, Ding YT. (2010a). Magnetically labelled mesenchymal stem cells after autologous transplantation into acutely injured liver. World Journal of Gastroenterology 16, 3674-3679.

Shi Y, Zhang JH, Jiang M, Zhu LH, Tan HQ, Lu B. (2010b). Synergistic genotoxicity caused by low concentration of Titanium dioxide nanoparticles and p – DDT in human hepatocytes. Environmental and Molecular Mutagenesis 51, 192-204.

Shing CM, Adams MJ, Fassett RG, Coombes JS. (2011). Nutritional compounds influence tissue factor expression and inflammation of chronic kidney patients *in vitro*. Nutrition 27, 967-972.

Shukla RK, Sharma V, Pandey AK, Singh S, Sultana S, Dhawan A. (2011). ROS-mediated genotoxicity induced by titanium dioxide nanoparticles in human epidermal cells. Toxicology *In Vitro* 25, 231-241.

Shono S, Habu Y, Nakashima M, Sato A, Nakashima H, Miyazaki H, Kinoshita M, Tsumatori M, Shinomiya N, Seki S. (2011). The immunological outcome of enhanced function of mouse liver lymphocytes and Kupffer cells by high fat and high cholesterol diet. Shock 36, 484-493.

Shvedova AA, Kisin ER, Mercer R, Murray AR, Johnson VJ, Potapovich AI, Tyurina YY, Gorelik O, Arepalli S, Schwegler-Berry D, Hubbs AF, Antonini J, Evans DE, Ku BK, Ramsey D, Maynard A, Kagan VE, Castranova V, Baron P. (2005). Unusual inflammatory and fibrogenic pulmonary responses to single walled carbon nanotubes in mice. American Journal of Physiology 289, 698-708.

Shvedova AA, Pietroiusti A, Fadeel B, Kagan VE. (2012). Mechanism of carbon nanotube-induced toxicity: Focus on oxidative stress. Toxicology and Applied Pharmacology – ahead of press.

Simon A, Gouget B, Mayne M, Herlin N, Reynaud C, Degrouard J, Carriere M. (2007). *In vitro* investigation of TiO_2, Al_2O_3, Au nanoparticles and multi-walled carbon nanotubes cyto- and genotoxicity on lung, kidney cells and hepatocytes. Toxicology Letters 172, 36-36.

Simon A, Reynaud C, Mayne M, Herlin N, Desqueyroux H, Gouget B, Carriere M. (2008). Cytotoxicity of metal oxide nanoparticles and multiwalled carbon nanotubes to lung, kidney and liver cells. Metal ions in Biology and Medicine 10, 310-314.

Singh R, Pantarotto D, Lacerda L, Pastorin G, Klumpp G, Parto M, Bianco A, Kostarelos K. (2006). Tissue bio-distribution and blood clearance rates of intravenously administered carbon nanotube radiotracers. Proceedings of the National Academy of Sciences 103, 3357-3362.

Song WH, Zhang JY, Guo J, Zhang JH, Ding F, Li LY, Sun ZT. (2010). Role of dissolved zinc ion and reactive oxygen species in cytotoxicity of ZnO nanoparticles. Toxicology Letters 199, 389-397.

Soto K, Garza KM, Murr LE. (2007). Cytotoxic effects of aggregated nanomaterials. Acta Biomaterialia 3, 351-358.

Speit G, Schutz P, Hoffmann H. (2004). Sensitivity of FPG protein towards alkylation damage in the comet assay. Toxicology Letters 146, 151-158.

Smith PJ, Giroud M, Wiggins HL, Gower F, Thorley JA, Stolpe B, Mazzolini J, Dyson RJ, Rappoport JZ. (2012). Cellular entry of nanoparticles via serum sensitive clathrin-mediated endocytosis and plasma membrane permeabilization. International Journal of Nanomedicine 7, 2045-2055.

Stern ST, Adiseshaiah PP, Crist RM. (2012). Autophagy and lysosomal dysfunction as emerging mechanisms of nanomaterial toxicity. Particle and Fibre Toxicology DOI: 10.1186/1743-8977-9-20.

Szalai AJ, Nataf S, Hu XZ, Barnum SR. (2002). Experimental allergic encephalomyelitis is inhibited in transgenic mice expressing human C reactive protein. The Journal of Immunology 168, 5792-5797.

Takenaka S, Karg E, Moller W, Roth C, Ziesenis A, Heinzmann U, Scharamel P, Heyder J. (2001). Pulmonary and systemic distribution of inhaled ultrafine silver particles in rats. Environmental Health Perspectives 4, 547-551.

Teigs G, Lohse AW. (2009). Immune tolerance: What is unique about the liver. Journal of Autoimmunity 34, 1-6.

Teixeira J., Soares P, Benfieto S, Gasper A, Garrido J, Murphy MP, Borges F. (2012). Rational discovery and development of mitochondria-targeted antioxidant based on cinnamic acid scaffold. Free Radical Research 46, 600-611.

Teow Y, Asharani PV, Hande MP, Valiyaveettil S. (2011). Health impact and safety engineered nanomaterials. Chemical Communications 47, 7025-7038.

Tetley TD. (2007). Health effects of nanomaterials. Bionanotechnology 35, 527-531.

Tredicucci A. (2009). Quantum dots: Long life in zero dimensions. Nature Materials 8, 775-776.

Tsuchiya T, Oguri I, Yamakoshi YN, Miyata N. (1996). Novel harmful effects of 60 fullerene on mouse embryos *in vitro* and *in vivo*. FEBS letters 393, 139-145.

Tsuji JS, Maynard AD, Howard PC, James JT, Lam CW, Warheit DB, Santamaria AB. (2006). Research strategies for safety evaluation of nanomaterials, part IV: risk assessment of nanoparticles. Toxicological Sciences 89, 42-50.

Vermeire S, Van Assche G, Rutgeerts P. (2005). The role of C-reactive protein as an inflammatory marker in gastrointestinal diseases. Nature Clinical Practice – Gastroenterology and Hepatology 2, 580-586.

Villar E, Polkinghorne KR, Chang SH, Chadban SJ, McDonald SP. (2009). Effect of type 2 diabetes on mortality risk associated with end-stage kidney disease. Diabetologia 52, 2536-2541.

Villeneuve JP, Pichette V. (2004). Cytochrome P450 and the liver diseases. Current Drug Metabolism 5: 273-282.

vom Dahl S, Hallbrucker C, Lang F, Gerok W, Häussinger D. (1991). Regulation of liver cell volume and proteolysis by glucagon and insulin. Biochemical Journal 278, 771–777.

Wagner V, Dullaart A, Bock AK, Zweck A. (2006). The emerging nanomedicine landscape. Nature Biotechnology 24, 1211-1217.

Walter PB, Fung EB, Killilea DW, Jiang Q, Hudes M, Madden J, Porter J, Evans P, Vichinsky E, Harmatz P. (2006). Oxidative stress and inflammation in iron-overloaded patients with beta-thalassaemia or sickle cell disease. British Journal of Haematology 135, 254–263.

Wang F, Gao F, Lan M, Yuan H, Huang Y, Liu J. (2009). Oxidative stress contributes to silica nanoparticle induced cytotoxicity in human embryonic kidney cells. Toxicology *in vitro* 23, 808-815.

Wang J, Li N, Zheng L, Wang SS, Wang Y, Zhao XY, Duan YM, Cui YL, Zhou M, Cai JW, Gong SJ, Wang H, Hong FS. (2011a). P38-Nrf-2 signalling pathway of oxidative stress in mice caused by nanoparticulate TiO_2. Biological Trace Element Research 140, 186-197.

Wang J, Zhou G, Chen C, Yu H, Wang T, Ma Y, Jia G, Gao Y, Li B, Sun J, Li Y, Jiao F, Zhao Y, Chai Z. (2007a). Acute toxicity and bio-distribution of different sized titanium dioxide particles in mice after oral administration. Toxicology Letters 168, 17-185.

Wang JJ, Sanderson BJ, Wang H. (2007b). Cyto- and genotoxicity of ultrafine TiO_2 particles in cultured human lymphoblastoid cells. Mutation Research 628, 99-106.

Wang YG, Aker WG, Hwang HM, Yedjou CG, Yu HT, Tchounwou PB. (2011b). A study of the mechanism of *in vitro* cytotoxicity of metal oxide nanoparticles using catfish primary heaptocytes and human HepG2 cells. Science of the Total Environment 409, 4753-4762.

Wanninger J, Neumeier M, Weigert J, Bauer S, Weiss TS, Schaffler A, Krempl C, Bleyl C, Aslanidis C, Scholmerich J, Buechler C. (2009). Adiponectin stimulated CXCL8 release in primary human hepatocytes is regulated by ERK1/ERK2, p38 MAPK, NF kappa B and STAT 3 signalling pathways. American Journal of Physiology-Gastrointestinal and liver Physiology 297, 611-618.

Westerink WMA, Schoonen WGEJ. (2007). Cytochrome P450 enzyme levels in HepG2 cells and cryopreserved primary human hepatocytes and their induction in HepG2 cells. Toxicology *in vitro* 21: 1581-1591.

Whelan RS, Kaplinskiy V, Kitsis RN. (2010). Cell death in pathogenesis of heart disease: mechanisms and significance. Annual Review of Physiology 72, 19-44.

Whitby KT, Clark WE, Marple VA, Sverdrup GM, Sem GJ, Willeke K, Liu BYH, Pui DYH. (1975). Characterisation of California aerosols size distribution of freeway aerosol. Atmospheric Environment 9, 463-482.

Wick P, Manser P, Limbach LK, Dettlaff-Weglikowska U, Jrumeich F, Roth S, Stark WJ, Bruinink A. (2007). The degree and kind of agglomeration affect carbon nanotube cytotoxicity. Toxicology Letters 168, 121-131.

Wildgoose GG, Wilkins SJ, Williams GR, France RR, Carnahan DL, Jiang L, Jones TG, Compton RG. (2005). Graphite powder and multi-walled carbon nanotubes chemically modified with 4-nitrobenzylamine. Chemphyschem 6, 352-362.

Wilklund SJ, Agurelli E. (2003). Aspects of design and statistical analysis in the Comet assay. Mutagenesis 18, 167-175.

Wong SWY, Leung PTY, Djurisic AB, Leung KMY. (2010). Toxicities of nano zinc oxide of five marine organisms: influences of aggregate sizes and ion solubility. Analytical and Bioanalytical Chemistry 396, 609-618.

Wongkajornslip A, Sa-Ngiamsuntorn K, Hongeng S. (2012). Development of immortalized Hepatocyte-like cells from hMSCs. Methods in Molecular Biology 826, 73-87.

Woodrow Wilson website - accessed 23-7-2012.
(http://www.nanotechproject.org/inventories/consumer/browse/products/)

World Health Organization, 2012. The Global UV project - acessed 6-7-2011.
(http://www.who.int/uv/publications/en/Intersunguide.pdf)

Wu HX, Liu G, Zhuang YM, Wu DM, Zhang HQ, Yang H, Hu H, Yang SP. (2011). The behaviour after intravenous injection in mice of multiwalled carbon nanotube/Fe_3O_4 hybrid MRI contrast agents. Biomaterials 21, 4867-4876.

Xia T, Kovochich M, Brant J, Hotze M, Sempf J, Oberley T, Sioutas C, Yeh JI, Wiesner MR, Nel AE. (2006). Comparison of the abilities of ambient and manufactured nanoparticles to induce cellular toxicity according to an oxidative stress paradigm. Nano Letters 6, 1794-1807.

Xia T, Kovochich M, Liong M, Madler M, Gilbert B, Shi H, Yeh JI, Zink JI, Nel AE. (2008). Comparison of mechanism of toxicity of zinc oxide and cerium oxide nanoparticles based on dissolution and oxidative stress properties. American Chemical Society 10, 2121-2134.

Xiong R, Lu W, Yue P, Xu R, Li J, Chen T, Wang P. (2008). Distribution of an intravenous injectable nimodipine nano-suspension in mice. The Journal of Pharmacy and Pharmacology 60, 1155-1159.

Yamanaka YJ, Leong KW. (2008). Enginnering strategies to enhance nanoparticle-mediated oral delivery. Journal of Biomaterials Science 19, 1549-1570.

Yang J, Srinivasan A, Sun Y, Mrazek J, Shu Z, Kickhoefer VA, Rome LH. (2012). Vault nanoparticles engineered with the protein transduction domain, TAT48, enhancer cellular uptake. Integrative Biology: quantitative biosciences from nano to micro – ahead of print.

Yang L, Froio RM, Sciuto TE, Dvorak AM, Alon R, Luscinskas FW. (2005). ICAM-1 regulates neutrophil adhesion and transcellular migration of TNF-α activated vascular endothelium under flow. Blood 15, 584-592.

Yokel RA, MacPhail RC. (2011). Engineered nanomaterials: exposures, hazards and risk preventation. Occupational Medicine and Toxicology 6, 7.

Yue ZG, Wei W, Lv PP, Yue H, Wang LY, Su ZG, Ma GH. (2011). Surface charges affects cellular uptake trafficking and intracellular of chitosan-based nanoparticles. Biomacromolecules 12, 2440-2446.

Zamjahn JB, Quinton LJ, Mack JC, Frevert CW, Nelson S, Bagby GJ. (2011). Differential flux of macrophage inflammatory protein-2 and cytokine induced neutrophil chemoattractant from the lung after intrapulmonary delivery. American Journal of Physiology – Lung cellular and Molecular Physiology 301, 568-574.

Zhang LW, Yu WW, Colvin VL, Monteiro-Riviere NA. (2008). Biological interactions of quantum dot nanoparticles in skin and in human epidermal keratinocytes. Toxicology and Applied Pharmacology 228, 200-211.

Zhao F, Zhao Y, Liu Y, Chang XL, Chen CY, Zhao YL. (2011). Cellular uptake, intracellular trafficking and cytotoxicity of nanomaterials. Small 7, 1322-1337.

Zheng XO, Wu R, Chen YG. (2011). Effects of ZnO nanoparticles on wastewater biological nitrogen and phosphorous removal. Environmental Science and Technology 45, 2826-2832.

Appendix

A1 Surface functionalisation of titanium dioxide

Briefly 300 g of 10 nm-sized rutile TiO_2 (NRCWE 001) was suspended in 1.5 l of 20% methanol in water. The suspension was stirred and 250 ml of 3-aminopropyltriethoxysilane (purity 99%, Sigma-Aldrich, Denmark) was added slowly. The reaction was sonicated with a Branson Sonifier S-450D (Branson, USA) mounted with a disruptor horn, on ice at full power for 1 hr with 10 s on and 10 s off cycles. The suspension was stirred for 24 hr at room temperature. The titanium dioxide product was collected and was washed sequentially with 100%, 50%, 20%, 10% and 0% methanol in water by centrifugation for 30 mins at 35000 g. The material was dried for 2 days at 110°C. The recovery product was 267 g of amino-TiO_2.

A total of 136 g of amino-TiO_2 (NRCWE 002) was suspended in 200 ml dry of toluene in a three-necked round bottom flask. This was followed by the addition of 100 g of succinic anhydride (99%) (Sigma-Aldrich, Denmark) in 200 ml of dry tetrahydrofuran was added slowly and the reaction was sonicated. The reaction was refluxed for 36 hr and the product was collected on a fine porosity glass filter funnel under a slight negative pressure. The product was washed by centrifugation (see above) twice in 100% and once in each 50% methanol, 0.1 M sodium acetate and twice in water. It was dried at 80°C for 2 days. The recovery amount was 90 g.

The zeta potential of the amino-TiO_2 was +35 mV and of the carboxy-TiO_2 was -29 mV at pH 7.4 in water (Malvern Nano ZetaSizer, Malvern Instruments, UK) and it was stable over 24 hr.

A2 Nanomaterial characterisation

Briefly, phase compositions and average crystallites sizes were determined from powder X-ray diffractograms obtained at room temperature (25°C) using a Bruker D8 Advanced diffractometer in reflection mode with Bragg-Brentano geometry. A sealed Cu X-ray tube was run at 40kV and 40 mA, wavelength Cu $K_{\alpha 1}$ 1.5406 Å from a primary beam Ge monochromator, fixed divergence slit 0.2°, step size 0.02, step time 1 s $step^{-1}$, linear PSD detector (Lynx-eye) with opening angle 3.3°. The sample holders used for the reflection data were either a standard sample holder containing an approximately 2 mm thick sample or a single Si sample holder. One NM 300 sample was measured as transmission in a capillary. The phases were identified by using the EVA 14.0 software from Bruker AXS (copyright 1996-2007 Bruker AXS). The ratios and size were calculated using Topas 4.1 from Bruker (copyright 1999, 2008 Bruker AXS).

The hydrodynamic size distributions of the NMs dispersed in biological media were determined in the 0.128 - 0.256 mg/ml concentration range (lower concentrations were too low for DLS measurements) by Dynamic Light Scattering (DLS) using a Nicomp Submicron Particle Sizer Autodilute® Model 370 (Santa Barbara, USA). The employed instrument can automatically recognize, in the 0.5 - 6000 nm range, up to three size distributions of materials concurrently present through a patented software algorithm. No significant size differences were found at different concentration levels.

A3 HE oxidation

The HK-2 cells were seeded in 12 well plates (10^4 cells per cm^2 in 1 ml of complete RPMI) and incubated for 48 hr at 37ºC and 5% CO_2. Cells were exposed to the materials or controls for 4 hr at 37ºC, 5% CO_2. The treatment was removed and the cells were washed with complete RPMI. Cells were then harvested with 0.05% trypsin/EDTA and centrifuged at 300 g for 5 min before being re-suspended in complete RPMI without phenol red containing 1 µM of dihydroethidium (HE) (Sigma, France) for 30 min at 37°C in the dark and analysed by CyAn ADP LX DakoCytomation cytometer (Beckman Coulter, France). Excitation and emission wavelengths were 488 and 620 nm respectively. Minimum of 10000 cells was analyzed after exclusion of cellular debris and NMs from the analysis by gating on the 620 nm Log versus FS area graph.

Hydroethidium is the chemically reduced form of the commonly used DNA intercalating dye ethidium bromide (Kalyanaraman., 2011). This reduced dye is therefore useful for detection of oxidative activities in viable intact cells. Only once it is internalized and dehydrogenated (oxidized) to ethidium, it can intercalate into DNA. Normally due to their compromised membranes, only dead cells are typically labelled by ethidium bromide when it selectively binds to DNA. However HE is a neutral probe and is able to penetrate the cell membrane of live cells, staining their cytoplasm blue as well as the chromatin/nucleus of living cells red.

Dihydroethidium was used for the flow cytometric measurement of superoxide production. Dihydroethidium is rapidly oxidized to ethidium (a red fluorescent compound) by H_2O_2 (in the presence of peroxidase) and superoxide. Ethidium is trapped in the nucleus by intercalating into DNA, leading to an increase of ethidium fluorescence.

A4 Intratracheal instillation

The mice were anesthetized using 4% isoflurane in an induction chamber. The anaesthesia was maintained using 2.5% isoflurane via an intubation aid (UNO BV, The Netherlands) during the intratracheal instillation as previously described (Sadauskas, *et al*., 2009b). A diode light was placed against the larynx, the tongue was pressed towards the lower jaw and the trachea was intubated using a 22 gauge with a shortened needle. A 50 µl suspension of the nanomaterials was instilled followed by 200 µl air. After the procedure the mice were transferred back to cages. Inter control mice were anaesthetised, but no instillation procedure was performed. Vehicle control mice received the dispersion media without nanomaterials (2% serum in MilliQ).

The study set-up included three animals per group and a dose-range of 0, 1, 4, 8, 16, 32, 64 and 128 µg/mouse of each NM. The animals were dissected 24 hr after instillation. The liver was then divided into five pieces. For the analysis reported here, the middle lobe was frozen in liquid nitrogen for GSH depletion measurements (about 0.4 g of tissue).

A5 Flow cytometry

Prior to fluorescence-associated cell sorting, the cells were fixed for 10 min in 4% paraformaldehyde and then washed in PBS. A CD163 Alexa-647-labelled antibody (MCA342A647) (AbD Serotec, UK) was used to detect Kupffer cells and a CD68-PE (MCA341PE) (AbD Serotec, UK) to detect non-resident macrophages and utilised as recommended by the manufacturer.

A6 Immunofluorescence

To detect phagocytic Kupffer cells, 200 nm fluorescent polystyrene beads were added to the cell cultures for 2 hr, before being rinsed out. The cells were then fixed with PFA, permeabilised, blocked with 10% FCS in PBS and stained with a sheep anti rat albumin antibody (1:500) (A110-134A) (Bethyl Laboratories, UK) and an anti-sheep Alexa-568 secondary antibody (1:1000) (Life Technologies, UK). Hoechst 33342 (Life Technologies, UK) was used as a nuclear stain.